UNIVERSITAT DE BARCELONA

Exploiting circulating lymphocytes and cell-free DNA as a source to develop minimally-invasive personalized T-cell therapies

Andrea Garcia Garijo

Universitat de Barcelona
Programa de doctorat en Biomedicina

Exploiting circulating lymphocytes and cell-free DNA as a source to develop minimally-invasive personalized T-cell therapies

Andrea Garcia Garijo
Doctoral Thesis
Barcelona, 2023

Thesis director: Alena Gros
Thesis tutor: Cristina Fillat

Acknowledgements

Abans de començar a parlar de tota la gent que ha format part d'aquesta etapa i a la qual li estic immensament agraïda per haver-me acompanyat tant i tan bé durant aquest procés, volia explicar breument el significat de la portada. Després de viure l'experiència d'escriure un llibre (check!), em semblava força important triar una portada que estigués a l'alçada del que ha suposat fer aquesta tesis doctoral i volia donar-li un significat tant científic, relacionat amb el tema de la tesis en si, com personal, intentant plasmar en una imatge tot el que han significat per mi aquests 6 anys de tesis. La part científica va relacionada amb una de les tècniques que més he utilitzat durant aquests quasi 6 anys, el FACS, ja que he hagut d'utilitzar molts colors per poder sortejar tota la ristra de poblacions que he arribat a sortejar de la sang, que no han sigut poques! Hi ha gent que m'ha dit que sembla un t-SNE plot, altres una cèl·lula, un tumor heterogeni amb T cells que se li aproximen... això ja és lliure a la imaginació de cadascú! I per altra banda, l'explosió de colors també té el seu significat emocional ja que representa tots els sentiments i totes les emocions viscudes durant aquests quasi 6 anys, que ha sigut ben bé una bona muntanya russa! Aprofito per començar amb el primer agraïment, a l'Alba, amiga de la Pepi i creadora d'aquesta fantàstica portada, no me la podia haver imaginat millor.

Si miro enrere, moltes coses han passat al llarg d'aquests quasi 6 anys... sembla mentida com ha canviat tot des de que vaig començar fins ara. Recordo perfectament quan estava fent la meva última estància de màster a Lausanne i vaig voler contactar l'Alena, que feia poc que havia obert el seu grup a Barcelona. El meu supervisor, el Pedro Romero, em va dir que era una idea fantàstica, que l'Alena era una crack i era el millor lloc al que podia anar si volia tornar a Barcelona. I recordo estar a Suïssa, després d'haver aconseguit una TC amb l'Alena, llegint els seus articles de TMGs... i no entendre **RES** i pensar: "doncs vaya a l'entrevista, anem fotuts!" Però després tot va ser molt fluït i fàcil. Tot i que la incertesa es va allargar més del que esperava perquè depenia d'un postDoc d'Argentina per poder entrar o no, finalment vaig aconseguir entrar com a PhD, i és el que m'ha permès arribar fins aquí. Per això, volia començar per donar-te les gràcies a tu, Alena, per donar-me aquesta gran oportunitat. Recordo amb especial carinyo i tendresa el meu inici, quan tu mateixa entraves amb mi a cultius i m'ensenyaves els protocols com el de fer dendrítiques. Gràcies a tu el meu primer dia a cultius de la 4ta planta està fotografiat! També recordo quan vas venir amb mi al primer sort al PRBB que ens vam equivocar d'hora perquè no ens vam entendre i jo no tenia la confiança per dir-te: "Alena, hauríem d'anar tirant...!". I les birres i sopars que fèiem freqüentment al sortir del lab sempre acompanyats dels nostres germans MALucos, quina gran època. Gràcies i mil gràcies per tot el que m'has ensenyat, he après moltíssim, no només de ciència, sinó també a ser crítica, a debatre, a resoldre problemes, a fer presentacions tenint clar el missatge que es vol donar en cada moment... I gràcies també per la confiança i la proximitat, per escoltar-me i entendre'm quan he passat per algun "entrebanc" personal o quan no he estat del tot bé al lab. Tot i que

les coses han evolucionat i han anat canviant perquè així havia de ser, jo m'emporto tot això i estic molt contenta d'haver-ho pogut viure d'aquesta manera. T'admiro molt.

Quan encara estava en el procés de selecció que no sabia si sí o si no, yo, poniendo toda la carne en el asador, vaig anar al laboratori per Setmana Santa a conèixer el lab. El que no sabia és que aquell dia també coneixeria a dues persones que acabarien sent dos dels més grans descobriments fets durant aquest temps i que es convertirien en dues persones indispensables a la meva vida. El lab en aquell moment estava format per l'Àlex, el tècnic i lab manager, i la Maria, que en aquell moment també feia de tècnic però la idea era que comencés a fer el PhD quan tot estigués una mica més assentat. Recordo la Maria apareixent per allà, coixa, que havia anat a esquiar i s'havia fet mal al genoll. Aquell dia ja corria, no seria cap novetat després. El mateix dia que jo vaig anar a conèixer el lab hi havia un altre noi, un tal Carlos, que s'entrevistava per començar com a PostDoc. Recordo que en aquell moment vaig pensar que no encaixaríem gaire. Segurament també mirat des del prisma que jo veia que ell sabia molt i jo no sabia res xD. I no podia estar més equivocada. Perquè el Carlos, alias Chals o Charlio, és un dels dos grans descobriments d'aquell dia. Charlio, amigo del alma, creo que me va a ser imposible darte las gracias lo suficiente solo escribiendo unas frases aquí. Gracias por tu presencia, por estar siempre cerca, por tus palabras de ánimos ("*Venga Andreita, que ya lo tienes!*"), por tu apoyo incondicional y por siempre creer en mí. Gracias por ayudarme tanto a lo largo de todos estos años, hasta el último momento corrigiendo la discusión conmigo el domingo antes de depositar. Te aseguro que hubiera sido mucho más difícil si no hubieras formado parte de toda esta etapa. Todo lo que pueda escribir aquí estoy segura que ya lo sabes, con lo moñas que soy seguro que ya te lo he repetido muchísimas veces. Estoy feliz de haber podido compartir esto contigo, te has convertido en una persona muy muy importante para mí y aunque quizás ahora es más difícil estar conectados día a día y es más difícil vernos, sé que estás ahí y te siento siempre cerca. Te quiero amigo.

I si el Charlio és una d'aquestes dues persones, ara tocarà parlar de l'altre. I òbviament és aquella noieta coixa amb una melena rizada despampanante, la Maria, també coneguda com a Meri, Meripein, Pepi, Pepinillo o Pepinillo picante si ha tingut un mal dia i no està de bon humor. Recordo que en els super inicis va ser ella la que li va escriure un e-mail a l'Alena dient-li que m'avisessin per inscriure'm a un congrés i allà va ser quan ens vam començar a enviar els primers e-mails tímids de compis de PhD. En aquell moment no sabíem tot el que teníem per davant Pepi, totes les històries i aventures, moments de felicitat, moments de tristesa i experiències que compartiríem, tant dins com fora del lab. Les tardes eternes processant sangs, les dos setmanes nadalenques ensenyant a la Jennifer (pa nah!), els screenings compartits dels Golden patients, l'screening fallit de 12 plaques amb la potencial peli + palomitas... No sé si en el meu primer positiu amb el pacient GOI-01 i les poblacions CD8+ estaves més emocionada tu o jo jaja. I totes les birres, sopars, noches en mi casita hablando hasta las mil, barbacoes, paelles, Altafulla, días de playita con la motico hasta Castelldefels. És realment impossible imaginar-me fent el Doctorat si tu no haguéssis estat al

meu costat, agafant-me de la maneta dia a dia i ajudant-me a tirar. No podria demanar una mejor compañera de viaje. I jo també sé que tu ho saps i, a més, sé que penses el mateix de mi. Ah! I per a que entengueu lo fons que han calat aquests anys... a dia d'avui, si crides Pepi, ella es gira!!!!!! Pepi, te quiero en mi equipo, ahora y siempre. T'estimo i et trobo a faltar.

Y ya que he empezado, voy a continuar con el equipito PhDs. Un any més tard que jo entrés va venir la petita Anna, l'Annita, también conocida com el carrito de Fontana o el torito de la 4ta. Al principi les PhDs mayores vam patir moooolt per perdre-la entre cafès i cafès i pel desterrament que va patir a l'arribar. Però poc a poc es va acabar convertint en una altra personeta molt molt important durant aquesta etapa. L'Anni també forma part de l'equip de runners, com la Pepi, sempre corrent d'aquí per allà. Però també sempre sempre sempre disposada a ajudar, en lo que le pongas, ni que sigui congelar REPs eterns amb noms infumables (GOI-01, CD8+ PD-1-CD39+ 4-1BB+ vs. KIAA1524 R1d14 ...). Crec que el fet que tant tu com jo haguem passat per una etapa difícil molt similar (bàsicament lo mateix però time-ponts pre i post-pandèmia) també va fer que poc a poc ens anéssim unint cada vegada més i t'acabessis convertint també en una peça clau d'aquesta etapa. Gràcies Anni, per ser sempre un suport, per estar sempre disposada a acompanyar-me a fer un piti si necessitava parlar, desfogar-me, plorar, o lo que fuera. Per sempre creure en mi *("Yo voy a ser la amiga de la que publicó un Nature!"*), per totes les birres, confessions i pel super viatge a Canadà que vam disfrutar com dos enanas. Crec que era una prova de foc passar 14 dies juntes, soles, fora de casa i amb una diferència horària tan gran y creo que la superamos con sobresaliente! Recordo amb molt de carinyo i amor les nostres converses profundes a Vancouver amb un cafè davant del mar... Tots aquests records els tindrem per sempre. Ah, i gràcies per sempre esperar-me pacientment a Fontana cada matí quan arribo tard a la nostra quedada. Encara ens queden moltes històries més per compartir i no et preocupis que, estigui on estigui, t'ajudaré amb tot el que necessitis i més en l'escriptura de la teva tesis, el disseny, les figures, y lo que haga falta. Creu-me, et quedarà una tesis espectacular perquè ets molt crack, una màquina, lo únic que et falta és creure-t'ho una mica més! Però ho passarem juntes, tus PhDs mayores estaran cerca.

Y finalmente llegamos a la PhD pequeña, la petita Jud, también conocida como Juditinha. Esta no solo forma parte del equipo runner, sinó que lo preside!! Que no os engañe, es un terremoto andante. La Judi és la força personificada, pot amb tot el que es proposi i més. I jo crec que lo únic que et falta a tu també és creure-t'ho una mica més. El dia que et paris a mirar enrere i a ser realment conscient de tot el que has tirat endavant pràcticament tu sola... veuràs lo molt que vals i en la gran científica que poc a poc t'has anat convertint. Crec que especialment l'Anni, tu i jo som persones molt auto-castigadores. És una llàstima que no et puguis veure per un segonet amb els meus ulls, perquè realment admiro la teva resiliència, la teva empenta per tirar endavant i aixecar un projecte tan complicat des de zero i la teva motivació per la ciència. Ah! I la teva energia matutina, tant de bo tingués una mica més d'això jo també. No et preocupis que no tinc CAP DUBTE que al congrés de Mainz ho petaràs, i allà

estarem l'Anni i jo per aixecar-nos i aplaudir en quan acabis. I també t'ajudaré amb el que necessitis amb l'escriptura de la tesis, ni ho dubtis. Per molt que potser no estigui físicament, no us lliurareu de mi tan fàcilment! Vull concloure aquesta part donant-vos unes gràcies molt molt sinceres i de cor a les tres, crec que l'equipito *Denia Felicidad* ha sigut indispensable en molts moments per poder tirar endavant i arribar on estem ara gràcies a tenir-nos les unes a les altres. Sou unes cracks.

Ara vull parlar en concret d'una altra persona molt especial, la meva tocaya, la meva partner in crime que ha tingut un paper fonamental en aquesta tesis i ha fet que tot això fos possible. La Imma, també coneguda com a Immiluki. Ella també té un dorsal en l'equip de runners, no us penseu pas que es queda fora. Tot i que ella fa més maratons, BST, VHIO, PRBB, BST, Clínic, VHIO... La Immi va entrar al lab pensant-se que seria tècnic, tindria una vida tranquila i feliç. Ja se li va complicar tot bastant quan la van posar a càrrec dels jaleitos amb el BST però no sabia que encara li venia lo pitjor: ajudar-me en el projecte per a que tot tirés més ràpid per arribar al deadline de la beca. Això sí que va ser una bogeria. Co-cultius de 10 plaques amb 36 poblacions a mig agost, "*venga yo pongo PBS y tu vas picando*", "*I: placa 1 ja està al FACS, ara preparo la 2 i la 3; A: vale, jo mentrestant revelo*". Infinites gràcies per tot el que has aportat en aquest temps, la teva ajuda ha sigut indispensable per arribar on estic ara. Gràcies per la teva calma, m'ha anat molt bé en molts moments. Per tots els gifs que ens hem arribat a enviar per whatsapp, em donaven la vida en molts moments. Gràcies per la teva paciència ETERNA quan cada dos per tres (no descarto seguir-te preguntant en un futur) et preguntava pels resultats de MotriColor, els minigenes testats, les reactivitats. Et mereixes un monument. Ha sigut un gran plaer treballar amb tu codo con codo i estic feliç que vagis a ser tu la persona que continui el meu projecte, no podria estar en millors mans. I igual que ho crec de la Jud i l'Anni, només et falta creure una mica més en tu per arribar allà on vulguis. Tu també ets molt crack i has après un montón des de que vas arribar fins al dia d'avui. I sé que encara et queda una etapa molt xula per començar i disfrutar que aviat arribarà. Però bueno ja saps... el río, el puente... pues eso.

Al lab hi ha altres membres que són essencials per a que el laboratori funcioni i els quals també han tingut un paper molt important en aquesta història. L'Albert, també conegut com "Alber", un personajillo como no los hay, amb les seves rutinetes i les seves maneres de fer. L'Alber té una gran facilitat per captar quan una persona del lab necessita ajuda i allà està ell, sempre disposat a ajudar o simplement per fer companyia. No oblidaré mai el dia del dipòsit de la meva tesis que tots estaven fent birres al Julio i tu et vas quedar amb mi ajudant-me amb tot el papeleo de la Universitat quan jo ja no veia res, ajudant-me a pujar tots els documents i revisar-los tots. Només tu vas estar present en el moment de clicar el botó "send" i això no ho oblidaré mai. Gràcies per la teva paciència, estic segura que per una persona tan ordenada com tu no ha sigut fàcil tenir-me a mi a l'escriptori del costat. Gràcies per ajudar-nos sempre amb el nitrogen *("Això per quan ho necessites?"; "Per quan abans millor..."*). Sóc la primera que et maleeixo cada vegada que te'n vas de vacances però això també demostra

lo molt important que ets. Tu també vas tenir un paper indispensable al principi d'aquest projecte processant les leucafèresis amb mi. Així que moltes gràcies per estar al meu costat des del ben principi fins al ben final d'aquesta història. Una altra peça extremadament clau en aquest laboratori és la Noe. La Noe és una màquina en tots els sentits, no conec a persona més eficient al planeta terra que ella. Jo seria incapaç de portar tot el que porta ella però Noe, por favor, frena un poco y recuerda que comer, se come cada dia!!!! Gracias por tu paciencia infinita, sé que soy tu hija tonta número uno, que ya te debes haber puesto en automático mandarme 3-4 reminders cada vez que tengo que hacer algo... prometo que en mi etapa postDoc voy a trabajar en eso. Gracias por tu calma (aunque a veces creo que es lo que vemos pero no lo que llevas dentro), eres el engranaje más importante para que este laboratorio siga funcionando. Ara parlem també del team postDocs. La PostDoc més antiga, la Jari. Jari quan penso en tu només em venen un munt de colors alegres. Sempre he pensat que ets la persona que millor combina tota la quantitat de colors amb que vesteixes, la teva jaqueta blava, la teva motxilla groga, les teves botes liles. I haig de dir-te que em vaig quedar impressionada quan vaig conèixer casa teva, perquè és exactament un reflex del que tu ets. I em va flipar. Tu també ets un dels pilars de la calma i la paciència del lab, l'experiència que dóna una mica de serenitat en els moments d'embogiment del sector PhD. Ha sigut genial compartir aquesta etapa amb tu també, ja tinc ganes de que tornis! Després tenim els dos PostDocs, el Pierre i l'Endika, que per fi han aportat una mica de testosterona a l'equip (a part de l'Alber, que estaba solo en eso). Merci beacoup/eskerrik asko por leeros pacientemente esta tesis eterna y darme los últimos comentarios, os lo agradezco un montón. Al Ricky, former postDoc, which was the wise of the molecular biology. Y finalmente gracias a Ricardo, también miembro honorífico del iTAG lab. Gracias por todos tus consejos, por los análisis y todo el tiempo invertido tanto en esta tesis como en el paper. Aunque al final ha habido algun gráfico que se ha quedado en la discusión, tu visión me ha sido muy útil para escribir la tesis. Muchas gracias. I no m'oblido de tots els master students (Helenita, Carla, Roc, Maria F., Carla, Alisha), que han anat passant i que d'una manera o una altra han deixat petjadeta. Overall, ha sigut i és un plaer formar part d'aquest equip humà tan genial que ha fet que aquesta etapa, que és como un programa de Gran Hermano, fos molt més divertida. Os porto a tots al cor (L).

Pero como ya he comentado antes, nosotros siempre hemos ido cogidos de la manita bien cerquita de nuestros vecinitos y hermanitos, los MALucos. Y esque todos vosotros también habéis sido una pieza clave durante todos estos años. Primero de todo, quería darte las gracias María, por ser también una persona tan cercana con la que he podido hablar de todo cuando lo necesitaba. Tu me cazabas por el pasillo y veías cuando algo no iba bien... te lo agradezco. Ha sido un placer compartir todas las cervezas, cenas y fiestas. Y también tener una colaboración en conjunto, ha sido muy guay trabajar contigo. Y de aquí me voy a la pequeña Olguita, con la que también he podido trabajar mano a mano. Ha sido un placer compartir el proyecto PD-L2 contigo, también formas parte de las persones más eficientes que conozco. Gracias Olgui, por también siempre tener un momento para compartir penas y alegrías, algun

que otro cafè y muchas historietes. Espero verte pronto. De la primera horneada de MALucos también tenemos a Elena, a Emanuela y a Iñaki. Elena, la PostDoc, la que siempre se enteraba de todo, hasta cuando ya no estaba en el VHIO! Aunque ahora ya hace unos años que te fuiste, estoy muy contenta de haber compartido la primera etapa de la tesis contigo. Siempre has aportado energia y buen rollo! Y Emanuela, que des de que aprendió castellano, creo que tiene un vocabulario más rico que el mío y todo. Una de las cosas que ha caracterizado estos años han sido tus frases celebres y tu tono de voz basal que hacía que siempre te oyeramos des de nuestro pasillo. Te echamos de menos! Y finalmente, Iñaki, el primer PhD del equipo niTAG-MAL y también conocido como el jefe del turno de noche. Cuando Iñaki entraba a cultivos... estabas jodido y se te había hecho muy tarde. Te confesaré que en tu etapa final sufrí un poquito por ti y por tu integridad. Pero como ya sabía, eres un crack y superaste la etapa con éxito. Me pareces un pozo sin fondo de sabiduría y has sido un gran descubrimiento. Gracias también por todas las charlas y momentos en cultivos, pasillo, por tu baile de Peter la Anguila, las fiestas y la facilidad de liarte, se agradece gente espontánea que no puede decir que no a una fiesta! Tenemos pendiente una visitilla a Cambridge, no os penséis que no vendremos a veros! Y después de esta primera horneada, llegaron Marta, Lluís y las dos nuevas PhDs, Marion y Alba. La Marta, que aportava dolçor i calma. I el Lluís que també aporta tranquil·litat, cordura i pau. A mi parlar amb tu Lluís, sempre em dona calma, em fas veure les coses amb molta més serenitat del que jo sóc capaç. La Marion, també una persona amb les coses molt clares, molt organitzada i eficient. Te confieso que te he cogido los markers muchas veces cuando trabajaba en la poyata frente a la tuya pero que siempre ponia mucha consciencia en devolverlos para que no se notara. Espero haberlo conseguido! Ha sido muy guay trabajar en ese lado estando vosotros al otro lado, siempre había alguna historieta que escuchar! I finalment la petita Albi, esta sí que és la dolçor i la tendresa en persona. Albi, tu també has sigut un dels grans descobriments d'aquesta etapa, ets de les persones més generoses i cuidadores que conec. Gràcies per estar sempre tan a prop, per totes les rosquilletes i els post-its que m'has anat deixant durant el període d'escriptura. Per preocupar-te per tot allò que a mi em preocupava, per sempre enrecordar-te de preguntar-me qualsevol cosa que sabies que havia de fer que era important. Gràcies per la constància, per acceptar totes les meves limitacions i no qüestionar-les, simplement fer que les coses siguin més fàcils (com per exemple, haver de pujar a casa amb mi perquè m'havia deixat la llum de la terrassa oberta i tenia por). Tot i que hem de seguir treballant amb el tema del compromís en els plans, jo sé que poc a poc ho aconseguirem. La Queri i jo anem fent feina, no tenim pressa. Pròxima parada: Bolívia 2023. I abans de parlar d'aquesta tal Queri, volia agraïr-vos, equipito de tres (Lluís, Marion i Alba) haver-me acollit al despatx mentre estava escrivint la tesis. Sempre era xuli sortir del despatx i veure algú de vosaltres tres que em preguntava com ho portava. Moltes gràcies.

I passem a l'altre membre del grup "Gracia girls", la Queralt, també coneguda com a Queri. Un altre gran descobriment d'aquesta etapa, si ja us dic que he tingut molta sort! Amb la Queri tot és molt fàcil, és alegria, bon rollo, felicitat i a més, tenim maneres molt similars

de fer i pensar. Queri, gràcies a tu també per cuidar-me tant i per estar sempre tan a prop. No oblidaré mai el dia que escrivint la tesis se'm va ficar al cap que volia croissants i tu vas demanar un glovo amb croissants de xocolata per fer-me feliç. Tens llum i la teva presència dona energia. Gràcies per estar sempre disposada a ajudar o a unir-te a qualsevol plan, ets una d'aquestes que també es lia fàcil y también por eso, te quiero en mi equipo siempre. Ara et toca a tu passar per l'escriptura però ho estàs fent genial i et quedarà una tesis espectacular. I ho celebrarem por todo lo alto, como a nosotras nos gusta!

I a més de tota aquesta gent que ja he nombrat del VHIO, molts altres també han estat presents i m'han acompanyat al llarg d'aquest camí. Gent de la 4ta planta com l'Ana i la Carlota, la Cris, el Dani i la Carlota d'hemato, la Mireia i la Chiara, la Saray, gent d'altres plantes com l'Ester Planas, l'Enrique, el Santi, la Garazi, la Irene, el Faiz... Gràcies a tots d'una manera o altra per fer d'aquesta etapa una etapa molt especial. I finalment, el petit comité con el que fácilmente compartimos unas birras los viernes: Nico, Sara, Juli... siempre va bien acabar la semana con una buena cerveza cogiendo aire fresco. Y no me olvido del VHIO finde comittee que algunos de ellos ya han salido como Emmanuela, Queri y Sara pero también faltan Fabio y Laia. Fue una pasada organizar el VHIO finde con vosotros y sinceramente fue un gran éxito! Esto también me lo llevo para siempre!

I tot i que una gran part del temps d'aquests quasi 6 anys l'he passat al VHIO, també ha sigut necessari i imprescindible comptar amb gent tan guai i especial fora per airejar-se una mica, desfogar-se o simplement desconnectar. Gràcies a l'equipito *Tremendo Kilombo*, entrenar i jugar amb vosaltres i compartir cerveses, dinars, sopars i findes ha sigut essencial per poder tirar endavant amb tot això. Especial menció a la meva peliroja prefe, la Clau, a la Rus i a la Yuli que sempre les he sentit molt a prop. Gràcies per ser-hi. També volia agrair-li al Marc, que, tot i que els nostres camins s'hagin separat, agraeixo tot l'esforç i implicació durant els primers anys de tesis amb viatges en moto a les 7 del matí per poder arribar dora al lab els dies de sort. A l'Anna, la Sara i la Júlia, pels sopars de riures i de posar-nos al dia. A la Sara, l'Amayita, la Nina, el Santi, por creer en mi y acompañarme en la distáncia. Aunque estemos lejos, yo sé que cuando nos vemos, parece que el tiempo no pase. Eso es lo más importante. A la Luli, la meva gran amiga de la Universitat amb la que vaig començar tota la carrera científica i que, any rere any, seguim tirant del carro juntes. Tot i que sigui més difícil veure'ns i potser no parlem tant en el dia a dia, et penso molt. I a la Jana, que també, tot i que visquis a Suïssa, sempre trobem un moment per veure'ns, posar-nos al dia i compartir vivències quan ens juntem.

Finalment, gràcies Marin i Euli, vosaltres dues també heu sigut un pilar durant aquest procés, sempre presents, disposades a ajudar, escoltar o preparar qualsevol plan per ajudar-me a desconnectar. Ja sabeu, capa més profunda de la ceba, per sempre. I òbviament, a mi amiga del alma, la Merin. Poques paraules són necessàries quan ens portem tatuades a la pell, creo que eso ya lo dice todo. Més que amigues som família, juntes hem compartit la vida. En tots els meus records hi ets tu, il·luminant-me amb la teva llum. No hi ha paraules suficients

per agrair-te tot el que fas constantment per mi, només amb la teva presència. Gràcies per SEMPRE creure en mi, m'has donat forces per seguir tirant.

Y obviamente no me olvido de ti Pauli, la que más ha sufrido el gremlin durante el periodo de escribir la tesis. Gracias por tu paciencia, templanza, cercanía, y por cuidar tanto de mi. Has sido un gran apoyo durante este tiempo y nunca podré agradecerte lo suficiente todo lo que has hecho. Tu también has sido un pilar en esta etapa final. Te prometo que lo peor ya ha pasado, ahora solo tenemos que estar preparadas para todas las aventuras que estan por venir!

I volia acabar amb un agraïment absolut i profund als meus pares pel seu recolzament incondicional. Sóc molt afortunada de tenir-vos i de poder comptar amb vosaltres sempre. Gràcies papi, per estar allà en els moments d'ofuscació i posar-li practicitat a tot, ajudar-me a sortir dels bucles i fer-me veure que la vida és més senzilla. Gràcies mami, pel teu amor incondicional, per cuidar tant de mi i per estar sempre al pie del cañón por si necesitaba un rescate. Gràcies Guille, el millor germà que podria tenir. Tu també has sigut una peça clau en aquest procés, sempre present i cuidador. Gràcies a la Lulu i al tiet, a l'Aleix i a la Bertuki. Y a la iaia, que siempre pide por mi para que todo me salga bien, que con lo mucho que yo estudio... no puede salir nada mal. Aquesta tesis també ha sigut possible gràcies a vosaltres. Somos una família pequeñita, pero partimos la pana allá donde vamos. No em podria imaginar una família millor. Gràcies a tots vosaltres he arribat on sóc i m'he convertit en la persona que sóc ara.

Com podeu veure, aquesta tesis l'he escrit jo però molta gent ha sigut necessària per a que això tirés endavant. Gràcies a tots, per formar part d'aquesta etapa tan especial. Ha sigut un plaer compartir-la amb tots vosaltres. Ara el més important és compartir la celebració post-defensa on ho petarem fort!!

Abbreviations

ACT	Adoptive T-cell transfer
ALL	Acute lymphoblastic leukemia
APCs	Antigen-presenting cells
CAR	Chimeric antigen receptor
CAR-T	CAR-transduced T
CD	Cluster of differentiation
CD39	Ectonucleoside triphosphate diphosphohydrolase 1
cfDNA	Cell-free DNA
CNAs	Copy number alterations
CRC	Colorectal cancer
CSF	Cerebrospinal fluid
CTCs	Circulating tumor cells
ctDNA	Circulating tumor DNA
CTLA-4	Cytotoxic T-lymphocyte antigen 4
ctRNA	Circulating tumor RNA
DCs	Dendritic cells
EBV	Epstein-Barr virus
EGFR	Epidermal growth factor receptor
ER	Endoplasmic reticulum
EVs	Extracellular vesicles
FACS	Fluorescence-activated cell sorting
FDA	Food and Drug Administration
GM-CSF	Granulocyte-macrophage colony-stimulating factor
H&N	Head and neck
HIV	Human immunodeficiency virus
HLA	Human leukocyte antigen
HPV	Human papillomavirus
ICB	Immune checkpoint blockade
IFN-γ	Interferon-γ
IL-2	Interleukin-2
IL-2R	IL-2 receptor
IVS	*In vitro* sensitization
LAG-3	Lymphocyte-activation gene 3
LCMV	Lymphocytic choriomeningitis virus
MART-1	Melanoma antigen recognized by T cells

MDSCs	Myeloid derived suppressor cells
MEP	Minimal epitope pool
MHC	Major histocompatibility complex
MLTCs	Mixed lymphocyte tumor cultures
MRD	Minimal residual disease
NK	Natural killer
NSCLC	Non-small cell lung carcinoma
NSMs	Non-synonymous somatic mutations
PAP	Prostatic acid phosphatase
PBLs	Peripheral blood lymphocytes
PBMCs	Peripheral blood mononuclear cells
PCR	Polymerase chain reaction
PD-1	Programmed death receptor-1
PD-L1 and PD-L2	Programmed death-ligand 1 and 2
PHA	Phytohemagglutinin
pHLA	Peptide-HLA
PP	Peptide pool
PSA	Prostate-specific antigen
RAG-2	Recombinase activating gene-2
REP	Rapid Expansion Protocol
SNVs	Single nucleotide variants
TALs	Tumor-associated lymphocytes
T-biAbs	T-cell engaging bi-specific antibodies
TCL	Tumor cell line
TCR	T-cell receptor
TEPs	Tumor-educated platelets
TILs	Tumor-infiltrating lymphocytes
TKIs	Tyrosine kinase inhibitors
TMG	Tandem minigene
TNF-α	Tumor necrosis factor-α
TuBx DNA	Tumor biopsy DNA
ULP-WGS	Ultra low-pass whole-genome sequencing
VAF	Variant allele frequency
WES	Whole-exome sequencing
WGS	Whole-genome sequencing
WT1	Wilms' tumor protein

Index

Summary

Adoptive cell transfer (ACT) of tumor-infiltrating lymphocytes (TILs) can mediate tumor regression in patients with metastatic melanoma. Retrospective studies of TIL products from responders and non-responders have shown that successful TIL-ACT is associated with an expansion of T cells targeting neoantigens, which are derived from tumor-specific non-synonymous somatic mutations (NSMs) and present exquisite tumor specificity. In addition, ACT with TIL products enriched for neoantigen recognition has demonstrated antitumor activity in selected patients with epithelial tumors other than melanoma, which has fueled the interest in personalized T-cell therapies targeting neoantigens. The identification and isolation of neoantigen-specific TILs has been possible due to advances in next-generation sequencing that enabled the rapid assessment of the tumor mutational landscape and the development of high-throughput personalized immunological screenings. However, the need of a tumor biopsy to both identify candidate neoantigens and reactive T cells limits the broad applicability of personalized T-cell therapies targeting neoantigens and can underestimate tumor heterogeneity in the advanced metastatic setting. Previous reports have shown that neoantigen-specific T cells can be enriched from peripheral blood by selecting programmed death receptor-1 (PD-1)-expressing lymphocytes in circulation. However, the frequency of neoantigen-specific T cells identified based on PD-1 expression remains very low and a tumor biopsy is still required to identify candidate NSMs.

In this thesis, we explored the use of peripheral blood as an alternative minimally-invasive source to identify tumor NSMs and isolate neoantigen-specific or tumor-reactive T lymphocytes in patients with metastatic breast, gynecological, colorectal and head and neck cancer or chordoma. We performed whole-exome sequencing (WES) of cell-free DNA (cfDNA) to identify tumor NSMs and compared these to those identified in DNA extracted from tumor biopsies (TuBx DNA). In parallel, we evaluated whether the selection of peripheral blood lymphocytes (PBLs) expressing a combination of cell-surface receptors, rather than the expression of PD-1 alone, could further enhance the frequency of neoantigen-specific T cells and T-cell receptors (TCR) detected or the number of neoantigens recognized.

To identify circulating tumor antigen-specific T cells, we sorted $CD8^+$ and $CD4^+$ PBLs of ten patients with different types of epithelial cancers based on the expression of PD-1 into $PD\text{-}1^{hi}$, $PD\text{-}1^{dim}$ and $PD\text{-}1^-$, and in combination with the cell-surface receptors CD27,

CD38, CD39, HLA-DR and 4-1BB, obtaining up to 35 $CD8^+$ and 35 $CD4^+$ T-cell populations for some of the patients studied. In parallel, we also expanded TILs from tumor biopsies and compared the reactivities detected in the two T-cell sources. *Ex vivo* expanded PBL subsets and TILs were screened using a personalized high-throughput screening strategy, which enabled the detection of T cells targeting neoantigens identified by WES from TuBx DNA and cfDNA as well as T cells recognizing cancer germline antigens. Using this approach, we detected tumor antigen-specific T cells in eight out of 10 patients analyzed. Both $CD8^+$ and $CD4^+$ tumor antigen-reactive T cells were preferentially enriched in T-cell subsets expressing high levels of PD-1, either alone or in combination with other cell-surface markers, being PD-$1^{hi}CD39^+$ the combination of markers that more consistently identified $CD4^+$ and $CD8^+$ tumor reactivities. More importantly, the frequency of tumor antigen-specific T lymphocytes contained in the $CD8^+$ PD-$1^{hi}CD39^+$ population was consistently higher than in any other $CD8^+$ population sorted. This was not observed in $CD4^+$ PBLs since the frequency of neoantigen-specific T cells was highly variable among PBL populations and none of them consistently displayed higher frequencies of neoantigen-reactive lymphocytes. The selection and expansion of $CD8^+$ PD-$1^{hi}CD39^+$ PBLs outperformed the classical non-specific TIL expansion in high-dose interleukin-2 (IL-2) at identifying anti-tumor $CD8^+$ T-cell responses. In contrast, despite the total number of $CD4^+$ reactivities detected considering all populations screened from blood was higher than in TILs, the $CD4^+$ PD-$1^{hi}CD39^+$ T-cell subpopulation identified fewer reactivities than unselected TILs. When comparing tumor and cfDNA, the overlap between NSMs identified in tumor and cfDNA varied notably between patients, with two out of six patients displaying no overlap between TuBx DNA and cfDNA WES. Moreover, WES of cfDNA from six patients preferentially identified clonal somatic mutations in tumor biopsies and enabled the identification of eight of 13 neoantigens in patients displaying some degree of overlap between tumor and cell-free NSMs. Our results underscore peripheral blood as an alternative source to identify cancer-specific neoantigens and $CD8^+$ and $CD4^+$ neoantigen-specific T lymphocytes and TCRs, with important implications for exploiting personalized T-cell responses in advanced cancer patients.

Resum

La teràpia adoptiva amb cèl·lules T infiltrants de tumor (TILs) ha demostrat capacitat de mediar regressió de lesions tumorals en pacients amb melanoma metastàtic. Estudis retrospectius dels productes cel·lulars utilitzats per tractar pacients que van respondre o no a la teràpia han demostrat que la resposta a la teràpia adoptiva amb TILs va associada a una major expansió de cèl·lules T amb capacitat de reconèixer neoantígens, els quals són pèptids que deriven de mutacions somàtiques no sinònimes (NSMs) específiques del tumor. A més, la teràpia adoptiva amb productes enriquits amb TILs específics contra neoantígens ha demostrat activitat antitumoral en pacients amb diferents tipus de tumors epitelials el que ha promogut l'interès en el desenvolupament de teràpies personalitzades amb limfòcits T reactius contra neoantígens. La identificació i aïllament de limfòcits T reactius contra neoantígens ha sigut possible gràcies als avenços en les tècniques de seqüenciació el que ha permès una ràpida avaluació del repertori mutacional del tumor així com el desenvolupament d'assajos personalitzats per testar el seu reconeixement. Tot i això, la necessitat d'accedir a una biòpsia tumoral tant per identificar els neoantígens candidats com per aïllar els limfòcits T ha limitat l'aplicabilitat de les teràpies personalitzades basades en cèl·lules T i a més a més, pot subestimar la heterogeneïtat tumoral en tumors metastàtics. Estudis previs han demostrat que els limfòcits T reactius contra neoantígens es poden identificar en sang perifèrica a través de la selecció de cèl·lules T amb expressió del receptor de mort programada tipus 1 (PD-1). Tanmateix, la freqüència de cèl·lules T reactives contra neoantígens després de seleccionar els limfòcits T que expressen PD-1 és molt baixa. A més, segueix sent necessària l'obtenció d'una biòpsia tumoral per tal de poder identificar les mutacions no sinònimes del tumor.

En aquesta tesi doctoral hem explorat com a teràpia mínimament invasiva l'ús de sang perifèrica per identificar les NSMs del tumor i per aïllar els limfòcits T específics contra neoantígens o contra altres antígens tumorals en pacients amb càncer de mama, ginecològic, colorectal, de cap i coll o cordoma, tots en estat metastàtic. Per això, hem seqüenciat l'ADN circulant aïllat de la sang per tal d'identificar mutacions que puguin provenir del tumor i les hem comparat amb aquelles identificades en l'ADN extret de biòpsies tumorals dels mateixos pacients. Paral·lelament, hem seleccionat limfòcits de la sang perifèrica en base a l'expressió simultània de diversos receptors de superfície amb l'objectiu de veure si la co-expressió de receptors pot millorar la freqüència de cèl·lules T específiques contra neoantígens o bé incrementar el repertori de receptors de cèl·lules T (TCRs) reconeixent un mateix neoantigen comparat amb l'expressió exclusiva de PD-1.

Per tal d'identificar cèl·lules T reactives contra neoantígens en la sang perifèrica, vam separar per citometria de flux limfòcits CD8 i CD4 de deu pacients amb diferents tipus de tumors epitelials en base al nivell d'expressió de PD-1 en els grups: PD-1^{hi}, PD-1^{dim}, PD-1^{-} i en combinació amb altres receptors de superfície com CD27, CD39, CD38, HLA-DR i 4-1BB, obtenint fins a 35 poblacions diferents tant pels limfòcits CD8 com pels CD4 per alguns dels pacients inclosos en l'estudi. Paral·lelament, també vam expandir els TILs de les biòpsies tumorals d'aquests pacients i vam comparar els neoantígens o antígens tumorals reconeguts per aquestes dues fonts de limfòcits T. Les cèl·lules T de sang perifèrica o infiltrants de tumor es van expandir *ex vivo* i es van testar en assajos funcionals personalitzats el que ens va permetre detectar cèl·lules T amb capacitat de reconèixer neoantígens identificats per seqüenciació de l'exoma tant de l'ADN extret de biòpsies tumorals com de l'ADN circulant i antígens tumorals de línia germinal expressats en la biòpsia tumoral. Utilitzant aquesta aproximació, es van detectar cèl·lules T reactives contra neoantígens en vuit dels deu pacients estudiats. En la majoria dels casos, els limfòcits CD8 i CD4 reactius es van identificar en poblacions que expressaven alts nivells de PD-1 (PD-1^{hi}), sol o en combinació amb altres marcadors, sent PD-1^{hi}CD39^{+} la combinació que identificava limfòcits T reactius contra antígens tumorals de manera més consistent. A més, en els limfòcits CD8^{+}, la població PD-1^{hi}CD39^{+} sempre contenia la freqüència més elevada de limfòcits reactius en el cas que aquests s'haguessin identificat en diferents poblacions separades de la sang. Aquesta darrera observació no aplica pels limfòcits CD4^{+} ja que en aquest cas cap de les poblacions contenia la freqüència més alta de limfòcits T reactius contra neoantígens de manera consistent. La selecció i expansió de limfòcits CD8^{+} PD-1^{hi}CD39^{+} de la sang perifèrica va permetre capturar un major nombre de reactivitats contra antígens tumorals que l'establert sistema d'expansió inespecífica de TILs en presència d'altes dosis d'interleuquina-2 (IL-2). Per altra banda, tot i que el nombre total de reactivitats identificades en les poblacions de limfòcits CD4^{+} aïllades de la sang perifèrica és superior a les identificades en els TILs, la combinació CD4^{+} PD-1^{hi}CD39^{+} identifica menys reactivitats que les detectades en els TILs. Pel que fa a les NSMs identificades en l'ADN tumoral i en l'ADN circulant, vam observar que el nombre de mutacions compartides entre les dues fonts d'ADN era altament variable, essent nul en dos dels sis pacients estudiats.

La seqüenciació d'exoma de l'ADN circulant dels sis pacients va identificar preferencialment mutacions somàtiques clonals en les biòpsies tumorals. També va

permetre la identificació de vuit dels 13 neoantígens detectats en pacients que mostraven un cert grau de solapament entre les NSMs detectades en l'ADN extret de la biòpsia tumoral i l'ADN circulant. En resum, els nostres resultats demostren que l'ús exclusiu de sang perifèrica permet detectar neoantígens i els limfòcits $CD4^+$ i $CD8^+$ capaços de reconèixer aquest tipus d'antígens tumorals el que té implicacions importants pel desenvolupament de teràpies cel·lulars personalitzades en pacients amb tumors avançats.

Introduction

1. Cancer and the T-cell immune response

Tumorigenesis is a multi-step process that can occur in most normal tissues. It is characterized by the progressive accumulation of genetic and epigenetic alterations that drive the gradual transformation of normal cells into malignant cells. Many types of cancer are diagnosed in the human population with an age-dependent incidence.

In the human body, which has more than 10^{14} cells, billions of cells experience mutations every day, which can disrupt their normal behavior. If a mutation confers a selective advantage to one particular cell, this cell will grow and divide slightly more vigorously and survive more readily than its neighbors subsequently becoming a founder of a malignant clone (1). Although this cell likely represents the origin of cancer, its progeny needs to acquire many additional mutations and epigenetic changes to finally drive tumor development and progression, a succession of events that can last many years.

In 2000, the hallmarks of cancer were proposed as a set of functional capabilities acquired by human normal cells during the process of malignant transformation that appeared to be critical for the onset of malignant tumors (2). Although only six

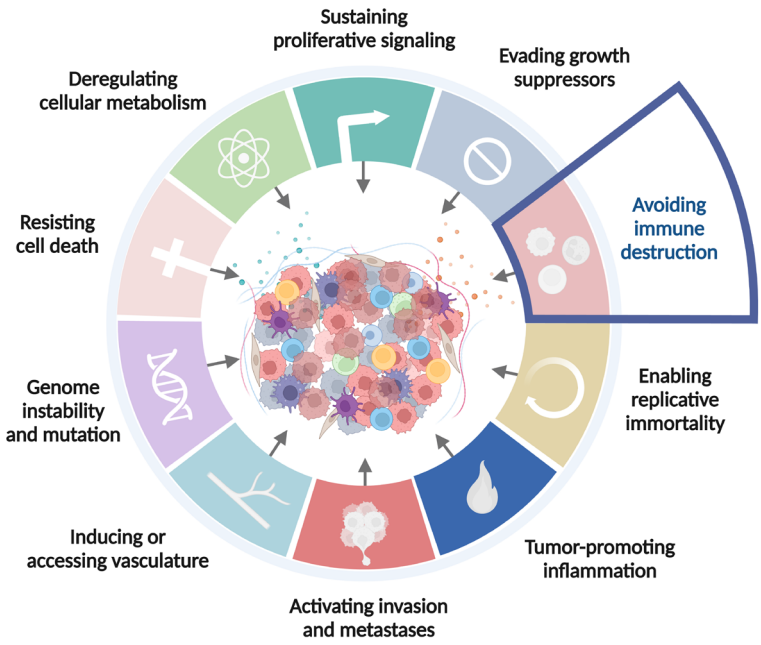

Figure 1. Current validated Hallmarks of Cancer. The eight core hallmarks of cancer and two enabling factors. Image adapted from Hanahan, 2022. Image created with BioRender.com.

distinct hallmarks of cancer were proposed at that point, the increased knowledge on the complexity of cancer pathogenesis over the years has expanded the number of recognized capabilities and enabling characteristics known to dictate malignant growth. In 2011, Hanahan and Weinberg introduced genome instability and tumor-promoting inflammation as enabling characteristics and the deregulation of cellular metabolism and the evasion of the immune system as emerging hallmark capabilities that have finally been postulated as core hallmarks of cancer 11 years later (3,4) (Figure 1).

The concept that the immune system plays a crucial role in preventing neoplastic cells from developing into tumors was proposed more than one century ago (5). This theory was further supported by Lewis Thomas in 1959 that suggested that the immune system could sense and eliminate neoplastic cells through the recognition of something foreign displayed at their surfaces that indicated their alien nature (6). Some years later, Burnet also claimed that tumor cell antigens induced an immunological reaction against cancer and formulated the concept of immune surveillance (7).

The concept of cancer immunosurveillance proposes that cells and tissues are constantly monitored by the immune system and that such immune surveillance is responsible for recognizing and eradicating most of the arising tumors. Although many experiments were pursued to validate this hypothesis, there was initially certain skepticism towards this concept because of a study with immunodeficient athymic nude mice that did not develop a significantly higher number of spontaneous tumors than control mice (8). Nevertheless, the demonstration that the lack of interferon-γ (IFN-γ) or perforin, two key immunologic molecules, enhanced the susceptibility to both chemically-induced and spontaneous tumors evidenced that components of the immune system were involved in controlling primary tumor development and further supported the immunosurveillance theory (9–11). The definitive evidence supporting the existence of a cancer immunosurveillance process and that showed it depends on lymphocytes was derived from experiments using mice in which the recombinase activating gene-2 (RAG-2) was selectively inactivated (12). Since this recombinase is involved in the repair of double-stranded DNA breaks and is exclusively expressed in the lymphoid compartment, RAG-2-deficient mice could not rearrange lymphocyte antigen receptors and subsequently lack T, B and natural killer (NK) T cells. The results of this study unequivocally showed that lymphocytes protect the host against the development of tumors, as RAG-2-deficient

mice developed chemically induced tumors more rapidly and in a greater frequency than genetically matched wild-type controls.

In addition to mice studies, epidemiologic studies of immunosuppressed transplant patients and of individuals with immunodeficient conditions showed a significantly higher risk for developing cancer, many of them of viral origin (13–17). This demonstrated the existence of cancer immunosurveillance in humans and further supported its key role in controlling tumor growth.

Nevertheless, why tumors were able to arise in healthy individuals despite immunosurveillance was still an unanswered question. Multiple studies demonstrated that tumors derived from mice having a certain immunodeficiency were more immunogenic than those arising in immunocompetent mice (12,18–21). Based on these findings, the immune system was postulated to not only protect the host from cancer disease but also to shape newly arising tumors, which led to the concept of cancer immunoediting (14).

Cancer immunoediting was proposed as a framework to integrate the dynamic process by which the immune system controls and sculpts cancer and has been divided into three phases (14) (Figure 2). It all starts with the elimination phase, in which the immune system can successfully eradicate the nascent tumor. If this is the case, it

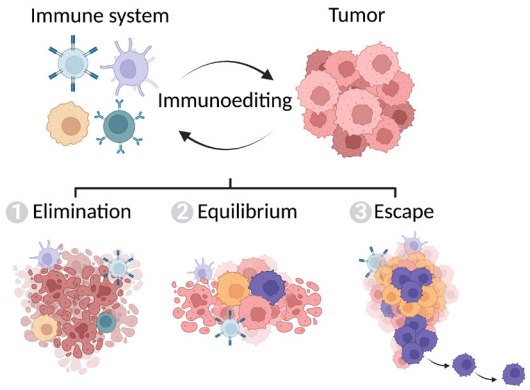

Figure 2. The cancer immunoediting process. Cancer immunoediting is a framework that integrates the dynamic process by which the immune system controls cancer. It consists in three phases. The first phase is elimination, in which the immune system acts and successfully destroys the emerging tumor. The second phase is equilibrium, in which the immune system can restrain tumor growth, but the tumor is not fully eliminated. Further immunologic sculpting of the tumor (resistant tumor clones) and establishment of a suppressive microenvironment leads to the escape phase, in which cancer becomes a clinically apparent disease and spreads to other organs forming metastatic tumor lesions. Image adapted from Gubin & Vesely, 2022. Image created with BioRender.com.

represents the complete editing process without going through the subsequent phases. If, however, the immune system fails to eliminate all cancer cells, the surviving cells and the immune system enter the equilibrium phase, in which the immune system can restrain the growth but not fully eliminate the tumor. Finally, surviving tumor cells that can no longer be targeted by the immune system due to acquired insensitivity to immunologic detection enter the escape phase, in which they accumulate genetic/epigenetic changes that confer them the potential to grow in an uncontrolled manner, subsequently forming clinically detectable tumors (13,14). The concept of cancer immunoediting has been widely accepted and it is currently thought to also occur during immunotherapy in human patients with cancer (22).

1.1. Antigen recognition by T cells

Conventional T lymphocytes recognize peptides bound to the major histocompatibility complex (MHC), also known as human leukocyte antigens (HLA), on the surface of target cells through their T-cell receptors (TCRs) (23). The peptide sequences that are recognized are called "epitopes", while their parent proteins are referred to as "antigens". In the context of cancer, these proteins are also known as tumor antigens.

T cells fall into two major classes that are distinguished by the expression of the cluster of differentiation (CD) markers CD8 and CD4. These two types of T cells exert different effector functions and recognize cognate epitopes in a different manner (1). On one hand, $CD8^+$ T cells recognize short peptides, typically eight to ten amino acids in length, that are derived from cytoplasmic proteins partially digested via proteasome and presented on the cell-surface of HLA-I molecules (Figure 3, left). On the other hand, $CD4^+$ T cells recognize longer peptides, which typically are 12-20 amino acids long, that derive from extracellular proteins previously endocytosed and delivered to endosomes and that are loaded and presented on the cell-surface on HLA-II molecules (Figure 3, right).

HLA-I and HLA-II molecules have distinct structures and are differentially expressed among different cell types, also reflecting the distinct effector functions of the T cells that recognize them. Almost all our nucleated cells express HLA-I constitutively, which present peptides to $CD8^+$ effector T cells that are specialized in killing any cell that they specifically recognize. In contrast, HLA-II expression is mainly expressed by antigen-presenting cells (APCs) although endothelial cells and some epithelial cells may

also express HLA-II under inflammatory stimuli. Tumor cells or other cell types can also express it upon stress or inflammation (24). In this case, peptides bound to MHC-II are presented to $CD4^+$ T cells whose main function is to activate other immune cells and help amplifying a potent immune response. The distinction between antigen-processing pathways for loading peptides on HLA-I and HLA-II molecules is not absolute and certain subsets of professional APCs, mainly dendritic cells (DCs), can present peptides derived from the phagocytosis of infected or malignant cells in the context of HLA-I, a process also known as cross-presentation.

T-cell-mediated immune responses are antigen specific. Thus, in order to protect the host from any infection or malignancy, a wide variety of TCRs recognizing distinct antigens need to be generated. During T-cell development, an extraordinarily high diversity (in the order of 10^{12} to 10^{15}) of TCRs are randomly generated in the thymus by somatic recombination of TCR genes, which are capable of recognizing virtually any pathogen but also self-antigens (25). Because of this, T cells need to undergo a process called central tolerance in which a broad representation of the self-proteins expressed in the body are potentially presented to immature T cells, which die by apoptosis upon strong TCR signaling. This leads to the elimination of a large proportion of self-reactive T-cell clones, which reduces the possibilities of T cells mounting an immune response upon recognition of host's own molecules and cells (26).

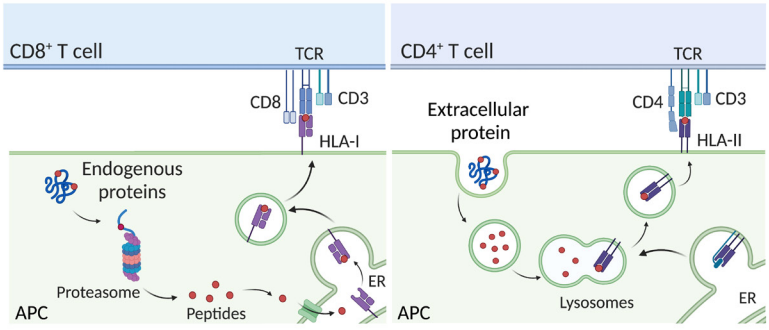

Figure 3. Antigen recognition by $CD8^+$ and $CD4^+$ T lymphocytes. $CD8^+$ and $CD4^+$ T cells recognize peptides bound to HLA molecules on the surface of target cells through their TCRs. On one hand, $CD8^+$ T cells recognize short peptides that are derived from cytoplasmic proteins partially digested via proteasome and presented on HLA-I molecules. On the other hand, $CD4^+$ T cells recognize longer peptides derived from extracellular proteins previously endocytosed that are loaded and presented on HLA-II molecules. Endoplasmic reticulum (ER). Image adapted from "MHC class I and II Pathways" by BioRender.com (2020).

Nevertheless, some self-reactive T cells escape and migrate to the periphery, because certain self-antigens are not expressed in the thymus and also because the threshold of affinity determining negative selection is variable and not totally forbidding. Because of this, peripheral tolerance mechanisms exist, which are also crucial to control tolerance of lymphocytes that first encounter their self-antigen outside the thymus. Despite this strict control during T-cell development, spontaneous T-cell responses recognizing self-proteins can be detected in certain autoimmune pathologies and in cancer patients, indicating that a fraction of T cells recognizing normal self-antigens escape the process of immunological tolerance.

In addition to conventional T lymphocytes, also known as αβ T cells based on their TCR composition, other types of lymphocytes can also mediate anti-tumor responses. This includes NK cells and a small population of T cells, known as γδ T lymphocytes, which can have anti-tumor activity that is via non-conventional HLA antigen presentation (27,28). Although they also participate in mounting an effective anti-tumor immune response, we will not develop their role further as it is not within the scope of this thesis.

1.2. Tumor antigens

Tumor antigens are defined as proteins expressed by tumor cells that are presented on HLA-I and HLA-II molecules and that can trigger a T-cell response. Since T cells recognizing tumor antigens can mediate tumor regression and are at the core of cancer immunotherapies, identifying tumor antigens and the T cells targeting them is of great interest in the field.

Although the involvement of the immune system in tumor rejection was demonstrated more than 50 years ago, it was not until 1989 that the molecular nature of some of the antigens expressed by tumors and recognized by cytotoxic T lymphocytes was discovered. In this pioneering study, Lurquin *et al.* identified a peptide that differed from the wild-type protein by a single-point mutation, which made it susceptible to T-cell recognition (29). Although this antigen was identified in mouse P815 tumor cells, the first human tumor antigen recognized by naturally occurring T cells was detected only two years later (30). Since then, many studies have been focused on their identification to exploit them therapeutically.

Tumor antigens have been classically categorized into two main groups based on

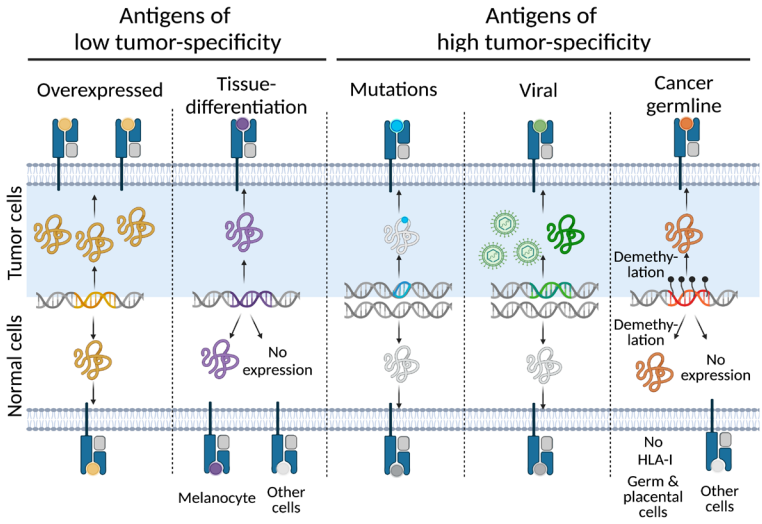

Figure 4. Classification of human tumor antigens. Expression and HLA-I presentation in tumor (top) and normal cells (bottom) of antigens with low or high-tumoral specificity are depicted from left to right, respectively. Antigens with low tumoral specificity include antigens overexpressed in tumor cells compared to normal cells and antigens derived from proteins involved in the differentiation of the specific tissue from which each tumor originates. Antigens with high tumoral specificity include antigens derived from tumor-specific mutations, viral proteins and cancer germline antigens. The latter are exclusively expressed in germline cells and tumor cells as a result of gene demethylation, but are not presented on the cell surface of germline cells due to the lack of HLA-I molecules. Adapted from Coulie *et al.*, 2014. Image created with BioRender.com.

their tumoral specificity (Figure 4): 1) antigens of low tumoral specificity, also known as tumor-associated antigens, which are mainly characterized by also being expressed, albeit at lower levels, in normal cells and 2) antigens of high tumoral specificity, also known as tumor-specific antigens, whose expression is restricted to tumor cells (31).

1.2.1. Antigens with low tumoral specificity

This group includes antigens encoded by non-mutated self-genes that are overexpressed in tumors but can also be expressed by normal cells. More specifically, it comprises differentiation antigens and antigens derived from proteins that are overexpressed in the tumor.

Differentiation antigens are expressed in tumor cells and in the differentiated normal tissue from which the tumor originated (Figure 4). In the literature, naturally occurring T cells recognizing differentiation antigens have been well documented in

patients with melanoma, which frequently target antigens derived from the proteins Tyrosinase (32), Melanoma antigen recognized by T-cells 1 (MART-1) (33) and gp100 (34). In addition, the prostate also expresses differentiation antigens such as prostate-specific antigen (PSA) and prostatic acid phosphatase (PAP), which are absent from other healthy tissues and spontaneous T-cell responses against them have also been described (35,36).

Overexpressed antigens are derived from normal genes that are constitutively expressed in multiple healthy tissues but have a higher level of expression in the tumor (Figure 4). T-cell responses against overexpressed antigens have been described in different tumor types. For instance, T cells recognizing the oncogene ERBB2 (also known as HER2), which is overexpressed in many epithelial tumors including ovarian and breast carcinomas, or the transcription factor Wilms' tumor protein (WT1), which is more highly expressed in leukemic cells than in normal cells, have been identified (37,38).

The fact that tumor antigen-specific T cells targeting these low tumor-specific antigens have been described indicates that central tolerance is not complete. However, only low-affinity TCRs are expected to be found since high-affinity TCRs against normal cellular proteins are usually eliminated during negative selection in the thymus.

1.2.2. Antigens with high tumoral specificity

This group comprises antigens that are not expressed by normal cells, which can be derived from mutations, viral proteins and cancer germline antigens.

Mutations accumulate during the process of carcinogenesis and can encode for mutated proteins, also known as neoantigens. These antigens emerge as a result of genomic alterations that are not present in the germline DNA and are therefore unique to malignant cells. In the exome, these alterations can be derived from multiple types of alterations including single nucleotide variants (SNVs), nucleotide insertions or deletions (indels) and gene fusions that generate new antigenic peptides by changing one amino acid, altering the phase of the reading frame, extending the coding sequence beyond the normal stop codon or by generating new DNA arrangements.

Neoantigens have also the advantage of being non-self antigens and thus, are more immunogenic. This is because T cells targeting them are not subjected to central tolerance and therefore are more frequently detected in periphery, since TCRs targeting them have not been depleted.

However, their variable expression within tumors and between primary lesions and metastasis in the same patient represents a daunting challenge for therapeutic strategies that aim at targeting them. Moreover, the majority of neoantigens arise from passenger mutations and are typically private for each patient (39). Only a small fraction of such antigens are shared across patients, also known as public neoantigens. These neoantigens are frequently localized in specific positions of oncogenic driver genes known as hotspot driver mutations (40).

A subset of cancers arises as a result of viral infection that can result in the expression of viral proteins that drive the oncogenic transformation (Figure 4). These oncogenic virus-derived antigens are not patient-specific and are shared by tumors of the same type. For instance, human papillomavirus (HPV) is associated with a subset of head and neck (H&N), cervical, penile and anal cancers that express oncoproteins (*e.g.* E6 and E7) that can be recognized by patients' T cells (41). This has also been shown for other virus-driven solid cancers, including Merkel cell carcinomas resulting from polyomavirus infection (42) and nasopharyngeal carcinomas that result from an Epstein-Barr virus (EBV) infection (43).

Lastly, cancer germline antigens are derived from non-mutated self-genes that are expressed during fetal development. These genes are epigenetically silenced in most normal adult tissues. Although they are expressed on germ cells and placental trophoblast, these cells do not express HLA class I and II molecules. Therefore, the presentation of cancer germline antigens on the cell surface of normal adult cells is generally lacking (Figure 4). As a result of DNA demethylation, cancer germline antigens can be re-expressed in multiple tumor types and naturally occurring T cells targeting them have been frequently observed in a variety of cancers (30,44).

1.3. Cancer immunity cycle

To develop an anti-cancer immune response that leads to effective killing of tumor cells, a series of stepwise events must be initiated and consecutively followed until complete tumor rejection. This process has been designated as the cancer immunity cycle (Figure 5) (45).

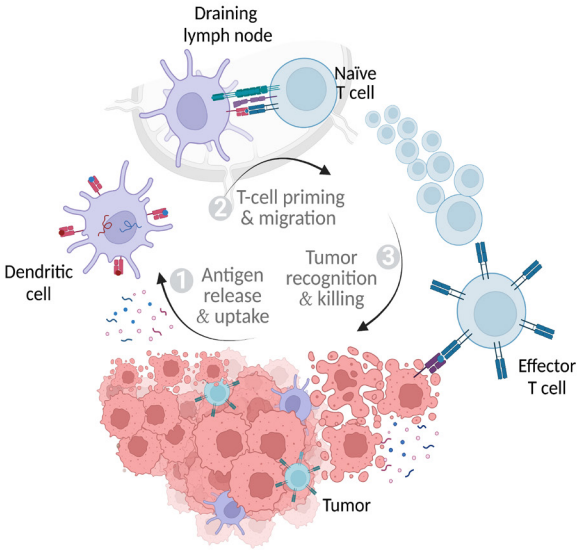

Figure 5. Cancer immunity cycle. (1) The first step comprises the release of tumor antigens that are captured by DCs and subsequently processed and cross-presented on HLA-I. (2) Next, these APCs migrate to lymph nodes where they interact with naïve $CD8^+$ T cells resulting in the priming and activation of effector T cells that recognize tumor-specific antigens. The stimulated T cells proliferate and differentiate into effector $CD8^+$ T cells, leave the lymph nodes and migrate to the tumor. (2) Activated effector T cells specifically recognize and kill tumor cells that are presenting their cognate antigen on HLA-I. This leads to the release of additional tumor antigens that increase the breadth and depth of the response in subsequent rounds of the cycle. Adapted from Chen & Mellman, 2013. Image created with BioRender.com.

The first step of the cycle comprises the release of tumor antigens expressed by tumor cells that are captured, processed and presented on HLA molecules by DCs. Thereafter, these APCs migrate to lymph nodes where they interact with naïve T cells resulting in the priming and activation of effector T cells that respond to tumor-specific antigens. At this point of the cancer immunity cycle, it is essential that DCs that have internalized tumor antigens cross-present such peptides on HLA-I molecules to prime naïve $CD8^+$ T cells (46). Moreover, for efficient priming of such T cells, the presentation of tumor antigens must be accompanied by co-stimulatory signals. Otherwise, naïve $CD8^+$ T cells may be tolerized instead of activated (47). Therefore, some subsets of DCs, which have the capability to cross-present and that express co-stimulatory molecules, play a key role in this step of the cycle. The activated effector $CD8^+$ T cells subsequently migrate to the tumor bed where, after specifically recognizing their cognate antigen, will mediate tumor cell killing. Additional tumor antigens will be released as a consequence of tumor cell death, a process generally known as antigen spreading, which may lead to the

expansion of the immune response by gaining breadth and depth in subsequent rounds of the cycle.

In cancer patients, this cycle is not functioning optimally, which leads to the formation of tumors. Each step of this cycle can be subjected to immune-modulatory mechanisms that facilitate the escape of tumor cells from immune pressure. This includes environmental factors that influence the efficacy of T-cell priming, infiltration and effector function. In addition to the production of soluble factors that modulate the tumor microenvironment and the downregulation of components of the antigen-presenting machinery by tumor cells to evade T-cell recognition, the local expression of inhibitory molecules also reduces T-cell function. Moreover, immune cells with immunosuppressive functions, including regulatory T cells and myeloid derived suppressor cells (MDSCs), are also recruited to the tumor site where they inhibit the action of effector T cells both by direct contact or by the production of soluble factors (48).

Together, these signals and immunosuppressive cells shape the states of intratumoral T cells, leading to the diverse spectrum of phenotypes and functionalities that can be observed at the tumor site and that determines the efficacy of anti-tumor T-cell responses.

1.4. T-cell activation and exhaustion

Upon recognition of their cognate antigen, T cells clonally expand and upregulate an array of co-stimulatory and co-inhibitory molecules that can either promote or inhibit T-cell activation and effector functions. In a setting of an acute infection, T cells downregulate the activation program of effector cells upon antigen clearance, which includes the downregulation of co-stimulatory/co-inhibitory molecules and only a small proportion of T cells survive and persist in the form of memory T cells. These T cells can persist overtime without the presence of the antigen and can rapidly and effectively mount a T-cell response upon re-infection (49,50).

In contrast, in the context of chronic infection and cancer, persistent exposure to antigens induces progressive changes in tumor antigen-specific T cells leading to a dysfunctional state. This state, also known as T-cell exhaustion, is characterized by the progressive and hierarchical loss of effector functions and proliferative capacity, the upregulation and sustained expression of co-inhibitory receptors and changes in

epigenetic, transcriptional and metabolic programs, which differ from those observed in effector and memory T cells (51). Moreover, dysfunctional T cells lose the homeostatic capacity to persist in an antigen-independent manner as memory T cells do.

T-cell exhaustion was first described in the context of chronic viral infections in lymphocytic choriomeningitis virus (LCMV)-infected mice (52,53). In these studies, virus-specific $CD8^+$ T cells showed a dysfunctional state and were not able to efficiently mediate viral pathogen clearance. Shortly after, a similar dysfunctional state was described in humans with chronic infections as human immunodeficiency virus (HIV) (54,55) and in cancer (56,57). In both mice and humans, intratumoral T cells frequently display characteristics associated with T-cell dysfunction. More importantly, this T-cell phenotype has been widely associated with tumor specificity (58,59), which underlines the relevance of dysfunctional T cells in anti-tumor immunity.

Although the precise definition of T-cell exhaustion is still under debate (60), this dysfunctional T-cell state is commonly understood as a progressive and stepwise process that can culminate in the physical deletion of antigen-specific T cells (Figure 6). Thus, T-cell dysfunction is not a binary but rather a gradual state that englobes T-cell populations with a remarkable phenotypic and functional diversity. Various combinations and levels of inhibitory and co-stimulatory receptors such as programmed cell death-1 (PD-1), T-cell immunoglobulin and mucin-domain containing-3 (TIM-3), Cytotoxic T-lymphocyte antigen 4 (CTLA-4), Lymphocyte-activation gene 3 (LAG-3), ectonucleoside triphosphate diphosphohydrolase 1 (CD39) and 4-1BB (also known as CD137) have been observed in intratumoral T cells displaying characteristics of dysfunction. Moreover, whilst IL-2 production is one of the first effector functions that is lost followed by tumor necrosis factor-α (TNF-α), the ability to produce IFN-γ is only impaired in most terminal stages of exhaustion (57,61). In the same line, recent single-cell transcriptome analysis of intratumoral T cells have distinguished between two T-cell populations with distinct transcriptional signatures but both bearing hallmarks of exhaustion, further supporting T-cell exhaustion as a gradual state (58,62) (Figure 6). This detailed characterization of single-cell transcriptomes led to the distinction between a less exhausted T-cell subset that maintained the ability to proliferate, also called progenitor or stem-like exhausted population and a highly exhausted population also called terminally-exhausted. Whilst progenitor exhausted T cells express high levels of co-stimulatory and low levels of co-

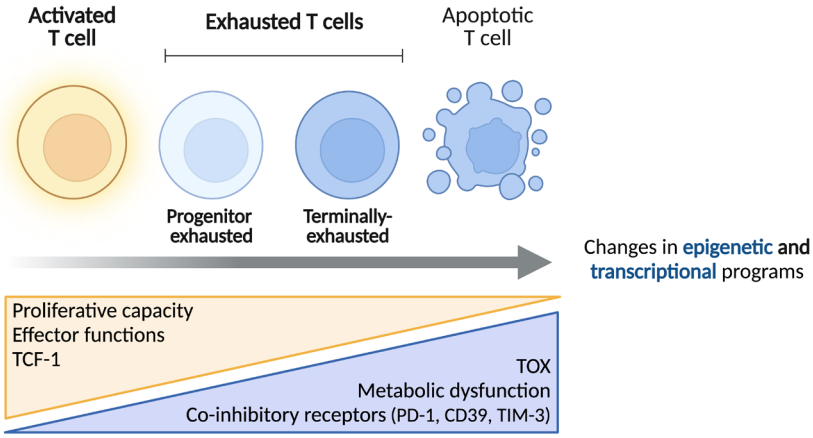

Figure 6. T-cell exhaustion is a progressive and stepwise process. Activated T cells that are persistently exposed to their cognate antigen can differentiate along a wide range of exhaustion states associated with different transcriptional and epigenetic programs and with the progressive loss of proliferative and functional capacity. These differential exhausted states span from progenitor-exhausted T cells to terminally-exhausted T cells that can ultimately undergo apoptosis due to overstimulation. Adapted from Chow *et al.*, 2022. Image created with BioRender.com

inhibitory receptors, terminally-exhausted T cells expressed high levels of multiple co-inhibitory receptors (*e.g.* PD-1, CD39, TIM-3) and produce granzyme molecules. These two populations also differ in their transcriptional program. More specifically, progenitor exhausted T cells express high levels of the transcription factor TCF-1 whereas terminally-exhausted T cells mainly express TOX, a transcription factor known to activate exhaustion programs (Figure 6). Of note, the progenitor exhausted T-cell population has been demonstrated to be particularly important for a durable response to immune checkpoint blockade (ICB) therapy (62,63). These findings together with the clinical success of ICB treatment support that T-cell exhaustion is not an irreversible terminal differentiation state. Rather, exhausted T cells, or at least a subset of them, can be reinvigorated by releasing the breaks that restrain their effector functions enabling to mediate anti-tumor immune responses.

1.4.1. Co-stimulatory, co-inhibitory, activation and exhaustion markers associated with TCR-triggered T-cell activation

Analyses of T cells from chronic infection and cancer have proven that the dysfunctional T-cell phenotype, characterized by an increased expression of co-

stimulatory and co-inhibitory molecules, is mainly observed in virus-specific or tumor-reactive T cells. Although the expression of many co-stimulatory and co-inhibitory receptors has been described to identify such virus- or tumor antigen-specific T cells, this section will be exclusively focused on describing those cell-surface receptors that have been further investigated in this thesis (Figure 7).

Given the parallelism between chronic viral infections and cancer, several markers expressed on antigen-specific activated T cells initially identified in the context of chronic infection have subsequently been demonstrated to be also expressed by tumor-reactive T lymphocytes.

One of such markers is **PD-1**, which is a co-inhibitory receptor that is expressed upon T-cell activation to prevent hyperactivation and autoimmunity by modulating T-cell responses. PD-1 exerts its suppressive functions upon engagement to its ligands, programmed death-ligand 1 and 2 (PD-L1 and PD-L2), inhibiting the activation of naïve and the effector T cells in multiple ways. PD-1 signals can decrease T-cell proliferation, IL-2 production and Bcl-xL expression. Moreover, it can inhibit master regulators of T-cell differentiation such as GATA-3, T-bet and Eomes subsequently controlling cell fate. PD-1 can also limit effector cell functions of committed effector $CD4^+$ and $CD8^+$ T cells, by reducing cytokine production and cytotoxic capacity (64).

Two other markers initially identified in the context of viral infection are the T-cell activation markers **CD38** and **HLA-DR**. CD38 is an ectoenzyme that regulates the

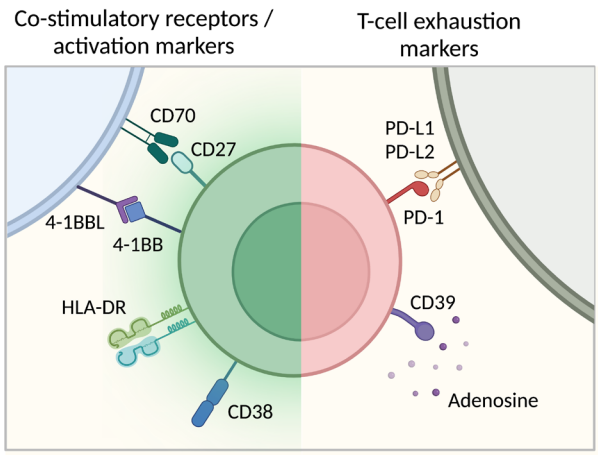

Figure 7. Activation and exhaustion markers associated with antigen-specific T lymphocytes.

Schematic overview of co-stimulatory, co-inhibitory and activation markers expressed on T lymphocytes and their ligands on APCs or tumor cells. Image created with BioRender.com.

production of NAD^+ and is naturally expressed by multiple immune cell types including DCs, macrophages, neutrophils, B and T lymphocytes and very distinctly in plasma cells. HLA-DR is involved in class II antigen presentation and is typically expressed by APCs, although its expression can be upregulated in other cell types upon stimulation. The expression of both CD38 and HLA-DR has been shown to identify human effector viral-specific $CD8^+$ T cells induced by vaccination (65).

CD27 is a co-stimulatory molecule of the TNF receptor family that is expressed in the lymphoid lineage, including NK, B and T cells and DCs. Upon binding to its ligand, CD70, CD27 signaling can lower the threshold of the TCR response to low-affinity antigens while enhancing proliferation and survival and promoting T-cell differentiation (66). Although CD27 expression has not been described to specifically identify virus- or tumor antigen-specific T lymphocytes, the engagement of CD27:CD70 has been shown to be essential for the efficient priming of $CD8^+$ T cells and effective anti-tumor immune responses in murine models (67–69).

Another member of the TNF receptor family is **4-1BB**, also known as CD137, which is an inducible co-stimulatory receptor transiently expressed on recently activated T cells and NK cells. Upon 4-1BB expression and engagement with its ligand, 4-1BBL, it promotes T-cell proliferation and survival and enhances cytokine secretion and T-cell effector functions.

Lastly, another cell-surface receptor whose expression on T cells has been linked to T-cell dysfunction is **CD39**. CD39 is an ectonucleotidase that catalyzes the conversion of ATP to AMP, which is subsequently converted to adenosine by another ectonucleotidase, CD73. Given that adenosine has been widely described as an immunosuppressive metabolite, the activity of CD39 together with CD73 can shift ATP-driven pro-inflammatory immune cell activity towards an anti-inflammatory state, inhibiting T-cell effector functions (70). CD39 is expressed by various immune cells, including macrophages, neutrophils and T cells, especially $CD4^+$ regulatory T cells (71). CD39 was described for the first time as a marker of T-cell exhaustion in chronic infection (72). In recent years, CD39 expression in $CD8^+$ T cells has also been associated with a terminally-exhausted signature and with tumor antigen specificity, enabling the distinction of tumor-reactive T cells from other

tumor-infiltrating bystander T cells (58, 73-75).

The fact that a fraction of tumor-infiltratin lymphocytes (TILs) commonly displays an exhausted phenotype that has been broadly associated with tumor specificity prompted the development of a wide range of immunotherapeutic strategies. These strategies aim at either reinvigorating the effector functions of those naturally occurring tumor-specific T cells or generating novel T-cell responses that could mediate anti-tumor immune responses.

2. Cancer immunotherapies

Cancer immunotherapy has revolutionized the field of oncology and is now achieving unprecedented bench-to-bedside clinical success. This area of immunological research has been highly active for the past 50 years and different modalities of cancer immunotherapies attempting to mobilize the immune system to recognize and kill cancer cells have been developed (Figure 8). In most of these immunotherapeutic strategies, T lymphocytes and their capacity for antigen-directed cytotoxicity have become the central focus for engaging the immune system in the fight against cancer. Thus, immunotherapies can be divided into two groups depending on if they aim to reinvigorate the naturally occurring anti-tumor immune response (*i.e.* interleukin-2 (IL-2), immune checkpoint inhibitors and co-stimulatory agonists, bi-specific antibodies or adoptive cell transfer (ACT) with TILs) or to generate *de novo* T-cell responses (*i.e.* ACT with chimeric antigen receptor (CAR) T cells, TCR-engineered T cells and vaccines).

2.1. IL-2

The systemic administration of IL-2 was the first effective immunotherapy applied in clinical trials and provided evidence that manipulation of the human immune system could reproducibly lead to durable tumor regressions (76).

This cytokine was identified in 1976 as a T-cell growth factor produced by lymphocytes cultured in media containing phytohemagglutinin (PHA) that, when continuously supplied, could sustain the growth of T lymphocytes *in vitro* (77). A decade later, the first proof-of-concept study with recombinant human IL-2 was performed and demonstrated that the administration of high doses of this cytokine mediated tumor regression in patients with solid tumors, including melanoma and renal cell carcinoma

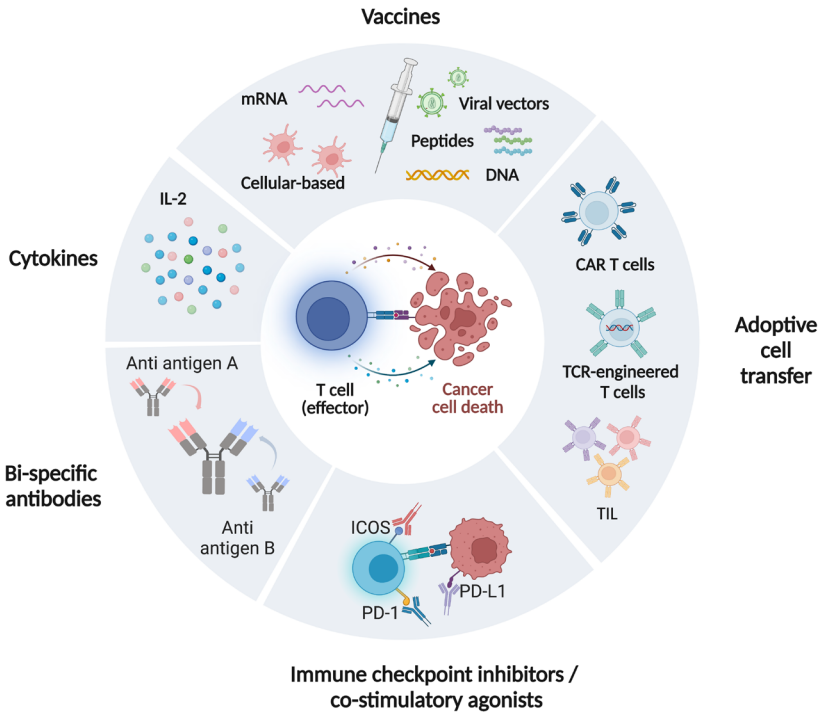

Figure 8. Cancer immunotherapies. Schematic overview of different modalities of cancer immunotherapies that have been developed attempting to mobilize the immune system to kill cancer cells. Most of these strategies are focused on T lymphocytes and their ability of antigen-directed cytotoxicity and can either aim at reinvigorating naturally occurring tumor-reactive T cells or generating *de novo* T-cell responses. Image created with BioRender.com.

generally reversible. These encouraging results led to an explosion of studies utilizing IL-2 in metastatic cancer patients (79,80). However, only rare responses were observed in patients with other tumor types. High-dose IL-2 was approved by The US Food and Drug Administration (FDA) for the treatment of metastatic renal cell carcinoma and metastatic melanoma in 1992 and 1998, respectively (76).

2.2. Immune checkpoint inhibitors and co-stimulatory agonists

Upon TCR engagement, T cells become activated, proliferate and start expressing inhibitory molecules to attenuate T-cell activation and prevent an unduly prolonged T-cell response that could potentially damage normal cells. As explained in section 1.4, the persistent exposure to antigens induces the continuous expression of these inhibitory molecules leading T cells into a dysfunctional state (51,81). These inhibitory molecules and the pathways involved are known as immune checkpoint receptors and are the main

targets of ICB therapies.

Immune checkpoint inhibitors are designed to interrupt inhibitory signals of T-cell activation to reinvigorate the anti-tumor immune response. Since many immune checkpoints are initiated by ligand-receptor interaction, they can be blocked by antibodies or modulated by recombinant forms of ligands or receptors. The first blocking antibody that demonstrated a survival benefit for patients with metastatic melanoma was Ipilimumab, a blocking antibody directed against the inhibitory receptor CTLA-4 (82). This blocking antibody was the first immune checkpoint inhibitor approved by the FDA in 2011 for the treatment of advanced melanoma patients. Subsequently, antibodies blocking the immune checkpoint PD-1 and its major ligand PD-L1 showed great promise in treating many diverse cancer types (83).

Despite the promising results observed in the clinic, most patients do not show long-lasting responses and several tumor types are refractory to this type of immunotherapy. Thus, a better understanding of the mechanism of action of PD-1 and CTLA-4 blockade would be important to explain the differences observed between patients regarding treatment efficacy (84).

So far, CTLA-4 and PD-1 are the two immune checkpoints most widely exploited therapeutically (85). These have led to a new array of treatment options available for patients with metastatic tumors. There are currently nine FDA-approved checkpoint inhibitors, covering more than 50 cancer indications (83). Although remarkable progress has been achieved with immune checkpoint inhibitor monotherapies, especially in melanoma, improving its efficacy across tumor types is an urgent clinical need. Since a primary resistance mechanism is the compensatory upregulation of additional immune checkpoint molecules, several strategies combining targeting of inhibitory (such as LAG-3, TIM-3, TIGIT, VISTA) and activation molecules (such as ICOS, OX40, GITR, 4-1BB, CD40) are currently being tested in clinical trials, some of them showing promising results (86). Moreover, the combination of anti-LAG-3 and anti-PD-1-blocking antibodies, relatlimab and nivolumab, has recently received the FDA approval for the treatment of adult and pediatric patients with unresectable or metastatic melanoma (87).

Nevertheless, there is still much to be learnt about how co-stimulatory and inhibitory molecules modulate T-cell activation, which would be critical for the development of novel approaches and continued improvement of immunotherapeutic

strategies.

2.3. Bi-specific antibodies

Bi-specific antibodies represent another immunotherapeutic strategy that aims at re-directing immune cells to the tumor (Figure 8). These are antibodies that are engineered to simultaneously bind to two different antigens, one typically expressed on tumor cells and the other on immune cells with the aim of bringing tumor cells and immune cells to close proximity to facilitate tumor cell killing. Thus far, the type of bi-specific antibodies that has dominated the cancer immunotherapy field are T-cell engaging bi-specific antibodies (T-biAbs), focused on activating T cells. The majority of T-biAbs use an anti-CD3 antibody fragment as a T-cell engaging arm, which triggers the activation of the signaling cascade of the TCR complex and mediates the formation of an immunologic synapse thereby promoting tumor cell lysis. This represents an advantage over immune checkpoint inhibitors since it circumvents the HLA restriction of the TCR to overcome immune escape.

The original concept of an antibody with two different antigen-binding sites was described over 60 years ago (88). However, it was not until 2014 that the first bi-specific antibody, which binds to CD3 and CD19, Blinatumomab, received FDA approval for the treatment of Philadelphia chromosome-negative relapsed or refractory B-cell precursor acute lymphoblastic leukemia (R/R ALL). The approval was supported by data from a clinical study in which 43% of patients treated showed complete regression (89).

Although the first bi-specific antibodies to reach patients have demonstrated clinical efficacy in the treatment of hematologic malignancies, the responses observed in solid tumors are scarce and no bi-specific antibodies have been approved for the treatment of this type of tumors so far. Novel bi-specific antibodies targeting two molecules expressed on the same cell are being investigated. This is the case of a bi-specific antibody that binds to PD-1 and the IL-2 receptor (IL-2R) on the same cell, which allowed the specific delivery of enhanced IL-2R agonism to PD-1$^+$ antigen-experienced T cells (90). The use of this bi-specific antibody led to the expansion of a highly proliferative and cytotoxic CD8$^+$ T-cell population that was associated with more potent anti-viral and anti-tumor responses. Moreover, it was recently shown to mediate tumor regression in a mouse model of pancreatic neuroendocrine cancer, a type of tumor that is resistant to ICB

treatment and other immunotherapies (90,91).

2.4. Vaccines

The large experience in producing preventive vaccines for pathogens has been used to develop therapeutic anti-tumor vaccines to treat cancer patients. Cancer vaccines aim to induce and amplify anti-tumor T-cell responses through active immunization of cancer patients to treat growing tumors. More specifically, they aim at boosting pre-existing $CD8^+$ and $CD4^+$ T-cell responses and also to activate and prime naïve T cells through the effective presentation of tumor antigens by APCs (92).

Early therapeutic vaccines for treating tumors were focused on the delivery of antigens that are aberrantly but not exclusively expressed by tumor cells and many clinical trials had been carried out targeting melanoma-differentiation antigens such as MART-1, gp100 or tyrosinase, cancer germline antigens such as NY-ESO-1, MAGE-A1 or MAGE-A3 or overexpressed antigens such as Her2/neu or PSA (93–96). In 2012, the first autologous therapeutic cancer vaccine was approved for the treatment of metastatic prostate cancer (97). This vaccine consisted in delivering autologous APCs previously incubated with a fusion protein of granulocyte-macrophage colony-stimulating factor (GM-CSF) and PAP, which ensures the presentation of PAP peptides by stimulated APCs. However, apart from this autologous therapeutic vaccine, the use of vaccines delivering antigens with low tumoral specificity has been largely unsuccessful in mediating clinically effective anti-tumor responses, probably owing to T cells being subjected to central or peripheral tolerance (95,98).

Advances in next-generation sequencing technologies provided the opportunity to systemically identify tumor-specific mutations encoding for potential neoantigens in individual patients in a timely and cost-effective manner. This led to the development of personalized therapeutic cancer vaccines that are tailored to the tumors of each patient to be treated. However, results from clinical trials treating cancer patients with such vaccines, either alone or in combination with immune checkpoint inhibitors, showed variable clinical effectiveness (99–101). Despite their limited efficacy observed so far, therapeutic vaccines are being actively explored in clinical trials, either alone or in combination with immune checkpoint inhibitors, using various adjuvants and delivery approaches (102).

2.5. Adoptive T-cell transfer

ACT is a type of immunotherapy that consists in the isolation and *ex vivo* expansion of T lymphocytes up to high numbers that are subsequently infused back into the patient (Figure 8 and 9). Thus, the efficacy of this therapy relies on the ability of the infused T-cell product to recognize and kill cancer cells. This therapy has several advantages over other immunotherapeutic strategies. For instance, *ex vivo* expansion of T cells allows such cells to be released from the immunosuppressive tumor microenvironment, which can hamper T-cell activation and proliferation. Moreover, this immunotherapy enables conditioning of the patient prior to cell transfer, thus providing a favorable microenvironment that better supports the anti-tumor activity of the transferred T cells. An example of this is the lymphodepleting preparative regimen that is typically administered before ACT, which eliminates endogenous T regulatory cells as well as endogenous lymphocytes that compete with the transferred cells for growth-promoting cytokines. Moreover, IL-2 can also be given following cell transfer to further support the growth and survival of the T cells infused. Nevertheless, the fact that ACT is a highly personalized treatment hinders its wide applicability since T-cell products with autologous T cells have to be prepared for each individual patient and this can only be done in a few specialized centers. This difficulty is currently being addressed by the use of allogeneic T-cell products or the generation of genetically modified peripheral blood lymphocytes (PBLs) that can be used as a universal donor for all patients.

3. ACT of TILs

The first evidence that ACT using TILs expanded in IL-2 could mediate a therapeutic effect against established tumors was provided by studies in murine tumor models (103–105). These findings were rapidly translated to humans and it was in 1986 when human TILs obtained from resected melanomas were shown to contain cells capable of recognizing autologous tumors *in vitro*. This represented an important step in the development of ACT to treat human cancers (106). In 1988, a clinical trial with ACT of *ex vivo* expanded autologous TILs with IL-2 showed that 11 of 20 patients with metastatic melanoma experienced an objective response. This was the first demonstration that autologous TILs could mediate the regression of large established tumors in patients with metastatic melanoma (107). Since then, ACT with autologous TILs has been used to treat many patients with this type of tumor and, more importantly, its use has also been extended

to patients with other epithelial cancers (108). Nevertheless, although 50% of metastatic melanoma patients responded to the treatment, objective responses in patients with other tumor types have been limited. These differences in therapy response between patients and cancer types lead researchers to study the specificity of TILs and how these T cells can mediate tumor regression. Indeed, retrospective studies of TIL products from responders and non-responders showed that successful TIL-ACT was associated with an expansion of T cells targeting differentiation and cancer germline antigens and more frequently, neoantigens (109–111). These retrospective studies suggest that selection and enrichment of T cells for tumor recognition prior to ACT may be critical for its success. Although TILs with high anti-tumor reactivity are frequently expanded from melanoma, T cells recognizing neoantigens can also be found in patients with other epithelial tumors, albeit probably at lower frequencies (39,112–116). Moreover, ACT with TIL products enriched for neoantigen recognition demonstrated anti-tumor activity leading to complete responses in selected patients with epithelial tumors other than melanoma (112,113,117). Overall, the clinical experience with this personalized T-cell therapy constitutes a solid proof of principle that it can mediate durable tumor regressions in metastatic melanoma and in selected patients with other epithelial tumors when the T-cell product is enriched with T cells capable of recognizing the tumor.

3.5.1. ACT of TCR-engineered T cells

While TIL therapy remains an important ACT modality, other strategies that aim at redirecting T cells against tumor cells have gained attention. One of these strategies is ACT with TCR-engineered T cells which consists in generating an infusion product with autologous T cells that have been genetically modified to express a specific TCR capable of recognizing the tumor (Figure 9). This therapy typically uses off-the-shelf TCRs whose specificity has been previously characterized. Moreover, to make this therapy widely applicable, most of the used TCRs are restricted to very frequent HLA alleles within the Caucasian population including HLA-A*01 or HLA-A*02. Because of this, only patients carrying these HLA alleles and whose tumors express the tumoral antigen targeted by the selected TCR would be eligible for this treatment.

In 2006, the first evidence that ACT with TCR-engineered T cells recognizing the melanoma-associated antigen MART-1 could mediate tumor regression in melanoma patients was reported (118). In this clinical trial, limited efficacy of TCR-engineered T

cells was observed since only four of 31 patients treated experienced objective responses without apparent toxicities, which was attributed to the moderate ability of the TCR to recognize low amounts of antigen. This led to a second study using high-affinity TCRs generated by immunizing mice that target MART-1 and gp100 melanoma-associated antigens (119). Although better objective responses were observed in both cases, patients also experienced severe toxicities in the retina and in the middle and inner ear associated with the destruction of melanocytes present in these organs.

ACT with TCR-engineered T cells targeting cancer germline antigens have also been used in the clinic and have mediated objective responses in distinct epithelial tumors (120,121). Nevertheless, these responses sometimes were associated with significant off-tumor and off-target toxicities that led to patients' death. This was the case of two clinical trials using genetically modified T cells with two distinct affinity-enhanced TCRs targeting the cancer germline antigen MAGE A3 that resulted in severe cardiovascular and brain toxicities due to the cross-recognition of highly homologous peptides that were expressed by normal cells (121, 122).

Similar complications have been observed when using TCRs targeting overexpressed antigens. For instance, T cells genetically modified to recognize the overexpressed protein carcinoembryonic antigen (CEA) resulted in objective tumor regression in one of three metastatic colorectal cancer (CRC) patients but all of them suffered from severe transient inflammatory colitis (123).

The clinical data related to the use of TCR-engineered T cells targeting tumor antigens whose expression is not restricted to tumor cells indicate that neoantigens are clearly more attractive therapeutic targets for developing TCR-based therapies. However, the fact that most neoantigens are private to each patient has hampered the development of such therapies and efforts have been focused at detecting TCRs targeting public neoantigens. Several reports have described TCRs specific against epitopes derived from hotspot driver genes such as KRAS, p53 and PIK3CA (113,124). Moreover, two recent reports showed that two TCRs targeting $KRAS_{p.G12D}$ and one targeting $p53_{p.R175H}$ mediated objective tumor regression in a patient with pancreatic ductal adenocarcinoma and a patient with breast cancer, respectively (125,126).

A novel clinical-grade approach has been recently described that is based on CRISPR-Cas9 non-viral precision genome-editing to simultaneously knockout the two

endogenous TCR genes (i.e. TRAC and TRBC) and insert into the TRAC locus two chains of a neoantigen-specific TCR isolated from circulating T cells of the same patient (127). This strategy was used in the first-in-human phase I clinical trial (NCT03970382) with patient-specific TCRs and 16 patients with different refractory solid cancers received up to three different neoantigen-specific TCR transgenic cell products. Although stable disease was the best response on the therapy, this study demonstrated the feasibility of isolating and cloning multiple TCR that recognize different neoantigens across multiple HLA alleles.

Overall, the use of TCR-engineered T cells is a promising strategy that has significantly expanded the range of tumors that can be treated by ACT including less immunogenic tumors such as pancreatic cancer (125). Nowadays, multiple TCRs that have shown promising clinical activity in patients with solid cancers are currently being tested in the clinic. Nonetheless, all clinical data collected so far emphasizes the critical

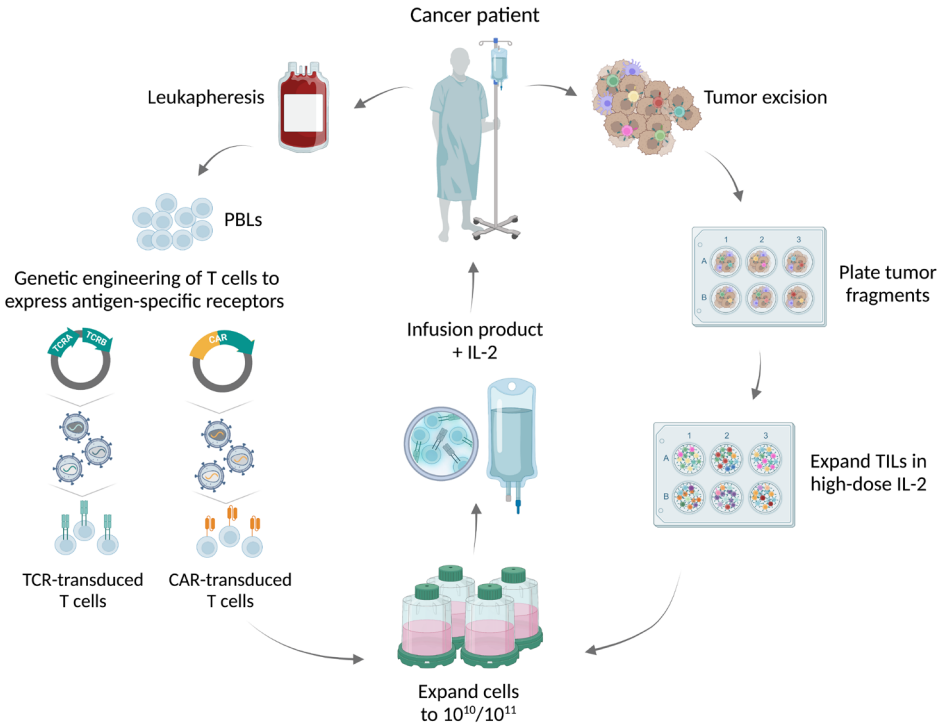

Figure 9. ACT of TILs or genetically-engineered T cells. Autologous lymphocytes are expanded up to high numbers and infused back into patients in the presence of IL-2 and after lymphodepleting chemotherapy. Two main modalities of ACT are currently used: (1) ACT with TILs that consists of the *ex vivo* expansion of TILs isolated from tumor biopsies or tumor resections (right). The tumor tissue is cut

into fragments and cultured in T-cell media containing high doses of IL-2 to promote the outgrowth of TILs. (2) ACT with genetically engineered T cells (left), which consists of the isolation of autologous PBLs that are subsequently transduced with viral vectors encoding the receptors of interest (TCR or CAR) targeting specific tumor antigens. Image created with BioRender.com.

importance of assessing potential TCR off-tumor toxicities prior to clinical development, both on-target or off-target due to cross-reactivity, especially when using affinity-enhanced TCRs.

3.5.2. ACT of CAR-engineered T cells

Another strategy to redirect T lymphocytes to recognize and eliminate tumor cells expressing a specific target antigen is ACT of T cells genetically modified to express a CAR (Figure 9). CARs are synthetic receptors that exploit the antigen specificity of the antigen-binding domains of monoclonal antibodies and combine it to the intracellular T-cell activation domains to trigger cytotoxic machinery and kill target cells (128). Therefore, CAR-transduced T (CAR-T) cells recognize natively folded proteins at the cell-surface of cancer cells independently of HLA molecules, thus overcoming clinical limitations imposed by the HLA restriction (129).

In 2010, the administration of T cells genetically engineered to express a CAR targeting CD19 to a patient with lymphoma was reported for the first time and showed remarkable long-lasting tumor regression (130). Subsequent studies using anti-CD19 CAR-T cells in B-cell lymphomas and leukemias showed impressive tumor regressions and resulted in the approval of this therapy by the FDA in 2017 (131–133). Despite the unprecedented success of anti CD19 CAR-T cell therapy in treating B-cell lymphomas and leukemias, clinical efficacy of CAR-T cells for the treatment of solid malignancies has been scarce (134). The lack of response in this type of tumors can be explained by several shortcomings of CAR-T-cell therapies that still need to be addressed, which include the limited persistence of CAR-T cells in circulation, their inefficient trafficking, their poor ability to infiltrate into the tumor and their susceptibility to the immunosuppressive microenvironment.

4. Identification of tumor-reactive T cells for the treatment of cancer

In order to generate infusion products for ACT with naturally occurring or TCR-

engineered T cells capable of recognizing and killing cancer cells, tumor-reactive T cells need to be previously identified from an endogenous T-cell source. Tumor-reactive and neoantigen-specific T cells are commonly found in patients with distinct solid tumors (39,135,136). In principle, any tissue or fluid from which T cells can be isolated and/or expanded can potentially contain such tumor-reactive T cells. However, their identification and isolation can be hindered by distinct factors including the lack of sampling material or their low frequency, which would in turn limit the development of personalized T-cell therapies. Because of this, multiple sources to isolate effector T cells as well as strategies to improve their comprehensive identification have been explored.

4.1. Sources of effector T-cell populations

4.1.1. TILs and other tumor-associated populations

Infiltration of human tumors by T cells is generally interpreted as a sign of tumor recognition. This is because the magnitude and composition of the intratumoral T-cell infiltrate have shown a clear correlation with clinical prognosis in multiple tumor types (137). Moreover, the TCR repertoire of TILs is typically more oligoclonal, probably as a result of local antigen-specific clonal expansion (138,139). Based on this, TILs are the preferred source to detect tumor-reactive T cells.

The first documented evidence that lymphocytes infiltrate the tumor dates to 1922. In that study, the post-operative survival rate was evaluated in 293 patients with distinct epithelial tumors and demonstrated that TILs were found in the tumors of patients who survived longer (140). Thereafter, thanks to the optimization of TIL culture conditions in the late 1980s, it has become possible to expand the relatively low numbers of T cells that can be naturally found infiltrating human tumors and to characterize their capacity to recognize the tumor (141).

Multiple studies have demonstrated the presence of T cells with tumor recognition potential at the tumor site (39,136,142). Nevertheless, several studies have also proven the presence of bystander cancer-unrelated T cells in the pool of TILs (74,143). Thus, the frequency of TILs capable of recognizing the tumor can be variable between patients and tumor types. Additional limitations for the isolation and expansion of tumor-reactive TILs include the variable success rate of TIL expansion from tumor biopsies and their heterogeneity even when expanded from contiguous tumor fragments. Moreover, their

isolation depends on the availability of tumor biopsies or resected tumoral tissue, which are not always available. Because of this, other T-cell sources have also been investigated with the aim of finding other natural sources of T cells capable of recognizing the tumor.

Fluids directly associated with particular solid tumors have been also used as sources for the expansion of tumor-associated lymphocytes (TALs). This is the case of pleural effusions from mesotheliomas (144,145) or urine in bladder cancer, where the TCR repertoire of urine-derived lymphocytes accurately maps that of T cells isolated from the primary tumor. Another example is ascites from ovarian cancer. In a study comparing the TCR repertoire derived from a series of primary cancers and ascites from 12 ovarian cancer patients, clonally expanded T cells were found in the ascites (146). However, only few TCR clonotypes coincided with those in the tumor, suggesting that the tumor-reactive T-cell population present in the primary tumor might be underrepresented in ascites. Nevertheless, the potential of using T cells from ascites to detect tumor-reactive T cells was demonstrated in another study where a neoantigen-specific T-cell clone was identified in the ascites of one patient with high-grade serous ovarian cancer at the time of recurrence but not in the primary tumor or in primary ascites (147). Cerebrospinal fluid (CSF) is another fluid that has been explored and demonstrated to contain T lymphocytes, as observed in a patient with diffuse intrinsic pontine glioma after DC vaccination (148). More recently, another study also showed that in patients with brain metastases, TCR clonotypes could be detected in CSF which matched those detected in metastatic brain lesions (149). All these studies have proven the potential of TALs as a source to detect T cells capable of recognizing the tumor.

4.1.2. Peripheral blood lymphocytes

Peripheral blood mononuclear cells (PBMCs) derived from blood samples are the most attractive non-invasive T-cell source to identify and isolate T cells capable of recognizing the tumor.

The first evidence of the existence of circulating tumor-reactive T cells was reported in 1987. In this study, mixed lymphocyte tumor cultures (MLTCs) were generated by successive rounds of stimulation of PBMCs with irradiated autologous tumor cell lines. These MLTCs were used as effector cells to evaluate tumor recognition and tumor-reactive MLTC clones were obtained (150). Nonetheless, multiple rounds of stimulation

were required to generate MLTC populations. The first study in which circulating T cells recognizing neoantigens were detected from unmanipulated PBMCs was in 2013 thanks to the improvement of HLA multimers technology (151). In this case, neoantigen-reactive T cells reactive against a neoantigen restricted to HLA-A*03:01 were detected in the circulation of a melanoma patient. Subsequent studies have further proven the existence of neoantigen-specific T cells in the peripheral blood of patients with distinct epithelial tumors evidencing that peripheral blood is a minimally-invasive T-cell source to isolate tumor-reactive T lymphocytes (58,152–156). More importantly, tumor antigen-specific T lymphocytes isolated from peripheral blood have been used in clinical trials to treat patients with metastatic melanoma (157–159).

4.2. Strategies for enrichment of tumor-antigen reactive T cells

Tumor-reactive T cells are frequently identified in cancer patients and have been proven to exist in distinct T-cell reservoirs. Nonetheless, studies have demonstrated that such T cells are present at relatively low frequencies in fresh tumor single-cell suspensions and are even more infrequent in other T-cell sources such as peripheral blood (151,154,160,161). Because of this, multiple enrichment strategies have been developed to increase the odds of detecting tumor-reactive T cells that otherwise would have been missed due to the limited sensitivity of the techniques in use. These strategies are: peptide-HLA (pHLA) multimers, *in vitro* sensitization (IVS) and surface marker-based isolation (Figure 10).

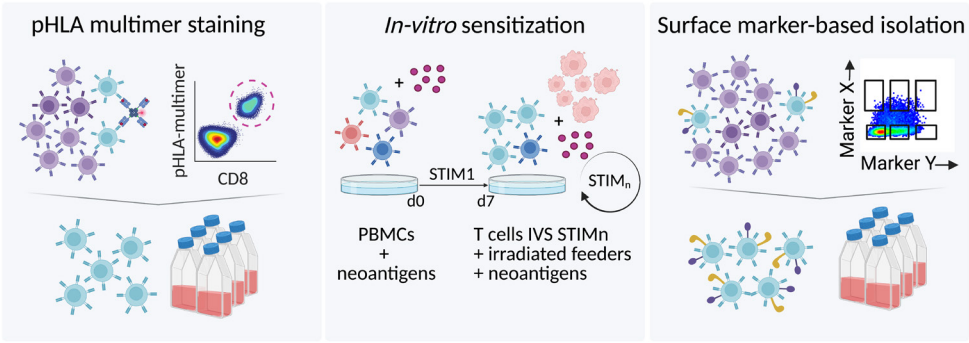

Figure 10. Enrichment strategies to identify neoantigen-specific or tumor-reactive T lymphocytes. Three enrichment strategies can be used to enrich for infrequent neoantigen-specific or tumor-reactive PBLs. One strategy uses pHLA-multimers that can be used to FACS neoantigen-specific T cells with known specificity (left). Another strategy is *in vitro* sensitization, which consists in the stimulation and expansion of T cells with antigens of interest either to generate *de novo* T-cell responses from the naïve compartment or to increase the frequency of infrequent naturally occurring T-cell reactivities (middle). Last, T-cell subsets from peripheral blood can be FACS based on the expression of

surface markers associated with tumor recognition to enrich for neoantigen-specific or tumor-reactive T lymphocytes (right). Image created with BioRender.com.

4.2.1. Multimers

One strategy to enrich for tumor-reactive T cells consists in the use of pHLA multimers, which can identify and be used for the isolation of tumor-reactive T cells with known specificity (Figure 10, left). This strategy relies on the detection of the interaction between the TCR and its cognate pHLA complex. Thus, pure antigen-specific T-cell populations can be isolated by staining with fluorescently-labeled pHLA multimers.

The first pHLA multimer was generated with HLA-A2 molecules loaded with HIV-derived or influenza A-derived peptides in 1996 (162). Since then, multiple tumor antigen-specific T-cell populations form either PBMCs or fresh tumor digests have been detected in patients with solid tumors and hematologic malignancies using this approach (160,163–165).

Although initially pHLA multimers had to be generated individually and the detection of T-cell populations with different antigen specificities in one sample was limited to the number of fluorochromes available, advances in multimer technologies have facilitated high-throughput production and testing of large libraries of pHLA complexes. Whilst the development of UV-exchangeable HLA ligands represented an important advance for the generation of large libraries of pHLA multimers by simple manipulations (166,167), fluorochrome-based combinatorial encoding increased the number of T-cell specificities that could be interrogated by flow cytometry in one sample (161,168). Other studies have developed similar strategies aiming at discovering tumor antigens and the T cells recognizing them in a high-throughput manner (169–172). For instance, a novel technology based on pHLA multimers labeled with individual DNA barcodes enabled to screen more than 1000 antigen specificities in a single sample and led to the detection of antigen-specific T cells from patients with melanoma and non-small cell lung carcinoma (NSCLC) against tumor-associated antigens and neoantigens (171). This technology has enabled the interrogation of large pHLA multimer libraries and has successfully identified neoantigen-specific T-cell populations in TILs and PBLs in patients with distinct epithelial cancers (156,173).

Despite all technological advances, pHLA multimers have been mainly applied for the detection and analysis of $CD8^+$ T-cell responses since technical challenges related to

the production of pHLA-II multimers have been encountered (174,175). Very recently, a novel HLA-sDM-based peptide exchange methodology has been developed to generate large panels of peptides-HLA-II complexes. This method functions as a universal exchange catalyst that can load antigenic peptides onto any natural HLA-II alleles. By using this platform, the authors were able to detect *de novo* neoantigen-specific $CD4^+$ T-cell responses in metastatic cancer patients after vaccination (176). Multimer technology with nonclassical HLA molecules has also been investigated (177–179). A recent study described the development of a method that allowed the high-throughput production of thermal-exchangeable pHLA multimers with the unconventional HLA-E molecule, which would subsequently enable the detection of T cells and NK cells that mediate anti-tumor responses by the recognition of HLA-E-restricted peptides (180).

4.2.2. *In vitro* sensitization

Another frequently used approach to enrich for tumor-reactive T lymphocytes is *in vitro* sensitization (IVS), which consists in the stimulation and expansion of T cells with the antigens of interest to either generate *de novo* T-cell responses from the naïve T-cell compartment or to increase the frequency of T cells that have previously seen their cognate antigen but are undetectable due to their low frequency (40,154,181,182) (Figure 10, middle). Although distinct IVS protocols have been described in the literature, all rely on the same principle. PBMCs or TILs are co-cultured during seven to 14 days, with or without irradiated feeders, with autologous APCs and pools of peptides encoding for candidate tumor antigens in the presence of cytokine cocktails, usually containing IL-2, IL-7, IL-15 and IL-21. After the first round of stimulation, T cells can either be screened for tumor antigen recognition or re-stimulated using the same approach. Multiple rounds of stimulation are frequently used to increase the odds of detecting very infrequent T-cell reactivities. Several modified versions have been used and all have proven to be useful for the enrichment of tumor antigen-specific T cells (154,183–185). For instance, if the autologous tumor cell line is available, it can be used instead of APCs for stimulation. Moreover, the candidate tumor antigens can be introduced in APCs in DNA or RNA format, instead of using pools of synthetic peptides. To get a purified population of tumor antigen-reactive T cells, IVS strategies can be combined with flow cytometry-based sorting of T cells expressing the activation markers 4-1BB, also known as CD137, or OX40, also known as CD134, after the screening for tumor antigen recognition (154) or directly by generating

a pHLA multimer with the peptide of interest and use it for sorting (186,187).

Since this approach can also generate *de novo* T-cell responses by priming and activating naïve T cells, several recent studies have used PBMCs from healthy donors to identify tumor antigen-specific T cells and TCRs, with a particular interest in detecting TCRs recognizing public neoantigens derived from recurrently mutated driver genes in patients with cancer (124,182,188,189).

4.2.3. Biomarker-based isolation

The biomarker-based isolation of T cells is the other enrichment strategy widely used to identify and isolate tumor antigen-specific T cells. This strategy exploits the differential phenotype observed on T cells upon recognition of their target characterized by the upregulation of co-stimulatory and co-inhibitory molecules, as described in section 1.4 (Figure 10, right).

To date, most of the cell-surface markers demonstrated to enrich tumor- or neoantigen-reactive T cells have been described in $CD8^+$ TILs from patients with different epithelial tumors. This includes PD-1, TIM-3 and LAG-3 in melanoma (138,190), high levels of PD-1 or the co-expression of CD39 and CD103 in NSCLC (73,191), co-expression of PD-1^{hi} and CD39 in endometrial cancer (192) and CD39 in lung cancer and CRC (74). A different approach isolates T cells based on 4-1BB expression after co-culture with autologous tumor cells, which also enriches tumor-reactive T lymphocytes (193,194). Nonetheless, three recent reports also identified certain receptors whose expression led to the selection of $CD4^+$ TILs capable of recognizing the tumor. More in detail, $CD4^+$ TILs expressing CD39 in HPV-induced squamous cell carcinomas or co-expressing PD-1 and ICOS in head and neck (H&N) and CRC led to the identification of a T-cell subset with enriched tumor recognition capacity (195,196). The expression of high levels of PD-1 also led to the detection of $CD4^+$ tumor-reactive TILs in endometrial cancer patients, which was irrespective of CD39 expression (192).

Although this strategy has been mainly used to enrich tumor-reactive T cells from TILs, some studies have also demonstrated its feasibility to enrich for T lymphocytes targeting neoantigens from peripheral blood. More in detail, PD-1 expression has been proven to guide the selection of $CD8^+$ and $CD4^+$ neoantigen-specific PBLs in patients with melanoma and gastrointestinal cancers (152,153). In another study, isolation of

$CD62L^+CD45RO^+$ memory T cells also enabled the identification of circulating neoantigen-specific T cells (154).

Although these surface receptors can identify neoantigen-specific or tumor-reactive T cells from circulation, the frequency of such T cells remains very low. Therefore, the selection of T cells expressing a combination of cell-surface receptors could further enhance the frequency of neoantigen-specific T cells. Thus, other markers previously described to be differentially expressed by effector T cells in chronic infection or in cancer could be investigated to improve the selection of PBLs capable of recognizing the tumor. One possibility could be to explore markers already described to enrich for neoantigen-specific or tumor-reactive T cells from tumor biopsies. In addition, other markers including CD38, HLA-DR and CD27 were shown to be expressed by proliferating $CD8^+PD\text{-}1^+$ T cells responding to anti-PD-1 therapy in patients with NSCLC (197), indicating that they could also be good candidates to improve the enrichment of tumor-reactive T cells from circulation.

5. Liquid biopsy: a new minimally-invasive diagnostic and monitoring tool for cancer

The gold-standard method for tumor profiling relies on sequencing of tumor samples. Nevertheless, this approach presents several limitations including the difficulty in acquiring tumor samples of the required size and quality, often limited by tumor accessibility and the clinical risk associated with invasive surgeries. Moreover, in patients with advanced metastatic tumors, tumor biopsies of a single lesion may not capture the genomic landscape of a patient's entire tumor burden thereby requiring multiple biopsies to obtain a comprehensive tumor profile.

Over the past decade, liquid biopsy has progressively emerged as a minimally-invasive surrogate for accessing the tumor genome and is slowly replacing invasive techniques for tumor diagnosis and monitoring. This technique overcomes several of the limitations associated with tumor resections and biopsies and offers an important advantage that is the ease of repeated sampling throughout treatment to monitor the tumor evolution in real-time.

Liquid biopsy consists of isolating tumor-derived components present in the body fluids of cancer patients and provide crucial genomic, epigenetic, transcriptomic and

proteomic information about primary tumors and metastatic lesions (198). Multiple body fluids such as saliva, pleural effusions, urine and CSF have been shown to contain tumor-derived materials and therefore can be used to profile the tumor (199–205) (Figure 11). Nevertheless, given that each of these body fluids is exclusively in contact with specific organs, they will only contain tumor-derived components from lesions arising in such organs. In contrast, peripheral blood represents a potential source of tumor-derived components from any given tumor lesion. Because of this and due to its easy accessibility, blood is the principal body fluid used and studied in the field of liquid biopsies (Figure 11) (206).

Multiple tumor-derived components can be obtained from liquid biopsies, which can provide longitudinal information and data from both primary and metastasized tumors. These include circulating tumor cells (CTCs), tumor-derived extracellular vesicles (EVs), tumor-educated platelets (TEPs), tumor metabolites, circulating cell-free RNA (ctRNA) composed of small RNAs and microRNAs and circulating tumor DNA (ctDNA) (Figure 11), the latter being the most widely used in the clinic and the one that has been investigated in this thesis.

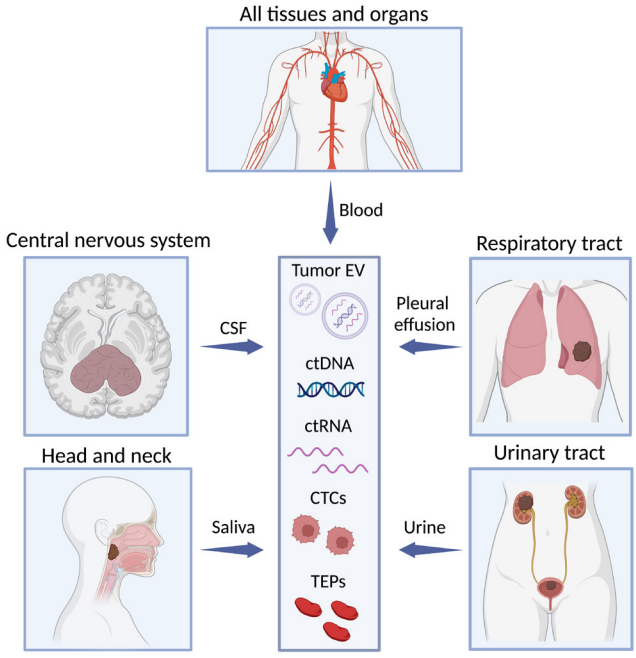

Figure 11. Liquid biopsies as a minimally-invasive surrogate to access the tumor. Liquid biopsies are used to isolate tumor-derived components present in the body fluids of cancer patients that can

provide crucial information of primary and metastatic tumor lesions. Body fluids that are in contact with certain organs, which include CSF, saliva, pleural effusions and urine, can contain tumor-derived material from tumors derived from such organs. Peripheral blood is the only body fluid that can contain tumor-derived components from any tumor since it is in contact with all the organs of the human body. Several tumor-derived components can be detected in such body fluids, which include circulating tumor cells (CTCs), circulating tumor RNA (ctRNA), tumor-educated platelets (TEPs), extracellular vesicles (EVs) and circulating tumor DNA (ctDNA). Nevertheless, not all of them are detected in liquid biopsies from all the body fluids mentioned. Image created with BioRender.com.

5.1. Circulating tumor DNA

In healthy individuals, cell-free DNA (cfDNA) is released into the circulation by normal cells, mostly originating from hematopoietic cells (207,208). However, in certain physiological or pathological conditions, such as exercise, pregnancy, organ transplantation and cancer, the tissues related to the specific condition could release additional DNA into peripheral blood (209,210). In cancer patients, higher levels of cfDNA have been observed compared to healthy individuals (211–213).

Tumor cells release ctDNA to the pool of cfDNA following apoptosis, necrosis or by active secretion (214). These single- or double-stranded DNA fragments present in plasma and serum are typically around 140-170 base pairs (bp) in length and have a half-life in the circulation that ranges from 16 minutes to 2.5 hours (215). ctDNA harbor many cancer-associated molecular signatures including somatic mutations, copy number alterations (CNAs) and methylation patterns (216,217). Multiple studies have demonstrated high concordance of somatic genomic alterations between cfDNA and matched tumor tissue in distinct types of epithelial tumors (218–222). Thus, ctDNA has been spotlighted as an attractive liquid biomarker that could be used for multiple clinical applications due to its easy accessibility, its capacity to recapitulate tumor lesions present in different tissues and its ability to represent the tumor genetic profile in real-time.

5.1.1. Tumor fraction in cfDNA

The contribution of tumor-derived DNA to cfDNA is also known as tumor fraction and has been shown to vary widely among cancer patients and among tumor types representing from 0.01-90% of the total cfDNA (223,224). Several biological factors have been shown to affect the amount of ctDNA shed into the circulation, including the location, size and vascularization of the tumor (212,225–227). Another factor that influences the levels of tumor fraction is the tumor stage as it has been found that higher levels of tumor fraction are more frequently detected in patients with advanced stage tumors (228,229).

Additionally, the source used to extract cfDNA also affects tumor fraction. This is because, although cfDNA can potentially be extracted from both serum and plasma, the latter represents a more suitable source for its extraction and analysis, as it contains lower levels of non-malignant DNA thereby yielding higher concentrations of ctDNA (230). In addition to biological factors, technical practices used to collect, store, extract and process cfDNA can also have an impact on the levels of tumor fraction (214). This was demonstrated in a study where the rate of detection of somatic mutations in cfDNA was decreased when the time between blood withdrawal and cfDNA extraction was more than four hours.

Overall, all these factors can affect the levels of tumor fraction that in turn have an impact on the representation and detectability of genetic alterations of the tumor in cfDNA. Because of this, determining the tumor fraction is crucial for the use of cfDNA in the clinic and can inform which is the most appropriate analysis method to be used in each case.

5.1.2. Methods for the detection of somatic genetic alterations

The levels of ctDNA in the circulation of cancer patients might be as low as 0.01% of total cfDNA which poses challenges in its detection. Over the last decade, methods to detect ctDNA have evolved from targeting individual mutations using polymerase chain reaction (PCR) (Figure 12) to using gene panels targeting dozens to hundreds of mutations. Additionally, whole-exome sequencing (WES) or whole-genome sequencing (WGS) analysis of cfDNA have also been used to identify genetic alterations across the entire exome and genome, respectively. Overall, all the strategies used to analyze ctDNA can be categorized into two groups: targeted and untargeted approaches.

Targeted approaches for ctDNA analysis are used to specifically detect a single or few tumor-specific mutations known to exist in the primary tumor. This includes PCR-based strategies such as quantitative PCR (qPCR) and digital PCR methods such as droplet digital PCR (ddPCR) and BEAMing (beads, emulsions, amplification and magnetics) and several sequencing-based methods, which have progressively improved the sensitivity of sequencing, including Safe-sequencing, cancer personalized profiling by deep sequencing (CAPP-Seq) and tagged-amplicon deep sequencing (TAmSeq). These strategies are commonly used in the clinic to identify specific genomic alterations in multiple tumor types, which can guide the selection of targeted therapies or can identify resistant mechanisms

after treatment. Genes that are frequently explored include epidermal growth factor receptor (EGFR) mutations in NSCLC, BRAF mutations in melanoma, KRAS mutations in CRC and HER2 amplification and PIK3CA mutations in breast cancer, among others (231–237). Targeted strategies can be extremely sensitive, as mutations can be detected at an allele frequency of down to 0.01% with high specificity (Figure 12). Nevertheless, these strategies cannot be used as discovery tools to identify new aberrations and require preconceived panels of genes whose mutational status has been previously assessed in the tumor.

Untargeted approaches are the second type of strategies used to investigate ctDNA and aim at an exome- or genome-wide analysis for copy number alterations (CNAs) or point mutations by either WES or WGS, respectively. These strategies are used as discovery tools since they can identify alterations that have not been previously detected in the primary tumor. Nevertheless, they have lower sensitivity and therefore require high concentrations of ctDNA to reliably identify tumor-specific genomic alterations (Figure 12). For this reason, the use of untargeted strategies is still challenging to confidently detect tumor variants, especially those that are at low frequencies in the circulation. In a recent study, Li *et al.*, developed cfSNV, a method that sensitively detects SNVs with variant allele frequencies (VAF) lower than 5%, which represents an improvement for the detection of infrequent variants in cfDNA of cancer patients (238,239).

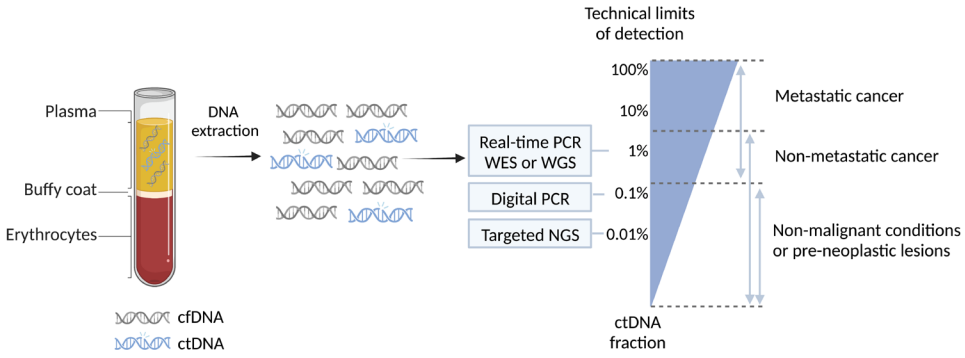

Figure 12. Analysis of ctDNA. cfDNA can be extracted from plasma. In cancer patients, a fraction of cfDNA is tumor-derived and it is also known as ctDNA. After cfDNA extraction from plasma, cfDNA can be analyzed using a variety of sequencing techniques that are based on PCR of next-generation sequencing. These techniques have different levels of sensitivity for the detection of NSMs. Adapted from Cabel *et al.*, 2018. Image created with BioRender.com.

5.1.3. Clinical applications of cfDNA

The possibility to analyze tumor-derived DNA by simply withdrawing blood without the need for an invasive tumor biopsy constitutes a critical advance with potentially transformative clinical applications, especially for those types of epithelial tumors that cannot easily be resected or biopsied, including lung, pancreatic, some H&N and brain tumors. Thus, cfDNA is gaining attention for its usage in multiple clinical applications (Figure 13).

ctDNA analysis can be used for early-diagnosis of tumors (Figure 13). A variety of tumor-specific genetic and epigenetic alterations are being investigated as possible early detection biomarkers from ctDNA, which can be assessed by using targeted strategies. The first ctDNA-based primary screening test designed was a qPCR assay directed to specific DNA sequences of Epstein Barr virus (EBV), which commonly drives the formation of several tumor types including gastric and H&N cancer. In this study, the use of EBV qPCR assay as a primary screening test in otherwise healthy adult individuals demonstrated high sensitivity and specificity for the detection of early-stage nasopharyngeal cancer and had a tremendous impact in progression-free survival rates after diagnosis (97%), which far exceeded historical controls for this disease (70%) (240). The use of cfDNA for early diagnosis faces several challenges including the inability to detect tumor mutations in early-stage patients with low cfDNA levels, the misclassification of patients due to the detection of mutations that can also be associated with non- or pre-malignant stages or the difficulty in determining the origin of the tumor-derived cfDNA. Although further research is needed, numerous studies demonstrated that cfDNA can detect tumor-derived mutations in early-stage disease and, importantly, before the development of symptoms, which support the potential use of cfDNA for the early detection and diagnosis of cancer (228,240–242).

Tumor molecular profiling using cfDNA can guide treatment selection through the identification of actionable gene targets (Figure 13). This ability of cfDNA is of great importance especially in those cases where tumor biopsies did not capture enough tumor material for sequencing, which can occur in 20 to 25% of needle biopsies (243,244). There is still much progress to be made to prove that cfDNA can be utilized for this purpose with confidence. Nonetheless, an FDA-approved application for cfDNA in routine clinical practice, the cobas EGFR Mutation Test v2, supports cfDNA

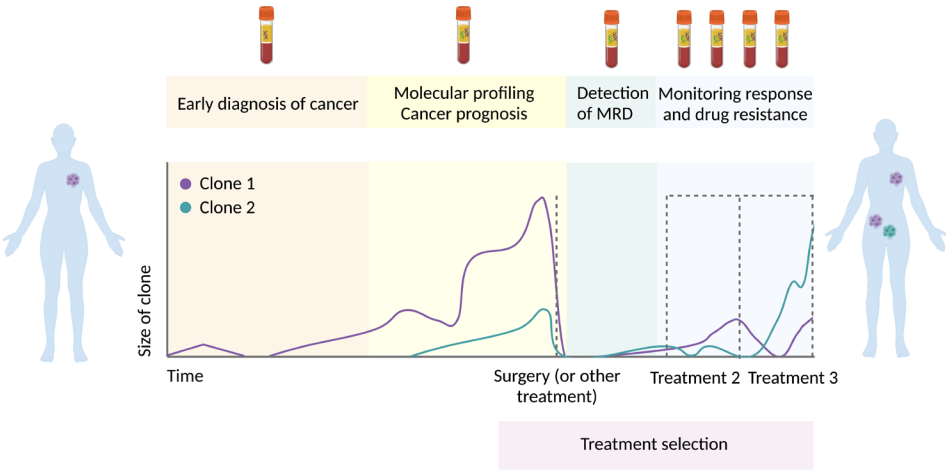

Figure 13. Clinical applications of ctDNA during the course of cancer disease. Schematic overview of a cancer patient that initially responds to surgery or other initial treatment but then has a relapse and receives other lines of treatment. All possible clinical applications of ctDNA in cancer management along the course of the disease are depicted. Adapted from Wan *et al.*, 2017. Image created with BioRender.com.

as a marker for cancer management. More in detail, this assay using cfDNA is designed to identify lung cancer patients that would benefit from EGFR tyrosine kinase inhibitors (TKIs) as initial therapy (245,246).

Since blood withdrawal is a simple procedure that can easily be used for repeated and serial testing after one or more lines of therapy, cfDNA also has an important role in tracking response to therapy, monitoring acquired drug resistance and detecting minimal residual disease (MRD) (Figure 13). ctDNA levels have also arisen as a biomarker of response to therapy since they correlate with changes in tumor burden and treatment response. Numerous studies that evaluated patients along treatment have shown that ctDNA levels drop drastically upon response to therapy in various cancers including CRC, ovarian, breast, NSCLC, melanoma and brain tumors (247–253). Similarly, an increase in ctDNA levels is frequently observed in progressors, which can even precede radiographic progression and correlate with poor survival rates (248,254,255).

Analysis of cfDNA represents an effective tool to identify emergent genetic alterations driving acquired resistance to therapy (Figure 13). Since resistance to treatment is often led by multiple resistant subclones that might co-exist in the same lesion or in

different metastatic lesions, cfDNA has demonstrated to outperform single-lesion tumor biopsies that underestimate tumor molecular heterogeneity in the detection of acquired resistant mechanisms (256–258). The ability of cfDNA to identify resistance alterations has been described in patients with several epithelial tumors including lung, breast and CRC (259,260).

Finally, cfDNA analysis has a great potential in detecting MRD after surgical resection. This can be determined by the presence of ctDNA in the plasma of patients after surgery. In a study in CRC patients, measurable ctDNA levels after 1-2 months of surgery accurately identified patients with later tumor recurrence (261). MRD can also be assessed by the post-operative detection of tumor-specific mutations in cfDNA, as observed in several studies in breast, lung, pancreatic and CRC patients (262–264).

Overall, cfDNA analysis has emerged as a novel technology that can potentially be used in multiple clinical applications. Nevertheless, a careful understanding of the advantages and limitations is essential for the effective clinical integration of this technology.

Hypothesis and Objectives

Identification of neoantigens targeted by lymphocytes is central to cancer immunotherapy strategies that take advantage of the spontaneous immune response to tumors.

The requirement of a tumor biopsy to identify candidate neoantigens and neoantigen-reactive T cells limits the scope of these personalized T-cell therapies. Moreover, the exclusive use of a single tumor biopsy to identify tumor somatic mutations can underestimate tumor heterogeneity in the metastatic setting, which may hamper treatment efficacy.

We hypothesize that:

1. Neoantigen-targeted T-cell therapies can be developed exclusively using peripheral blood, making these therapies more broadly applicable.
2. Tumor somatic mutations can be detected by performing WES of cfDNA isolated from plasma and may capture the mutational landscape of metastatic tumors.
3. T cells targeting neoantigens can be identified, isolated and expanded from peripheral blood and co-expression of two or more exhaustion/activation markers may better define and enhance the detection of circulating neoantigen-reactive T cells.

The **overall objective** of this thesis is:

To develop T-cell therapies exclusively using the peripheral blood of patients with metastatic epithelial tumors. We aim to mine the WES data of cfDNA to detect tumor somatic mutations and neoantigens and to identify and isolate circulating T lymphocytes and TCRs targeting them.

The **specific objectives** are the following:

1. Identify tumor-specific somatic mutations by performing WES of cfDNA extracted from plasma.
2. Compare the phenotypic profile of circulating T lymphocytes in healthy individuals compared to metastatic cancer patients.
3. Improve the detection of circulating neoantigen-specific $CD8^+$ and $CD4^+$ lymphocytes and TCRs beyond what was previously reported by exploring the

co-expression of cell-surface receptors associated with activation/exhaustion and refining the phenotypic signature of neoantigen-targeted T-cell responses in peripheral blood.

4. Characterize and compare the specificity and diversity of the neoantigen-specific responses derived from circulating $CD8^+$ and $CD4^+$ T lymphocytes and TILs.
5. Evaluate the ability of WES of cfDNA to identify neoantigens and compare them to those identified in tumor biopsies.
6. Determine which factors influence the efficiency of the methods applied to identify tumor somatic mutations and neoantigens in cfDNA.

Materials and methods

Patient samples

This study included patients with advanced metastatic epithelial cancers treated at Vall d'Hebrón Hospital or Hospital Universitari Bellvitge.

Table 1. Patients' characteristics and analysis in which they were involved

Patient	Cancer type	Age/sex	Phenotypic analysis	Cell sorting and T-cell screening
VHIO-08	H&N[a]	61/M	Yes	-
VHIO-09	H&N	55/M	Yes	-
VHIO-29	Melanoma	76/F	Yes	-
VHIO-35	Penile squamous cell carcinoma	83/M	Yes	-
VHIO-38	Hepatocellular carcinoma	44/M	Yes	-
VHIO-59	Merkell cell carcinoma	77/M	Yes	-
VHIO-75	Testicular germ cell tumor	36/M	Yes	-
VHIO-84	Melanoma	75/F	Yes	-
VHIO-89	CRC[b]	61/F	Yes	-
VHIO-90	CRC	63/M	Yes	-
VHIO-91	CRC	76/M	Yes	-
VHIO-92	CRC	66/M	Yes	-
VHIO-93	CRC	73/M	Yes	-
VHIO-100	CRC	44/M	Yes	-
VHIO-106	Stomach adenocarcinoma	63/M	Yes	-
CRC MSI-01	CRC	68/M	Yes	-
CRC MSI-04	CRC	35/M	Yes	-
CRC MSI-08	CRC	61/F	Yes	-
CRC MSI-11	CRC	77/M	Yes	-
CRC MSI-12	CRC	43/M	Yes	-
GOI-01	Breast	46/F	-	Yes
GOI-02	Breast	68/F	-	Yes
GOI-03	H&N	57/M	-	Yes
GOI-04	H&N	37/M	-	Yes
GOI-05	CRC	72/F	Yes	Yes
GOI-06	CRC	67/F	Yes	Yes
GOI-07	Ovarian	54/F	-	Yes
GOI-08	CRC	70/M	-	Yes
GOI-09	Chordoma	70/M	Yes	Yes
GOI-10	Chordoma	70/M	Yes	Yes

[a]Head and neck. [b]Colorectal

Patients were chosen on the basis of the availability of pre-treatment peripheral blood samples. Written informed consent was obtained from all patients before enrollment. Most patients received a wide range of prior therapies, but all were immunotherapy naïve. The hospital Institutional Review Board approved the study in accordance with the principles of Good Clinical Practice, the Declaration of Helsinki (protocol PR(AG)482/2017) and other applicable local regulations. A summary of clinical details and the protocols carried out with their tissue and blood samples is given in Table 1.

Establishment of patient-derived tumor cell line (TCL)

A small fragment (2-4 mm^3) of a tumor biopsy or surgically resected tumor was cultured in RPMI 1640 plus (Lonza) containing 10% FBS Hyclone (GE Healthcare), 100 U/mL penicillin (Lonza), 100 µg/mL streptomycin (Lonza) and 25 mM HEPES (Thermo Fisher Scientific) at 37°C in 5% CO_2. The medium was replaced once every month until the TCL was established and then further expanded in media containing RPMI 1640 plus (Lonza), 20% FBS (Gibco), 100 U/mL penicillin (Lonza), 100 µg/mL streptomycin (Lonza) and 25 mM HEPES (Thermo Fisher Scientific) or cryopreserved until used. Established TCLs were regularly tested for mycoplasma and were authenticated based on the identification of patient-specific somatic mutations and HLA typing.

TIL expansion

Small tumor fragments (2-4 mm^3) were cultured in individual wells of a 24-well plate in T-cell medium consisting of RPMI 1640 plus (Lonza) supplemented with 10% human AB serum (Banc de Sang i Teixits, Barcelona, Spain), 100 U/mL penicillin (Lonza), 100 µg/mL streptomycin (Lonza), 2 mM L-Glutamine (Lonza), 25 mM HEPES (Thermo Fisher Scientific) and $6x10^6$ IU IL-2 (Proleukin) at 37°C and 5% CO_2. Fresh media containing IL-2 was added on day 5 and media was changed or TIL were split when confluent every other day after that. T cells were expanded independently for 15-30 days and cryopreserved until use.

PBMCs isolation

PBMCs were obtained using a Ficol density gradient (Lymphoprep, Stem cell) from pheresis or whole blood and cryopreserved for cell sorting, DNA extraction for WES and to expand B cells *ex vivo*.

Flow cytometry analysis and fluorescence-activated cell sorting (FACS)

To phenotype $CD4^+$ and $CD8^+$ T lymphocytes from peripheral blood by flow cytometry,

an extracellular panel of human-specific antibodies was designed (Table 2). Briefly, PBMCs were thawed and rested overnight in the absence of cytokines. Cells were stained with LIVE/DEAD™ Fixable Yellow (ThermoFischer) for 30 minutes and washed in PBS (Biowest) before staining with surface marker antibodies.

Table 2. List of antibodies used and their applications

Target	Conjugate	Clone	Application	Supplier	Catalog number
CD3	Pe-Cy7	SK7	Phenotyping	BD Biosciences	557851
CD8	APC-H7	SK1	Phenotyping	BD Biosciences	560176
CD4	BV510	SK3	Phenotyping	BioLegend	344534
PD-1	PE	EH12.2H7	Phenotyping	BioLegend	329906
CD28	Pe-Cy5	CD28.2	Phenotyping	BioLegend	302910
CD27	FITC	BV650	Phenotyping	BioLegend	302828
CD38	APC	HIT2	Phenotyping	BioLegend	303510
CD39	FITC	A1	Phenotyping	Thermo Fisher	11-0399-42
HLA-DR	BV605	L243	Phenotyping	BioLegend	307640
LAG 3	AF488	11C3C65	Phenotyping	BioLegend	369326
ICOS	BV785	C398.4A	Phenotyping	BioLegend	313534
CD3	APC-H7	SK7	FACS	BD Biosciences	560176
CD3	Pe-Cy7	SK7	FACS	BD Biosciences	557851
CD8	Pe-Cy7	RPA-T8	FACS	BD Biosciences	557746
CD8	APC-H7	SK1	FACS	BD Biosciences	560176
CD4	BV510	SK3	FACS	BioLegend	344534
CD4	AF700	SK3	FACS	BioLegend	344622
PD-1	PE	EH12.2H7	FACS	BioLegend	329906
PD-1	PE/Dazzle 594	EH12.2H7	FACS	BioLegend	329939
CD27	FITC	O323	FACS	BioLegend	302806
CD39	FITC	A1	FACS	Thermo Fisher	11-0399-42
CD39	BV421	A1	FACS	BioLegend	328214
CD38	APC	HIT2	FACS	BioLegend	303510
4-1BB	PE	4B4-1	FACS	Miltenyi Biotec	130-093-475
HLA-DR	BV605	L243	FACS	BioLegend	307640
CD3	APC-H7	SK7	co-culture	BD Biosciences	560176
CD8	Pe-Cy7	SK1	co-culture	BD Biosciences	557746
CD4	PE	RPA-T4	co-culture	BD Biosciences	555347
4-1BB	APC	4B4-1	co-culture	BioLegend	550890
OX40	FITC	ACT35	co-culture	BD Biosciences	555837
moTCR β	FITC	H57-597	co-culture	Invitrogen	11-5961_85

To isolate $CD8^+$ and $CD4^+$ subpopulations based on the expression of PD-1, CD27, CD38, CD39, HLA-DR and 4-1BB from peripheral blood by FACS, PBMCs were thawed and rested overnight without cytokines but in the presence of DNAse (Pulmozyme, Roche). Following $CD8^+$ or $CD4^+$ enrichment using CD8 or CD4 microbeads (Miltenyi Biotec), respectively, the Fc receptor was blocked (Miltenyi Biotec) and cells were washed and stained with the corresponding antibody mix (Table 2) for 30 minutes at 4°C. Single stain controls for each marker and fluorescence minus one controls for PD-1, CD27, CD38, CD39, HLA-DR and 4-1BB were also included. Cells were isolated using the BD FACS Aria™. FACS-sorted cell populations were expanded using a rapid expansion protocol (REP) explained below.

Rapid Expansion Protocol (REP)

To expand T cells *ex vivo* we used a REP that lasts 14 days. T cells are cultured in T25 flasks in T-cell medium containing 30 ng/mL anti-CD3 (OKT3, Miltenyi), $3x10^3$ IU/mL IL-2 (Proleukin) and irradiated PBMCs pooled from at least 3 allogeneic donors. After day 6, half of the medium was replaced with fresh T-cell medium containing IL-2 every other day. Cells were split when confluent, harvested on day 14 and used in co-culture analysis or cryopreserved until further use.

DNA and RNA extraction

DNA was extracted from leukocytes (germline DNA) or from a cell pellet of patient-derived TCL using the Allprep DNA/RNA mini kit (Qiagen, Germany). CfDNA was extracted from plasma samples using the QIAamp Circulating Nucleic Acid kit (Qiagen) according to the manufacturer's instructions. Genomic DNA and total RNA were purified from 10-µm OCT sections using DNeasy Blood and Tissue kit (Qiagen). In all cases, the extraction was performed according to the manufacturer's instructions. The DNA and RNA amounts were quantified with a Qubit™ Fluorometer (Thermofisher, USA) or with Nanodrop, respectively and reported in total nanograms (ng). The 4200 TapeStation (Agilent, USA) was used to assess the quality and fragment size distribution of the pre-processed and post-processed DNA samples and libraries.

Exome sequencing and RNA sequencing

Sequencing libraries of cfDNA plasma samples were prepared using the SMARTer ThruPLEX Plasma-seq Kit (Takara). Barcode indexes were added to samples during seven PCR cycles of template preparation and 550 ng of each library was captured using the SureSelectXT Target Enrichment System (Agilent SureSelect V6). xGen Blocking Oligos (IDT, Iowa, USA) were used following the Takara compatibility manual. Captured targets were subsequently enriched by 11 cycles of PCR with KAPA HiFi HotStart (Kapa Biosystems), with

a Tann of 60° and the following primers, which target generic ends of Illumina adapters: AATGATACGGCGACCACCGAGAT and CAAGCAGAAGACGGCATACGAGAT. Sequencing was carried out in the Illumina NovaSeq 6000 platform at Macrogen.

Genomic tumor and normal DNA WES library construction were performed by exome capture of approximately 20,000 exome sequences of coding genes using SureSelect human All exon V6 kit (Agilent Technologies) and paired-end sequencing was performed on a HiSeq sequencer (Illumina) at Macrogen. The average sequencing depth ranged from 150-300X for each of the individual libraries generated.

Alignments of WES to the reference human genome build hg19 were done using NovoAlign MPI from Novocraft (http://www.novocraft.com/). Duplicates were marked using Picard's MarkDuplicates tool (picard/releases/tag/1.127). Indels realignment and base recalibration were performed according to Genome Analysis Toolkit (GATK) best practices (https://www.broadinstitute.org/gatk/). SAMtools was used to create tumor and normal pileup files.

An mRNA sequencing library was also prepared from tumor biopsy of patients GOI-05, -06 and -07 and patient-derived TCL of patient GOI-07 using TruSeq RNA library prep kit. RNA alignment was performed using STAR. Duplicates were marked using Picard's Mark Duplicate tools. Transcripts per million (TPM) normalization was applied to the raw gene counts obtained from feature counts and used to evaluate gene expression.

Bionformatics analysis to call and filter mutations varied slightly over the execution of the project for pipeline optimization (Table 3). For the analysis of WES data of patients GOI-01, -02, -03, -04, -07, -08, -09 -10, four independent mutation callers (Varscan, SomaticSniper, Mutect and Strelka) were applied to call somatic NSMs according to the following criteria: minimum coverage of 10 reads, minimum four variant reads, greater than 3% VAF and 5X the VAF in normal DNA or having a 0% of VAF in normal DNA and called by two or more callers for SNVs or one for indels and annotated as coding mutation in two of the three annotation data sets (RefGene, University of California, Santa Cruz, Ensembl). While WES data of patients GOI-01, -02, -03 and -04 was analyzed with the first version of the pipeline (v1), an updated version (v2) was used for WES analysis of patients GOI-07, -08, -09 and -10 (Table 3).

Table 3. Source of DNA used to detect NSMs and the version of the pipeline used for WES and clonality analysis

Patient	Cancer type	Source of DNA used to detect NSMs	Pipeline used to detect NSMs and generate TMGs/PPs	Pipeline used for clonality analysis
GOI-01	Breast	TuBx DNA and cfDNA	Pipeline v1	Pipeline v1
GOI-02	Breast	TuBx DNA and cfDNA	Pipeline v1	Pipeline v1
GOI-03	H&N	TuBx DNA and cfDNA	Pipeline v1	Pipeline v1
GOI-04	H&N	TuBx DNA and cfDNA	Pipeline v1	Pipeline v1
GOI-05	CRC	TuBx DNA and cfDNA	Pipeline v3	Pipeline v1
GOI-06	CRC	TuBx DNA	Pipeline v3	-
GOI-07	Ovarian	TuBx DNA	Pipeline v2	-
GOI-08	CRC	TuBx DNA and cfDNA	Pipeline v2	Pipeline v1
GOI-09	Chordoma	TuBx DNA	Pipeline v2	-
GOI-10	Chordoma	TuBx DNA	Pipeline v2	-

A modified version of the pipeline (v3) was used for the analysis of WES data of patients GOI-05 and -06. In this case, the filters applied to identify NSMs were: minimum coverage of 10 reads, minimum four variant reads, greater than 7% tumor VAF. Only SNVs were considered in this analysis, which had to be called for at least two callers. Moreover, RNA sequencing was used to exclude those variants that were not expressed in the tumor.

Prioritization of NSMs for immunological screenings

In patients GOI-01, -02, -03, -04, -07, -09 and -10 all NSMs detected in both DNA sources or only detected in TuBx DNA or cfDNA were tested in immunological screenings. In contrast, in patients GOI-05, -06 and -08 which harbored over 300 NSMs, mutations were prioritized based on HLA binding prediction. Two different HLA prediction algorithms were used: NetMHCCons prediction tool was used for patients GOI-05 and -06 and NetMHCpan version 4.1 was used for patient GOI-08. For patient GOI-05, NSMs exclusively detected in cfDNA were not tested in immunological screenings.

Determination of allele-specific copy number analysis and mutation clustering

In order to enable comparison of clonality among mutations identified in patients GOI-01, -02, -03, -04, -05 and -08, patient data was reanalyzed using v1 of the pipeline and used to perform copy number and clonality (Table 3). The segmented copy number, cellularity and ploidy were determined using Sequenza version 2.1.2 with normal sample as references and hg19 coordinates. The cancer cell fraction (CCF) of each mutation was estimated by integration of the local copy number, tumor purity (obtained from Sequenza) and VAF. The mutations were classified as either clonal or subclonal based on the confidence interval of the CCF. Mutations were defined as clonal if the 95% confidence interval overlapped 1 and subclonal otherwise. All mutations with read depth greater than 4 and VAF greater than 7% were clustered using PyClone version 1.3.0 Dirichlet process clustering. PyClone allows clustering to simply group clonal and subclonal mutations based on their CCF estimates. PyClone was run using 50.000 iterations and a burn-in of 1000.

Ultra low-pass whole-genome sequencing (ULP-WGS) and analysis of cfDNA tumor fraction using ichorCNA

An ULP-WGS from cfDNA libraries was carried out to assess the presence of detectable ctDNA. Constructed libraries were sequenced using 150 bp paired-end run over 1x lane on a NovaSeq6000 (Illumina). Thereafter, ichorCNA was used for the analysis as previously described (222).

Generation of autologous APCs

Autologous B cells were isolated from cryopreserved PBMCs by positive selection using $CD19^+$ microbeads (Miltenyi Biotec) and expanded through CD40-CD40L stimulation by culturing cells for 4-5 days with irradiated NIH3T3 feeder cells constitutively expressing CD40L at 37°C in 5% CO_2 in B-cell medium (Iscove's IMDM media (Gibco) containing 10% human AB serum (Biowest), 100 U/mL Penicillin and 100 µg/mL streptomycin (Lonza), 2 mM L-Glutamine (Lonza) and supplemented with 200 U/mL IL-4 (Peprotech). Cultures underwent up to three consecutive rounds of stimulation and expansion. At day 5-6, B cells were used in co-culture experiments or cryopreserved until use. When used after cryopreservation, B cells were thawed in B-cell medium containing DNAse (Pulmozyme, Roche) 20h before use in co-culture assays.

Alternatively, $CD4^+$ T cells were isolated from PBMCs by positive selection using $CD4^+$ microbeads (Miltenyi Biotec) or FACS and subsequently expanded through a REP as explained above.

Tandem minigenes (TMGs) construction, cloning, *in vitro* transcription of RNA and electroporation

TMGs were constructed following two different strategies. For patients GOI-01, -02, -03, -04, -07, -08, -09 and -10, TMGs were constructed as previously described (265). Briefly, for each nonsynonymous variant identified by WES, we constructed a "minigene", consisting of the mutant amino acid flanked by 12 amino acids of the wild-type protein sequence. Up to 24 minigenes were concatenated to generate a TMG construct. TMG constructs were codon optimized and subcloned into pcDNA3.1 using HindIII and BamHI (New England Biolabs).

The HLA sequences of interest were also cloned into pcDNA3.1 using BamHI and EcoRI containing a Kozak motif upstream of the start codon. HLA-I sequences were obtained from IPD-IMGT/HLA data base and were codon optimized. All TMGs and HLA-I sequence oligonucleotides were supplied by GenScript Biotech (Rijswijk, Netherlands).

One microgram of linearized (NotI; New England Biolabs) TMG plasmid RNA was used as a template to generate *in vitro* transcribed TMG RNA using the HiScribe T7 ARCA mRNA Kit (with tailing) (New England Biolabs) as instructed by the manufacturer. RNA was precipitated using $LiCl_2$ and RNA concentration was measured using a NanoDrop spectrophotometer. RNA was resuspended at 1 µg/mL and stored at -80ºC until use.

For patients GOI-05 and -06, we constructed minigenes for each nonsynonymous variant by placing the mutant amino acid in the middle and flanked by 12 amino acids of the wild-type protein sequence on each side. We concatenated up to 21 minigenes and the linear sequences of each TMG were supplied by Twist Bioscience, CA, USA. Each TMG sequence had a T7 promoter followed by β-globin 5'UTR and a kozak sequence upstream of the start codon and a stop codon followed by 3' β-globin and a unique site of restriction of the BsrD1 restriction enzyme in the 3' end.

For these patients, deconvolution experiments to identify the reactive minigene from a TMG were also performed with DNA fragments encoding for each minigene separately. In this case, each minigene had a T7 promoter followed by β-globin 5'UTR, a kozak sequence and a ubiquitin site upstream of the minigene sequence and a stop codon and the β-globin 3' UTR with the restriction site of the BsrD1 restriction enzyme in the 3' end.

In this case, 200 ng of each construct was used as a template to generate *in vitro* transcribed TMG RNA using the HiScribe T7 ARCA mRNA Kit (with tailing) (New England Biolabs) as instructed by the manufacturer. RNA was precipitated using $LiCl_2$ and RNA concentration was measured using a NanoDrop spectrophotometer. RNA was resuspended at 1 µg/mL and stored at -80ºC until use.

Peptide synthesis and peptide pulsing

The amino acid sequences of 25-mer peptides, each including one NSMs detected by WES were purchased from JPT Peptide Technologies (Berlin, Germany) at crude grade and used for the initial *in vitro* screening of T cells. To validate the reactivities observed in the initial screen, we used high-performance liquid chromatography (HPLC)-purified mutant peptides and their wild-type counterparts purchased from JPT Peptide Technologies or Thermo fisher Scientific (Massachusetts, USA). Autologous APCs (B cells or $CD4^+$ T cells) were harvested, washed and resuspended at $2x10^6$ to $5x10^6$ cells/mL in their corresponding media with 5 µg/mL or 1 µg/mL for long peptides (13-mer to 25-mer) and minimal epitopes, respectively. Peptide pools were used a final concentration of 5 µg/mL per peptide. Long peptides were pulsed overnight while minimal epitopes were only pulsed for 2h. After pulsing, APCs were washed with PBS, resuspended in T-cell medium and immediately used in co-culture assays.

HLA identification and minimal epitope pulsing

HLA haplotypes were inferred from the WES data using the PHLAT algorithm(266). To predict candidate minimal epitopes capable of binding to their autologous HLA-I alleles we used NetMHCpan version 4.1 (267).

Co-culture assays: IFN-γ enzyme-linked immunospot (ELISPOT) assays and detection of activation marker 4-1BB using flow cytometry

T cells were thawed into T-cell medium supplemented with $3x10^3$ IU IL-2 (Proleukin) and DNAse (Pulmozyme, Roche) three to four days before co-incubation with target cells. All co-cultures were performed in the absence of exogenously added cytokines. After 20h of co-culture, cells were stained with an extracellular panel of human-specific antibodies (Table 2) for 30 minutes at 4°C, washed with staining buffer containing PI (1:1000) and acquired in BD FACSCanto™ or BD FACSLyric™. In parallel, IFN-γ secretion was detected using IFN-γ capture and detection antibodies (MABtech technologies) assessed by ELISPOT assay following manufacturer instructions. ELISPOT plates were analyzed and counted in ELISPOT reader. For all the assays, plate-bound OKT3 (1 µg/mL; Biolegend) was used as a positive control. Media and/or autologous APCs electroporated or pulsed with irrelevant TMG or peptides, respectively, were used as negative controls.

For the detection of T-cell responses, from $2x10^4$ to $7.5x10^4$ *ex vivo* expanded TILs, sorted PBLs or enriched populations of tumor-reactive lymphocytes were co-cultured with either $1.5x10^5$ to $2x10^5$ peptide-pulsed or $3x10^5$-$4x10^5$ electroporated autologous APCs (either B cells, or $CD4^+$ T cells). T-cell reactivities were considered positive if: 1) the number of IFN-γ spots were greater than 13 spots and 5 times the amount of the irrelevant control condition or 2)

the number of IFN-γ spots were greater than 50 spots and twice the amount of the irrelevant control condition. Additionally, reactivities had to be observed in at least two independent experiments. Crude peptide preparations were used for screening and the reactivities were further confirmed with HPLC-grade peptides. All experiments were performed at least twice.

Enrichment of tumor-reactive and antigen-specific T lymphocytes

To enrich for tumor-reactive and antigen-specific T cells, either expanded TILs or $CD8^+$ and $CD4^+$ PBLs were co-cultured with an autologous TCL or with autologous APCs either electroporated with TMGs or pulsed with mutated peptides for 20h. $CD3^+CD8^+$ or $CD3^+CD4^+$ cells expressing 4-1BB or OX40 were sorted in BD FACS Aria™ and expanded using a REP as previously specified. The same antibodies used for co-cultures (Table 2) were scaled up and used for sorting $4\text{-}1BB^+$ or $OX40^+$ T cells.

HLA-I restriction

To determine the HLA restriction element of the peptides recognized, COS-7 cells were co-transfected with plasmids encoding the individual HLA molecules and plasmids encoding for TMGs using Lipofectamine 2000 (Life Technologies). After resting overnight, cells were harvested, washed and used as targets in co-culture assays.

TCR sequencing and PBL transduction

The TCR locus was sequenced by multiplex single-cell RNA sequencing of enriched antigen-specific T-cell populations. The samples were multiplexed using TotalSeq™ barcodes. Sequencing was carried out in an Illumina NS6000 with an S1 flowcell and v1 chemistry. For mapping, quantification and clonotype definitions we used cell ranger multi software (version 6.1.1 with vdj_GRCh38_alts_ensembl-5.0.0 as reference). Demultiplexing and subsequent analysis was done in R using the packages Seurat (version 4.0.3) and scRepertoire (version 1.3.5); Seurat::HTODemux was run using default parameters to obtain singlets.

TRA V-J-encoding sequences and TRB V-D-J-encoding sequences were combined to sequences encoding the mouse constant TRA and TRB chains, respectively (268). Mouse constant regions were modified, as previously described (269,270). The full-length TRB and TRA chains were cloned separated by a furin SGSG P2A linker, into pMSGV1 retroviral vector (GenScript). The use of the modified mouse TCR constant regions promotes pairing of the introduced TCR and also facilitates the identification of positively transduced human T cells by flow cytometry using an antibody specific for the mouse TCR-β chain.

To generate transient retroviral-rich supernatants, the retroviral vector MSGV1 encoding the antigen-specific TCR and the plasmid encoding for the envelope (RD114) were co-

transfected into the retroviral packaging cell line 293GP cells, which had been plated the day prior to transfection, using Lipofectamine 2000 (Life Technologies). Retroviral supernatants were harvested at 24 and 48 hours after transfection, centrifuged to discard cell debris and diluted 1:1 with DMEM medium (Gibco) and then centrifuged onto retronectin-coated (10 µg/mL, Takara), non-tissue culture-treated 24-well plates at 2000 g for 2h at 32ºC. Donor PBMCs, which had been activated in T-cell medium supplemented with 50 ng/mL anti-CD3 and 300 IU/mL IL-2 during 3 days before retroviral transduction, were harvested, added onto the plates containing the retrovirus and centrifuged for 10 minutes at 300g. Activated T cells were transduced overnight, removed from retronectin-coated plates and further cultured in T-cell medium containing IL-2. Cells were typically assayed 10-14 days post-retroviral transduction.

Media for cell culture and other reagents

T-cell medium comprised a 1:1 mix of RPMI 1640 with L-glutamine (Lonza) and AIM-V (Thermo Fisher Scientific) supplemented with 100 U/mL penicillin, 100 µg/mL streptomycin, 12.5 mM HEPES (Thermo Fisher Scientific) and 5% human serum (prepared in-house) without cytokines. T-cell medium was supplemented with IL-2 as specified in each section. Staining buffer contained PBS supplemented with 0.5% FBS and 2 mM EDTA (Sigma-Aldrich). B-cell medium comprised IMDM (Quality Biological Inc.) supplemented with 10% human AB serum (processed in-house), 100 U/mL penicillin, 100 µg/mL streptomycin, 2 mM L-glutamine and 200 U/mL IL-4. IFN-γ was purchased from PeproTech.

Correlation and statistical analyses

Correlation analyses were performed by the non-parametric Spearman rank-order correlation test. To evaluate statistical significance, Shapiro-Wilk normality test was performed and depending on the data distribution, either one-way ANOVA, parametric Tukey's or non-parametric Kruskal-Wallis, Mann-Whitney or Dunn's multiple comparisons test were used, as indicated. Significance was set at $p \leq 0.05$. All analyses were performed with GraphPad PRISM 8 software and R version 4.2.2 using tableOne package (The R Foundation for Statistical Computing, Vienna, Austria).

Data analysis and visualization

All flow cytometry data were analyzed with FlowJo software v7.6.5 and v10 (Tree Star). Data were represented with GraphPad PRISM 8 software and SPICE software, NIH, Bethesda, USA.

Results

1. Design of a minimally-invasive strategy to identify and isolate neoantigen-specific T cells exclusively using peripheral blood

The main goal of this thesis was to investigate the feasibility and reproducibility of identifying neoantigen-reactive T cells exclusively using peripheral blood. Simultaneously, we also wanted to understand the advantages and limitations of such an approach compared to the standard, which relies on candidate neoantigen identification from tumor DNA and *ex vivo* expansion of TILs to detect neoantigen-reactive T cells. To this end, we conceived the strategy depicted in Figure 14 which consisted in: (1) the identification of tumor NSMs by performing WES of cfDNA and comparison to the standard source, TuBx DNA, (2) the biomarker-guided isolation of circulating T-cell populations as well as obtention of *ex vivo* expanded TILs and (3) subsequent screening of the T-cell populations for neoantigen recognition.

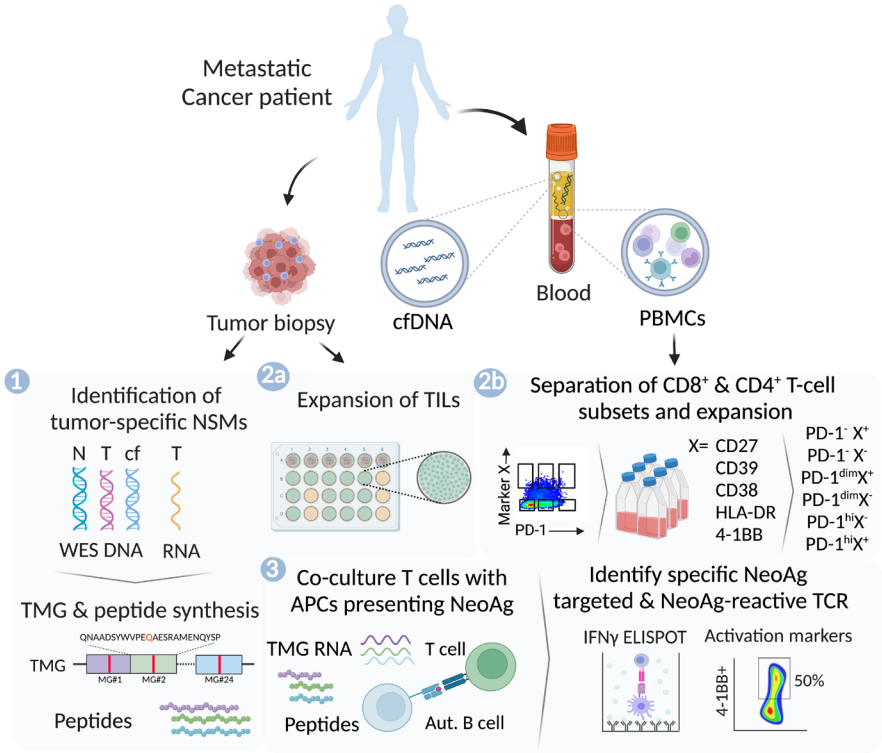

Figure 14. Schematic representation of the personalized strategy used to identify and isolate neoantigen-specific T lymphocytes from peripheral blood of patients with epithelial cancers. Tumor biopsies and leukapheresis or blood samples were obtained from each cancer patient included in the study. Tumor biopsies were used to isolate TuBx DNA and to expand TILs. Either leukapheresis or

blood samples were used to isolate PBMCs and extract genomic DNA. Plasma samples were collected for a fraction of patients and were used for cfDNA extraction. (1) To identify tumor NSMs, WES of TuBx DNA, cfDNA and normal DNA was performed. In the cases where we were able to isolate RNA from tumor biopsies, we also performed RNA sequencing. Somatic mutations detected in TuBx DNA, cfDNA or in both DNA sources were used to design and generate TMGs. Synthetic peptides were purchased and pooled together to generate PPs. (2a) Tumor biopsies were cut in tumor fragments and cultured separately in high dose IL-2 to expand TILs. (2b) In parallel, $CD8^+$ and $CD4^+$ T-cell populations were isolated from circulation based on the differential expression of PD-1 alone or in combination with selected cell-surface markers including CD27, CD38, CD39, HLA-DR and 4-1BB by FACS ($PD\text{-}1^-$, $PD\text{-}1^{dim}$, $PD\text{-}1^{hi}$, $PD\text{-}1^-$marker X^-, $PD\text{-}1^-$marker X^+, $PD\text{-}1^{dim}$marker X^-, $PD\text{-}1^{dim}$marker X^+, $PD\text{-}1^{hi}$marker X^-, $PD\text{-}1^{hi}$marker X^+). T cells were *ex vivo* expanded for 14 days using REP. (3) The sorted subpopulations and TILs were tested for neoantigen recognition via a co-culture with autologous B cells electroporated or pulsed with TMGs and PPs, respectively. Tumor recognition was assessed 20h later by measuring the upregulation of the activation markers 4-1BB or OX40 on $CD8^+$ or $CD4^+$ T cells by flow cytometry, and by measuring IFN-γ production using an IFN-γ ELISPOT assay.

All cancer patients included in the study had metastatic solid tumors that progressed on chemotherapy and/or radiotherapy but were immunotherapy naïve. From each patient included (n=10), we received a tumor biopsy that was used to isolate TuBx DNA and to *ex vivo* culture and expand TILs. We also received either a leukapheresis or a peripheral blood sample that was used to isolate PBMCs and extract normal DNA. In addition, for six of ten patients, a plasma sample was collected from which cfDNA was extracted. This enabled us to study and compare candidate neoantigen identification in cfDNA and TuBx DNA in a total of six patients. Moreover, we explored the detection of neoantigen-reactive PBLs and TILs in all ten patients.

To detect putative neoantigens, we performed WES of cfDNA and of TuBx DNA and compared to matched DNA from non-malignant PBMCs to identify putative tumor NSMs (Figure 14.1). Thereafter, minigenes encoding for the NSMs detected were synthesized. Briefly, each 25-mer minigene encoded for one NSM identified by WES flanked by 12 amino acids of the wild-type sequence on each side. Up to 25 minigenes were concatenated to generate each TMG and multiple TMGs were designed and constructed to encode for all or a selection of NSMs identified. Additionally, 25-mer peptides were synthesized and grouped into PPs matching the composition of the TMGs (*i.e.* PP-1 contained the same 25-mers as those encoded by TMG1). In some cases, we also generated a minimal epitope pool (MEP) composed of the top 30 best peptides predicted to bind to the patient HLA alleles based on NetMHCPan4.0.

In parallel, we expanded TIL lines from independent tumor fragments derived

from one tumor biopsy (Figure 14.2a) and we sorted circulating T lymphocytes from peripheral blood based on the differential expression of selected biomarkers and expanded them *in vitro* using a REP (Figure 14.2b). To test whether the sorted circulating T-cell populations or *ex vivo* expanded TILs were capable of recognizing neoantigens, autologous *ex vivo* expanded B cells expressing the patient-specific HLA-I and HLA-II molecules, were used as target cells. B cells were either electroporated with TMGs or pulsed with PPs or MEP. Thereafter, these autologous B cells potentially presenting neoantigens were co-cultured with circulating T-cell subsets or expanded TILs to evaluate neoantigen recognition (Figure 14.3). T-cell responses were assessed by measuring the secretion of IFN-γ and the upregulation of activation cell-surface markers by flow cytometry (*i.e.* 4-1BB for $CD8^+$ and 4-1BB or OX40 for $CD4^+$ T cells). Whilst IFN-γ ELISPOT is a highly sensitive technique capable of detecting very infrequent T-cell responses, flow cytometric analysis measures activation regardless of the specific cytokine released and can distinguish between $CD8^+$ or $CD4^+$ reactivities. Thus, both readouts were used to better characterize the T-cell responses.

2. WES of cfDNA identifies putative tumor NSMs in patients with epithelial cancers

We first evaluated the potential of cfDNA as a source to identify putative tumor NSMs. To this end, we extracted cfDNA from plasma samples of six cancer patients with distinct epithelial tumors, including breast and H&N cancer and CRC (Table 4).

Table 4. Number of NSMs detected by WES of distinct sources of DNA

Patient	Cancer type	Concentration (ng/ml)	Number of NSMs in cfDNA only (%)	Number of NSMs in TuBx only (%)	Number of NSMs in TuBx and cfDNA (%)
GOI-01	Breast	14.04	87 (46.28%)	31 (16.49%)	70 (37.23%)
GOI-02	Breast	6	86 (43.22%)	111 (55.78%)	2 (1.01%)
GOI-03	H&N	11.8	55 (23.81%)	176 (76.19%)	0 (0%)
GOI-04	H&N	18.8	73 (70.19%)	16 (15.38%)	15 (14.42%)
GOI-05	CRC	10.2	535 (20.60%)	721 (27.76%)	1341 (51.64%)
GOI-08	CRC	6.2	144 (37.99%)	130 (34.30%)	105 (27.70%)

The amount of cfDNA extracted from plasma varied among patients, ranging from 6 to 18.8 ng/mL. We next performed WES of matched cfDNA and TuBx DNA and compared the NSMs identified in the two DNA sources. WES of cfDNA identified a variable number of somatic NSMs in all evaluated patients, ranging from 55 to 1876 and representing from 23.81% to up to 84.61% of the total NSMs identified in each patient (Figure 15; Table 4). Importantly, all patients except for GOI-03 contained mutations that were shared between cfDNA and TuBx DNA, validating that at least a fraction of the NSMs detected in cfDNA derived from tumor. The frequency of shared NSMs between cfDNA and TuBx DNA was highly variable and differed from 0% to 51.64% of the total NSMs identified (Figure 15; Table 4). Of note, in some patients we detected more somatic mutations in cfDNA than in TuBx DNA. Although this could be indicative of sequencing artifacts, which has previously been reported (271,272), it is also compatible with our hypothesis that WES of cfDNA could potentially capture tumor heterogeneity, detecting somatic mutations expressed either in other regions of the same tumor or in other tumor lesions. Overall, these results suggest that cfDNA is a viable source to identify putative neoantigens and the number of mutations is highly variable from patient to patient.

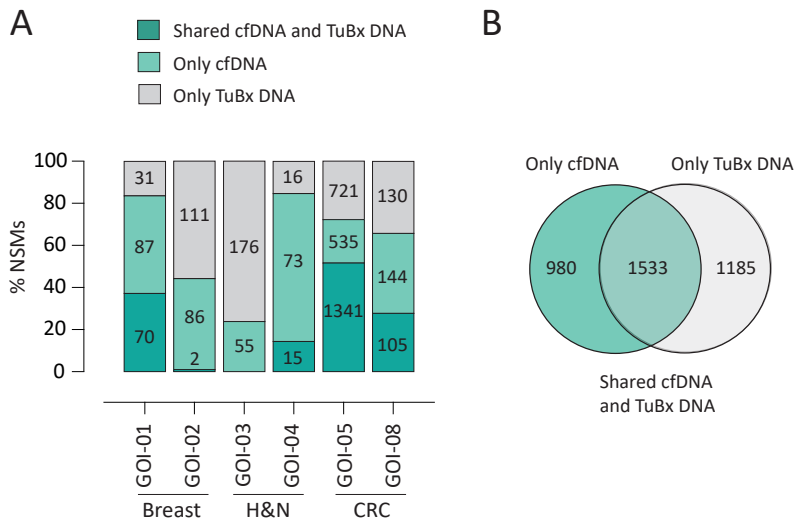

Figure 15. Frequency of NSMs detected in the distinct sources of tumor DNA in the six epithelial cancer patients studied. Three categories of mutations were defined: 1) NSMs shared: those identified both in TuBx and cfDNA, 2) NSMs TuBx: those uniquely identified in TuBx DNA and 3) NSMs cfDNA: those uniquely identified in cfDNA. (**A**) Frequency of NSMs shared, only detected in cfDNA or only detected in TuBx DNA in each of the six patients analyzed. The absolute number of mutations of each category is depicted in the bars. (**B**) Venn diagram showing the absolute number of NSMs detected only in cfDNA, only in TuBx or shared between the two DNA sources. The number of NSMs from each category is the sum of the NSMs detected in each of the patients analyzed.

2.1. Generation of TMGs and PPs of candidate neoantigens for immunological screenings

As explained in section 1, we wanted to evaluate the ability of sorted circulating T cells and expanded TILs to recognize neoantigens. To this end, we used WES from TuBx DNA and, when available, cfDNA to identify tumor-specific NSMs and subsequent candidate neoantigens of the ten patients included in the study.

The total number of candidate neoantigens varied widely among patients and tumor types, ranging from 27 to 1068 NSMs (Table 5). Using the aforementioned TMG and PP strategy, we were able to interrogate all candidate neoantigens in seven out of ten patients studied but not in the three CRC patients (*i.e.* GOI-05, GOI-06 and GOI-08), which harbored over 300 mutations (Table 5). This is due to TMG and PP screening cost and sample limitations. For these patients with such high mutational load, 205, 182 and 254 candidate neoantigens, respectively, were prioritized based on binding affinity to the corresponding HLA alleles and were included in TMGs and PPs.

In patient GOI-07 in which WES of TuBx DNA only detected 27 NSMs, cancer

Table 5. Information of somatic NSMs detected, candidate neoantigens or cancer germline antigens evaluated, and the reagents generated to screen for T-cell recognition in all cancer patients studied

Patient	Tumor type	Total somatic NSMs	Candidate neoantigens evaluated[a]	Number of candidate neoantigens in				Cancer Germline antigens tested[b]	Minigenes /25-mers included in TMGs/PPs	TMG and PP generated
				cfDNA only	TuBx only	TuBx& cfDNA	TCL only			
GOI-01	Breast	154	133	33	28	72	n.e.	-	16-17	8
GOI-02	Breast	157	118	31	86	1	n.e.	-	14-15	8
GOI-03	H&N	192	191	24	167	0	n.e.	-	16-21	10
GOI-04	H&N	62	64	33	15	16	n.e.	-	13-20	4
GOI-05	CRC	1068	226	0	130	96	n.e.	-	16-21	11
GOI-06	CRC	1302	182	n.e.	182	n.e.	n.e.	-	2-21	11
GOI-07	Ovarian	27	23	n.e.	20	n.e.	3	16	11-12	2
GOI-08	CRC	381	255	60	51	144	n.e.	-	10-25	12
GOI-09	Chordoma	44	50	n.e.	50	n.e.	n.e.	-	16-17	3
GOI-10	Chordoma	71	77	n.e.	77	n.e.	n.e.	-	12-22	4

[a]Epitopes were selected for screening as explained in detail in Methods. [b]Cancer germline antigens were selected based on their gene transcript expression level (>30% gene percentile) assessed by RNA sequencing. n.e. not evaluated

germline antigens were also included in the T-cell screening to increase the probabilities of detecting T-cell responses against tumor antigens. In total, 16 cancer germline antigens were selected based on their gene transcript expression level (*i.e.* >30% gene percentile) as assessed by tumor RNA sequencing (Appendix Table 1). The autologous TCL of patient GOI-07 was also derived in our laboratory and was subsequently included in the screening to evaluate the tumor reactivity of circulating T-cell subsets and expanded TILs.

3. Phenotypic characterization of PBLs from cancer patients and healthy donors

As mentioned in the introduction, the persistent exposure of T cells to their cognate antigen during chronic infection and cancer induces, among many other pathways, the continuous co-expression of co-stimulatory and co-inhibitory receptors leading T cells into a dysfunctional state (51). This differential expression of certain biomarkers has been explored to identify neoantigen-specific or tumor-reactive TILs. Phenotypic studies of TIL infiltrating different cancer types have shown that $CD8^+$ T cells frequently display co-expression of multiple biomarkers associated with activation/exhaustion and some of them have been demonstrated to be preferentially expressed by neoantigen-specific TILs (73,74,138,191,192,195,196). Although there are also reports of biomarkers, such as PD-1 expression or T-cell effector memory markers, that can be used to enrich for circulating neoantigen-specific T cells (153,154,273), their frequency following biomarker selection is still low. Thus, we reasoned that by combining the expression of multiple biomarkers we could improve the selection efficiency of circulating neoantigen-specific T cells.

3.1. T cells expressing high levels of PD-1 co-express cell-surface receptors associated with activation and/or exhaustion

We wanted to explore and better define what cell-surface receptors could better distinguish circulating tumor- and neoantigen-reactive T cells from irrelevant cells. For this, we phenotypically characterized circulating T lymphocytes from a cohort of 24 patients with different epithelial tumors that had received on average 1.6 lines of treatment but were immunotherapy naïve and compared them with circulating $CD8^+$ and $CD4^+$ T cells from healthy individuals. We reasoned that cell-surface markers that were preferentially co-expressed in cancer patients could be good candidates to further explore their ability to enrich for tumor reactivity.

We previously reported PD-1 as a biomarker that could guide the enrichment of circulating T cells capable of recognizing neoantigens (152,153). Because of this, we stratified $CD4^+$ and $CD8^+$ T cells into three populations based on PD-1 expression levels: cells lacking PD-1 expression ($PD\text{-}1^-$) and cells expressing intermediate ($PD\text{-}1^{dim}$) or high ($PD\text{-}1^{hi}$) levels of PD-1 (defined as the top 2% of PD-1-expressing cells). The frequency of $CD8^+$ and $CD4^+$ T cells expressing $PD\text{-}1^{hi}$ in cancer patients and healthy donors only represented a minor fraction of the total pool of $CD8^+$ and $CD4^+$ T cells ranging from 0.27%-1.36%±0.26 and from 0.37-1.48%±0.27, respectively (Figure 16A).

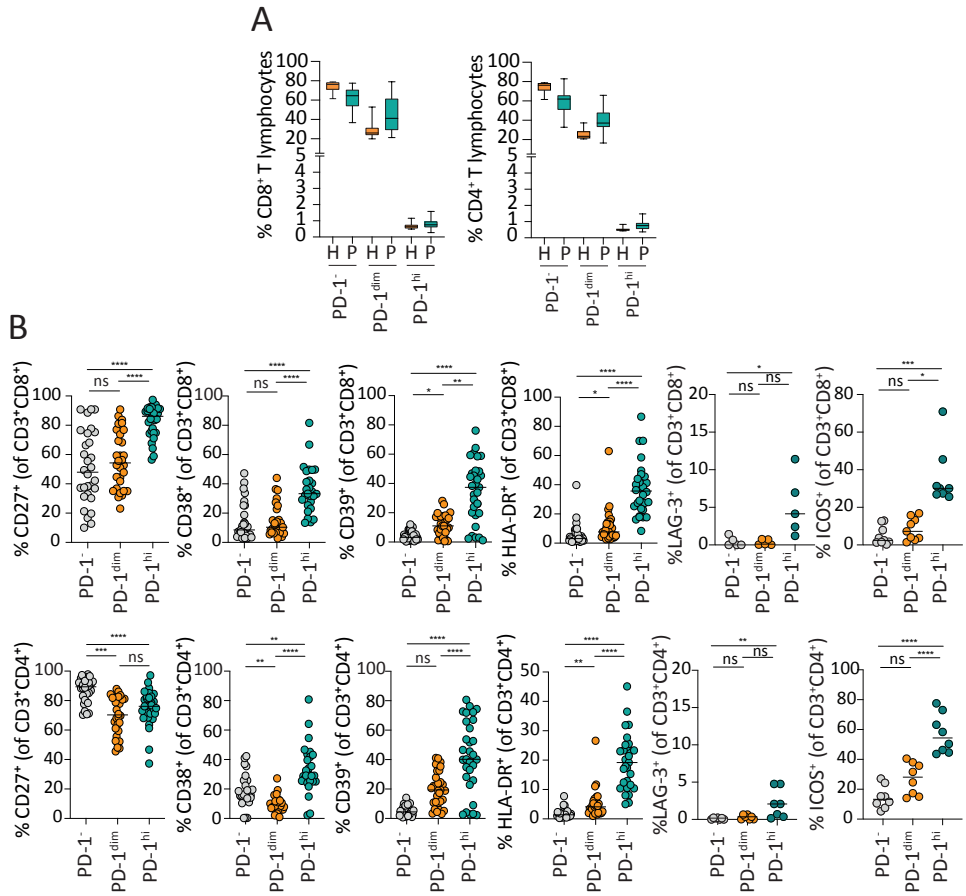

Figure 16. Phenotypic characterization of circulating T cells in cancer patients. $CD8^+$ and $CD4^+$ PBLs were stratified in three populations based on PD-1 expression into $PD\text{-}1^-$, $PD\text{-}1^{dim}$ and $PD\text{-}1^{hi}$. **(A)** Box plot showing the mean ± SD of the frequency of $CD8^+$ and $CD4^+$ T cells of cancer patients (P) and healthy donors (H) expressing high ($PD\text{-}1^{hi}$) or intermediate ($PD\text{-}1^{dim}$) levels of PD-1 or not expressing PD-1 ($PD\text{-}1^-$). **(B)** Frequency of $CD8^+$ (top) and $CD4^+$ (bottom) T cells expressing the selected cell-surface markers CD27, CD38, CD39, HLA-DR, LAG-3 and ICOS within the three PD-1-expressing populations. Statistical significance was analyzed by unpaired non-parametric Dunn's multiple comparisons test. *p<0.05, **p<0.001, ***p<0.0001; ns, not significant.

Next, we measured the cell-surface expression of biomarkers known to be associated with T-cell activation/exhaustion in the context of chronic infection and cancer including co-stimulatory (CD27 and ICOS) and co-inhibitory (LAG-3) receptors, markers of activation (CD38 and HLA-DR) and the ectoenzyme involved in adenosine production (CD39) within the PD-1^{-}, PD-1^{dim} and PD-1^{hi} T-cell populations.

In cancer patients, the expression of the selected biomarkers was significantly higher in CD8^{+} and CD4^{+} PD-1^{hi} T-cell subsets compared to PD-1^{dim} and PD-1^{-}, except for CD27 in CD4^{+} T cells in which the highest expression was observed in the PD-1^{-} population (Figure 16B). We also determined the co-expression pattern of four of the biomarkers studied (*i.e.* CD27, CD38, CD39 and HLA-DR) within the three populations stratified based on PD-1 expression by performing Boolean gating analysis. While the cumulative frequency of T cells co-expressing three or four markers accounted for 27.54% and 16.85% of CD8^{+} and CD4^{+} PD-1^{hi} T cells, respectively, it did not exceed 4% of CD8^{+} and CD4^{+} PD-1^{dim} and PD-1^{-} T-cell populations (Figure 17; Appendix Table 2).

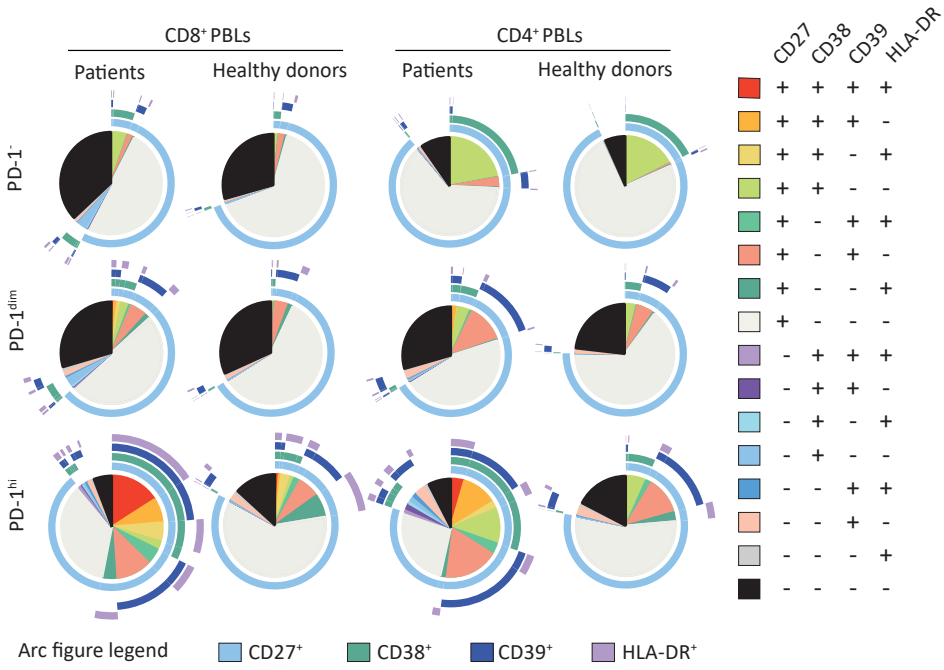

Figure 17. Co-expression profile of CD27, CD38, CD39 and HLA-DR according to PD-1 expression levels in CD8^{+} and CD4^{+} PBLs of cancer patients and healthy donors. Boolean analysis of co-expression were performed after stratifying CD8^{+} and CD4^{+} T cells in three populations based on PD-1 expression levels (*i.e.* PD-1$^{-/dim/hi}$). Boolean analysis was imported into SPICE for final data analysis and

visualization. Pie charts display the frequency of the distinct subpopulations expressing 0, 1, 2, 3 and 4 of the cell-surface markers studied. The expression of each specific cell-surface receptor is represented by the arcs depicted around the pie chart.

Thus, although $CD8^+$ and $CD4^+$ $PD\text{-}1^{hi}$ T cells represent a small fraction of all circulating lymphocytes, this subset accumulated higher levels of co-inhibitory/co-stimulatory receptors as compared to the $PD\text{-}1^{dim}$ and $PD\text{-}1^-$ populations and exhibited the highest frequency of T cells co-expressing three or four of the biomarkers studied.

Next, we also compared the expression level and co-expression profile of the selected biomarkers in $CD8^+$ and $CD4^+$ T cells according to their PD-1 expression level in cancer patients and healthy individuals. As in cancer patients, $CD8^+$ and $CD4^+$ $PD\text{-}1^{hi}$ T-cell subsets from healthy donors also contained the highest frequency of T cells co-expressing three or four markers compared to $PD\text{-}1^{dim}$ and $PD\text{-}1^-$ populations (Figure 17). Nevertheless, when comparing the co-expression pattern of the four biomarkers in the $CD8^+$ and $CD4^+$ $PD\text{-}1^{hi}$ of healthy individuals and cancer patients, substantial differences were observed. While cumulative frequency of T cells co-expressing three or four markers in cancer patients accounted for 27.54% and 16.85% of $CD8^+$ and $CD4^+$ $PD\text{-}1^{hi}$ T cells, respectively, it only represented the 6.06% and 2.2% of $CD8^+$ and $CD4^+$ $PD\text{-}1^{hi}$ T cells in healthy individuals (Figure 17; Appendix Table 2). When we looked at the relative increase in the frequency of each population in cancer patients compared to healthy individuals, we observed that multiple T-cell subsets co-expressing two, three or four biomarkers were more represented in cancer patients (Figure 18). More specifically, the populations that were more significantly increased in $CD8^+$ and $CD4^+$ T cells from cancer patients were expressing CD39 and CD38. Moreover, in the case of $CD8^+$ PBLs, the population co-expressing these two biomarkers together with HLA-DR was also significantly increased in cancer patients.

Altogether, despite their paucity, circulating $CD8^+$ and $CD4^+$ $PD\text{-}1^{hi}$ PBLs populations in cancer patients showed an overall upregulation of biomarkers typically associated with T-cell activation and dysfunction and a unique co-expression profile that was clearly different from that observed in the other populations defined by the PD-1 expression level. This profile was also different from that observed in healthy individuals. Thus, these results prompted us to study the neoantigen or tumor reactivity of circulating T-cell subsets expressing a combination of these cell-surface receptors in more detail.

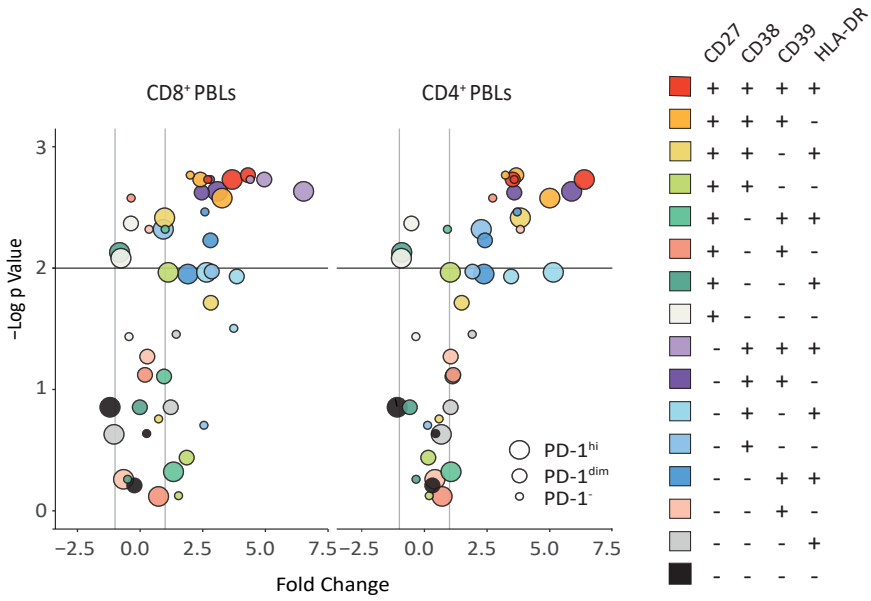

Figure 18. The frequency of CD8⁺ and CD4⁺ T-cell populations, generally co-expressing three or four biomarkers, is increased in cancer patients compared to healthy individuals. Volcano plot showing the relative increase in the frequency of PD-1⁻, PD-1^{dim} and PD-1^{hi} in CD8⁺ and CD4⁺ lymphocytes displaying the co-expression patterns in cancer patients compared to healthy donors.

3.2. Isolation of circulating T-cell subsets based on the expression of activation/exhaustion biomarkers

The identification of neoantigen-specific T lymphocytes from the peripheral blood of cancer patients is particularly difficult because their frequency in circulation is relatively low (151,160). To overcome this limitation, we selected circulating T-cell subpopulations expressing selected biomarkers to increase the odds of detecting them. Based on our own experiments and the literature, the biomarkers we decided to pursue were CD27, CD38, CD39, HLA-DR and 4-1BB in combination with PD-1 (138,192,273–275). The selected T-cell populations were expanded *ex vivo* for 14 days and used in immunological screenings to evaluate their reactivity to tumor antigens including neoantigens and, in one case, cancer germline antigens. When available, we also evaluated the reactivity against the autologous TCL.

In order to isolate CD8⁺ and CD4⁺ PBLs, we used the gating strategy depicted in Figure 19. We set an initial gate on total lymphocytes based on their size and complexity.

After gating on single and live cells, we gated on $CD3^+$ and subsequently on $CD8^+$ and $CD4^+$. Thereafter, within $CD3^+CD8^+$ and $CD3^+CD4^+$ cells, we set the gates needed for sorting specific populations based on the differential expression of PD-1 and the selected biomarkers. Hence, $CD8^+$ and $CD4^+$ T cells were sorted into three populations based on PD-1 expression levels as performed for the phenotypic analysis: cells lacking PD-1 expression ($PD\text{-}1^-$) and cells expressing intermediate ($PD\text{-}1^{dim}$) or high ($PD\text{-}1^{hi}$) levels of PD-1. In this case, $PD\text{-}1^{hi}$ cells were defined as the top 1.5% of PD-1-expressing cells as we wanted to be more restrictive at the time of cell sorting. Finally, T cells were also sorted based on PD-1 expression in combination with CD27, CD38, CD39, HLA-DR and 4-1BB. For some patients, we also sorted $CD8^+$ and $CD4^+$ T cells based on the expression of CD39 alone (*i.e.* $CD39^+/CD39^-$). In total, up to 35 $CD8^+$ and 35 $CD4^+$ T-cell subpopulations were sorted from peripheral blood and subsequently expanded using a REP. These T cells were then used in immunological screenings to evaluate T-cell responses as explained in section 1.

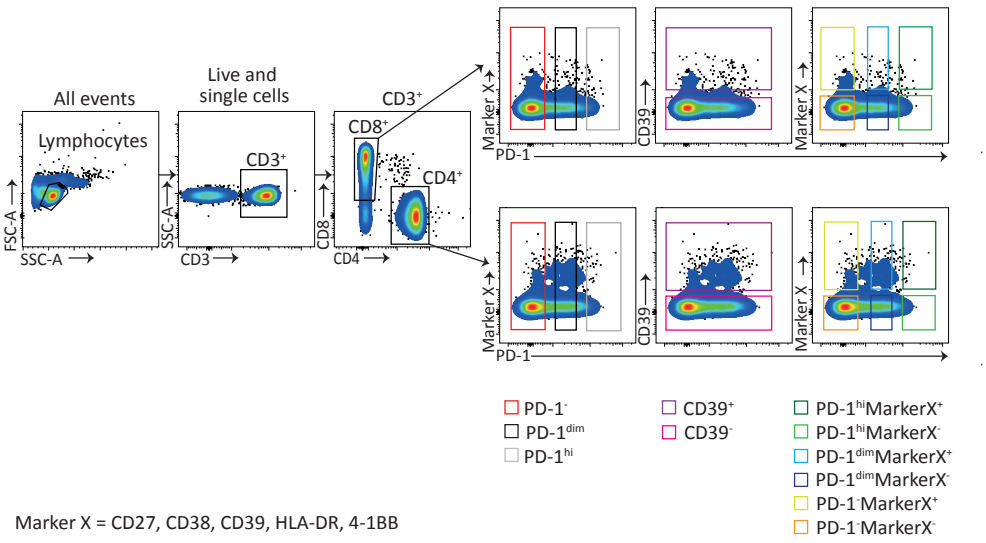

Figure 19. FACS of $CD8^+$ and $CD4^+$ T-cell populations from peripheral blood of cancer patients. Representative flow cytometry dot plots displaying the gating strategy used for sorting $CD8^+$ and $CD4^+$ PBLs from cancer patients based on the expression of PD-1 (*i.e.* $PD\text{-}1^{-/dim/hi}$), CD39 ($CD39^{+/-}$) or the co-expression of PD-1 with $CD27^{+/-}$, $CD38^{+/-}$, $CD39^{+/-}$, $HLA\text{-}DR^{+/-}$ and $4\text{-}1BB^{+/-}$. Following cell separation, cells were expanded for 14 days through a REP. The gates used for sorting lymphocytes with either unique or combined expression of markers are displayed in different colors.

4. Functional screening for neoantigen recognition of an extensive panel of sorted circulating T-cell subsets

To evaluate whether we could improve the enrichment of $CD8^+$ and $CD4^+$ circulating neoantigen-specific T cells by biomarker-based sorting beyond the enrichment obtained with PD-1 alone (152,153), we isolated an extensive number of circulating T-cell subpopulations following the gating strategy shown in section 3.2 and evaluated their ability to recognize neoantigens by immunological screenings. These analyses were performed with circulating T lymphocytes from three patients with metastatic tumors: one patient with breast cancer (*i.e.* GOI-01) and two patients with H&N cancer (*i.e.* GOI-03 and -04).

Table 6 summarizes the number of T-cell subsets sorted from peripheral blood, NSMs identified and the corresponding TMGs and PPs generated to investigate the reactivity to all NSMs identified for each of the patients analyzed. T-cell subsets and TILs were co-cultured with autologous APCs modified to express candidate neoantigens and T-cell responses were assessed by measuring IFN-γ release by ELISPOT and upregulation of the activation marker 4-1BB (for $CD8^+$ and $CD4^+$) and OX40 (for $CD4^+$) by flow cytometry. If $CD8^+$ or $CD4^+$ neoantigen reactivities were detected, neoantigen-reactive T cells were enriched by FACS to better characterize the specificity of the reactive cells.

Table 6. Reagents generated to screen for neoantigen reactivities in selected cancer patients

Patient	Cancer type	Biomarker-based sorted T-cell subsets from leukapheresis		Total number of putative neoantigens screened[a]	Putative neoantigens screened			Number of TMG and PP synthesized
		$CD8^+$	$CD4^+$		cfDNA only	TuBx DNA only	TuBx DNA & cfDNA	
GOI-01	Breast	33	33	133	33	28	72	8
GOI-03	H&N	35	35	191	24	167	0	10
GOI-04	H&N	35	35	64	33	15	16	4

[a]Putative NSMs were defined by: minimum coverage of 10 reads, minimum four variant reads, greater than 3% VAF and supported by at least one variant caller for indels or two variant callers for SNVs.

4.1. Identification of circulating neoantigen-specific T cells in a patient with metastatic breast cancer

The first patient studied was GOI-01, a patient with metastatic $ER^{+}PR^{-}HER2^{-}$ breast cancer. We sorted 33 $CD8^{+}$ and 33 $CD4^{+}$ T-cell subpopulations from peripheral blood that were *in vitro* expanded and tested for neoantigen recognition (Table 6). WES of TuBx DNA and cfDNA identified a total of 133 NSMs. All NSMs were synthesized as minigenes or 25-mer peptides and concatenated to generate eight TMGs or grouped into eight PPs. Additionally, a MEP containing the 30 minimal epitopes with the highest binding score for the patient's HLA alleles according to NetMHCPan4.0, was generated and included in the functional immunological screening.

4.1.1. Co-expression of PD-1^{hi} with CD27, CD39, HLA-DR or lacking 4-1BB expression identifies $CD8^{+}$ circulating neoantigen-specific T cells in patient GOI-01

Figure 20 shows the results of the functional screening of 33 $CD8^{+}$ PBL subsets sorted and expanded from patient GOI-01 upon co-culture with autologous B cells expressing neoantigens. The upper, medium and lower panels depict the results of PD-1^{hi}, PD-1^{dim} and PD-1^{-} T-cell populations, respectively. As previously mentioned, T-cell activation was measured by the secretion of IFN-γ (left panels) and the upregulation of 4-1BB by flow cytometry (right panels). We detected neoantigen-specific $CD8^{+}$ T cells recognizing a mutated peptide encoded by TMG1 and included in the MEP in distinct circulating T-cell subsets, all expressing PD-1^{hi} either alone or co-expressed with CD27, CD39, HLA-DR, or negative for 4-1BB expression (Figure 20, top). Although we observed that $CD8^{+}$ PD-$1^{dim}CD39^{+}$ recognized TMG7, this reactivity was not reproducible and, thereby, was not considered a positive hit. Thus, no reactivities were observed in any of the PD-1^{dim} nor PD-1^{-} $CD8^{+}$ PBL subsets (Figure 20, middle and bottom). Of note, based on the upregulation of the activation marker 4-1BB by flow cytometry, the frequency of neoantigen-specific T cells within each subpopulation varied notably (Figure 20, right). The population co-expressing PD-1^{hi} and CD39 showed the greatest frequency of neoantigen-reactive lymphocytes with up to 33.4% and 40% of $CD8^{+}$ 4-$1BB^{+}$ cells after co-culture with B cells electroporated with TMG1 RNA or pulsed with the MEP, respectively.

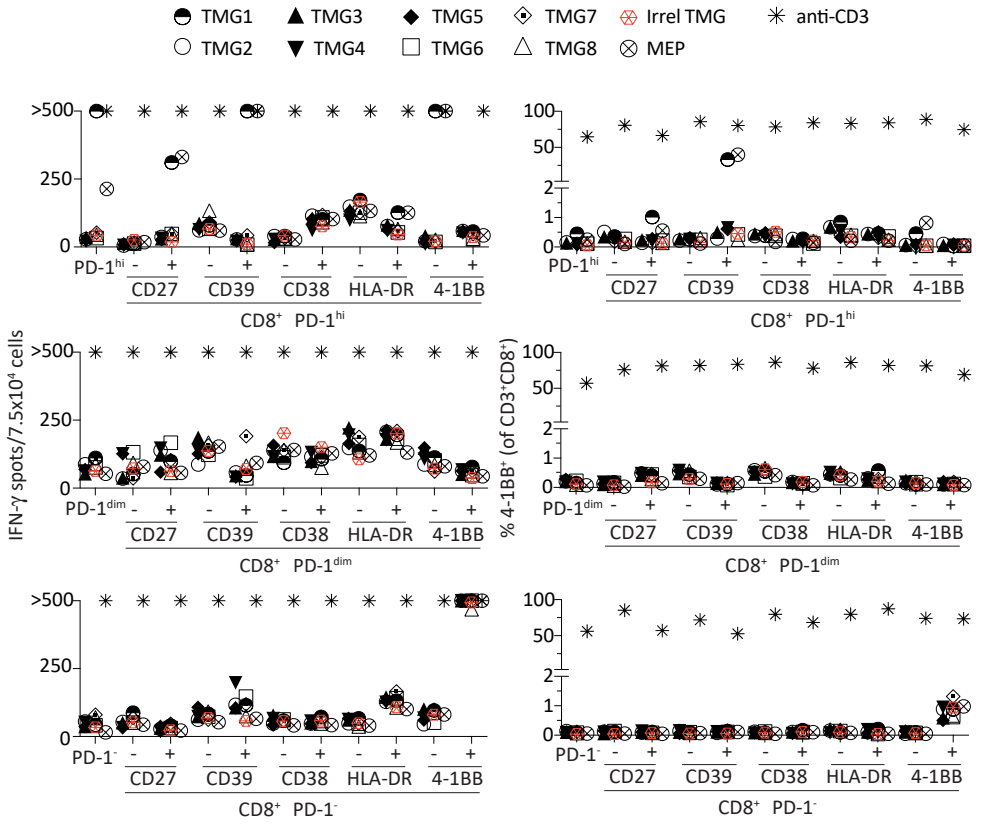

Figure 20. Screening of CD8⁺ PBL subsets for neoantigen recognition. Autologous B cells electroporated with TMGs encoding for neoantigens or pulsed with a MEP were co-cultured with the 33 CD8⁺ T-cell populations sorted from peripheral blood of patient GOI-01. After 20h, T-cell responses were evaluated by measuring the number of IFN-γ spots using IFN-γ ELISPOT (left) and upregulation of 4-1BB by flow cytometry analysis (right). Data is representative from two independent experiments.

To identify the mutated peptide/s encoded in TMG1 recognized by CD8⁺ T cells, we performed deconvolution assays with the TMG1-reactive T-cell populations. Briefly, T-cell subsets containing TMG1-reactive cells were co-cultured with autologous B cells pulsed with individual 25-mer peptides included in TMG1/PP-1. As observed in Figure 21, all T-cell populations containing TMG1-reactive T cells recognized the same 25-mer (i.e. PP-1-12) encoding for the mutated peptide KIAA1524$_{p.S57I}$. CD8⁺ PD-1^{hi}HLA-DR⁺ also showed recognition of an additional mutated peptide encoded by TMG1/PP-1 (*i.e.* CDH24$_{p.G59W}$) but this reactivity was not confirmed when testing for reactivity to the high-performance liquid chromatography (HPLC) purified version of the mutated peptide.

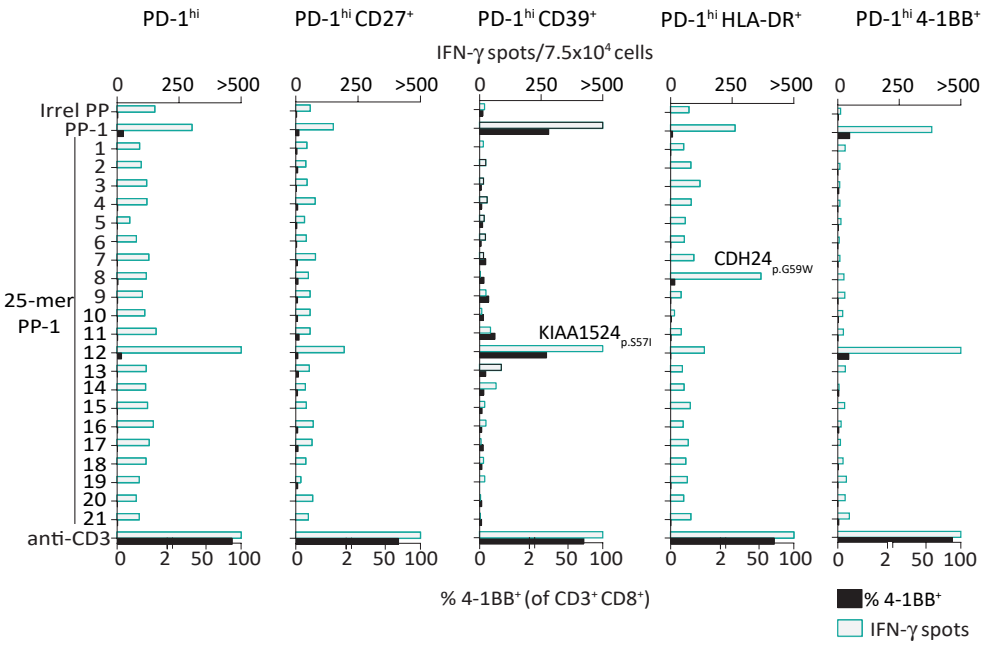

Figure 21. CD8⁺ T-cell populations reactive against TMG1 and MEP recognize a neoantigen derived from KIAA1524$_{p.S57I}$ identified by WES of TuBx DNA and cfDNA. To determine the mutation specifically recognized, 25-mer peptides encoding the individual NSMs contained in TMG1 were independently pulsed onto autologous B cells at 5 µg/mL overnight. B cells were then washed and co-cultured with the CD8⁺ T-cell subsets that previously showed reactivity against TMG1. After 20h, T-cell responses were evaluated by measuring IFN-γ production and upregulation of 4-1BB by flow cytometry as indicated in the x axis. The specific mutated protein and amino acid change are annotated. Autologous B cells pulsed with an irrelevant PP and anti-CD3 were used as negative and positive controls, respectively. Data is representative from two independent experiments.

Overall, T cells expressing PD-1^{hi}, either alone or in combination with CD27, CD39, HLA-DR or T cells expressing PD-1^{hi} but not 4-1BB enriched for CD8⁺ neoantigen-specific T cells from peripheral blood of patient GOI-01.

4.1.2. Characterization of neoantigen-specific T-cell responses in CD8⁺ PBLs

We next characterized the neoantigen specificity of the CD8⁺ T-cell response detected in the CD8⁺ PD-1^{hi}CD39⁺ population, containing the greatest frequency of neoantigen-reactive T cells and compared to the CD8⁺ PD-1^{hi} population. To this end, we enriched for KIAA1524$_{p.S57I}$-specific lymphocytes from both populations by FACS of 4-1BB⁺ T lymphocytes after co-culture with autologous B cells pulsed with KIAA1524$_{p.S57I}$ 9-mer,

which was included in the MEP and expanded them *in vitro* through a REP.

We used this strategy to prevent loss of neoantigen recognition, which can sometimes occur after long-term culture of T cells, particularly if cells are expanded through a REP with non-specific stimulation.

Figure 22 shows the 4-1BB expression before and after sorting CD8$^+$ 4-1BB$^+$ T cells

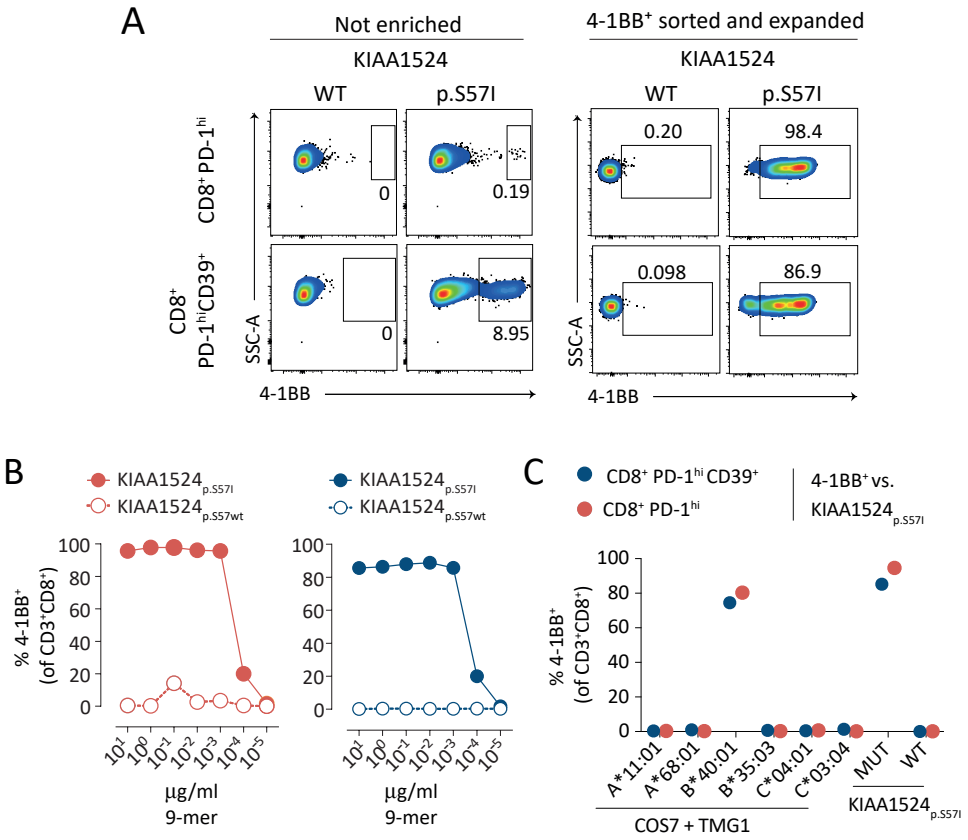

Figure 22. Enrichment and characterization of CD8$^+$ PD-1^{hi} and CD8$^+$ PD-1^{hi}CD39$^+$ T cells reactive against KIAA1524$_{p.S57I}$. (**A**) KIAA1524$_{p.S57I}$-reactive T cells detected in the PBL CD8$^+$ PD-1^{hi} and CD8$^+$ PD-1^{hi}CD39$^+$ subpopulations were enriched by FACS based on 4-1BB expression after a 20h co-culture with B cells pulsed with KIAA1524$_{p.S57I}$ mutated peptide. Cells were expanded *ex vivo* for 14 days. Plots show gates used for 4-1BB$^+$ sorting (left) and the frequency of 4-1BB expression on CD8$^+$ T cells following co-culture with autologous B cells pulsed with KIAA1524$_{p.S57I}$ mutated peptide after expansion (right). Autologous B cells pulsed with the wild-type version of KIAA1524$_{p.S57I}$ peptide were used as negative control of T-cell activation. (**B**) Reactivity of enriched KIAA1524$_{p.S57I}$-specific T-cell populations derived from PBL CD8$^+$ PD-1^{hi} (left) and CD8$^+$ PD-1^{hi}CD39$^+$ (right) to B cells pulsed with serial dilutions of the wild-type (KIAA1524$_{p.S57wt}$) or mutant (KIAA1524$_{p.S57I}$) peptides. T-cell reactivity was evaluated by measuring upregulation of 4-1BB expression after 20h. (**C**) To determine the HLA restriction element, COS7 cells were co-transfected with the indicated individual HLA-I alleles and TMG1 encoding for KIAA1524$_{p.S57I}$ and were co-cultured with the enriched populations from (A). T-cell activation was assessed by measuring upregulation of 4-1BB by flow cytometry. Data from (B-C) is representative from two independent experiments.

upon co-culture with autologous B cells pulsed with the mutated KIAA1524$_{p.S57I}$ minimal epitope. After selection and expansion of 4-1BB-sorted cells, the frequency of KIAA1524$_{p.S57I}$–reactive cells within CD8$^+$ PD-1^{hi} and CD8$^+$ PD-1^{hi}CD39$^+$ T-cell populations increased from 0.19% and 8.95% to 98.4% and 86.9%, respectively, indicating successful enrichment of neoantigen-reactive T cells (Figure 22A). Importantly, KIAA1524$_{p.S57I}$–reactive CD8$^+$ T cells specifically recognized the mutated version of KIAA1524$_{p.S57I}$ peptide but not the wild-type counterpart (Figure 22B) and its recognition was restricted to HLA-B*40:01 (Figure 22C). The circulating neoantigen-reactive T cells were capable of detecting down to 0.1 ng/mL of peptide, supporting a high avidity for neoantigen recognition.

4.1.3. Identification of KIAA1524$_{p.S57I}$ -specific TCRs from CD8$^+$ PD-1^{hi} and PD-1^{hi}CD39$^+$ PBLs

In order to further study the diversity and magnitude of the KIAA1524$_{p.S57I}$ response in the CD8$^+$ PD-1^{hi}CD39$^+$ and CD8$^+$PD-1^{hi} PBLs of patient GOI-01, we aimed to evaluate the TCR repertoire and isolate and clone the TCRs specific for KIAA1524$_{p.S57I}$ in these two different populations. For this, we performed single-cell RNA sequencing of the neoantigen-specific CD8$^+$ T-cell populations enriched by FACS. These analyses revealed multiple dominant TCR clonotypes in the KIAA1524$_{p.S57I}$-reactive PD-1^{hi} and PD-1^{hi}CD39$^+$ PBL subsets (Figure 23A). Interestingly, only one TCR was shared between the two populations, which was the most frequent TCR in both of them (*i.e.* TRB-CDR3-CASSVTGGTAYEQYF). To evaluate whether the TCRs identified displayed specific recognition of KIAA1524$_{p.S57I}$, we cloned the top four and three most dominant αβ TCR pairs detected in the KIAA1524$_{p.S57I}$–enriched CD8$^+$ PD-1^{hi}CD39$^+$ or CD8$^+$PD-1^{hi} PBLs, respectively, into a retroviral vector that was then used to transduce PBLs with each of the TCRs. Each TCR was constructed using the murine TRA and TRB constant region to reduce mispairing of the endogenous TCR and enabling us to specifically track the TCR-transduced cells using an anti-mouse TRB antibody.

As shown in Figure 23B, all evaluated TCRs recognized the mutated KIAA1524$_{p.S57I}$ peptide, but not the wild-type counterpart. These results confirmed that all the different clonotypes identified were neoantigen-specific, highlighting the polyclonal nature of both KIAA1524$_{p.S57I}$-specific CD8$^+$PD-1^{hi} and CD8$^+$PD-1^{hi}CD39$^+$ populations isolated from peripheral blood.

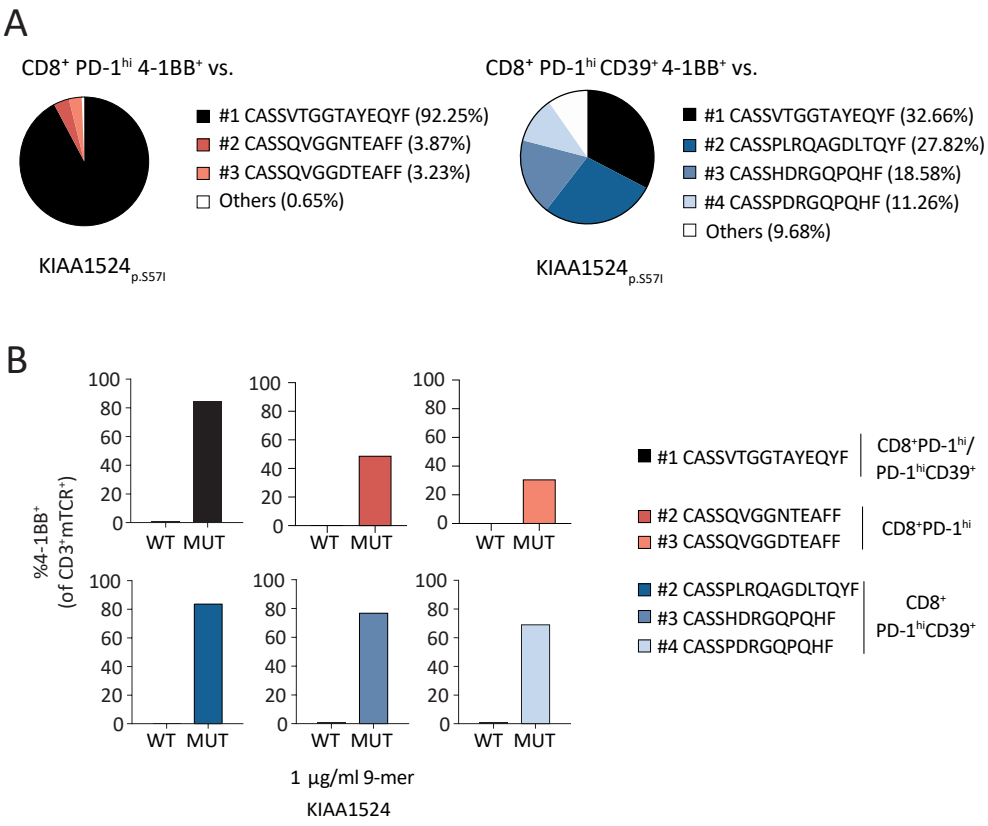

Figure 23. Single-cell RNA sequencing of CD8⁺4-1BB⁺neoantigen-specific lymphocytes identified multiple dominant TCRs reactive against KIAA1524$_{p.S57I}$ peptide in breast cancer patient GOI-01. (**A**) Pie charts show the frequency of the most dominant TCRs identified by single-cell RNA sequencing of neoantigen-reactive T-cell populations enriched from CD8⁺ PD-1^{hi} (left) and PD1^{hi}CD39⁺ (right) T-cell subsets. (**B**) Reactivity of gene-engineered PBLs with dominant KIAA1524$_{p.S57I}$ -specific candidate TCRs. Frequency of 4-1BB⁺ cells gated on CD3⁺mTCR⁺ after 20h co-culture with B cells pulsed with the mutated and wild-type minimal epitope of KIAA1524$_{p.S57I}$. Sequences of the CDR3 locus of the TCR-β chain of each TCR are annotated. Data from (B) is representative from two independent experiments.

4.1.4. CD4⁺ PBL subsets co-expressing PD-1^{hi} and CD39$^{+/-}$ contained neoantigen-specific T cells in patient GOI-01

We also investigated whether CD4⁺ T-cell subsets isolated from the peripheral blood of patient GOI-01 harbored neoantigen reactivities by applying the same strategy used to identify neoantigen-specific CD8⁺ T cells explained in section 1 and at the beginning of section 4. We observed that of the 33 PBL subsets isolated from GOI-01, the CD4⁺PD-1^{hi} T cells expressing different levels of CD39 (*i.e.* PD-1^{hi}CD39⁺ and PD-1^{hi}CD39^{-}) contained neoantigen-reactive T cells against PP-2 and PP-4, respectively, as shown by the secretion of IFN-γ (Figure 24, top).

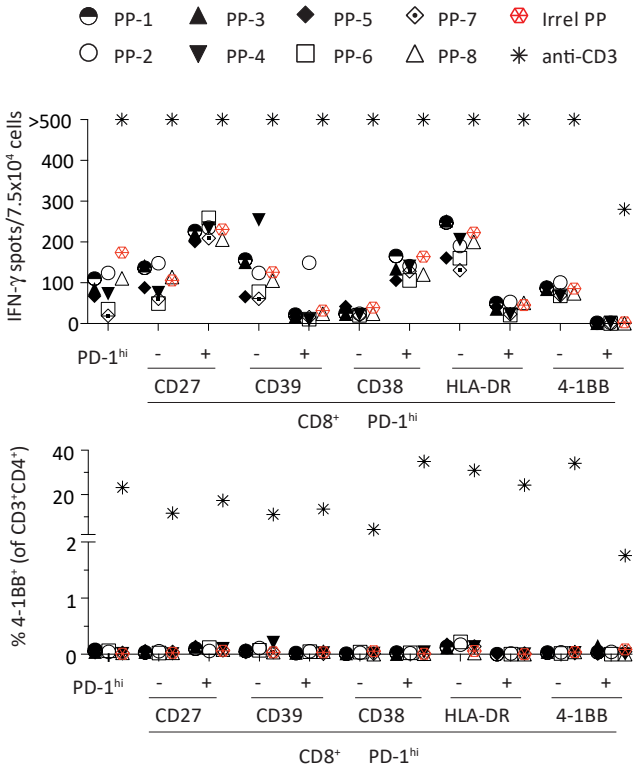

Figure 24. PD-1^{hi}CD39$^{+/-}$ CD4^{+} PBL subsets contained neoantigen-specific T cells recognizing two distinct neoantigens in breast cancer patient GOI-01. Autologous B cells pulsed with PP encoding for neoantigens were co-cultured with the 33 CD4^{+} T-cell populations sorted from peripheral blood of patient GOI-01. After 20h, T-cell responses were evaluated by measuring the number of IFN-γ spots using IFN-γ ELISPOT assay (top) and the upregulation of 4-1BB by flow cytometry analysis (bottom). Data is representative from two independent experiments.

However, the reactivities were not above the detection level when using 4-1BB upregulation as a read-out, at least using such small number of effector cells, suggesting these reactivities were rare (Figure 24, bottom). CD4^{+} PD-1^{hi} T cells did not show recognition of any neoantigen tested. Moreover, in line with the results of CD8^{+} T cells, no reactivities were detected neither in PD-1^{dim} nor in PD-1^{-} CD4^{+} T-cell populations (Appendix Figure 1).

Next, we enriched for PP-reactive T cells. Although, according to our screening, expression of 4-1BB on the reactive T-cell subsets was rare, we were able to sort and expand 4-1BB^{+} T cells after co-culture with PP-pulsed autologous B cells as explained in section 4.1.2, possibly because we used a higher number of T cells for FACS (Figure 25A). Thereafter, long peptides encoding the individual mutated peptides contained in PP-2 or in PP-4 were independently tested to determine the specific mutated peptide recognized within the pool. CD4^{+} PD-1^{hi}CD39^{+} PP-2- and CD4^{+} PD-1^{hi}CD39^{-} PP-4-enriched populations

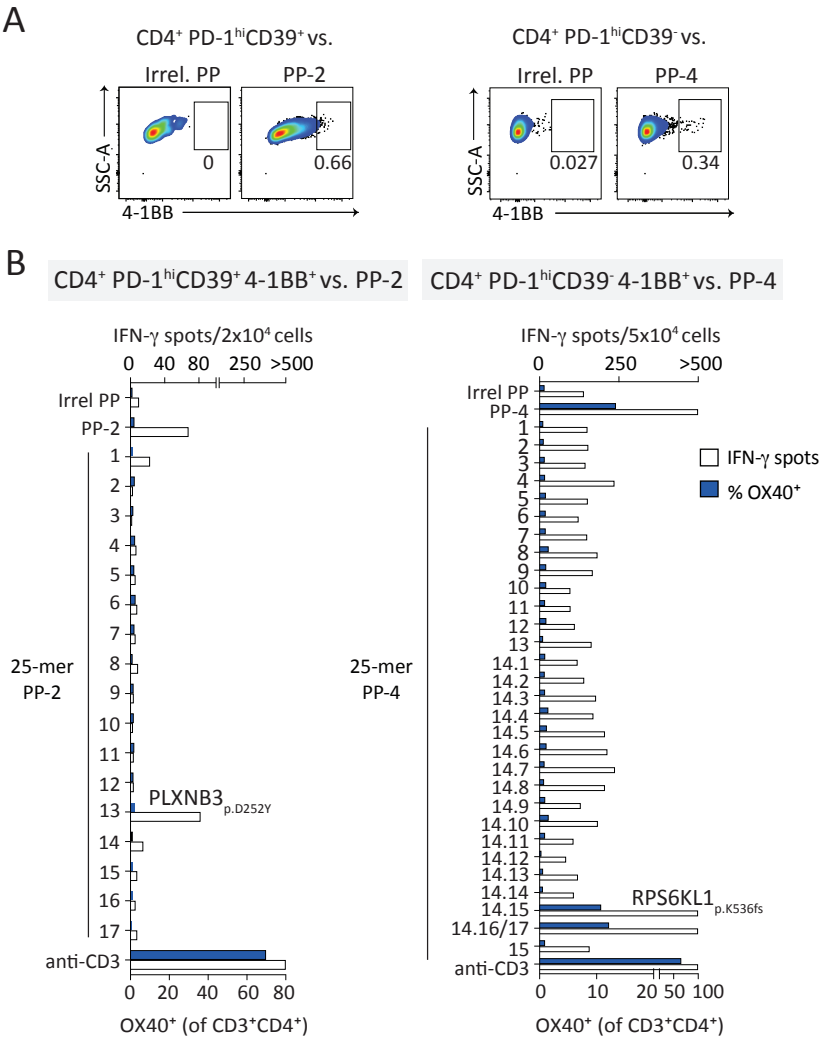

Figure 25. Neoantigen-specific CD4⁺ T cells enriched from CD4⁺ PD-1^{hi}CD39⁺ and PD-1^{hi}CD39⁻ PBL subsets each recognized one unique neoantigen derived from PLXNB3$_{p.D252Y}$ and RPS6KL1$_{p.K536fs}$ identified using WES of TuBx and cfDNA. (**A**) Flow cytometry plots showing the expression of 4-1BB of CD4⁺PD-1^{hi}CD39⁺ and PD-1^{hi}CD39⁻ upon co-culture with autologous B cells pulsed with the PP-2 and PP-4, respectively and an irrelevant PP that was used as a control. Neoantigen-reactive T cells were enriched by FACS of CD4⁺OX40⁺ T cells and were subsequently *ex vivo* expanded for 14 days. (**B**) Reactivity of the specified circulating enriched CD4⁺ T-cell populations to autologous B cells pulsed with individual 25-mers from PP-2 (left) and PP-4 (right), respectively. Reactivity was measured by IFN-γ ELISPOT assay and the upregulation of 4-1BB by flow cytometry as indicated in the axis. The specific mutated protein and amino acid change are noted. Autologous B cells pulsed with an irrelevant PP were used as a negative control. Data from (B) is representative from two independent experiments.

recognized the mutated peptides PLXNB3$_{p.D252Y}$ and RPS6KL1$_{p.K536fs}$, respectively (Figure 25B). This demonstrated that the CD39⁻ and CD39⁺ CD4⁺ T-cell subsets within the PD-1^{hi}

population, each contained circulating $CD4^+$ T cells recognizing one distinct neoantigen.

Of note, the mutated peptide recognized by $CD4^+$ PP-4-enriched T cells arose from a mutation causing a frameshift, which generated a foreign peptide of 185 amino acids until the next stop codon. Thus, we had to generate 17 25-mers having an overlap of 11 amino acids between them to cover the entire mutated sequence in the screening. This explains the observed recognition of both peptide 14.15 and the pool of 14.16 and 14.17 from PP-4 as they are consecutive 25-mers covering contiguous mutated regions of $RPS6KL1_{p.K536fs}$ (Figure 25B, right).

4.1.5. Isolation of neoantigen-specific TCRs from enriched $CD4^+$ reactive T cells by single-cell TCR sequencing

To evaluate the TCR clonotypic frequency and neoantigen specificity of the enriched PP-2- and PP-4-reactive $CD4^+$ T-cell populations, we obtained their TCR sequences by single-cell RNA sequencing of the TCR genes. In the case of $CD4^+$ PD-$1^{hi}CD39^+$ T cells enriched for PP-2 recognition, a clear dominant TCR clonotype was detected in 98.79% of the T cells sequenced, followed by two other TCR clonotypes detected at a frequency of 0.56% and 0.32% (Figure 26A, left). A higher TCR diversity was observed in the PP-4-enriched $CD4^+$ PD-$1^{hi}CD39^-$ population with at least two expanded TCR clonotypes detected at 52.08% and 20.94% (Figure 26A, right). To evaluate whether the enriched TCRs were mutation-reactive, we followed the same strategy as for $CD8^+$ by cloning and transducing PBLs with the most frequent TCRs (explained in section 4.1.3). Given that we detected a clear dominant TCR in the PP-2-enriched population but the reactivity against the individual mutated peptide was very low (Figure 25B, left; Figure 26A; left), we reasoned that the most expanded clonotype might not be specific for the mutated peptide $PLXNB3_{p.D252Y}$. Thus, we decided to also clone the second and the third most frequent TCR that only accounted for 0.56% and 0.32% of the total lymphocytes sequenced to increase the odds of finding the TCR of interest. In the case of PP-4-enriched $CD4^+$ PD-$1^{hi}CD39^-$ T cells, we also synthesized and cloned the two most frequent TCRs.

Upon immunological testing of the TCR-transduced cells, we identified two neoantigen-specific TCRs, one recognizing the mutated peptide $PLXNB3_{p.D252Y}$ and the other recognizing $RPS6KL1_{p.K536fs}$ (Figure 26B). In the two cases, the TCRs were mutation-specific since TCR-transduced cells recognized the peptide containing the mutation, but not the wild-type counterpart. Of note, the most dominant TCRs of the two populations

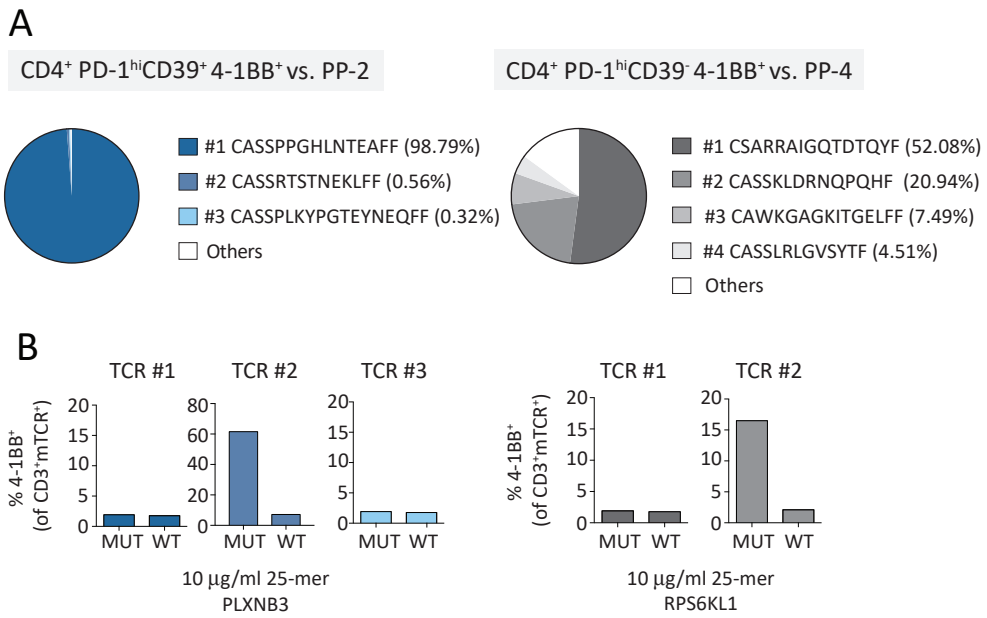

Figure 26. Single-cell TCR sequencing of neoantigen-reactive enriched CD4⁺ T-cell populations identified two TCRs recognizing neoantigens. (**A**) Pie charts show the frequency of the most dominant TCRs identified by single-cell TCR sequencing of neoantigen-reactive T-cell populations enriched from CD4⁺ PD-1^{hi}CD39⁺ (left) and PD1^{hi}CD39⁻ (right) T-cell subsets. (**B**) Reactivity of gene-engineered PBLs with the most frequent PLXNB3$_{p.D252Y}$ -specific (left) and RPS6KL1$_{p.K536fs}$-specific (right) candidate TCRs. Frequency of 4-1BB⁺ cells gated on CD3⁺mTCR⁺ after 20h co-culture with B cells pulsed with the mutated and wild-type PLXNB3$_{p.D252Y}$ and RPS6KL1$_{p.K536fs}$ peptides is plotted. Data from (B) is representative from two independent experiments.

sequenced were not neoantigen-specific.

Overall, our results showed that the selection of CD4⁺ T cells co-expressing high levels of PD-1 and CD39$^{+/-}$ enriched for neoantigen-reactive CD4⁺ T cells. Unexpectedly, we did not observe any neoantigen reactivity within the PD-1^{hi} T-cell population despite both PD-1^{hi}CD39⁺ and PD-1^{hi}CD39⁻ T-cell subsets contained neoantigen-reactive T cells. These discrepancies might be due to two reasons. First, it is plausible that although being sorted at the beginning, the neoantigen-specific T cells in the PD-1^{hi} population were outgrown by bystander T cells during the expansion after sorting, rendering them undetectable in the subsequent immunological screenings. Second, it is important to consider that infrequent populations are more affected by random and small sampling, which can lead to the lack of detection of rare neoantigen reactivities existing in specific T-cell populations.

4.2. Selection of PBLs co-expressing PD-1^{hi} and CD39 reproducibly enriches for CD8$^+$ and CD4$^+$ circulating neoantigen-reactive T cells in three cancer patients

In addition to patient GOI-01, we studied two additional patients with H&N cancer using the same strategy to identify circulating neoantigen-specific T cells. For these two patients, we sorted CD8$^+$ and CD4$^+$ T cells based on the expression of CD39 alone (*i.e.* CD39$^+$/CD39$^-$) in addition to the 33 CD8$^+$ and 33 CD4$^+$ PBL subsets, as with GOI-01 (Table 6). WES from cfDNA and TuBx DNA led to the identification of 191 and 64 NSMs in patients GOI-03 and GOI-04, respectively. All NSMs were included in TMGs and PPs and were used in immunological screenings to evaluate T-cell responses.

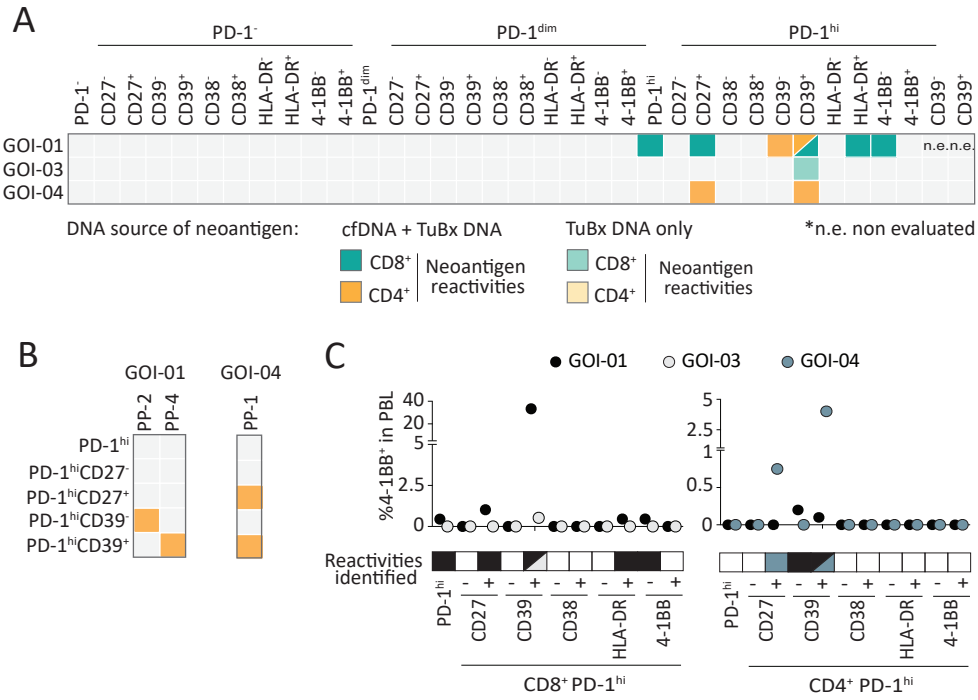

Figure 27. Summary of neoantigen reactivities detected in circulating CD8$^+$ and CD4$^+$ T-cell subsets of three patients with breast or H&N cancers. (**A**) Heat map showing the neoantigen reactivities detected in the different CD8$^+$ and CD4$^+$ T-cell subpopulations sorted by the expression of PD-1, CD39 or the co-expression of PD-1 with CD27, CD38, CD39, HLA-DR and 4-1BB. Screenings were carried out after *ex vivo* expansion of each population. Green and orange shaded cells indicate CD8$^+$ and CD4$^+$ neoantigen reactivities, respectively. The DNA source where neoantigens were detected is also annotated. (**B**) Heat map showing CD4$^+$ neoantigen reactivities identified in patient GOI-01 and -04 circulating T-cell subsets. (**C**) Frequency of neoantigen-reactive T cells as measured by 4-1BB upregulation detected in each of the peripheral blood CD8$^+$ (left) and CD4$^+$ (right) PD-1^{hi} T-cell subsets from the three patients studied. Only the frequencies of populations recognizing neoantigens are shown. Data from (C) is representative from two independent experiments. n.e. not evaluated.

Similar to patient GOI-01, in patients GOI-03 and GOI-04 only $CD8^+$ and $CD4^+$ T lymphocytes expressing PD-1^{hi} contained neoantigen-reactive T cells, as opposed to PD-1^{dim} and PD-1^- T-cell populations (Figure 27A; Appendix Figure 2 and 3). In addition, the selection of $CD8^+$ and $CD4^+$ T cells expressing PD-1^{hi} did not capture several of the reactivities identified in smaller T-cell subsets derived from this population (Figure 27A). In contrast, $CD8^+$ PBLs expressing PD-$1^{hi}CD39^+$ and $CD4^+$ PBLs expressing PD-1^{hi} $CD39^{+/-}$ captured all neoantigen reactivities identified in the three patients studied (Figure 27A-B). We also determined the frequency of neoantigen-reactive T cells within each T-cell population. In all cases where the same neoantigen reactivity was detected in more than one T-cell population, $CD8^+$ and $CD4^+$ T cells co-expressing PD-1^{hi} and CD39 displayed the highest frequency of neoantigen-specific T cells in two of three patients studied (Figure 27C).

Altogether, these results from the screening of an extensive number of T-cell subsets from three patients showed that the co-expression of PD-1^{hi} and CD39 displayed a promising ability to enrich for circulating neoantigen-specific T cells beyond what was observed with PD-1^{hi} alone. These results highlight the importance of combining two markers to enhance the identification of tumor-reactive T cells from peripheral blood of cancer patients.

4.3. WES of cfDNA identified all neoantigens targeted by PBLs in patients harboring NSMs shared between TuBx DNA and cfDNA in the three patients studied

Next, we wanted to determine the DNA source where the neoantigens targeted by circulating T-cell populations were identified. As explained in section 2.1, for these three patients (*i.e.* GOI-01, -03 and -04) we performed WES of cfDNA in addition to TuBx DNA and detected NSMs that were either shared with TuBx DNA or only found in cfDNA. In patients GOI-01 and -04, all neoantigens targeted by $CD8^+$ and $CD4^+$ T-cell populations were detected in cfDNA but also in TuBx DNA (Figure 27A). In contrast, the neoantigen recognized by $CD8^+$ T cells in patient GOI-03 was exclusively detected in TuBx DNA. Given that NSMs shared between the two sources of DNA were only detected in patients GOI-01 and -04, but not in patient GOI-03, our data suggested that WES of cfDNA identified neoantigens preferentially in those patients having a certain overlap between TuBx DNA and cfDNA.

Overall, we were able to identify neoantigen reactivities in two of three patients by exclusively using peripheral blood. In patient GOI-01 and -04, we identified circulating neoantigen-reactive T cells targeting three and one different neoantigens, respectively, completely overcoming the need for a tumor biopsy. This is important since in a sizable proportion of cases, access to tumor tissue may not be feasible or only a small biopsy would be obtained, which could hinder the detection of neoantigen-specific T cells.

5. Validation of PD-1 and CD39 as biomarkers to identify neoantigen-reactive PBLs in patients with metastatic epithelial tumors

Based on the results obtained in section 4, we wanted to further explore the ability of the combined expression of PD-1 and CD39 to reproducibly detect and enrich for circulating neoantigen-specific PBLs. Moreover, we wanted to exploit whether this combination could also be used to enrich for neoantigen-specific circulating $CD4^+$ and $CD8^+$ T cells in patients with other epithelial tumors. For this purpose, seven additional patients with distinct epithelial tumors (*i.e.* breast cancer, CRC, ovarian cancer and chordoma) were evaluated.

5.1. Peripheral blood sorted T-cell populations and detection of candidate neoantigens

We screened $CD8^+$ and $CD4^+$ PBLs sorted according to PD-1 or CD39 expression alone or by the co-expression of both markers for neoantigen recognition. A total of 11 $CD8^+$ and 11 $CD4^+$ T-cell subsets were obtained except for patient GOI-10, from which single marker $CD39^{+/-}$ populations could not be sorted. The number of NSMs identified by WES of TuBx DNA and, when available, cfDNA, ranged from 27 to 1068 (Table 5). The number of putative neoantigens included in each TMG/PP is shown in Table 5. As explained in section 1.2, for patient GOI-07 (ovarian cancer), in which only 27 NSMs were detected, we also screened for recognition of 16 cancer germline antigens selected on the basis of gene transcript expression (*i.e.* >30% gene percentile) as assessed by RNA sequencing (Appendix Table 1). In addition, for this patient, we also evaluated the recognition of the autologous TCL that was previously established in our laboratory.

In total, using the personalized immunological screening detailed in section 1, we were able to identify circulating T cells targeting tumor antigens in eight out of ten

patients screened (Figure 28 and 31; Table 7; Appendix Figure 4-6). More specifically, we detected a total of eight and seven tumor antigens recognized by distinct CD8⁺ and CD4⁺ T-cell populations, respectively.

5.2. Selection of CD8⁺ T cells expressing PD-1^{hi}CD39⁺ enriches for neoantigen- and tumor-reactive circulating T lymphocytes

In the case of CD8⁺ T cells, we were able to identify CD8⁺ PBLs capable of recognizing tumor antigens in six out of ten patients studied (Figure 28A).

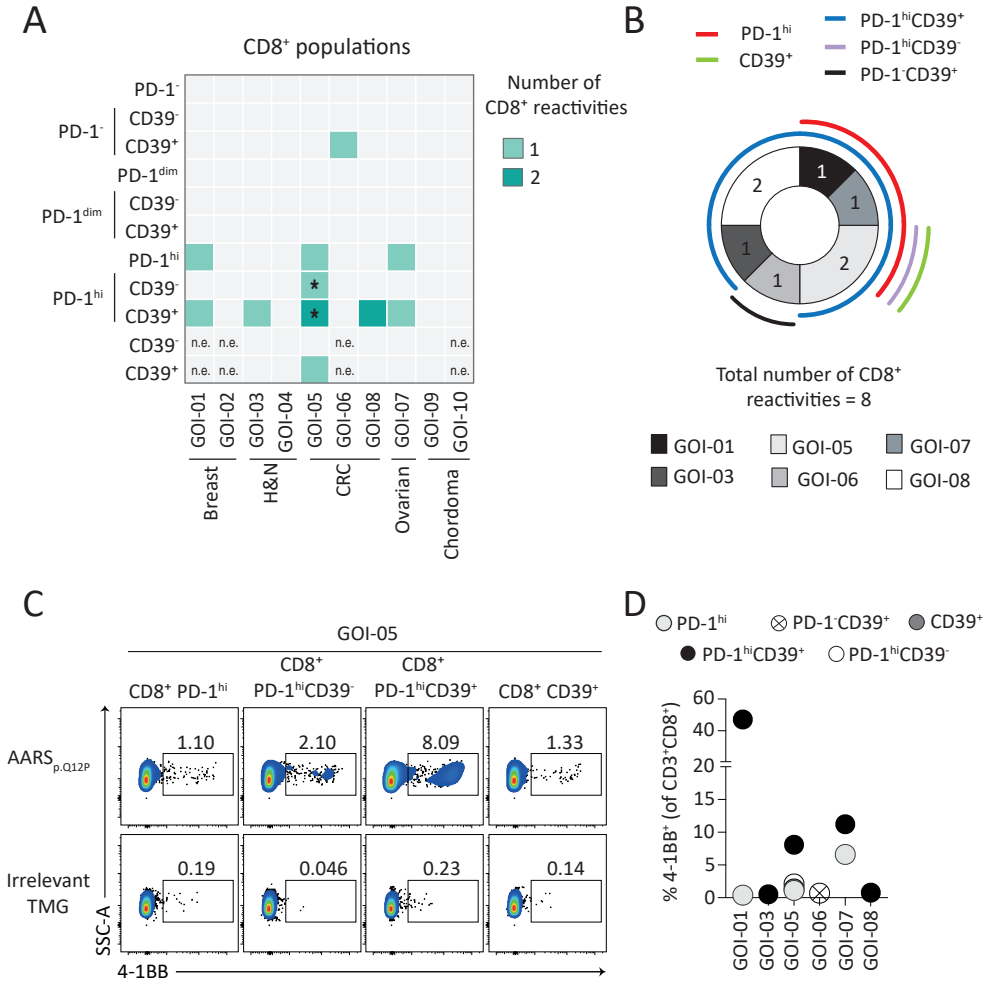

Figure 28. The selection of CD8⁺ PBLs based on the co-expression of PD-1^{hi} and CD39 reproducibly captures and markedly enhances the detection of neoantigen reactivities in patients with epithelial cancers. (A) Heat map displaying the number of neoantigen reactivities detected in the CD8⁺ T-cell populations isolated and expanded from peripheral blood based on PD-1 and CD39 expression

in ten patients with different epithelial cancers. (**B**) Donut plot depicts the number of CD8$^+$ neoantigen reactivities identified per patient and the specific circulating T-cell subpopulation where each was detected. (**C**) Representative flow cytometry plots of patient GOI-05 showing the frequency of AARS$_{p.Q12P}$-reactive T cells within the different subpopulations harboring neoantigen-reactive cells upon co-culture with autologous B cells electroporated with a minigene encoding for AARS$_{p.Q12P}$. Reactivity was measured by 4-1BB upregulation. Autologous B cells electroporated with an irrelevant TMG were used as a negative control. (**D**) Frequency of CD8$^+$ T cells recognizing tumor antigens in each of the specific circulating subsets harboring reactivity. The sum of the percentage of 4-1BB$^+$ cells measured following co-culture with each of the antigens recognized was used as a surrogate to measure the frequency of tumor antigen reactive-T cells. * indicates T-cell populations were sorted and tested twice.

Importantly, seven out of eight CD8$^+$ reactivities were detected in the CD8$^+$ PD-1^{hi}CD39$^+$ population, being the population that most consistently detected CD8$^+$ neoantigen-specific or tumor-reactive T lymphocytes (Figure 28B). The unique reactivity that was not detected by CD8$^+$ PBLs co-expressing PD-1^{hi} and CD39 was identified in the CD8$^+$ PD-1$^-$CD39$^+$ T-cell subset. The fact that all except one neoantigen reactivity were identified in PD-1^{hi} T-cell populations was consistent with previous studies (152,153). However, combining PD-1^{hi} with CD39 expression was necessary to more reproducibly detect neoantigen-specific PBLs, since CD8$^+$ T cells selected based on the expression of PD-1^{hi} alone missed some. Moreover, the CD8$^+$ PD-1^{hi}CD39$^+$ T-cell subset consistently contained the highest frequency of T lymphocytes targeting tumor antigens when the same reactivity was detected in multiple subpopulations (Figures 28C and D). Thus, the combination of PD-1^{hi} and CD39 enriches for CD8$^+$ neoantigen-specific and tumor-reactive T cells from peripheral blood to a greater extent than PD-1^{hi} alone in patients with different epithelial tumors.

5.2.1. CD8$^+$ PD-1^{hi}CD39$^+$ PBLs from GOI-07 recognize the cancer germline antigen MAGE A4 and the autologous tumor

Patient GOI-07 was one of the six patients in which we detected CD8$^+$ T cells capable of recognizing tumor antigens (Figure 28A). In this case, we identified CD8$^+$ T cells targeting the cancer germline antigen MAGE A4 in two different T-cell subsets (Figure 29A). More specifically, CD8$^+$ T cells expressing PD-1^{hi} and those expressing PD-1^{hi}CD39$^+$, each contained T cells targeting one unique minimal epitope from MAGE A4 (Figure 29B). Importantly, CD8$^+$ PD-1^{hi}CD39$^+$, but not CD8$^+$ PD-1^{hi} T cells, also recognized the autologous TCL pre-treated with IFN-γ (Figure 29A). To better characterize the specificity of CD8$^+$ T cells recognizing MAGE A4 or the autologous TCL, we enriched the MAGE A4-specific lymphocytes from the CD8$^+$ PD-1^{hi} and CD8$^+$ PD-

1^{hi}CD39^{+} PBL subsets. Moreover, we also selected for tumor-specific T lymphocytes from the CD8^{+} PD-1^{hi}CD39^{+} T-cell subset. In all cases, we followed the enrichment strategy explained in section 4.1.2 (Figure 29C). As shown in Figure 29D, MAGE A4-reactive T cells sorted from CD8^{+} PD-1^{hi} and CD8^{+} PD-1^{hi}CD39^{+} PBL subsets recognized MAGE A4.

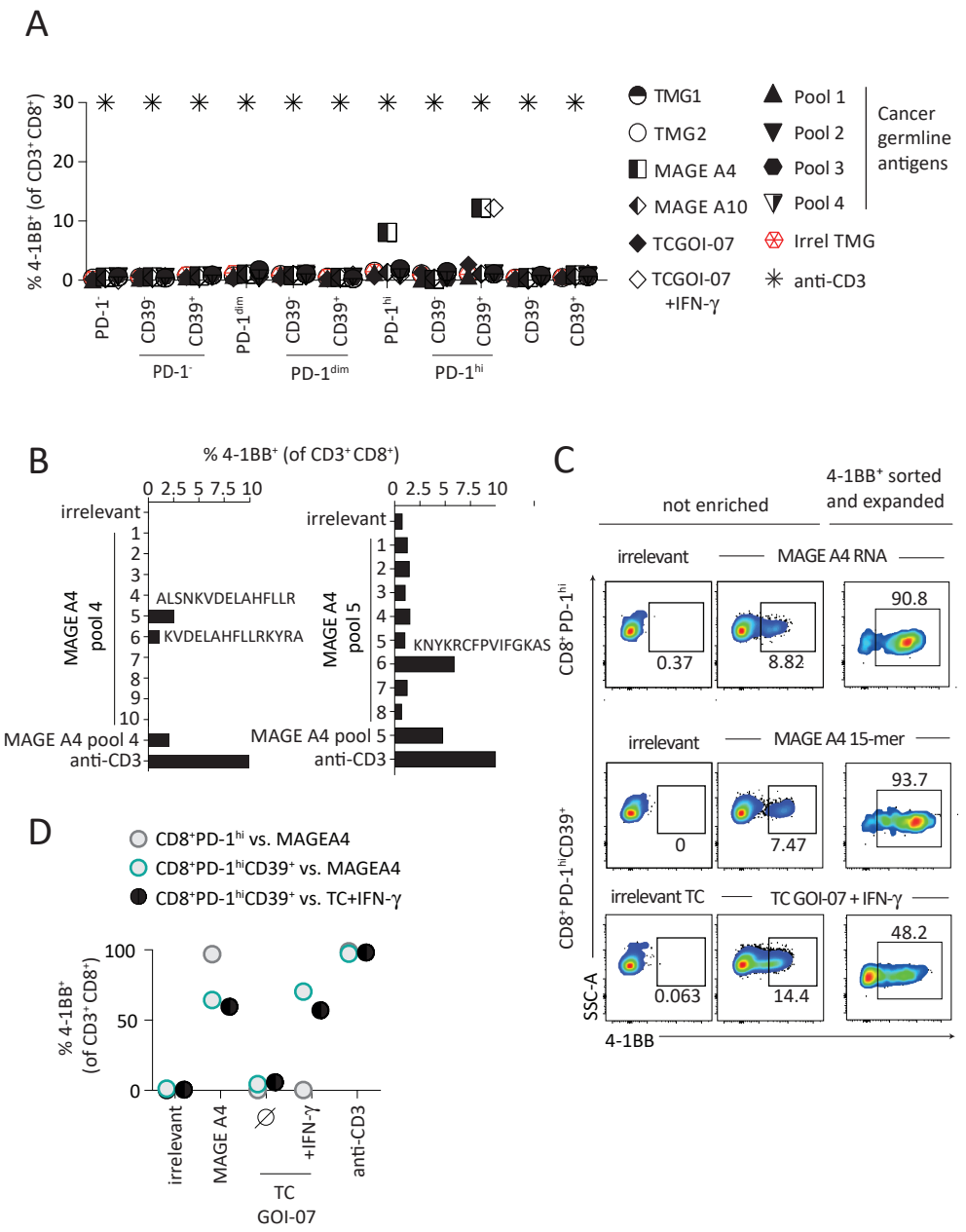

Figure 29. CD8^{+} T cells expressing PD-1^{hi} alone or co-expressed with CD39 recognize the cancer germline antigen MAGE A4 but only CD8^{+} PD-1^{hi}CD39^{+} can recognize tumor cells. (A) Reactivity of circulating CD8^{+} T-cell subsets sorted by PD-1 and CD39 against neoantigens, cancer germline

antigens or the autologous TCL untreated or pre-treated with IFN-γ. Reactivity was measured by the upregulation of 4-1BB by flow cytometry analysis after 20h co-culture with autologous B cells electroporated with TMGs encoding for neoantigens and cancer germline antigens or with the autologous TCL. Autologous B cells electroporated with an irrelevant TMG were used as a negative control. (**B**) $CD8^+$ $PD\text{-}1^{hi}$ (left) and $PD\text{-}1^{hi}CD39^+$ (right) T cells reactive against MAGE A4 were co-cultured with autologous B cells pulsed with individual peptides of MAGE A4 to identify the minimal epitope that was recognized by each MAGE A4-reactive population. (**C**) $CD8^+PD\text{-}1^{hi}$ (top) and $CD8^+PD\text{-}1^{hi}CD39^+$ (middle) T cells recognizing MAGE A4 and $CD8^+PD\text{-}1^{hi}CD39^+$ T cells (bottom) recognizing the autologous TCL treated with IFN-γ were enriched by FACS based on 4-1BB expression after 20h co-culture with the corresponding targets. Plots show gates used for sorting (left) and recognition of the corresponding target after expansion (right). Autologous B cells electroporated or pulsed with an irrelevant TMG or PP and an irrelevant TCL were used as a negative control to set the gates for sorting. (**D**) Frequency of sorted $CD8^+$ T cells recognizing MAGE A4 and the autologous TCL after sorting based on 4-1BB expression and 14 days of expansion. Data from (A-B) and (D) is representative from two independent experiments.

However, only those sorted from $CD8^+$ $PD\text{-}1^{hi}CD39^+$ T-cell population were also able to recognize the autologous TCL treated with IFN-γ.

Next, we performed single-cell TCR sequencing of the neoantigen-specific or tumor-reactive $CD8^+$ enriched T-cell populations. MAGE A4-enriched T cells from $PD\text{-}1^{hi}$ and $PD\text{-}1^{hi}CD39^+$ T-cell populations did not share any TCR clonotype, which was consistent with the fact that they recognized two different epitopes from MAGE A4 (Figure 30A). Moreover, $CD8^+$ $PD\text{-}1^{hi}CD39^+$ but not $CD8^+$ $PD\text{-}1^{hi}$ T cells enriched for MAGE A4 recognition shared the two most frequent TCRs with the T-cell population enriched for recognition of the autologous tumor cell line treated with IFN-γ (Figure 30A).

We then tested the three most frequent TCRs isolated from one of the two MAGE A4-enriched T-cell populations. More specifically, we selected the most frequent TCR detected in MAGE A4-enriched T cells from $CD8^+$ $PD\text{-}1^{hi}$ PBLs and the two most frequent TCRs from MAGE A4-enriched T cells from $CD8^+$ $PD\text{-}1^{hi}$ $CD39^+$ PBLs, which were shared with the T-cell population enriched for recognition of the autologous TCL. To evaluate their specificity, the selected TCRs were transduced into PBLs as explained in section 2.1.3.

As observed in Figure 30B, the three tested TCRs recognized MAGE A4. However, only the two TCRs identified in the $CD8^+$ $PD\text{-}1^{hi}CD39^+$ population, but not the one from $CD8^+$ $PD\text{-}1^{hi}$ T-cell subset, recognized the autologous TCL treated with IFN-γ, consistent with previous observations. These results indicated that the selection of $CD8^+$ T cells expressing $PD\text{-}1^{hi}$ and CD39 can enrich not only for neoantigen-specific T cells, but also for T cells recognizing other tumor antigens such as cancer germline antigens. Moreover, they can also recognize the autologous tumor.

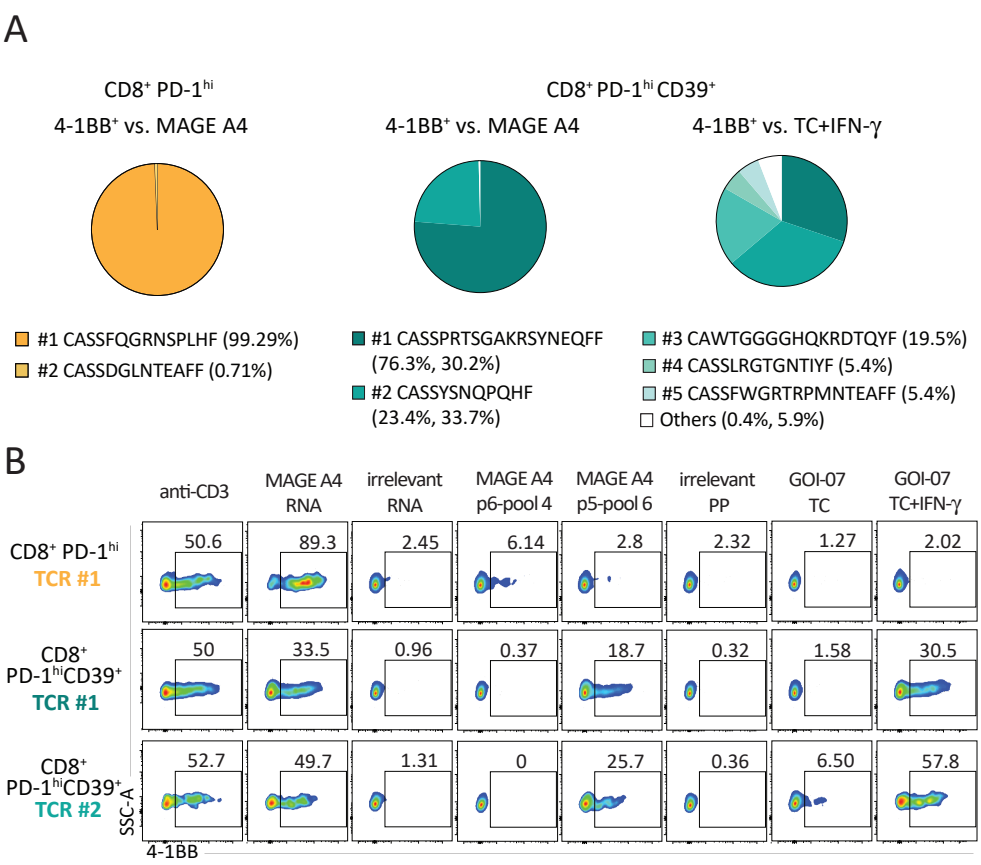

Figure 30. Single-cell RNA sequencing analysis revealed multiple TCRs reactive against MAGE A4 and capable of recognizing the autologous tumor in ovarian cancer patient GOI-07. (**A**) Pie charts show the frequency of the most dominant TCRs identified by single-cell RNA sequencing of MAGE A4-reactive T-cell populations enriched from CD8$^+$ PD-1^{hi} (left) or from CD8$^+$ PD-1^{hi} CD39$^+$ (middle) T-cell populations or of tumor-reactive T cells enriched from CD8$^+$PD1^{hi}CD39$^+$ T-cell subset (right). (**B**) Flow cytometry plots show the reactivity of PBLs transduced with the three most frequent TCRs derived from MAGE A4-reactive T-cell populations. TCR#1 depicted in orange was isolated from the CD8$^+$ PD-1^{hi} T-cell population enriched for MAGE A4 recognition whereas TCR#1 and TCR#2 depicted in green were the two most frequent TCRs detected in CD8$^+$PD-1^{hi}CD39$^+$ T-cell population sorted based on the recognition of MAGE A4 but also when sorted based on the recognition of the autologous TCL treated with IFN-γ. Data from (B) is representative from two independent experiments.

5.3. The CD4$^+$ PD-1^{hi}CD39$^+$ PBL subset contains the largest number of CD4$^+$ neoantigen reactivities across cancer patients

In the case of CD4$^+$, we were able to identify seven neoantigen reactivities in five out of ten patients analyzed (Figure 31A). In contrast to CD8$^+$, all CD4$^+$ neoantigen reactivities were identified within T-cell populations expressing PD-1^{hi}, either alone or in combination with CD39$^{+/-}$ (Figure 31A; Table 7). Although the CD4$^+$ PD-1^{hi}CD39$^+$ T-cell population contained the largest number of neoantigen reactivities across patients, it missed three of

seven CD4⁺ reactivities that were detected either in the PD-1^{hi} or PD-1^{hi}CD39^{-} T-cell subsets (Figure 31B). Moreover, when we looked at the frequency of neoantigen-specific T cells within each population, the proportion of relevant T cells was highly variable and none of the subpopulations consistently contained the highest frequency of neoantigen-specific T cells (Figure 31C). Therefore, although the CD4⁺ PD-1^{hi}CD39⁺ T-cell population contained the largest number of neoantigen reactivities, it did not capture all. Hence, it is plausible that additional cell-surface receptors, others than CD39, which are more specifically expressed on neoantigen-reactive CD4⁺ T cells, could further improve their identification in combination with PD-1^{hi}.

Altogether, we captured a total of 15 CD8⁺ and CD4⁺ reactivities against tumor antigens including neoantigens and cancer germline antigens in the peripheral blood of ten patients with different epithelial tumors (Table 7). Our results show that CD8⁺ and CD4⁺ T cells co-expressing PD-1^{hi} and CD39 contain the greatest number of neoantigen reactivities

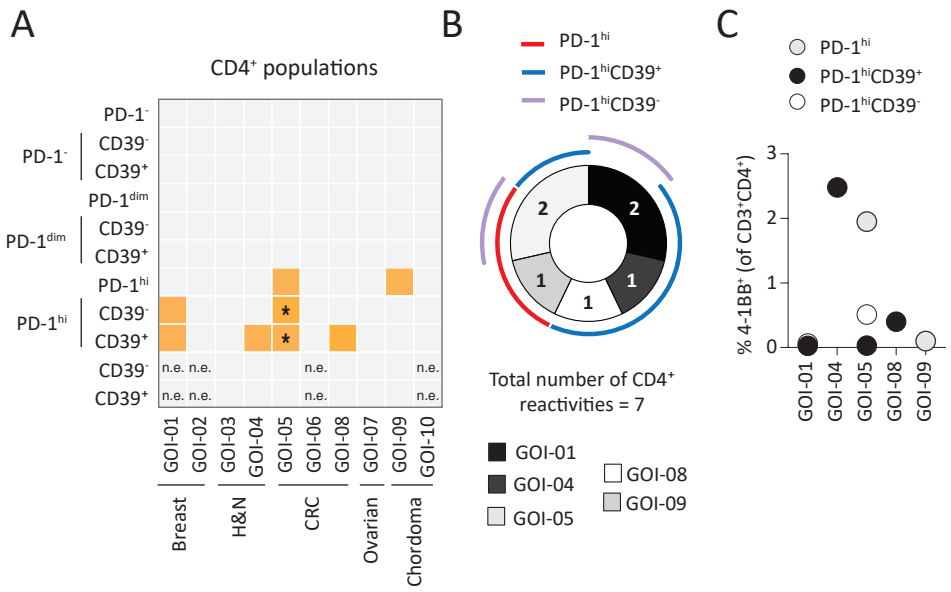

Figure 31. Co-expression of PD-1^{hi} and CD39 in circulating CD4⁺ T cells reproducibly guides the detection of neoantigen reactivities in patients with epithelial cancers (n=10). (**A**) Heat map displaying the number of neoantigen reactivities detected in the CD4⁺ T-cell populations isolated and expanded from peripheral blood based on PD-1 and CD39 expression in 10 cancer patients analyzed. (**B**) Donut plot depicts the number of CD4⁺ neoantigen reactivities identified per patient and the specific circulating T-cell subpopulation where each was detected. (**C**) Frequency of CD4⁺ T cells recognizing tumor antigens in each of the specific circulating subsets harboring reactivity. The sum of the percentage of 4-1BB⁺ cells measured following co-culture with each of the antigens recognized was used as a surrogate to measure the frequency of tumor antigen reactivity. n.e. not evaluated. * indicates T-cell populations that have been sorted twice.

detected. Moreover, in the case of $CD8^+$, this population consistently contained the highest frequency of T cells recognizing tumor antigens. Thus, the combination of PD-1^{hi} and CD39 outperforms PD-1^{hi} alone in the identification of circulating neoantigen-specific T cells in patients with epithelial tumors.

Table 7. Tumor rejection antigens targeted by $CD8^+$ and $CD4^+$ PBLs and TILs from patients with metastatic epithelial cancers

Patient ID	Tumor type	Number of somatic NSMs	Number of mutated epitopes evaluated[a]	Number of cancer germline antigens evaluated[b]	PBL subset/TILs with neoantigen reactivity	Mutated protein recognized	Amino acid position and change
GOI-01	Breast	124	133	-	$CD8^+$ PD-1^{hi}	KIAA1524	p.S57I
					$CD8^+$ PD-$1^{hi}CD27^+$	KIAA1524	p.S57I
					$CD8^+$ PD-$1^{hi}CD39^+$	KIAA1524	p.S57I
					$CD8^+$ PD-1^{hi}HLA-DR^+	KIAA1524	p.S57I
					$CD8^+$ PD-1^{hi}4-1BB^-	KIAA1524	p.S57I
					$CD4^+$ PD-$1^{hi}CD39^+$	PLXNB3	p.D252Y
					$CD4^+$ PD-$1^{hi}CD39^-$	RPS6KL1	p.K536fs
					TIL $CD4^+$	n.e. (TMG2)	n.e.
GOI-02	Breast	118	118	-	-	-	-
GOI-03	H&N	197	191	-	$CD8^+$ PD-$1^{hi}CD39^+$	TMTC3	p.L242F
GOI-04	H&N	65	64	-	$CD4^+$ PD-$1^{hi}CD27^+$	LASP1	p.G84S
					$CD4^+$ PD-$1^{hi}CD39^+$	LASP1	p.G84S
GOI-05	CRC	1068	226	-	$CD8^+$ PD-1^{hi}	AARS	p.Q12P
					$CD8^+$ PD-$1^{hi}CD39^-$	AARS	p.Q12P
					$CD8^+$ $CD39^+$	AARS	p.Q12P
					$CD8^+$ PD-$1^{hi}CD39^+$	AARS	p.Q12P
					$CD8^+$ PD-$1^{hi}CD39^+$	WDR90	p.T214M
					$CD4^+$ PD-$1^{hi}CD39^+$	WDFY3	p.T3011I
					$CD4^+$ PD-1^{hi}	SLC25A22	p.A163T
					$CD4^+$ PD-$1^{hi}CD39^-$	SLC25A22	p.A163T
					TIL $CD4^+$	SLC25A22	p.A163T
GOI-06	CRC	1302	182	-	$CD8^+$PD-1^-CD39^+	TEX264	p.S40L
GOI-07	Ovarian	27	23	16	$CD8^+$ PD-1^{hi}	MAGE A4	-
					$CD8^+$ PD-$1^{hi}CD39^+$	MAGE A4	-
					TIL $CD8^+$	MAGE A4	-
GOI-08	CRC	381	255	-	$CD8^+$ PD-$1^{hi}CD39^+$	GINS1	p.D163N
					TIL $CD4^+$	GINS1	p.D163N
					$CD8^+$ PD-$1^{hi}CD39^+$	SART1	p.G15W
					$CD4^+$ PD-$1^{hi}CD39^+$	CACNA2D	p.W233L
					TIL $CD4^+$	POLR3A	p.N1277K
GOI-09	Chordoma	44	50	-	$CD4^+$ PD-1^{hi}	CWC15	p.Y30C
					TIL $CD4^+$	CWC15	p.Y30C
GOI-10	Chordoma	71	77	-	-	-	-

[a]Epitopes were selected for screening as explained in detail in Methods. [b]Cancer germline antigens were selected based on their gene transcript expresion (>30% gene percentile) assessed by RNA sequencing. n.e. not evaluated.

6. Characterization of neoantigen-specific T-cell responses detected in TILs and PBLs

Given that expanded TILs are the classical T-cell source commonly used to identify and isolate neoantigen-specific T lymphocytes, we wanted to study the T-cell responses detected in expanded TILs from tumor biopsies and compare them to those already identified in T-cell subsets isolated from peripheral blood of cancer patients.

6.1. Expansion of TILs from tumor biopsies

As mentioned in section 1, we also expanded TILs from several small tumor fragments cultured independently in high doses of IL-2 to preserve, as much as possible, intratumoral heterogeneity. As summarized in Table 8, we were able to successfully expand TILs from at least two tumor fragments for each of the patients studied. The frequency of $CD8^+$ and $CD4^+$ TILs varied notably among tumor fragments and patients (Figure 32A; Table 8). Nevertheless, both $CD8^+$ and $CD4^+$ TILs were successfully expanded in the majority of patients except for GOI-05, -08 and -10, in which more than 95% of TILs were $CD4^+$.

Table 8. Number of TIL fragments expanded and the average frequency of $CD8^+$ and $CD4^+$ TILs from each patient

Patient ID	Tumor type	TIL fragments expanded/seeded	TIL frequency[a]	
			$CD4^+$	$CD8^+$
GOI-01	Breast	6/6	74.7%	25.3%
GOI-02	Breast	4/6	33.1%	66.9%
GOI-03	H&N	2/6	48.8%	51.2%
GOI-04	H&N	5/6	31.7%	68.3%
GOI-05	CRC	5/6	95.8%	4.2%
GOI-06	CRC	2/6	50.1%	49.9%
GOI-07	Ovarian	3/6	38.9%	61.1%
GOI-08	CRC	12/12	96.4%	3.6%
GOI-09	Chordoma	13/18	47.2%	52.8%
GOI-10	Chordoma	2/6	97.5%	2.5%

[a]The frequency of $CD4^+$ and $CD8^+$ TILs is the average of all TIL fragments expanded from each patient.

6.2. Selection of circulating T-cell subsets identifies more neoantigen reactivities than the non-specific expansion of TILs in high dose IL-2

Although we were able to expand and screen TILs for neoantigen recognition in all ten patients, only six antigens were recognized by CD8⁺ and CD4⁺ TILs (Figure 32A; Table 8). We detected five neoantigen reactivities in CD4⁺ TILs in four of the patients evaluated. In contrast, no CD8⁺ neoantigen-specific TILs were detected in any of the patients evaluated. Only CD8⁺ TILs targeting MAGE A4 were identified in patient GOI-07. Thus, the number of reactivities detected in TILs was substantially lower than those detected in specific T-cell subsets selected and expanded from PBLs, since only six antigens were recognized by CD8⁺ and CD4⁺ TILs compared to the 15 antigens recognized by CD8⁺ and CD4⁺ PBL subsets (Figure 32A-B). Moreover, while ten of the antigens recognized by PBL subsets were not recognized by TILs, the majority of the neoantigen reactivities detected in CD4⁺ TILs were captured in PBLs. In fact, only two neoantigen-specific T-cell responses identified in GOI-08 TILs were not captured by circulating CD4⁺ T-cell subsets (Figure 32C).

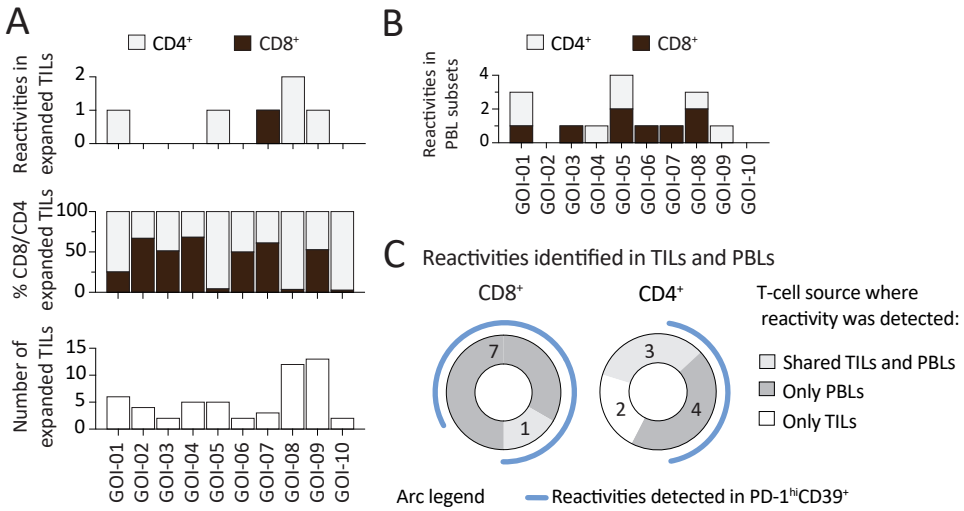

Figure 32. Isolation of specific CD8⁺ and CD4⁺ T-cell subsets from peripheral blood captures a greater number of neoantigen reactivities compared to unselected *ex vivo* expanded TILs. (**A**) Bar plots showing the number of expanded TIL fragments per patient (bottom), the average frequency of CD8⁺ and CD4⁺ T cells in the expanded TILs and the number of neoantigen reactivities detected in CD8⁺ and CD4⁺ TILs in ten patients with epithelial cancers. (**B**) Number of neoantigen reactivities detected in CD8⁺ and CD4⁺ PBL subsets in ten patients with epithelial cancers. (**C**) Pie charts show the total number of reactivities detected in the ten patients studied and the T-cell source where they were identified depending on if they were only identified in TILs, PBLs or were found both in TILs and PBLs. The reactivities that were detected in CD8⁺ and CD4⁺ PD-1^{hi} CD39⁺ PBLs are depicted with a blue arch.

Next, we more specifically looked at the reactivities detected in $CD8^+$ and $CD4^+$ PBL subsets co-expressing PD-1^{hi} and CD39 since these were the subpopulations containing the greatest number of reactivities and compared to those detected in TILs. As shown in Figure 32C, the selection and expansion of $CD8^+$ PD-$1^{hi}CD39^+$ PBLs outperformed the classical non-specific TIL expansion in high-dose IL-2 at identifying anti-tumor $CD8^+$ T-cell responses. In contrast, despite the total number of $CD4^+$ reactivities detected in blood was higher than in TILs, the $CD4^+$ PD-$1^{hi}CD39^+$ T-cell subpopulation identified fewer reactivities than unselected TILs. These results are in line with those from section 5.3 further indicating that, although the $CD4^+$ PD-$1^{hi}CD39^+$ T-cell population identifies neoantigen reactivities, it still misses several $CD4^+$ neoantigen-specific PBLs.

Altogether, these results underscore the use of peripheral blood as an alternative source of neoantigen-specific and tumor-reactive T cells that could make personalized T-cell therapies more widely applicable.

7. WES of cfDNA identifies tumor NSMs and neoantigens targeted by TILs and PBLs

Since we aimed to develop a minimally-invasive strategy for the detection of neoantigen-specific T cells through the exclusive usage of peripheral blood, we also wanted to determine whether WES of cfDNA reproducibly identified neoantigens. In section 1.1, we already showed that WES of cfDNA was able to identify NSMs in six patients studied (Figure 15). Moreover, in the first three patients analyzed, cfDNA WES identified three and one neoantigens in patients GOI-01 and GOI-04 but it did not detect the neoantigen recognized by $CD8^+$ T cells in patient GOI-03 (section 4.2 and 4.3). Hence, we wanted to further explore the ability of cfDNA to detect neoantigens in the remaining three patients from which we extracted cfDNA.

Figure 33 shows the percentage of shared NSMs, the number of neoantigens identified out of the candidate neoantigens tested and the source of DNA where they were detected. The percentage of neoantigens recognized of the total number of NSMs tested in all patients studied was lower than 3%, ranging from 0 to 2.9% (Figure 33A), which is in line with previous studies done in TILs (39). Of note, cfDNA captured eight out of 13 neoantigens in four out of five patients harboring neoantigen reactivities and all of them were shared between the two sources of DNA (Figure 33A-B). The remaining

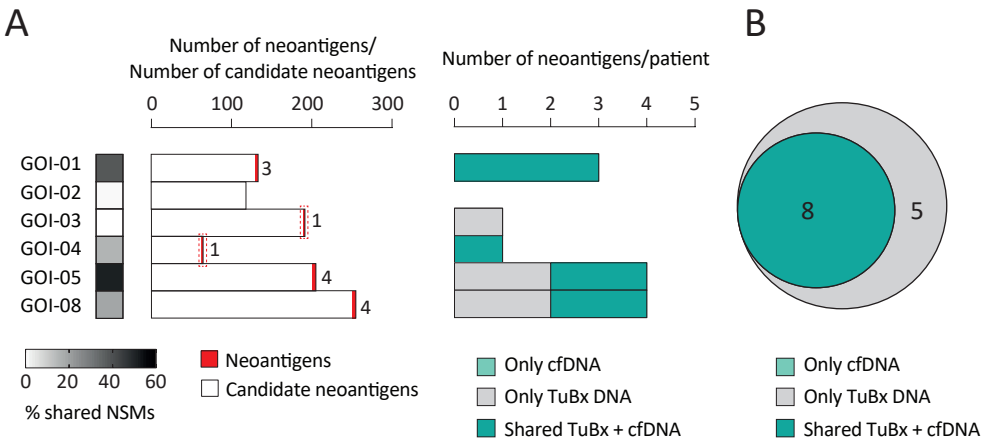

Figure 33. WES of cfDNA can be exploited to identify neoantigens targeted by circulating T cells and TILs. (**A**) Number of immunogenic neoantigens of the total candidate neoantigens tested (left) and source of DNA where the immunogenic neoantigens were identified (right). The frequency of shared tumor and circulating NSMs in each patient is specified on the far left. (**B**) Venn diagram showing the total number of neoantigens detected in cfDNA and TuBx DNA or only detected in TuBx DNA in the six patients analyzed.

five neoantigens were exclusively identified in TuBx DNA (Figure 33A-B). Although we did not include any NSMs only detected in cfDNA in the immunological screenings of patient GOI-05, we did not identify any neoantigen exclusively detected in this source of DNA in any other patient. Overall, our results demonstrate that WES of cfDNA can be used to identify neoantigens in cancer patients with different epithelial tumors.

Importantly, the only patient for which cfDNA did not identify any neoantigen was patient GOI-03, which was also the only patient in which no overlap was observed between the NSMs detected in cfDNA and TuBx DNA (Figure 15 and Figure 33A). This prompted us to investigate what could explain the differences in the number of NSMs shared between TuBx and cfDNA, which could in turn influence the ability of cfDNA to detect neoantigens.

7.1. The tumor fraction of cfDNA does not correlate with the frequency of NSMs identified in cfDNA

We observed differences between cancer patients in the frequency of shared NSMs between cfDNA and TuBx DNA and in the number of neoantigens detected in cfDNA. Because of this, we carried out different analyses to investigate the factors that could affect the performance of cfDNA at identifying tumor NSMs and neoantigens.

As discussed in the introduction, ctDNA might represent only a very small fraction

of the total cfDNA. Thus, we reasoned that the differences in the overlap of NSMs between cfDNA and TuBx DNA could be explained by differences in the tumor fraction of cfDNA. To answer this question, we performed shallow WGS and used ichorCNA, an algorithm that predicts regions with CNA and estimates tumor content in cfDNA (222). Our results showed that the relative amount of tumor-derived DNA in the cfDNA, also known as tumor fraction, varied notably between patients ranging from 0 to 40%, irrespective of the tumor type. Nevertheless, we did not observe any correlation between the tumor fraction of cfDNA and the frequency of NSMs identified in this source of DNA (Figure 34, left) nor with the frequency of shared NSMs (Appendix Figure 7A). We also investigated whether the frequency of total NSMs identified in cfDNA could be correlated with tumor burden. Although there were differences in tumor burden between patients, the total tumor volume did not correlate either with the frequency of NSMs in cfDNA (Figure 34, right) or with the frequency of shared NSMs (Appendix Figure 7B). Thus, our results showed that the differences in the identification of NSMs and neoantigens observed in cfDNA among patients were not explained either by differences in tumor fraction or tumor burden. Thus, having certain levels of tumor fraction does not guarantee the detection of mutations that are shared by cfDNA and TuBx DNA.

Of note, while it seemed obvious that having a minimum tumor fraction in cfDNA would be essential for the identification of NSMs in this DNA source, NSMs were detected in cfDNA of patient GOI-02, in which the tumor fraction of cfDNA was 1.25%.

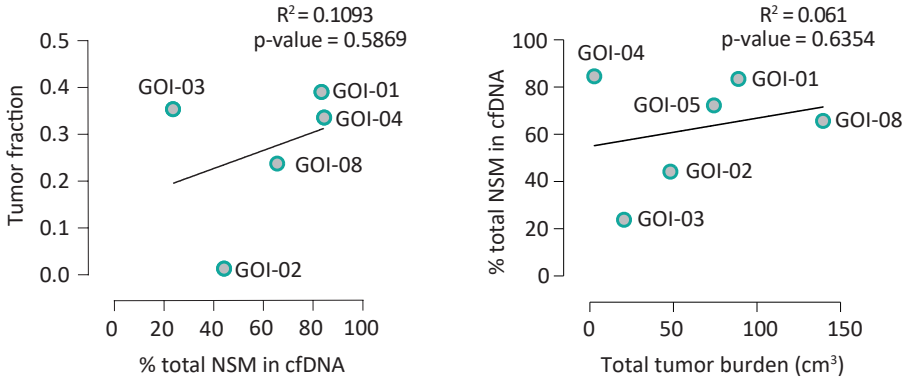

Figure 34. Identification of NSMs by cfDNA WES is not correlated with cfDNA tumor fraction nor total tumor burden in six patients with metastatic epithelial cancers. Correlation between the frequency of total NSMs detected in cfDNA and the tumor fraction of cfDNA (left) or the total tumor burden (right) of each patient.

More specifically, 44.23% of the total NSMs detected were identified in cfDNA. Nevertheless, only 1.01% of the NSMs were shared with TuBx DNA (Figure 15). These observations were unexpected and prompted us to further explore the NSMs that were exclusively detected in cfDNA.

7.2. NSMs exclusively detected in cfDNA contained a higher proportion of indels as opposed to NSMs shared or only detected in TuBx DNA

Based on the unexpected findings in patient GOI-02 in which 44.23% of the total NSMs were detected in cfDNA but displayed barely any overlap with NSMs from TuBx DNA and had a tumor fraction close to 0, we wanted to further characterize the NSMs exclusively detected in cfDNA.

NSMs exclusively detected in cfDNA could potentially derive from other regions of the biopsied lesion or other tumor lesions that shed tumor DNA into the circulation. Despite we could not explore this hypothesis since we only obtained one single biopsy from each patient, the undetectable tumor fraction in the cfDNA of patient GOI-02 (Figure 34A) suggests this assumption is flawed. Another possible explanation is that NSMs only detected in cfDNA are artefactual products generated during sequencing or *in silico* analysis. This could more frequently happen in patients with low levels of cfDNA tumor fraction in which NSMs in ctDNA would thereby be less represented.

To explore this, we characterized the type of mutations identified in each source of DNA. The bioinformatics pipeline used to analyze WES data can detect SNVs and indels. Therefore, we classified NSMs based on the type of mutation and on the DNA source where they were detected.

As shown in Figure 35, NSMs only detected in cfDNA contained a higher proportion of indels compared to NSMs shared or only detected in TuBx DNA (Figure 35A). This increase in the frequency of indels among mutations uniquely identified in cfDNA was not only explained by the results of one patient, since a similar distribution pattern was observed across the six patients analyzed except for GOI-05 (Figure 35B). In contrast, in most of the patients, shared NSMs displayed similar frequencies of SNVs and indels to NSMs exclusively detected in TuBx DNA, being SNVs the main type of NSMs identified (Figure 35A-B).

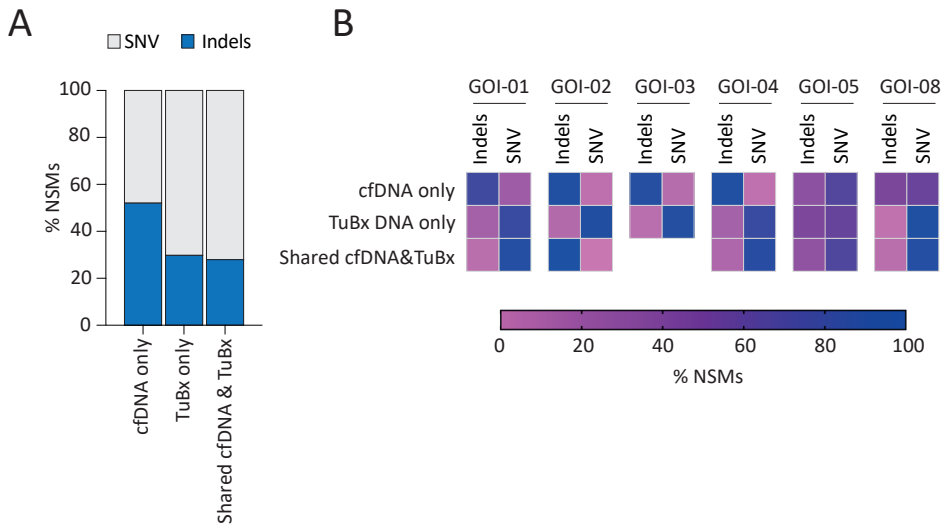

Figure 35. A higher frequency of indels is observed in NSMs only detected in cfDNA compared to NSMs shared or only detected in TuBx DNA. (**A**) Frequency of SNVs and indels within the total NSMs only detected in cfDNA, only detected in TuBx DNA or shared between the two DNA sources in the six patients analyzed. (**B**) Heat map showing the frequency of indels and SNVs within the NSMs only detected in cfDNA, only detected in TuBx DNA or shared between the two DNA sources. The information of each patient is plotted separately.

These results, together with the fact that no neoantigens were exclusively detected in cfDNA, suggested that at least a fraction of NSMs only detected in cfDNA might be artifacts generated during sequencing or the *in silico* analysis.

7.3. WES of cfDNA captures a higher frequency of tumor clonal mutations in cancer patients harboring shared NSMs between TuBx and cfDNA

Next, since all neoantigens identified in cfDNA of the six patients analyzed were shared with TuBx DNA, we wanted to determine whether there were any molecular features that characterize shared NSMs and differentiate them from those exclusively identified in TuBx DNA. As previously mentioned, a low tumor fraction in cfDNA would accordingly decrease the probability to detect tumor-derived NSMs in blood, especially when using WES for cfDNA analysis due to its low sensitivity. Hence, following what is frequently done in the field, we set a cutoff value of tumor fraction and only plasma samples in which the tumor fraction in cfDNA accounted for over >10% were included in this analysis (222,276). We distinguished clonal and subclonal events estimating the proportion of an observed somatic event out of the total tumor-derived DNA from tumor

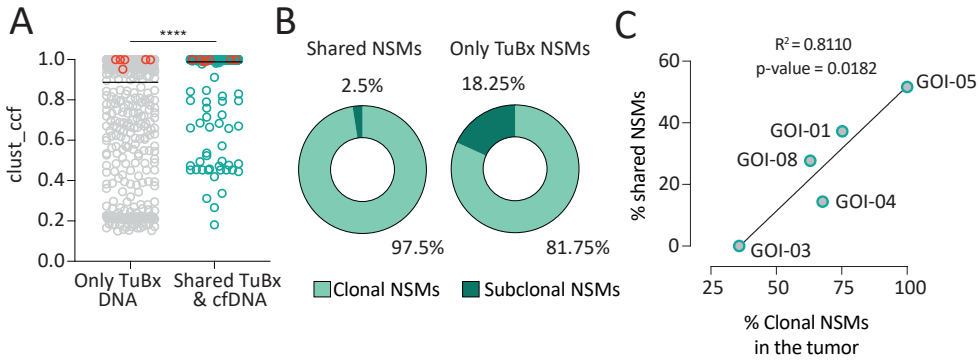

Figure 36. Clonal mutations in the tumor are more frequently detected in cfDNA in cancer patients having a certain overlap between cfDNA and TuBx DNA. (**A**) Tumor clonality of NSMs identified in cfDNA and TuBx DNA or uniquely in TuBx DNA as determined by clust_ccf of TuBx DNA. Clonality of all the neoantigens identified is depicted in red. (**B**) Percentage of tumor clonal and subclonal mutations detected in TuBx and cfDNA or only in TuBx DNA. (**C**) Correlation between the frequency of shared NSMs between cfDNA and TuBx DNA and the frequency of clonal mutations in the tumor. Statistical significance was analyzed using an unpaired non-parametric Mann Whitney test. *p<0.05, **p<0.001, ***p<0.0001; ns, not significant.

biopsies taking into account CNA by using clust_ccf. Of note, mutations shared between TuBx and cfDNA were significantly more clonal than those exclusively identified in TuBx DNA (Figure 36A). Similarly, whilst only the 2.5% of all shared NSMs were subclonal mutations, they represented the 18.25% of NSMs exclusively identified in TuBx DNA (Figure 36B; Appendix Figure 7C). Moreover, the frequency of shared NSMs was positively correlated with the frequency of clonal mutations within the tumor (r^2= 0.81, p= 0.0182) (Figure 36C).

These results indicate that tumor clonal mutations are more frequently identified in cfDNA than subclonal mutations. This is of great importance since all neoantigens identified were derived from clonal mutations (Figure 36A). Thus, cfDNA would better capture NSMs and neoantigens in patients with a high proportion of clonal mutations.

Altogether, our results show that cfDNA can detect tumor NSMs, preferentially those that are clonal in the tumor. Therefore, according to our data, in patients having a tumor fraction >10%, the tumor mutational landscape of a highly clonal tumor would be better represented in cfDNA than heterogeneous tumors. These results underscore cfDNA as a source of tumor DNA to identify tumor NSMs that could overcome the need of a tumor biopsy. Thus, performing WES of cfDNA and isolating circulating $CD8^+$ and $CD4^+$ T lymphocytes expressing PD-1^{hi} and CD39 would enable the development of personalized

T-cell therapies targeting neoantigens exclusively using a liquid biopsy. This could make personalized T-cell therapies more widely applicable, even in patients with unresectable tumors or whose tumors cannot be biopsied due to their localization or the health state of the patient.

Discussion

In this thesis, we aimed to mine WES from cfDNA to detect somatic NSMs and to identify and isolate T lymphocytes targeting neoantigens using peripheral blood of patients with metastatic epithelial cancer in order to develop personalized T-cell therapies without the need of a tumor biopsy.

By performing cfDNA WES and leveraging the expression of cell-surface markers to isolate distinct T-cell subsets from peripheral blood, we were able to identify neoantigens recognized by circulating $CD8^+$ or $CD4^+$ T cells that elicited T-cell responses in patients with distinct histological cancer types. These results showed that the selection of peripheral blood $CD8^+$ and $CD4^+$ T lymphocytes co-expressing PD-1^{hi} and CD39 reproducibly captured circulating T cells targeting neoantigens and, in the case of $CD8^+$ lymphocytes, this subpopulation consistently contained the highest frequency of reactive T cells. Moreover, isolation of circulating $CD8^+$ and $CD4^+$ T-cell subsets from peripheral blood identified a greater number of neoantigen reactivities compared to unselected TILs expanded in high-dose IL-2, which is the gold standard method currently used in adoptive cell transfer.

Hence, we provide proof of principle for a minimally-invasive strategy based on the use of peripheral blood to develop personalized T-cell therapies targeting neoantigens without the need of a tumor biopsy. This strategy could be exploited to treat patients with unresectable tumors that currently cannot benefit from ACT.

cfDNA WES coupled with selection and expansion of a specific circulating T-cell subpopulation can detect neoantigen-specific PBLs and their target neoantigens in peripheral blood

We explored peripheral blood as an alternative source to detect cancer-specific neoantigens and to identify and isolate $CD8^+$ and $CD4^+$ neoantigen-specific T lymphocytes and TCRs from patients with epithelial cancers. To this end, we followed two parallel strategies: 1) Perform WES of cfDNA to detect tumor NSMs and 2) use a biomarker-based isolation method to detect circulating neoantigen-specific T cells.

By using WES, we identified tumor NSMs in the cfDNA of the six cancer patients studied. Other exploratory strategies such as WGS could have been used to sequence cfDNA and would have covered a larger part of the genome also detecting non-canonical neoantigens. Nevertheless, considering the high cost of sequencing technologies together

with our recent work that demonstrated that non-canonical neoantigens are very infrequent (277), WES represented the most cost-effective technique to cover a wide spectrum of candidate neoantigens potentially involved in tumor clearance. Importantly, our results showed that cfDNA WES could be used to identify neoantigens, since it detected eight out of 13 neoantigens in five of the six patients studied, further supporting that it could be used for the development of minimally-invasive T-cell therapies.

To identify tumor antigen-specific PBLs, we used a biomarker-based isolation method coupled with functional immunological screenings. This strategy allowed the identification of 15 T-cell reactivities against tumor antigens in the peripheral blood of eight of 10 patients with different epithelial tumors.

Other strategies have been previously described to enrich for circulating neoantigen-specific T lymphocytes, including multimer staining and IVS (151,154,160,183). However, these two strategies have certain limitations that hamper the reproducible identification of recall T-cell responses in circulation (reviewed in Garcia-Garijo, Fajardo and Gros 2019) (278). For instance, although pHLA multimers enable the detection of infrequent neoantigen-specific PBLs, prior knowledge of the specific minimal epitope and HLA restriction is required for multimer generation, which is only available for a limited number of HLA molecules. This would represent an important limitation in our study since the patients analyzed have not been selected based on any specific HLA typing and their tumors can harbor over 300 mutations. Moreover, the detection of neoantigen-specific T lymphocytes by pHLA multimer staining does not necessarily determine functional T-cell responses (164). Therefore, functional immunological screenings following pHLA multimer staining would still be required.

The fact that IVS is typically performed with pools of peptides to ensure testing of all candidate neoantigens may also hamper the detection of the entire neoantigen-specific T-cell repertoire. This is because the simultaneous presentation of several epitopes during IVS might favor the enrichment of neoantigen-specific PBLs recognizing immunodominant peptides, thereby underrepresenting the neoantigen-specific T-cell repertoire present in the starting population. Although T lymphocytes could be stimulated with APCs pulsed with each individual peptide separately to solve this hurdle, this strategy would not be feasible to test many of our patients that harbor a high number of mutations. Moreover, T-cell reactivities detected through IVS can originate from the naïve rather than

the antigen-experienced T-cell compartment if the tumor does not express the peptide used for stimulation (26). Thus, T-cell responses that did not naturally occur in the tumor might also be detected.

The use of our strategy enabled the identification of T-cell responses in eight of 10 patients with different epithelial tumors, including breast, CRC, H&N, ovarian cancer and chordoma. Nevertheless, we are aware that the number of patients included in the study was limited, especially for the detection of tumor NSMs by cfDNA WES, for which only samples from six patients were analyzed. Thus, these analyses should be performed in a larger cohort of patients to further support our encouraging data from the detection of tumor NSMs and neoantigens by using a liquid biopsy. Similarly, we could not obtain apheresis in six out of 10 patients included in the study due to their frail medical status. Thus, in those six patients, the analyses were performed by exclusively using 10-20 mL of blood. Although this also underscores the strength of our method, the shortage of material could affect the results, especially when sorting infrequent populations from peripheral blood that can be affected by random sampling. Overall, while working with human samples makes our study highly valuable, it is challenging to obtain samples from big and representative cohorts of cancer patients.

A small fraction of PBLs from cancer patients express high levels of PD-1 and contain most of the T-cell reactivities detected in circulation

T-cell phenotypic studies in cancer patients have predominantly been focused on TILs and have revealed that a fraction of them typically display a dysfunctional phenotype characterized by the co-expression of multiple activation and exhaustion markers (73,74,138,191,192,195,196). With few exceptions, this dysfunctional phenotype has been associated with tumor recognition and has been exploited to enrich for T cells capable of recognizing the tumor. Several surface markers have been described to distinguish neoantigen-specific or tumor-reactive TILs within the heterogeneous TIL population in multiple epithelial tumors (73,74,138,192,193,195,196). All this work done in TILs provides valuable information about the phenotypic and functional state of tumor-reactive T cells in the tumor. However, we cannot assume that neoantigen-specific or tumor-reactive T cells existing in the circulation exhibit a similar phenotype to that observed in TILs. Indeed, a previous study showed that $CD8^+$ TILs from melanoma patients displayed an

increased expression and co-expression of activation and exhaustion markers such as PD-1, LAG-3, TIM-3 and 4-1BB compared to PBLs (138). Therefore, it is plausible that PBLs do not exhibit such a dysfunctional phenotype since they are not usually chronically exposed to their cognate antigen nor to the immunosuppressive microenvironment. Despite this, other studies have demonstrated that the selection of circulating PD-1^{+} T cells enriches for neoantigen-specific T lymphocytes in the circulation (152,153), indicating that tumor-reactive or neoantigen-specific PBLs might express, although at lower levels or in a smaller fraction of the total PBLs, specific cell-surface receptors associated with persistent TCR stimulation.

In our analysis, the phenotypic characterization of PBLs from the extensive cohort of cancer patients revealed that a very small subpopulation of CD4^{+} and CD8^{+} PBLs displayed a dysfunctional phenotype that could resemble TILs. We observed that CD4^{+} and CD8^{+} PD-1^{hi} T-cell subsets in cancer patients, but not PD-1^{dim} or PD-1^{-}, exhibited higher expression of most of markers studied, accompanied by a unique co-expression profile, which was characterized by the co-expression of three or four of the activation/exhaustion markers evaluated. The division of PD-1^{+} cells into subpopulations based on their expression levels in PBLs from cancer patients showed phenotypic differences between these subpopulations as previously described in TILs (191,192,279), further supporting the phenotypic similarities of the PD-1^{hi} PBL subset with dysfunctional TILs.

In addition, the co-expression profile was more evident in the PD-1^{hi} PBLs of cancer patients as compared to PD-1^{hi}, PD-1^{dim} and PD-1^{-} PBLs from healthy donors (Figure 17). Of note, a fraction of PBLs from healthy donors expressed PD-1, which would be unexpected if PD-1 expression would be exclusively associated with a dysfunctional state. Nevertheless, it is important to keep in mind that in addition to exhaustion, PD-1 is also associated with activation as it is transiently expressed on T cells upon recognition of their cognate antigen (81,280). In fact, high levels of PD-1 have been observed in the periphery of healthy individuals and are mainly expressed by effector-memory T cells (281). Nevertheless, circulating PD-1^{hi} CD8^{+} PBLs from healthy donors were not enriched with an exhausted phenotype as they did not co-express multiple of the evaluated cell-surface receptors, which is the case of cancer patients. Thus, although PD-1 expression has emerged as a hallmark of T-cell exhaustion, its expression is not necessarily associated with a dysfunctional phenotype as its main role is to act as a regulatory mechanism on

activated T cells to balance T-cell responses.

The differences in the phenotypic profile observed between PD-1^{-}, PD-1^{dim} and PD-1^{hi} subpopulations in cancer patients prompted us to study these markers and their potential to detect neoantigen-specific T cells in circulation in more detail. Functional immunological screenings evaluating neoantigen recognition of an extensive panel of PBL subsets sorted based on the differential expression of surface markers demonstrated that 14 of 15 CD4^{+} and CD8^{+} T-cell reactivities detected in peripheral blood were contained in T-cell populations expressing PD-1^{hi}. More specifically, these 14 reactivities were detected in populations expressing PD-1^{hi}, either alone or co-expressed with CD27^{+}, CD39$^{+/-}$, HLA-DR^{+} or 4-1BB^{-}. Importantly, circulating CD8^{+} and CD4^{+} neoantigen-specific PBLs targeting the same neoantigen were detected in multiple T-cell subsets selected based on the expression of different combinations of markers (Figure 21; Figure 27B; Figure 28C). This indicates that many receptors can be co-expressed on tumor-reactive T cells, as has also been observed in the aforementioned studies in TILs. Nevertheless, which marker or combination of markers most efficiently captures the tumor-reactive T-cell repertoire in patients remains unclear. Moreover, it is possible that cell-surface receptors that guide the identification of tumor-reactive or neoantigen-specific TILs might not be useful to identify their counterparts in circulation. For instance, the only neoantigen reactivity detected in a population sorted based on 4-1BB expression was detected in the PD-1^{hi}4-1BB^{-} CD8^{+} subpopulation indicating that circulating neoantigen-specific T cells did not express 4-1BB, which is contrary to what has been described for TILs (193,275,282). Since 4-1BB is an early activation marker that is transiently upregulated early after T-cell activation (283,284), the lack of reactivities in the circulating 4-1BB-expressing T-cell subsets can be explained by the fact that these T cells might not have encountered their cognate antigen very recently, contrary to what happens with TILs.

CD8^{+} and CD4^{+} PBLs co-expressing PD-1^{hi} and CD39 identify reactivities against tumor antigens in cancer patients

Our results showed that CD8^{+} PBLs co-expressing PD-1^{hi} and CD39 most reproducibly identified T cells recognizing tumor antigens and consistently contained the highest frequency of CD8^{+} reactive T cells (Figure 28). Both PD-1 and CD39 have been described as biomarkers to enrich for CD8^{+} tumor-reactive or neoantigen-specific T cells

at the tumor site (73,74,138,191,192). Moreover, PD-1 has also been demonstrated to enrich for neoantigen-specific PBLs and CD39 was recently shown to be preferentially expressed by this subset of T cells in peripheral blood (156). We also isolated $CD8^+$ populations based on the exclusive expression of PD-1 or CD39. However, these populations failed to identify the vast majority of reactivities against the detected tumor antigens. We cannot rule out the possibility that these subpopulations initially contained the neoantigen-specific T cells although at a lower frequency than the PD-$1^{hi}CD39^+$. It is possible that less dysfunctional T cells with a higher proliferative capacity also present in the culture outgrow neoantigen-specific T cells during the T-cell expansion after cell sorting, rendering them undetectable. To avoid losing T-cell reactivities, TCR sequencing could be performed immediately after sorting, which would ensure the identification of neoantigen-specific TCRs if they were ever present in the starting population.

Although $CD8^+$ PBLs sorted based on the expression of PD-1^{hi} and CD39 contained the highest frequency of neoantigen-specific T lymphocytes, only a small fraction of the entire subpopulation were neoantigen-specific. Therefore, a question that remains unanswered is what the rest of $CD8^+$ PD-$1^{hi}CD39^+$ PBLs recognize. For the three CRC patients whose tumors harbored over 300 mutations, $CD8^+$ PD-$1^{hi}CD39^+$ T cells potentially recognize additional neoantigens that were not included in our screenings. Another possibility is that these T cells are tumor reactive but recognize nonmutant tumor antigens. This was observed in a study with metastatic melanoma patients in which circulating PD-1^+ PBLs showed recognition of one or more cancer germline antigens or melanoma differentiation antigens (152). In the only patient in which we tested reactivity against self-antigens, GOI-07, we detected a reactivity against the cancer germline antigen MAGE A4. Therefore, broadening the spectrum of antigens tested could potentially identify more tumor-reactive T cells within this subpopulation. Nonetheless, we cannot rule out the possibility that a fraction of the expanded T cells are bystanders that were sorted and outgrew the neoantigen-specific T lymphocytes. In our analysis, the $CD8^+$ PD-1^{hi} $CD39^+$ population, from which we sorted the lowest number of cells (*i.e.* 69 cells), was the population that resulted in the highest frequency of neoantigen-specific T lymphocytes (40% of reactivity). This might indicate that, if there were bystander T cells, the frequency of these T cells was so low that they were not able to outgrow neoantigen-specific T cells. However, this is purely speculative and whether the frequency of neoantigen-specific PBLs after sorting and before the expansion was higher than after expansion is unknown.

CD4$^+$ PBLs co-expressing PD-1^{hi} and CD39 also detected the greatest number of neoantigen reactivities (Figure 31). Nevertheless, this population missed several reactivities, which were captured in the PD-1^{hi} or PD-1^{hi}CD39$^-$ subpopulations. Our laboratory recently reported similar observations in CD4$^+$ TILs from endometrial cancer patients (192). Thus, PD-1^{hi}CD39$^+$ might not be the best combination of biomarkers to comprehensively identify CD4$^+$ neoantigen-specific or tumor-reactive T cells neither in the tumor nor in peripheral blood. Most of the work in the field of tumor-reactive or neoantigen-specific T cells has been focused on the CD8$^+$ compartment. Thus, less evidence is available about what tumor-reactive or neoantigen-specific CD4$^+$ T cells express in the tumor and in circulation. A recent study described that CD4$^+$ TILs co-expressing CD39 and ICOS are enriched with tumor-reactive T cells at the tumor site. Thus, other markers or other combinations should be explored to determine which would be the combination that best guides the detection of circulating CD4$^+$ neoantigen-specific or tumor-reactive T cells.

CD8$^+$ and CD4$^+$ sorted PBLs detected a greater number of neoantigen reactivities than unselected TILs expanded in high dose IL-2

In addition to PBLs, we also screened *ex vivo* expanded TILs against tumor antigens, as they have classically been the preferred source to obtain neoantigen-reactive lymphocytes. Our results showed that the selection of specific peripheral blood subsets identified a greater number of neoantigen reactivities than using the classical non-specific TIL expansion in high-dose IL-2. This was mainly observed for CD8$^+$ TILs as we did not capture any neoantigen reactivity, despite being expanded from the tumor lesion (Figure 32A). Thus, unselected TILs expanded in high dose IL-2 were less efficient at capturing neoantigen reactivities. Moreover, all but two neoantigen reactivities detected in TILs were also identified in peripheral blood. This demonstrates a high degree of similarity between the neoantigens targeted by T cells isolated from the circulation or from the tumor site, which is consistent with previous studies (152–154).

In contrast to circulating lymphocytes that were selected from peripheral blood based on the expression of specific cell-surface markers, TILs were expanded from the tumor biopsy in the presence of high dose IL-2 but without any previous enrichment. Thus, the most likely explanation is that the different strategies used to expand the TILs and the

PBLs affected the number of neoantigen reactivities detected. It is possible that selecting TILs based on their phenotype would have improved the identification of neoantigen-specific TILs as previously reported (73,74,191,192,195,196). Nevertheless, the isolation of tumor-reactive TILs also faces other hurdles. Although TILs capable of recognizing the tumor are enriched at the tumor site, their isolation from a tumor biopsy might be compromised by multiple factors including the limited amount of tumor material resected, the high heterogeneity within the tumor microenvironment and, more importantly, the abundance and the diversity of TILs in different tumor regions (285). Moreover, *in vitro* expansion of TILs in the presence of high dose IL-2 can significantly bias the frequency of antigen-specific T cells, which could potentially lead to the loss of specific reactivities, thereby underestimating the initial T-cell repertoire (160,286). Despite being at far lower frequencies in the circulation, the pool of T cells present in peripheral blood might capture a larger breadth of the anti-tumor response as it could, theoretically, include T cells recognizing neoantigens from distinct lesions and others that are trafficking from lymph nodes. Thus, developing efficient strategies to specifically select circulating T lymphocytes targeting neoantigens or capable of recognizing the tumor is crucial for the development of T-cell-based therapies and has the potential to outperform the detection of neoantigen-specific TILs from a tumor biopsy.

The selection of PBL subsets based on the expression of cell-surface markers might underrepresent the neoantigen-specific TCR repertoire

Although the surface marker-based isolation strategy enabled the identification of neoantigen-specific PBLs in eight out of 10 patients studied, this method also has certain limitations that are worth mentioning.

One potential concern of our strategy is the loss of reactivities and clonotype diversity that can occur during the *in vitro* expansion of sorted T-cell populations, which lasts 14 days (287). Although the sorted T-cell populations are enriched in neoantigen-specific T cells, these are likely still mixed subpopulations that also contain bystander T cells. Thus, the presence of non-reactive T cells in the selected T-cell population could lead to the overgrowth of bystander T cells thereby diluting the reactive cells (286). This limitation represents a common concern in the field and has been previously reported. For instance, Yossef *et al.* developed a strategy that consisted in isolating TILs expressing

PD-1 and/or activation markers such as 4-1BB or OX40 followed by microwell culturing at a density of 3 cells/well to avoid overgrowth of non-reactive T cells (282). Using this strategy, the authors detected 13 new neoantigens that were missed using the standard TIL *ex vivo* expansion. Nevertheless, generating microwell cultures of 3 cells/well might be highly laborious and hard to handle when working with peripheral blood due to the low frequency of neoantigen-specific T cells in circulation. Other strategies aim at detecting the TCR clonotypes directly after sorting specific T-cell populations from fresh tumor specimens prior to *in vitro* T-cell expansion. For instance, Pasetto et al., performed TCRβ deep sequencing followed by matching TRA-TRB by pairSEQ of sorted $CD8^+$ $PD\text{-}1^+$ T cells from fresh metastatic melanomas and identified up to five tumor-reactive TCRs in 11 out of 12 patients (139). More recently, TCRs derived from TILs have been directly identified from fresh tumor digests without using any pre-enrichment strategy in patients with different epithelial tumors (58,143). This approach enabled the interrogation of the entire TCR repertoire initially present in the tumor without the loss of any TCR clonotype, which can potentially occur in other strategies that require additional manipulation of the T-cell population prior to TCR sequencing.

Another limitation of our method is that sorting $CD8^+$ and $CD4^+$ T cells based on the expression of selected cell-surface receptors can skew our results towards a particular combination of biomarkers leaving many others overseen. Although we included a large panel of circulating T-cell populations to detect neoantigen reactivities in three cancer patients, it is technically challenging and laborious to cover all markers and all possible combinations using our approach. In the last years, multiple studies have used single-cell RNA and TCR sequencing analysis of tumor biopsies coupled with immunological screenings and have identified multiple tumor-reactive TCRs in TILs of different solid cancers, all presenting a gene signature associated with a dysfunctional phenotype (58,59,115,155,288). More recently, single-cell RNA sequencing analyses have also been coupled with CITE-seq to concomitantly assess cell-surface expression of >100 markers at protein level and thereby extract the highest amount of information on TIL populations including T-cell differentiation state, specificity and functionality. The use of this strategy based on single-cell RNA sequencing analysis could overcome the inherent bias in marker selection and the potential loss of reactive clonotypes during T-cell expansion. Moreover, it also allows TCR clonotype tracking along treatment to better monitor T-cell responses and clonal expansion after treatment with immunotherapy (58,289). Nonetheless, the

low prevalence of the tumor-reactive clonotypes in the blood would likely still require some level of enrichment prior to single-cell sequencing. In this regard, our work shows that selection and single-cell sequencing of PD-1 and CD39-expressing PBLs may greatly improve the number of neoantigen- and tumor-reactive TCRs identified.

cfDNA as an alternative source to identify candidate neoantigens

Analysis of cfDNA from peripheral blood for tumor molecular profiling represents a critical advance that offers a wide range of minimally-invasive clinical applications (206). Using our pipeline, we identified putative NSMs in the cfDNA of all patients analyzed and observed a certain degree of overlap with the NSMs identified in TuBx DNA in five of six patients. More importantly, WES of cfDNA successfully detected eight of 13 neoantigens in four of five cancer patients containing neoantigen reactivities, all of them also detected in TuBx DNA, further supporting their tumor-specificity. These findings demonstrate the feasibility and reproducibility of our approach and show that the WES sequencing depth used in our study (300X) provides enough sensitivity to identify tumor NSMs in cfDNA. Nonetheless, we cannot rule out the possibility that more neoantigens would have been detected if other inclusion criteria would have been used in our analysis. The criteria applied for selecting cfDNA variants varies considerably among studies, some selecting NSMs exclusively based on a minimum VAF of 1% (290,291). Considering this and the usual low representation of tumor-derived DNA within the total pool of cfDNA, using less stringent criteria to select cfDNA variants could increase the identification of neoantigens. Nevertheless, it would be important to find the most suitable filters to ensure selection of the maximum number of NSMs without including too many sequencing errors or artifacts generated during the generation of the WES library and *in silico* analysis.

Which factors could account for the differences observed between somatic mutations detected by WES of cfDNA and TuBx DNA?

In our study, the frequency of cfDNA NSMs over the total NSMs varied widely among patients and high levels of discordance between matched tumor and cfDNA samples were observed in some patients (*e.g.* patient GOI-03). These discordances have been previously reported in the literature and have been associated with biological and

preanalytical factors that will be further discussed in this section (292).

The ability to detect somatic mutations in cfDNA could be explained by different levels of tumor fraction in cfDNA, which represents the proportion of the total cfDNA that derives from tumor. In a systematic review analyzing 20 studies that used WES for tumor molecular profiling, the number of detected SNVs was correlated with the amount of tumor fraction of cfDNA (293). In contrast, the differences in the identification of NSMs in cfDNA could not be attributed to the tumor content in cfDNA in our cohort of patients. Given the low sensitivity of cfDNA WES in identifying tumor-derived genetic alterations (293), we considered essential to set a cfDNA tumor fraction cutoff value to pre-select samples for WES. Previous studies have established tumor fraction levels of 10% or 25% as pre-selection criteria for cfDNA WES analysis (222,294). Thus, we decided to exclude plasma samples having a tumor fraction <10% from our clonality analysis. Additional patients should be evaluated to confidently determine the tumor fraction cutoff value that would ensure the identification of tumor NSMs in cfDNA using WES. Such a cutoff could also be used as an inclusion criterion if finally applying this minimally-invasive T-cell therapy in the clinic to select patients.

Another factor that can explain discordances between tumor NSMs detected in cfDNA and TuBx DNA is the presence of spatial and temporal tumor heterogeneity (Figure 37). An example of this is a study conducted in patients with renal cell carcinoma where 65% of somatic genomic alterations were not detectable in every region of the primary and metastatic lesions(295). Similarly, a study that assessed a panel of 54 genes in cfDNA and primary and metastatic lesions in patients with metastatic breast cancer showed that cfDNA not only identified 97.2% of the variants present in primary and metastatic lesions but also detected 13 variants that were also present in the metastatic lesion but not in the primary tumor (296). Based on this, it is possible that subclones that exist in the primary tumor evolve and expand through disease progression, leading to the divergence of tumor genomic landscapes. Thus, NSMs exclusively found in cfDNA could be derived from tumor clones that were not captured by the core biopsy of a single lesion. This is because cfDNA potentially captures intra- and inter-tumor heterogeneity as the tumor DNA shed from distinct lesions in the same individual is mixed in the circulation (297) (Figure 37). Studies comparing cfDNA to tumor regional sampling supported this hypothesis as they observed that a great number of the SNVs initially identified only in cfDNA as compared to TuBx

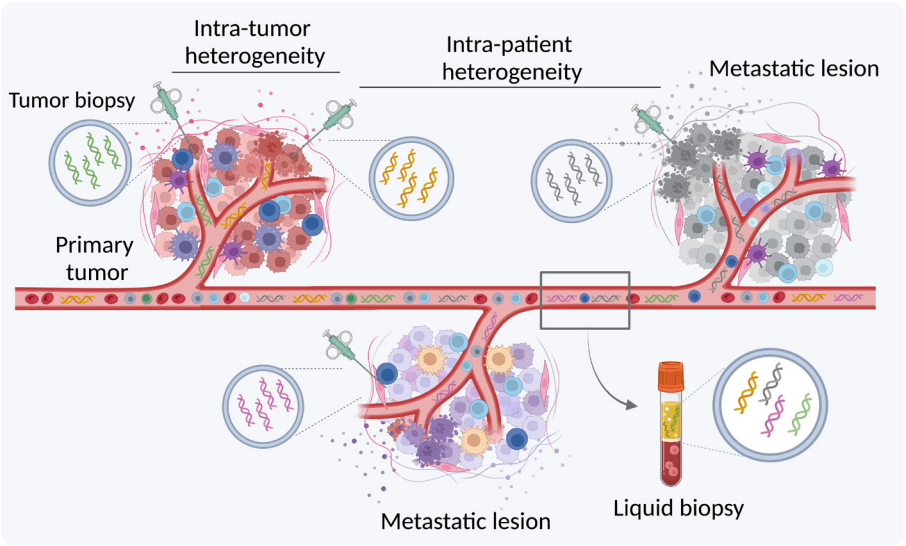

Figure 37. cfDNA can capture genomic tumor heterogeneity. During cancer progression, subclones that exist in the primary tumor might evolve and expand leading to the divergence of tumor genomic landscapes. Single tumor biopsies might not captured somatic alterations present in other regions of the same tumor or in other metastatic lesions. In contrast, since cfDNA can be shed from different tumor lesions and be mixed in the circulation, it potentially reflects intra- and inter-tumor heterogeneity. Image created with BioRender.com.

DNA were prospectively found in additional tumor regional biopsies (298,299). Although it is a potential explanation and would represent an advantage of using WES of cfDNA over TuBx DNA, we did not detect any reactivity against any NSM exclusively identified in cfDNA, which would have supported this hypothesis.

In addition to tumor heterogeneity, we cannot exclude the possibility that NSMs only detected in cfDNA are an artefactual product generated by sequencing errors or even during *in silico* analysis. This represents a technical limitation that is aggravated in WES of cfDNA due to the low representation of ctDNA (271,292,300). Other techniques are currently used to detect somatic variants in cfDNA, which include PCR-based and small-panel sequencing approaches. These techniques have higher sensitivity than WES or WGS but cannot be used as an exploratory tool to detect tumor NSMs, thereby only being able to detect mutations in a specific gene or panel of genes (271). Nonetheless, performing targeted sequencing and selected mutations uniquely identified through WES of cfDNA using conventional sequencing methods could help confirm whether these are indeed artifacts or real and this is pending.

By analyzing the type of mutations that were detected in the distinct sources of

DNA, we noticed that the frequency of frameshift mutations within NSMs detected exclusively in cfDNA was higher compared to those that were detected in the two DNA sources or exclusively detected in TuBx DNA (Figure 35). Moreover, somatic mutations shared between cfDNA and TuBx DNA or only detected in TuBx DNA were mainly SNVs and shared a similar pattern that was different from that observed in mutations exclusively detected in cfDNA. The differences observed between NSMs from cfDNA or from TuBx DNA are probably influenced by interpretation parameters. For instance, since the filters applied to include frameshift mutations are more relaxed than those used for SNVs (*i.e.* SNVs need to be called by two or more variant callers, as compared to only one for frameshifts), it is plausible that sequencing errors that generate frameshift mutations at low frequency in cfDNA were considered positive events whereas errors generating SNVs were excluded. Thus, it is tempting to speculate that at least a fraction of frameshifts exclusively detected in cfDNA corresponds to artifacts related to sequencing errors or *in silico* analysis rather than to tumor heterogeneity. Fine-tuning of sequencing methods and more sensitive filters is warranted to dissect and distinguish heterogeneity from artifacts, which would be essential to confidently detect tumor NSMs by sequencing cfDNA.

In addition to variations that could be applied to the *in silico* analysis of WES, we reasoned that molecular traits of NSMs might influence their identification in cfDNA. One possibility is the clonal status of NSMs in the tumor. Different mutational processes happen during tumor evolution, leading to tumor heterogeneity and the appearance of tumor subclones that can subsequently lead to no or variable representation of subclonal populations within cfDNA. Thus, clonal mutations, which are more represented in the tumor, might be better captured by WES of cfDNA. A study analyzing the concordance between clonal and subclonal events in tumor tissue and cfDNA supported this hypothesis since 88% of tumor clonal mutations were confirmed to be present in cfDNA, as opposed to the 47% of subclonal mutations (222). Similarly, our findings showed that WES of cfDNA preferentially captured clonal NSMs from tumor tissues and the frequency of clonal mutations in the biopsied tumor positively correlated with the frequency of shared NSMs identified. This observation further supports the use of cfDNA to develop minimally-invasive T-cell therapies as it would indirectly preferentially identify clonal neoantigens, which have been shown to be more clinically relevant (161). In line with this, all neoantigens detected in our cohort of patients were derived from clonal tumor NSMs, based on TuBx DNA WES. Overall, based on the differences observed in the frequency of shared NSMs

and the neoantigens identified, it would be of great interest to find a feature enabling the selection of patients whose cfDNA will consistently identify neoantigens. Although tumor clonality allows making this distinction, a tumor biopsy is needed to perform such analysis. Thus, increasing the number of cfDNA and matched tumor samples analyzed would be essential to explore other variables that could further enhance detection of the most clinically relevant NSMs using cfDNA WES.

Development of T-cell products for ACT from PBLs expressing PD-1^{hi}CD39^{+}

The fact that our strategy leverages the co-expression of PD-1^{hi} and CD39 for the enrichment of circulating neoantigen-specific T cells could raise some concern for the development of T-cell products for ACT. The expression of these two cell-surface markers has been widely described to be related to a dysfunctional state characterized by low proliferation capacity and functional impairment, which could compromise the efficacy of ACT therapy (71,301). T-cell intrinsic factors have been associated with ICB response in several murine and human studies, all of them demonstrating that a "progenitor-exhausted" T-cell population with stemness properties such as self-renewing capacity is needed for ICB response (62,63,302,303). This population is characterized by the expression of the transcription factor TCF-1 while not expressing inhibitory markers such as TIM-3 and CD39. Although most of the work has been done in ICB-treated cancer patients, a more recent study also demonstrated that melanoma cancer patients that respond to TIL-ACT retained a CD39^{-}CD69^{-} stem-like T-cell population recognizing neoantigens that had a higher capacity of self-renewal, persistence and presented a superior antitumor response *in vivo* (304). In our work, the T-cell population from which we sorted the smallest number of cells was PD-1^{hi}CD39^{+}, especially in CD8^{+}, from which we could only sort 69 T cells for patient GOI-01 (Figure 38, top). The second less-represented population was PD-1^{hi}CD39^{-} followed by PD-1^{-}CD39 (Figure 38, top). Contrary to what has been published for *ex vivo* expanded TILs, the proliferative capacity of circulating CD4^{+} and CD8^{+} T-cell populations expressing CD39 is not inferior to that observed in CD39^{-} populations (Figure 38, bottom). Notably, T-cell dysfunctionality has been described as a gradual state that encompass T-cell populations with a remarkable phenotypic diversity reflected by various combinations and levels of inhibitory and co-stimulatory markers (305). Therefore, it is tempting to speculate that our circulating PD-1^{hi}CD39^{+} T-cell populations might not be

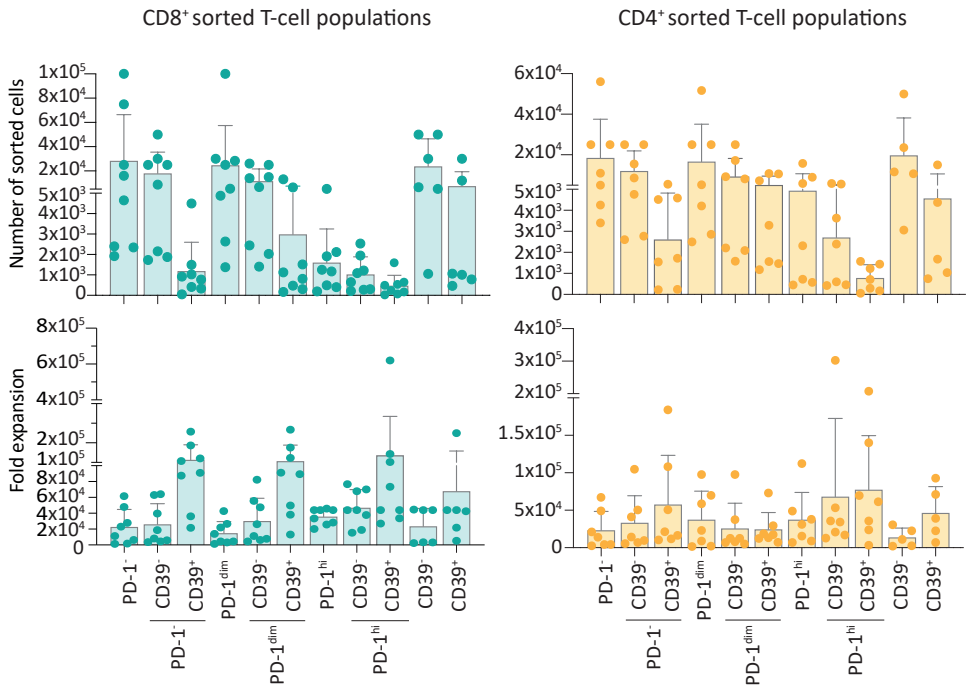

Figure 38. CD8⁺ and CD4⁺ PBL subsets sorted based on the expression of PD-1 and CD39 could be expanded from peripheral blood of all cancer patients studied. (**A**) Number of sorted circulating CD8⁺ and CD4⁺ T cells from peripheral blood of each individual. (**B**) Fold expansion of sorted CD8⁺ and CD4⁺ PBLs after a 14 days REP.

in a terminally-exhausted state but rather in an intermediate state that still maintains proliferative capacity and at least some levels of IFN-γ.

To unravel whether this circulating T-cell population would be suitable for the development of T-cell products for ACT, a more extensive phenotypic and transcriptional characterization to determine their differentiation state would be needed. Moreover, evaluating their effector functions together with their capacity to proliferate and persist *in vivo* would also be essential before developing novel T-cell products for ACT treatment.

Where are circulating neoantigen-specific T cells coming from or going to?

We have observed that co-expression of PD-1^{hi} and CD39 reproducibly identifies circulating CD8⁺ and CD4⁺ neoantigen-specific T cells. Our data, together with recent publications, demonstrate that tumor and neoantigen-reactive T cells can frequently be

detected in peripheral blood of cancer patients (58,152–156,288,306). However, the origin and/or destination of these tumor-reactive T cells has not been studied in detail and is still a matter of debate.

The natural development of anti-tumor T-cell responses is a process that involves several steps occurring at different locations. It is thought that T cells are forced to migrate and traffic through peripheral blood to reach different specialized niches. Priming of naïve T cells generally occurs in tumor-draining lymph nodes where migratory DCs loaded with tumor antigens present them to T cells. Thereafter, T cells recognizing tumor antigens get activated, clonally expand, start differentiating towards a more effector phenotype and migrate to peripheral tissues (Figure 39). In principle, we might be able to capture circulating neoantigen-specific T cells at this point. Nevertheless, the fact that we identified circulating neoantigen-specific T cells based on the co-expression of PD-1^{hi} and CD39, does not favor this hypothesis. Although PD-1 and CD39 are markers naturally expressed upon antigen-driven activation, such high levels of PD-1 co-expressed with CD39 would have typically been associated with chronically stimulated T cells. A recent study with murine models also does not support this hypothesis. In this study, they demonstrated that tumor-specific $CD8^+$ T cells are initially primed in the lymph nodes where they maintained a stem-like phenotype, but it is not until they infiltrate the tumor bed that they acquire the effector program by additional co-stimulation from APCs (307). Nevertheless, we cannot rule out the possibility that T lymphocytes become exhausted in the lymph nodes as they can contain or can be replaced by tumor cells in metastatic tumors. Another option is that the detected circulating neoantigen-specific T cells left the tumor bed and reentered the circulation, possibly to migrate to other tumor-draining lymph nodes or to sequentially patrol multiple metastases. In a recent paper, a subset of tissue-resident memory T cells in the skin was shown to be able to enter the circulation, where they remained transcriptionally representative of the skin-resident population (308). In cancer, using a Kaede transgenic mice developing Lewis lung carcinoma tumors, the authors described a tumor-experienced T-cell population that egressed the primary tumor and migrated to tumor-draining lymph nodes and distant metastasis (309). Although the specificity of the emigrant T cells was not evaluated, this study proved that T cells can leave the tumor niche. However, while emigrant T cells were activated and showed clear effector functions, T cells that persisted in the tumor expressed co-inhibitory receptors such as TIM-3 and PD-1, possibly because of a hampered migration capacity (310).

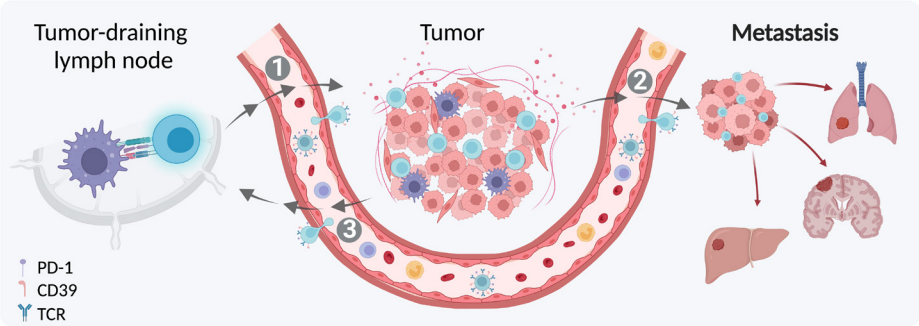

Figure 39. Neoantigen-specific and tumor-reactive T cells can be found in the circulation at different time points of the anti-tumor T-cell response. The development of anti-tumor T-cell responses is a process that involves several steps occurring at different locations. T cells need to migrate and traffic through peripheral blood to reach the different specialized niches, making them detectable in peripheral blood at different time points in the course of the response against tumor. Image created with BioRender.com.

Further studies are needed to unravel this conundrum and to better characterize circulating neoantigen-specific T cells to gain more insights into their differentiation status. Moreover, whether exhausted T cells detected in the blood, as opposed to the tumor, may also have altered motility and homing properties remains to be investigated.

Development of a personalized minimally-invasive T-cell therapy to treat patients with metastatic epithelial cancers

Personalized cancer immunotherapies with T-cell products enriched with neoantigen-specific T cells have been used to treat patients with metastatic epithelial cancers. Although objective responses have only been observed in selected patients (112,113,116,311), this therapy demonstrated to have the potential to mediate tumor regression in the advanced metastatic setting. In line with this, retrospective studies of TIL products from responders and non-responders of melanoma patients demonstrated that successful TIL-ACT is associated with an expansion of T cells targeting neoantigens supporting the important role of these T cells in mediating antitumor responses (173,312,313). Nevertheless, recent data has also shown the limitations of this therapeutic approach as neoantigen-specific T cells were detected in the tumor and blood of patients not responding to anti-PD-1 treatment (306). Although the existence of tumor-reactive or neoantigen-specific T cells is critical for mediating anti-tumor T-cell responses, there is still much to be learned in how such T cells mediate tumor cell clearance upon

immunotherapy and whether they require other factors for efficiently exerting their effector functions. So far, the development of neoantigen-targeted T-cell therapies and monitoring of neoantigen-specific T cells in cancer patients rely on tumor biopsies to both identify candidate neoantigens and reactive T cells or TCRs, limiting their therapeutic applicability and potentially underestimating tumor heterogeneity in the advanced metastatic setting.

In this thesis, we devised a strategy to simultaneously identify NSMs through WES and isolate neoantigen-specific $CD8^+$ and $CD4^+$ T cells or TCRs from cancer patients solely using peripheral blood (Figure 40). Our results demonstrated that the selection of circulating $CD8^+$ and $CD4^+$ T lymphocytes co-expressing PD-1^{hi} and CD39 coupled with WES of cfDNA enables the identification of $CD8^+$ and $CD4^+$ neoantigen-reactive T lymphocytes in patients with distinct epithelial tumors including breast, H&N and CRC. Hence, we provide a minimally-invasive strategy based on the use of peripheral blood to develop personalized T-cell therapies targeting neoantigens without the need of a tumor biopsy, which could be exploited to treat patients with unresectable tumors. Although we have already discussed several important considerations that still need to be addressed before applying this strategy to the clinics, this minimally-invasive approach could be used to treat patients with metastatic epithelial solid tumors that nowadays cannot benefit from currently used ACT treatments.

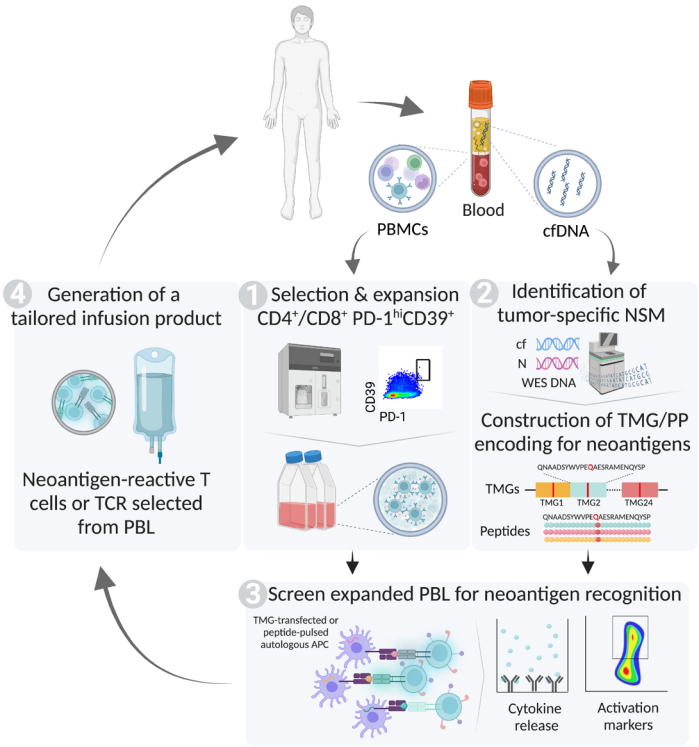

Figure 40. Schematic representation of the proposed strategy to simultaneously identify NSMs through WES of cfDNA and isolate neoantigen-specific CD8⁺ and CD4⁺ T cells or TCRs from cancer patients solely using peripheral blood. A peripheral blood sample would be used for (1) isolate CD4⁺ and CD8⁺ T cells based on the co-expression of PD-1^{hi} and CD39 and (2) isolate cfDNA to perform WES and identify putative NSMs, which would then be included in TMGs and PPs. (3) The sorted subpopulations would then be tested for neoantigen recognition via a co-culture with autologous B cells electroporated or pulsed with TMGs and PPs, respectively, and neoantigen-specific T cells would be selected based on the expression of the activation markers 4-1BB or OX40 on CD8⁺ or CD4⁺ T cells and expanded *ex vivo* to generate a T-cell product enriched with neoantigen-specific PBLs that would be re-infused back to the patient. Image created with BioRender.com.

Conclusions

The use of WES of cfDNA combined with the isolation of $CD8^+$ and $CD4^+$ $PD\text{-}1^{hi}$ $CD39^+$ PBLs enables the development of personalized T-cell therapies targeting neoantigens by the exclusive use of peripheral blood in a proportion of patients with metastatic epithelial cancers.

1. WES of cfDNA identified somatic mutations that were either shared with TuBx DNA or exclusively detected in the peripheral blood of patients with metastatic epithelial tumors.

2. In cancer patients, $CD8^+$ and $CD4^+$ $PD\text{-}1^{hi}$ PBLs displayed an overall upregulation of biomarkers typically associated with T-cell activation and dysfunction.

3. $CD8^+$ and $CD4^+$ $PD\text{-}1^{hi}$ PBLs from cancer patients represent rare subpopulations that show a unique co-expression profile of activation/exhaustion markers resembling the dysfunctional phenotype typically observed in TILs.

4. $CD8^+$ PBLs co-expressing $PD\text{-}1^{hi}$ and CD39 most reproducibly identify neoantigen-specific T cells, exceeding the number of reactivities detected by T-cell populations uniquely sorted based on $PD\text{-}1^{hi}$ expression. Moreover, this subpopulation consistently contained the highest frequency of neoantigen-specific lymphocytes.

5. While $CD4^+$ $PD\text{-}1^{hi}$ $CD39^+$ PBLs identified a higher number of neoantigen reactivities, it did not consistently result in a greater frequency of neoantigen-specific T cells and it missed some neoantigen reactivities.

6. The selection of $CD8^+$ PBLs expressing $PD\text{-}1^{hi}$ and CD39 leads to the detection of a greater number of T-cell reactivities targeting tumor antigens than the classical non-specific TIL expansion in high-dose IL-2.

7. Overall, WES of cfDNA identified 61.5% of all neoantigens in four of five patients harboring neoantigen reactivities. None of the candidate neoantigens tested exclusively identified in cfDNA were recognized by T cells.

8. The tumor fraction of cfDNA and the tumor clonality of each NSMs are two factors that influence the detection of tumor somatic mutations and neoantigens in cfDNA.

   8.1. A certain level of tumor fraction in cfDNA is essential but does not guarantee the detection of mutations shared with TuBx DNA.

   8.2. WES of cfDNA was capable of frequently detecting shared mutations, which

were predominantly clonal. This is critical since all the neoantigens identified in our study derived from clonal mutations.

References

1. Alberts B. Molecular Biology of the Cell. 2015.

2. Hanahan D, Weinberg RA. The Hallmarks of Cancer Review evolve progressively from normalcy via a series of pre. Vol. 100, Cell. 2000.

3. Hanahan D, Weinberg RA. Hallmarks of cancer: The next generation. Vol. 144, Cell. 2011. p. 646–74.

4. Hanahan D. Hallmarks of Cancer: New Dimensions. Vol. 12, Cancer Discovery. American Association for Cancer Research Inc.; 2022. p. 31–46.

5. Ehrlich P. Ueber den jetzigen Stand der Karzinomforschung. Ned Tijdschr Geneeskd. 1909;

6. Thomas L. Discussion. In Cellular and Humoral Aspects of the Hypersensitive States [Internet]. Shaftesbury Ave. 1959. Available from: http://jama.jamanetwork.com/

7. Burnet FM. The Concept of Immunological Surveillance. Vol. 13, Progr. exp. Tumor Res. Karger; 1970.

8. Rygaard J, Povlsen CO. THE MOUSE MUTANT NUDE DOES NOT DEVELOP SPONTANEOUS TUMOURS. An Argument Against Immunological Surveillance. Acta Pathologica Microbiologica Scandinavica Section B Microbiology and Immunology. 1974;82 B(1):99–106.

9. Dighe AS, Richards E, Old LJ, Schreiber RD. Enhanced in vivo growth and resistance to rejection of tumor cells expressing dominant negative IFNγ receptors. Immunity [Internet]. 1994 Sep 1;1(6):447–56. Available from: https://doi.org/10.1016/1074-7613(94)90087-6

10. van den Broek M, Ossendorpfl Ren F, SpirosVamvakas T, Lutz WK, Melieffl Rolf M Zinkernagel CJ, Hengartner H. Decreased Tumor Surveillance in Perforin-deficient Mice. Journal Experimental Medicine [Internet]. 1996; Available from: http://rupress.org/jem/article-pdf/184/5/1781/1396694/1781.pdf

11. Kaplan DH, Shankaran V, Dighe AS, Stockert E, Aguet M, Old LJ, et al. Demonstration of an interferon γ-dependent tumor surveillance system in immunocompetent mice. Proc Natl Acad Sci U S A. 1998 Jun 23;95(13):7556–61.

12. Shankaran V, Ikeda H, Bruce AT, White JM, Swanson PE, Old LJ, et al. IFNγ and lymphocytes prevent primary tumour development and shape tumour

immunogenicity. Nature [Internet]. 2001;410(6832):1107–11. Available from: https://doi.org/10.1038/35074122

13. Dunn GP, Old LJ, Schreiber RD. The immunobiology of cancer immunosurveillance and immunoediting. Immunity. 2004;21(2):137–48.

14. Dunn GP, Bruce AT, Ikeda H, Old LJ, Schreiber RD. Cancer immunoediting: from immuno-surveillance to tumor escape [Internet]. 2002. Available from: http://www.nature.com/natureimmunology

15. Penn I. Posttransplant Malignancies. 1999.

16. Gatti RA, Good RA. Occurrence of malignancy in immunodeficiency diseases - A Literature Review. 1971.

17. Boshoff C, Weiss R. Aids-related malignancies. Nat Rev Cancer [Internet]. 2002;2(5):373–82. Available from: https://doi.org/10.1038/nrc797

18. Street SEA, Cretney E, Smyth MJ. Perforin and interferon-activities independently control tumor initiation, growth, and metastasis [Internet]. 2001. Available from: http://ashpublications.org/blood/article-pdf/97/1/192/1670448/192.pdf

19. Engel AM, Svane IM, Rygaard J, Werdelin O. MCA sarcomas induced in scid mice are more immunogenic than MCA sarcomas induced in congenic, immunocompetent mice. Scand J Immunol. 1997;45(4):463–70.

20. Street SEA, Trapani JA, MacGregor D, Smyth MJ. Suppression of lymphoma and epithelial malignancies effected by interferon γ. Journal of Experimental Medicine. 2002 Jul 1;196(1):129–34.

21. Svane IM, Engel AM, Nielsen MB, Ljunggren HG, Rygaard J, Werdelin O. Chemically induced sarcomas from nude mice are more immunogenic than similar sarcomas from congenic normal mice. Eur J Immunol. 1996;26(8):1844–50.

22. Gubin MM, Vesely MD. Cancer Immunoediting in the Era of Immuno-oncology. Vol. 28, Clinical Cancer Research. American Association for Cancer Research Inc.; 2022. p. 3917–28.

23. Strominger JL. Human histocompatibility proteins. Immunol Rev [Internet]. 2002 Jul 1;185(1):69–77. Available from: https://doi.org/10.1034/j.1600-065X.2002.18508.x

24. Neefjes J, Jongsma MLM, Paul P, Bakke O. Towards a systems understanding of MHC class i and MHC class II antigen presentation. Vol. 11, Nature Reviews Immunology. 2011. p. 823–36.

25. Irla M. Annual Review of Immunology Instructive Cues of Thymic T Cell Selection. 2022; Available from: https://doi.org/10.1146/annurev-immunol-101320-

26. Morris GP, Allen PM. How the TCR balances sensitivity and specificity for the recognition of self and pathogens. Vol. 13, Nature Immunology. 2012. p. 121–8.

27. de Vries NL, van de Haar J, Veninga V, Chalabi M, Ijsselsteijn ME, van der Ploeg M, et al. γδ T cells are effectors of immunotherapy in cancers with HLA class I defects. Nature [Internet]. 2023;613(7945):743–50. Available from: https://doi.org/10.1038/s41586-022-05593-1

28. Long EO. Tumor cell recognition by natural killer cells. Semin Cancer Biol [Internet]. 2002;12(1):57–61. Available from: https://www.sciencedirect.com/science/article/pii/S1044579X01903980

29. Lurquin C, Van Pel A, Mariamé B, De Plaen E, Szikora JP, Janssens C, et al. Structure of the gene of tum- transplantation antigen P91A: The mutated exon encodes a peptide recognized with Ld by cytolytic T cells. Cell [Internet]. 1989 Jul 28;58(2):293–303. Available from: https://doi.org/10.1016/0092-8674(89)90844-1

30. van der Bruggen P, Traversari C, Chomez P, Lurquin C, De Plaen E, Van den Eynde B, et al. A Gene Encoding an Antigen Recognized by Cytolytic T Lymphocytes on a Human Melanoma. Science (1979) [Internet]. 1991 Dec 13;254(5038):1643–7. Available from: https://doi.org/10.1126/science.1840703

31. Coulie PG, Van Den Eynde BJ, Van Der Bruggen P, Boon T. Tumour antigens recognized by T lymphocytes: At the core of cancer immunotherapy. Vol. 14, Nature Reviews Cancer. 2014. p. 135–46.

32. Brichard V, Pel A Van, W6lfel T, W61fel C, De Plaen E, Leth6 B, et al. The Tyrosinase Gene Codes for an Antigen Recognized by Autologous Cytolytic T Lymphocytes on HLA-A2 Melanomas. Available from: http://rupress.org/jem/article-pdf/178/2/489/1267835/489.pdf

33. Coulie PG, Brichard V, Pel A Van, W61fel T, Schneider J, Traversari C, et al. A

New Gene Coding for a Differentiation Antigen Recognized by Autologous Cytolytic T Lymphocytes on HLA-A2 Melanomas. Journal Experimental Medicine [Internet]. 1994; Available from: http://rupress.org/jem/article-pdf/180/1/35/1105507/35.pdf

34. Barker ABH, Schreurs MWJ, Tafazzul G, De Boer AJ, Kawakami Y, Adema GJ, et al. Identification of a novel peptide derived from the melanocyte-specific gp100 antigen as the dominant epitope recognized by an HLA-A2.1-restricted anti-melanoma CTL line. Int J Cancer [Internet]. 1995 Jul 4;62(1):97–102. Available from: https://doi.org/10.1002/ijc.2910620118

35. Correale P, Walmsley K, Nieroda C, Zaremba S, Zhu M, Schlom J, et al. In Vitro Generation of Human Cytotoxic T Lymphocytes Specific for Peptides Derived From Prostate-Specific Antigen. J Natl Cancer Inst [Internet]. 1997; Available from: https://academic.oup.com/jnci/article/89/4/293/2526832

36. Olson BM, Frye TP, Johnson LE, Fong L, Knutson KL, Disis ML, et al. HLA-A2-restricted T-cell epitopes specific for prostatic acid phosphatase. Cancer Immunology, Immunotherapy [Internet]. 2010;59(6):943–53. Available from: https://doi.org/10.1007/s00262-010-0820-6

37. Rezvani K, Brenchley JM, Price DA, Kilical Y, Gostick E, Sewell AK, et al. T-cell responses directed against multiple HLA-A*0201-restricted epitopes derived from Wilms' tumor 1 protein in patients with leukemia and healthy donors: Identification, quantification, and characterization. Clinical Cancer Research. 2005 Dec 15;11(24):8799–807.

38. Fisk B, Blevins TL, Wharton JT, Ioannides CG. Identification of an Immunodominant Peptide of HER-2/neu Protooncogene Recognized by Ovarian Tumor-specific Cytotoxic T Lymphocyte Lines. Journal experimental medicine. 1995;

39. Parkhurst MR, Robbins PF, Tran E, Prickett TD, Gartner JJ, Li J, et al. Unique neoantigens arise from somatic mutations in patients with gastrointestinal cancers. Cancer Discov. 2019 Aug 1;9(8):1022–35.

40. Malekzadeh P, Yossef R, Cafri G, Paria BC, Lowery FJ, Jafferji M, et al. Antigen experienced T cells from peripheral blood recognize p53 neoantigens. Clinical Cancer Research. 2020 Mar 15;26(6):1267–76.

41. Eberhardt CS, Kissick HT, Patel MR, Cardenas MA, Prokhnevska N, Obeng RC, et

al. Functional HPV-specific PD-1+ stem-like CD8 T cells in head and neck cancer. Nature [Internet]. 2021;597(7875):279–84. Available from: https://doi.org/10.1038/s41586-021-03862-z

42. Iyer JG, Afanasiev OK, McClurkan C, Paulson K, Nagase K, Jing L, et al. Merkel cell polyomavirus-specific CD8+and CD4+ T-cell responses identified in Merkel cell carcinomas and blood. Clinical Cancer Research. 2011 Nov 1;17(21):6671–80.

43. Lee SP, Chan ATC, Cheung ST, Thomas WA, CroomCarter D, Dawson CW, et al. CTL Control of EBV in Nasopharyngeal Carcinoma (NPC): EBV-Specific CTL Responses in the Blood and Tumors of NPC Patients and the Antigen-Processing Function of the Tumor Cells. The Journal of Immunology. 2000 Jul 1;165(1):573–82.

44. Almeida LG, Sakabe NJ, de Oliveira AR, Silva MCC, Mundstein AS, Cohen T, et al. CTdatabase: A knowledge-base of high-throughput and curated data on cancer-testis antigens. Nucleic Acids Res. 2009;37(SUPPL. 1).

45. Chen DS, Mellman I. Oncology meets immunology: The cancer-immunity cycle. Vol. 39, Immunity. 2013. p. 1–10.

46. Cruz FM, Colbert JD, Merino E, Kriegsman BA, Rock KL. The Biology and Underlying Mechanisms of Cross-Presentation of Exogenous Antigens on MHC-I Molecules. 2017; Available from: https://doi.org/10.1146/annurev-immunol-

47. Lenschow DJ, Walunas TL, Bluestone JA. CD28/B7 SYSTEM OF T CELL COSTIMULATION [Internet]. Vol. 14, Annu. Rev. Immunol. 1996. Available from: www.annualreviews.org

48. Tie Y, Tang F, Wei Y quan, Wei X wei. Immunosuppressive cells in cancer: mechanisms and potential therapeutic targets. J Hematol Oncol [Internet]. 2022;15(1):61. Available from: https://doi.org/10.1186/s13045-022-01282-8

49. Virgin HW, Wherry EJ, Ahmed R. Redefining Chronic Viral Infection. Vol. 138, Cell. Elsevier B.V.; 2009. p. 30–50.

50. Kaech SM, Wherry EJ. Heterogeneity and Cell-Fate Decisions in Effector and Memory CD8+ T Cell Differentiation during Viral Infection. Vol. 27, Immunity. 2007. p. 393–405.

51. Mclane LM, Abdel-Hakeem MS, Wherry EJ. CD8 T Cell Exhaustion During

Chronic Viral Infection and Cancer. 2019; Available from: https://doi.org/10.1146/annurev-immunol-041015-

52. Zajac AJ, Blattman JN, Murali-Krishna K, Sourdive DJD, Suresh M, Altman JD, et al. Viral Immune Evasion Due to Persistence of Activated T Cells Without Effector Function [Internet]. Vol. 188, J. Exp. Med. 1998. Available from: http://www.jem.org

53. Gallimore A, Glithero A, Godkin A, Tissot AC, Plückthun A, Elliott T, et al. Induction and Exhaustion of Lymphocytic Choriomeningitis Virus-specific Cytotoxic T Lymphocytes Visualized Using Soluble Tetrameric Major Histocompatibility Complex Class I-Peptide Complexes [Internet]. Vol. 187, J. Exp. Med. 1998. Available from: http://www.jem.org

54. Kostense S, Vandenberghe K, Joling J, Van Baarle D, Nanlohy N, Manting E, et al. Persistent numbers of tetramer+ CD8+ T cells, but loss of interferon-γ+ HIV-specific T cells during progression to AIDS. Blood. 2002 Apr 1;99(7):2505–11.

55. Shankar P, Russo M, Harnisch B, Patterson M, Skolnik P, Lieberman J. Impaired function of circulating HIV-specific CD8+ T cells in chronic human immunodeficiency virus infection. Blood. 2000 Nov 1;96(9):3094–101.

56. Thommen DS, Schumacher TN. T Cell Dysfunction in Cancer. Vol. 33, Cancer Cell. Cell Press; 2018. p. 547–62.

57. Pauken KE, Wherry EJ. Overcoming T cell exhaustion in infection and cancer. Vol. 36, Trends in Immunology. Elsevier Ltd; 2015. p. 265–76.

58. Oliveira G, Stromhaug K, Klaeger S, Kula T, Frederick DT, Le PM, et al. Phenotype, specificity and avidity of antitumour CD8+ T cells in melanoma. Nature. 2021 Aug 5;596(7870):119–25.

59. Lowery FJ, Krishna S, Yossef R, Parikh NB, Chatani PD, Zacharakis N, et al. Molecular signatures of antitumor neoantigen-reactive T cells from metastatic human cancers [Internet]. 2022. Available from: https://www.science.org

60. Blank CU, Haining WN, Held W, Hogan PG, Kallies A, Lugli E, et al. Defining 'T cell exhaustion'. Nat Rev Immunol. 2019 Nov 1;19(11):665–74.

61. Yi JS, Cox MA, Zajac AJ. T-cell exhaustion: Characteristics, causes and conversion. Vol. 129, Immunology. 2010. p. 474–81.

62. Miller BC, Sen DR, Al Abosy R, Bi K, Virkud Y V., LaFleur MW, et al. Subsets of

exhausted CD8+ T cells differentially mediate tumor control and respond to checkpoint blockade. Nat Immunol. 2019 Mar 1;20(3):326–36.

63. Siddiqui I, Schaeuble K, Chennupati V, Fuertes Marraco SA, Calderon-Copete S, Pais Ferreira D, et al. Intratumoral Tcf1 + PD-1 + CD8 + T Cells with Stem-like Properties Promote Tumor Control in Response to Vaccination and Checkpoint Blockade Immunotherapy. Immunity. 2019 Jan 15;50(1):195-211.e10.

64. Kuchroo JR, Hafler DA, Sharpe AH, Lucca LE. The double-edged sword: Harnessing PD-1 blockade in tumor and autoimmunity. Sci Immunol [Internet]. 2023 Mar 15;6(65):eabf4034. Available from: https://doi.org/10.1126/sciimmunol.abf4034

65. Miller JD, van der Most RG, Akondy RS, Glidewell JT, Albott S, Masopust D, et al. Human Effector and Memory CD8+ T Cell Responses to Smallpox and Yellow Fever Vaccines. Immunity. 2008 May 16;28(5):710–22.

66. Goronzy JJ, Weyand CM. T-cell co-stimulatory pathways in autoimmunity. Vol. 10, Arthritis Research and Therapy. 2008.

67. Bak SP, Barnkob MS, Bai A, Higham EM, Wittrup KD, Chen J. Differential Requirement for CD70 and CD80/CD86 in Dendritic Cell-Mediated Activation of Tumor-Tolerized CD8 T Cells. The Journal of Immunology. 2012 Aug 15;189(4):1708–16.

68. French RR, Taraban VY, Crowther GR, Rowley TF, Gray JC, Johnson PW, et al. Eradication of lymphoma by CD8 T cells following anti-CD40 monoclonal antibody therapy is critically dependent on CD27 costimulation. Blood. 2007 Jun 1;109(11):4810–5.

69. Taraban VY, Rowley TF, Kerr JP, Willoughby JE, Johnson PMW, Al-Shamkhani A, et al. CD27 costimulation contributes substantially to the expansion of functional memory CD8+ T cells after peptide immunization. Eur J Immunol. 2013;43(12):3314–23.

70. Antonioli L, Pacher P, Sylvester Vizi E, rgy Haskó G. CD39 and CD73 in immunity and inflammation. Trends Mol Med [Internet]. 2013;19:355–67. Available from: http://dx.doi.org/10.1016/j.molmed.2013.

71. Moesta AK, Li XY, Smyth MJ. Targeting CD39 in cancer. Nat Rev Immunol [Internet]. 2020;20(12):739–55. Available from: https://doi.org/10.1038/s41577-020-0376-4

72. Gupta PK, Godec J, Wolski D, Adland E, Yates K, Pauken KE, et al. CD39 Expression

Identifies Terminally Exhausted CD8+ T Cells. PLoS Pathog. 2015;11(10).

73. Duhen T, Duhen R, Montler R, Moses J, Moudgil T, De Miranda NF, et al. Co-expression of CD39 and CD103 identifies tumor-reactive CD8 T cells in human solid tumors. Nat Commun. 2018 Dec 1;9(1).

74. Simoni Y, Becht E, Fehlings M, Loh CY, Koo SL, Teng KWW, et al. Bystander CD8+ T cells are abundant and phenotypically distinct in human tumour infiltrates. Nature. 2018 May 24;557(7706):575–9.

75. Chow A, Uddin FZ, Liu M, Dobrin A, Nabet BY, Mangarin L, et al. The ectonucleotidase CD39 identifies tumor-reactive CD8+ T cells predictive of immune checkpoint blockade efficacy in human lung cancer. Immunity. 2023 Jan 10;56(1):93-106.e6.

76. Rosenberg SA. IL-2: The First Effective Immunotherapy for Human Cancer. The Journal of Immunology. 2014 Jun 15;192(12):5451–8.

77. Morgan DA, Ruscetti FW, Gallo R. Selective in Vitro Growth of T Lymphocytes from Normal Human Bone Marrows. Science (1979) [Internet]. 1976 Sep 10;193(4257):1007–8. Available from: https://doi.org/10.1126/science.181845

78. Rosenberg SA, Lotze MT, Muul LM, Leitman S, Chang AE, Ettinghausen SE, et al. Observations on the Systemic Administration of Autologous Lymphokine-Activated Killer Cells and Recombinant Interleukin-2 to Patients with Metastatic Cancer. New England Journal of Medicine [Internet]. 1985 Dec 5;313(23):1485–92. Available from: https://doi.org/10.1056/NEJM198512053132327

79. Rosenberg SA, Yang JC, Topalian SL, Schwartzentruber DJ, Weber JS, Parkinson DR, et al. Treatment of 283 Consecutive Patients With Metastatic Melanoma or Renal Cell Cancer Using High-Dose Bolus Interleukin 2. JAMA [Internet]. 1994 Mar 23;271(12):907–13. Available from: https://doi.org/10.1001/jama.1994.03510360033032

80. Yang JC, Sherry RM, Steinberg SM, Topalian SL, Schwartzentruber DJ, Hwu P, et al. Randomized Study of High-Dose and Low-Dose Interleukin-2 in Patients With Metastatic Renal Cancer. Journal of Clinical Oncology [Internet]. 2003 Aug 15;21(16):3127–32. Available from: https://doi.org/10.1200/JCO.2003.02.122

81. Wherry EJ, Kurachi M. Molecular and cellular insights into T cell exhaustion.

Nat Rev Immunol [Internet]. 2015;15(8):486–99. Available from: https://doi.org/10.1038/nri3862

82. Hodi FS, O'Day SJ, McDermott DF, Weber RW, Sosman JA, Haanen JB, et al. Improved Survival with Ipilimumab in Patients with Metastatic Melanoma. New England Journal of Medicine. 2010 Aug 19;363(8):711–23.

83. Sharma P, Siddiqui BA, Anandhan S, Yadav SS, Subudhi SK, Gao J, et al. The next decade of immune checkpoint therapy. Vol. 11, Cancer Discovery. American Association for Cancer Research Inc.; 2021. p. 838–57.

84. Wei SC, Duffy CR, Allison JP. Fundamental mechanisms of immune checkpoint blockade therapy. Vol. 8, Cancer Discovery. American Association for Cancer Research Inc.; 2018. p. 1069–86.

85. Sharpe AH, Pauken KE. The diverse functions of the PD1 inhibitory pathway. Vol. 18, Nature Reviews Immunology. Nature Publishing Group; 2018. p. 153–67.

86. Khair DO, Bax HJ, Mele S, Crescioli S, Pellizzari G, Khiabany A, et al. Combining immune checkpoint inhibitors: Established and emerging targets and strategies to improve outcomes in melanoma. Vol. 10, Frontiers in Immunology. Frontiers Media S.A.; 2019.

87. Tawbi HA, Schadendorf D, Lipson EJ, Ascierto PA, Matamala L, Castillo Gutiérrez E, et al. Relatlimab and Nivolumab versus Nivolumab in Untreated Advanced Melanoma. New England Journal of Medicine. 2022 Jan 6;386(1):24–34.

88. Nisonoff A, Wissler FC, Lipman LN. Properties of the Major Component of a Peptic digest of Rabbit Antibody. Science (1979). 1960;

89. Topp MS, Gökbuget N, Stein AS, Zugmaier G, O'Brien S, Bargou RC, et al. Safety and activity of blinatumomab for adult patients with relapsed or refractory B-precursor acute lymphoblastic leukaemia: A multicentre, single-arm, phase 2 study. Lancet Oncol. 2015;16(1):57–66.

90. Codarri Deak L, Nicolini V, Hashimoto M, Karagianni M, Schwalie PC, Lauener L, et al. PD-1-cis IL-2R agonism yields better effectors from stem-like CD8+ T cells. Nature. 2022 Oct 6;610(7930):161–72.

91. Tichet M, Wullschleger S, Chryplewicz A, Fournier N, Marcone R, Kauzlaric A,

et al. Bispecific PD1-IL2v and anti-PD-L1 break tumor immunity resistance by enhancing stem-like tumor-reactive CD8+ T cells and reprogramming macrophages. Immunity. 2023 Jan 10;56(1):162-179.e6.

92. Blass E, Ott PA. Advances in the development of personalized neoantigen-based therapeutic cancer vaccines. Vol. 18, Nature Reviews Clinical Oncology. Nature Research; 2021. p. 215–29.

93. Disis ML, Wallace DR, Gooley TA, Dang Y, Slota M, Lu H, et al. Concurrent trastuzumab and HER2/neu-specific vaccination in patients with metastatic breast cancer. Journal of Clinical Oncology. 2009 Oct 1;27(28):4685–92.

94. Karbach J, Neumann A, Atmaca A, Wahle C, Brand K, Von Boehmer L, et al. Efficient in vivo priming by vaccination with recombinant NY-ESO-1 protein and CpG in antigen naïve prostate cancer patients. Clinical Cancer Research. 2011 Feb 15;17(4):861–70.

95. Hollingsworth RE, Jansen K. Turning the corner on therapeutic cancer vaccines. Vol. 4, npj Vaccines. Nature Publishing Group; 2019.

96. Vansteenkiste J, Zielinski M, Linder A, Dahabreh J, Gonzalez EE, Malinowski W, et al. Adjuvant MAGE-A3 immunotherapy in resected non–small-cell lung cancer: Phase II randomized study results. Journal of Clinical Oncology. 2013 Jul 1;31(19):2396–403.

97. Gardner TA, Elzey BD, Hahn NM. Sipuleucel-T (Provenge) autologous vaccine approved for treatment of men with asymptomatic or minimally symptomatic castrate-resistant metastatic prostate cancer. Vol. 8, Human Vaccines and Immunotherapeutics. Landes Bioscience; 2012. p. 534–9.

98. Pedersen SR, Sørensen MR, Buus S, Christensen JP, Thomsen AR. Comparison of Vaccine-Induced Effector CD8 T Cell Responses Directed against Self- and Non–Self-Tumor Antigens: Implications for Cancer Immunotherapy. The Journal of Immunology. 2013 Oct 1;191(7):3955–67.

99. Ott PA, Hu-Lieskovan S, Chmielowski B, Govindan R, Naing A, Bhardwaj N, et al. A Phase Ib Trial of Personalized Neoantigen Therapy Plus Anti-PD-1 in Patients with Advanced Melanoma, Non-small Cell Lung Cancer, or Bladder Cancer. Cell. 2020 Oct 15;183(2):347-362.e24.

100. Burris III HA, Patel MR, Cho DC, Clarke JM, Gutierrez M, Zaks TZ, et al. A phase

1, open-label, multicenter study to assess the safety, tolerability, and immunogenicity of mRNA-4157 alone in subjects with resected solid tumors and in combination with pembrolizumab in subjects with unresectable solid tumors (Keynote-603). J Glob Oncol [Internet]. 2019 Oct 7;5(suppl):93. Available from: https://doi.org/10.1200/JGO.2019.5.suppl.93

101. Sahin U, Oehm P, Derhovanessian E, Jabulowsky RA, Vormehr M, Gold M, et al. An RNA vaccine drives immunity in checkpoint-inhibitor-treated melanoma. Nature. 2020 Sep 3;585(7823):107–12.

102. Shemesh CS, Hsu JC, Hosseini I, Shen BQ, Rotte A, Twomey P, et al. Personalized Cancer Vaccines: Clinical Landscape, Challenges, and Opportunities. Vol. 29, Molecular Therapy. Cell Press; 2021. p. 555–70.

103. Cheever MA, Greenberg PD, Fefer A, Gillisi S. AUGMENTATION OF THE ANTI-TUMOR THERAPEUTIC EFFICACY OF LONG-TERM CULTURED T LYMPHOCYTES BY IN VIVO ADMINISTRATION OF PURIFIED INTERLEUKIN 2*. Journal of experimental medicine [Internet]. 1982; Available from: http://rupress.org/jem/article-pdf/155/4/968/1393726/968.pdf

104. Eberlein TJ, Rosenstein M, Rosenberg SA. REGRESSION OF A DISSEMINATED SYNGENEIC SOLID TUMOR BY SYSTEMIC TRANSFER OF LYMPHOID CELLS EXPANDED IN INTERLEUKIN 2. Journal of experimental medicine. 1982;

105. Rosenberg SA, Spiess P, Lafreniere R. A New Approach to the Adoptive Immunotherapy of Cancer with Tumor-Infiltrating Lymphocytes. Science (1979) [Internet]. 1986 Sep 19;233(4770):1318–21. Available from: https://doi.org/10.1126/science.3489291

106. Muul LM, Nason-Burchenal K, Carter CS, Cullis H, Slavin D, Hyatt C, et al. Development of an automated closed system for generation of human lymphokine-activated killer (LAK) cells for use in adoptive immunotherapy. J Immunol Methods [Internet]. 1987;101(2):171–81. Available from: https://www.sciencedirect.com/science/article/pii/0022175987901487

107. Rosenberg SA, Packard BS, Aebersold PM, Solomon D, Topalian SL, Toy ST, et al. Use of Tumor-Infiltrating Lymphocytes and Interleukin-2 in the Immunotherapy of Patients with Metastatic Melanoma. New England Journal of Medicine [Internet]. 1988 Dec 22;319(25):1676–80. Available from: https://doi.org/10.1056/NEJM198812223192527

108. Rosenberg SA, Restifo NP. Adoptive cell transfer as personalized immunotherapy for human cancer. Science (1979) [Internet]. 2015 Apr 3;348(6230):62–8. Available from: https://doi.org/10.1126/science.aaa4967

109. Kristensen NP, Heeke C, Tvingsholm SA, Borch A, Draghi A, Crowther MD, et al. Neoantigen-reactive CD8+ T cells affect clinical outcome of adoptive cell therapy with tumor-infiltrating lymphocytes in melanoma. J Clin Invest [Internet]. 2022 Jan 18;132(2). Available from: https://doi.org/10.1172/JCI150535

110. Robbins PF, Lu YC, El-Gamil M, Li YF, Gross C, Gartner J, et al. Mining exomic sequencing data to identify mutated antigens recognized by adoptively transferred tumor-reactive T cells. Nat Med. 2013 Jun;19(6):747–52.

111. Lu YC, Yao X, Crystal JS, Li YF, El-Gamil M, Gross C, et al. Efficient identification of mutated cancer antigens recognized by T cells associated with durable tumor regressions. Clinical Cancer Research. 2014 Jul 1;20(13):3401–10.

112. Tran E, Turcotte S, Gros A, Robbins PF, Lu YC, Dudley ME, et al. Cancer Immunotherapy Based on Mutation-Specific CD4+ T Cells in a Patient with Epithelial Cancer. Science (1979). 2014;344(6184):638–41.

113. Tran E, Robbins PF, Lu YC, Prickett TD, Gartner JJ, Jia L, et al. T-Cell Transfer Therapy Targeting Mutant KRAS in Cancer. New England Journal of Medicine. 2016 Dec 8;375(23):2255–62.

114. Zacharakis N, Lutfi ;, Huq M, Seitter SJ, Kim SP, Gartner JJ, et al. Breast Cancers Are Immunogenic: Immunologic Analyses and a Phase II Pilot Clinical Trial Using Mutation-Reactive Autologous Lymphocytes. J Clin Oncol [Internet]. 2022;40:1741–54. Available from: https://doi.

115. Hanada K ichi, Zhao C, Gil-Hoyos R, Gartner JJ, Chow-Parmer C, Lowery FJ, et al. A phenotypic signature that identifies neoantigen-reactive T cells in fresh human lung cancers. Cancer Cell. 2022 May 9;40(5):479-493.e6.

116. Stevanović S, Pasetto A, Helman SR, Gartner JJ, Prickett TD, Howie B, et al. Landscape of immunogenic tumor antigens in successful immunotherapy of virally induced epithelial cancer. Science (1979). 2017;

117. Zacharakis N, Chinnasamy H, Black M, Xu H, Lu YC, Zheng Z, et al. Immune

recognition of somatic mutations leading to complete durable regression in metastatic breast cancer. Nat Med. 2018 Jun 1;24(6):724–30.

118. Morgan RA, Dudley ME, Wunderlich JR, Hughes MS, Yang JC, Sherry RM, et al. Cancer Regression in Patients After Transfer of Genetically Engineered Lymphocytes. Science (1979) [Internet]. 2006; Available from: www.sciencemag.org

119. Johnson LA, Morgan RA, Dudley ME, Cassard L, Yang JC, Hughes MS, et al. Gene therapy with human and mouse T-cell receptors mediates cancer regression and targets normal tissues expressing cognate antigen. Blood. 2009;114(3):535–46.

120. Robbins PF, Morgan RA, Feldman SA, Yang JC, Sherry RM, Dudley ME, et al. Tumor regression in patients with metastatic synovial cell sarcoma and melanoma using genetically engineered lymphocytes reactive with NY-ESO-1. Journal of Clinical Oncology. 2011 Mar 1;29(7):917–24.

121. Linette GP, Stadtmauer EA, Maus M V, Rapoport AP, Levine BL, Emery L, et al. Cardiovascular toxicity and titin cross-reactivity of affinity-enhanced T cells in myeloma and melanoma. 2013; Available from: http://ashpublications.org/blood/article-pdf/122/6/863/1374971/863.pdf

122. Morgan RA, Chinnasamy N, Abate-Daga D, Gros A, Robbins PF, Zheng Z, et al. Cancer Regression and Neurological Toxicity Following Anti-MAGE-A3 TCR Gene Therapy [Internet]. 2013. Available from: http://www.clinicaltrials.gov

123. Parkhurst MR, Yang JC, Langan RC, Dudley ME, Nathan DAN, Feldman SA, et al. T cells targeting carcinoembryonic antigen can mediate regression of metastatic colorectal cancer but induce severe transient colitis. Molecular Therapy. 2011;19(3):620–6.

124. Chandran SS, Ma J, Klatt MG, Dündar F, Bandlamudi C, Razavi P, et al. Immunogenicity and therapeutic targeting of a public neoantigen derived from mutated PIK3CA. Nat Med. 2022 May 1;28(5):946–57.

125. Leidner R, Sanjuan Silva N, Huang H, Sprott D, Zheng C, Shih YP, et al. Neoantigen T-Cell Receptor Gene Therapy in Pancreatic Cancer. New England Journal of Medicine. 2022 Jun 2;386(22):2112–9.

126. Kim SP, Vale NR, Zacharakis N, Krishna S, Yu Z, Gasmi B, et al. Adoptive Cellular Therapy with Autologous Tumor-Infiltrating Lymphocytes and T-cell Receptor-

Engineered T Cells Targeting Common p53 Neoantigens in Human Solid Tumors. Cancer Immunol Res. 2022 Aug 1;10(8):932–46.

127. Foy SP, Jacoby K, Bota DA, Hunter T, Pan Z, Stawiski E, et al. Non-viral precision T cell receptor replacement for personalized cell therapy. Nature. 2022;

128. Sterner RC, Sterner RM. CAR-T cell therapy: current limitations and potential strategies. Vol. 11, Blood Cancer Journal. Springer Nature; 2021.

129. Maus M V., June CH. Making better chimeric antigen receptors for adoptive T-cell therapy. Clinical Cancer Research. 2016 Apr 15;22(8):1875–84.

130. Kochenderfer JN, Yu Z, Frasheri D, Restifo NP, Rosenberg SA. Adoptive transfer of syngeneic T cells transduced with a chimeric antigen receptor that recognizes murine CD19 can eradicate lymphoma and normal B cells. Blood. 2010 Nov 11;116(19):3875–86.

131. Neelapu SS, Locke FL, Bartlett NL, Lekakis LJ, Miklos DB, Jacobson CA, et al. Axicabtagene Ciloleucel CAR T-Cell Therapy in Refractory Large B-Cell Lymphoma. New England Journal of Medicine. 2017 Dec 28;377(26):2531–44.

132. Maude SL, Laetsch TW, Buechner J, Rives S, Boyer M, Bittencourt H, et al. Tisagenlecleucel in Children and Young Adults with B-Cell Lymphoblastic Leukemia. New England Journal of Medicine. 2018 Feb;378(5):439–48.

133. Schuster SJ, Svoboda J, Chong EA, Nasta SD, Mato AR, Anak Ö, et al. Chimeric Antigen Receptor T Cells in Refractory B-Cell Lymphomas. New England Journal of Medicine. 2017 Dec 28;377(26):2545–54.

134. Chandran SS, Klebanoff CA. T cell receptor-based cancer immunotherapy: Emerging efficacy and pathways of resistance. Vol. 290, Immunological Reviews. Blackwell Publishing Ltd; 2019. p. 127–47.

135. Junker N, Andersen MH, Wenandy L, Dombernowsky SL, Kiss K, Sørensen CH, et al. Bimodal ex vivo expansion of T cells from patients with head and neck squamous cell carcinoma: A prerequisite for adoptive cell transfer. Cytotherapy. 2011;13(7):822–34.

136. Dudley ME, Wunderlich JR, Shelton TE, Even J, Rosenberg SA. Generation of Tumor-Infiltrating Lymphocyte Cultures for Use in Adoptive Transfer Therapy for Melanoma Patients. 2003.

137. Fridman WH, Pagès F, Sautès-fridman C. The immune contexture in human

tumours : impact on clinical outcome. Nat Rev Cancer [Internet]. 2012;12(4):298–306. Available from: http://dx.doi.org/10.1038/nrc3245

138. Gros A, Robbins PF, Yao X, Li YF, Turcotte S, Tran E, et al. PD-1 identifies the patient-specific CD8+ tumor-reactive repertoire infiltrating human tumors. Journal of Clinical Investigation. 2014;124(5):2246–59.

139. Pasetto A, Gros A, Robbins PF, Deniger DC, Prickett TD, Matus-Nicodemos R, et al. Tumor- and neoantigen-reactive T-cell receptors can be identified based on their frequency in fresh tumor. Cancer Immunol Res. 2016 Sep 1;4(9):734–43.

140. Carty WC Mac. FACTORS WHICH INFLUENCE LONGEVITY IN CANCER* A STUDY OF Q93 CASES. 1922.

141. Topalian SL, Muul LM, Solomon D, Rosenberg SA. Expansion of human tumor infiltrating lymphocytes for use in immunotherapy trials. J Immunol Methods [Internet]. 1987;102(1):127–41. Available from: https://www.sciencedirect.com/science/article/pii/S0022175987800182

142. Westergaard MCW, Andersen R, Chong C, Kjeldsen JW, Pedersen M, Friese C, et al. Tumour-reactive T cell subsets in the microenvironment of ovarian cancer. Br J Cancer. 2019 Feb 19;120(4):424–34.

143. Scheper W, Kelderman S, Fanchi LF, Linnemann C, Bendle G, de Rooij MAJ, et al. Low and variable tumor reactivity of the intratumoral TCR repertoire in human cancers. Nat Med. 2019 Jan 1;25(1):89–94.

144. Chee J, Watson MW, Chopra A, Nguyen B, Cook AM, Creaney J, et al. Tumour associated lymphocytes in the pleural effusions of patients with mesothelioma express high levels of inhibitory receptors 11 Medical and Health Sciences 1107 Immunology. BMC Res Notes. 2018 Dec 5;11(1).

145. Wong YNS, Joshi K, Khetrapal P, Ismail M, Reading JL, Sunderland MW, et al. Urine-derived lymphocytes as a non-invasive measure of the bladder tumor immune microenvironment. Journal of Experimental Medicine. 2018 Nov 1;215(11):2748–59.

146. Jang M, Yew PY, Hasegawa K, Ikeda Y, Fujiwara K, Fleming GF, et al. Characterization of T cell repertoire of blood, tumor, and ascites in ovarian cancer patients using next generation sequencing. Oncoimmunology. 2015 Nov 2;4(11).

147. Wick DA, Webb JR, Nielsen JS, Martin SD, Kroeger DR, Milne K, et al. Surveillance of the tumor mutanome by T cells during progression from primary to recurrent ovarian cancer. Clinical Cancer Research. 2014;20(5):1125–34.

148. Benitez-Ribas D, Cabezón R, Flórez-Grau G, Molero MC, Puerta P, Guillen A, et al. Immune response generated with the administration of autologous dendritic cells pulsed with an allogenic tumoral cell-lines lysate in patients with newly diagnosed diffuse intrinsic pontine glioma. Front Oncol. 2018 Apr 26;8(APR).

149. Rubio-Perez C, Planas-Rigol E, Trincado JL, Bonfill-Teixidor E, Arias A, Marchese D, et al. Immune cell profiling of the cerebrospinal fluid enables the characterization of the brain metastasis microenvironment. Nat Commun. 2021 Dec 1;12(1).

150. Hérin M, Lemoine C, Weynants P, Vessière F, Van Pel A, Boon T, et al. Production of stable cytolytic T-cell clones directed against autologous human melanoma. Int J Cancer. 1987;39(3):390–6.

151. van Rooij N, van Buuren MM, Philips D, Velds A, Toebes M, Heemskerk B, et al. Tumor Exome Analysis Reveals Neoantigen-Specific T-Cell Reactivity in an Ipilimumab-Responsive Melanoma [Internet]. 2013. Available from: www.jco.org

152. Gros A, Parkhurst MR, Tran E, Pasetto A, Robbins PF, Ilyas S, et al. Prospective identification of neoantigen-specific lymphocytes in the peripheral blood of melanoma patients. Nat Med. 2016 Apr 1;22(4):433–8.

153. Gros A, Tran E, Parkhurst MR, Ilyas S, Pasetto A, Groh EM, et al. Recognition of human gastrointestinal cancer neoantigens by circulating PD-1+ lymphocytes. Journal of Clinical Investigation. 2019 Nov 1;129(11):4992–5004.

154. Cafri G, Yossef R, Pasetto A, Deniger DC, Lu YC, Parkhurst M, et al. Memory T cells targeting oncogenic mutations detected in peripheral blood of epithelial cancer patients. Nat Commun. 2019 Dec 1;10(1).

155. Oliveira G, Stromhaug K, Cieri N, Iorgulescu JB, Klaeger S, Wolff JO, et al. Landscape of helper and regulatory antitumour CD4+ T cells in melanoma. Nature. 2022 May 19;605(7910):532–8.

156. Holm JS, Funt SA, Borch A, Munk KK, Bjerregaard AM, Reading JL, et al. Neoantigen-specific CD8 T cell responses in the peripheral blood following PD-L1 blockade might

predict therapy outcome in metastatic urothelial carcinoma. Nat Commun. 2022 Dec 1;13(1).

157. Yee C, Thompson JA, Byrd D, Riddell SR, Roche P, Celis E, et al. Adoptive T cell therapy using antigen-specific CD8+ T cell clones for the treatment of patients with metastatic melanoma: In vivo persistence, migration, and antitumor effect of transferred T cells. Proc Natl Acad Sci U S A. 2002 Dec 10;99(25):16168–73.

158. Chandran SS, Paria BC, Srivastava AK, Rothermel LD, Stephens DJ, Dudley ME, et al. Persistence of CTL clones targeting melanocyte differentiation antigens was insufficient to mediate significant melanoma regression in humans. Clinical Cancer Research. 2015 Feb 1;21(3):534–43.

159. Hunder N, Wallen H, Cao J, Hendricks D, Reilly J, Rodmyre R, et al. Treatment of Metastatic Melanoma with Autologous CD4+ T Cells against NY-ESO-1. N Engl J Med [Internet]. 2008; Available from: www.nejm.org

160. Cohen CJ, Gartner JJ, Horovitz-Fried M, Shamalov K, Trebska-McGowan K, Bliskovsky V V., et al. Isolation of neoantigen-specific T cells from tumor and peripheral lymphocytes. Journal of Clinical Investigation. 2015 Oct 1;125(10):3981–91.

161. McGranahan N, Furness A, Rosenthal R, Ramskov S, Lyngaa R, Saini SK, et al. Clonal neoantigens elicit T cell immunoreactivity and sensitivity to immune checkpoint blockaed. Science (1979). 2016 Mar 25;351(6280):1463–9.

162. Altman JD, Moss PAH, Goulder PJR, Barouch DH, McHeyzer-Williams MG, Bell JI, et al. Phenotypic Analysis of Antigen-Specific T Lymphocytes. Science (1979) [Internet]. 1996 Oct 4;274(5284):94–6. Available from: https://doi.org/10.1126/science.274.5284.94

163. Rizvi NA, Hellmann MD, Snyder A, Kvistborg P, Makarov V, Havel JJ, et al. Mutational landscape determines sensitivity to PD-1 blockade in non – small cell lung cancer. Science (1979). 2015;348(6230):124–9.

164. Tubb VM, Schrikkema DS, Croft NP, Purcell AW, Linnemann C, Freriks MR, et al. Isolation of T cell receptors targeting recurrent neoantigens in hematological malignancies. J Immunother Cancer. 2018 Jul 13;6(1).

165. Andersen RS, Andersen SR, Hjortsø MD, Lyngaa R, Idorn M, Køllgård TM, et al. High frequency of T cells specific for cryptic epitopes in melanoma patients. Oncoimmunology.

2013;2(7).

166. Toebes M, Rodenko B, Ovaa H, Schumacher TNM. Generation of Peptide MHC Class I Monomers and Multimers Through Ligand Exchange. Curr Protoc Immunol [Internet]. 2009 Nov 1;87(1):18.16.1-18.16.20. Available from: https://doi.org/10.1002/0471142735.im1816s87

167. Rodenko B, Toebes M, Hadrup SR, van Esch WJE, Molenaar AM, Schumacher TNM, et al. Generation of peptide–MHC class I complexes through UV-mediated ligand exchange. Nat Protoc [Internet]. 2006;1(3):1120–32. Available from: https://doi.org/10.1038/nprot.2006.121

168. Hadrup SR, Bakker AH, Shu CJ, Andersen RS, van Veluw J, Hombrink P, et al. Parallel detection of antigen-specific T-cell responses by multidimensional encoding of MHC multimers. Nat Methods [Internet]. 2009;6(7):520–6. Available from: https://doi.org/10.1038/nmeth.1345

169. Luimstra JJ, Garstka MA, Roex MCJ, Redeker A, Janssen GMC, van Veelen PA, et al. A flexible MHC class I multimer loading system for large-scale detection of antigen-specific T cells. Journal of Experimental Medicine. 2018 May 1;215(5):1493–504.

170. Leisner C, Loeth N, Lamberth K, Justesen S, Sylvester-Hvid C, Schmidt EG, et al. One-pot, mix-and-read peptide-MHC tetramers. PLoS One. 2008 Feb 27;3(2).

171. Bentzen AK, Marquard AM, Lyngaa R, Saini SK, Ramskov S, Donia M, et al. Large-scale detection of antigen-specific T cells using peptide-MHC-I multimers labeled with DNA barcodes. Nat Biotechnol [Internet]. 2016;34(10):1037–45. Available from: https://doi.org/10.1038/nbt.3662

172. Zhang SQ, Ma KY, Schonnesen AA, Zhang M, He C, Sun E, et al. High-throughput determination of the antigen specificities of T cell receptors in single cells. Nat Biotechnol [Internet]. 2018;36(12):1156–9. Available from: https://doi.org/10.1038/nbt.4282

173. Kristensen NP, Heeke C, Tvingsholm SA, Borch A, Draghi A, Crowther MD, et al. Neoantigen-reactive CD8+ T cells affect clinical outcome of adoptive cell therapy with tumor-infiltrating lymphocytes in melanoma. Journal of Clinical Investigation. 2022 Jan 18;132(2).

174. Niemiec PK, Read LR, Sharif S. Synthesis of chicken major histocompatibility

complex class II oligomers using a baculovirus expression system. Protein Expr Purif [Internet]. 2006;46(2):390–400. Available from: https://www.sciencedirect.com/science/article/pii/S1046592805003098

175. Vollers SS, Stern LJ. Class II major histocompatibility complex tetramer staining: progress, problems, and prospects. Immunology [Internet]. 2008 Mar 1;123(3):305–13. Available from: https://doi.org/10.1111/j.1365-2567.2007.02801.x

176. Vyasamneni R, Kohler V, Karki B, Mahimkar G, Esaulova E, McGee J, et al. A universal MHCII technology platform to characterize antigen-specific CD4+ T cells. Cell Reports Methods. 2023 Jan 23;3(1).

177. Rahimpour A, Koay HF, Enders A, Clanchy R, Eckle SBG, Meehan B, et al. Identification of phenotypically and functionally heterogeneous mouse mucosal-associated invariant T cells using MR1 tetramers. Journal of Experimental Medicine. 2015 Jun 29;212(7):1095–108.

178. Crowley MP, Fahrer AM, Baumgarth N, Hampl J, Gutgemann I, Teyton L, et al. A population of murine γδ T cells that recognize an inducible MHC class Ib molecule. Science (1979). 2000;287(5451):314–6.

179. Sidobre S, Kronenberg M. CD1 tetramers: a powerful tool for the analysis of glycolipid-reactive T cells. J Immunol Methods [Internet]. 2002;268(1):107–21. Available from: https://www.sciencedirect.com/science/article/pii/S0022175902002041

180. Ruibal P, Derksen I, van Wolfswinkel M, Voogd L, Franken KLMC, El Hebieshy AF, et al. Thermal-exchange HLA-E multimers reveal specificity in HLA-E and NKG2A / CD94 complex interactions . Immunology. 2022 Mar 20;

181. Smith KN, Llosa NJ, Cottrell TR, Siegel N, Fan H, Suri P, et al. Persistent mutant oncogene specific T cells in two patients benefitting from anti-PD-1. J Immunother Cancer. 2019 Feb 11;7(1).

182. Hoyos D, Zappasodi R, Schulze I, Sethna Z, de Andrade KC, Bajorin DF, et al. Fundamental immune–oncogenicity trade-offs define driver mutation fitness. Nature. 2022 Jun 2;606(7912):172–9.

183. Bobisse S, Genolet R, Roberti A, Tanyi JL, Racle J, Stevenson BJ, et al. Sensitive and frequent identification of high avidity neo-epitope specific CD8 + T cells in

immunotherapy-naive ovarian cancer. Nat Commun. 2018 Dec 1;9(1).

184. Meng Q, Valentini D, Rao M, Moro CF, Paraschoudi G, Jäger E, et al. Neoepitope targets of tumour-infiltrating lymphocytes from patients with pancreatic cancer. Br J Cancer. 2019 Jan 8;120(1):97–108.

185. Wölfel T, Hauer M, Schneider J, Serrano M, Wölfel C, Klehmann-Hieb E, et al. A p16INK4a-Insensitive CDK4 Mutant Targeted by Cytolytic T Lymphocytes in a Human Melanoma. Science (1979) [Internet]. 1995 Sep 1;269(5228):1281–4. Available from: https://doi.org/10.1126/science.7652577

186. Ali M, Foldvari Z, Giannakopoulou E, Böschen ML, Strønen E, Yang W, et al. Induction of neoantigen-reactive T cells from healthy donors. Nat Protoc. 2019 Jun 1;14(6):1926–43.

187. Danilova L, Anagnostou V, Caushi JX, Sidhom JW, Guo H, Chan HY, et al. The mutation-associated neoantigen functional expansion of specific T cells (MANAFEST) assay: A sensitive platform for monitoring antitumor immunity. Cancer Immunol Res. 2018 Aug 1;6(8):888–99.

188. Bear AS, Blanchard T, Cesare J, Ford MJ, Richman LP, Xu C, et al. Biochemical and functional characterization of mutant KRAS epitopes validates this oncoprotein for immunological targeting. Nat Commun. 2021 Dec 1;12(1).

189. Choi J, Goulding SP, Conn BP, McGann CD, Dietze JL, Kohler J, et al. Systematic discovery and validation of T cell targets directed against oncogenic KRAS mutations. Cell Reports Methods. 2021 Sep 27;1(5).

190. Inozume T, Hanada KI, Wang QJ, Ahmadzadeh M, Wunderlich JR, Rosenberg SA, et al. Selection of CD8 + PD-1 + Lymphocytes in Fresh Human Melanomas Enriches for Tumor-reactive T Cells [Internet]. 2010. Available from: www.immunotherapy-journal.com

191. Thommen DS, Koelzer VH, Herzig P, Roller A, Trefny M, Dimeloe S, et al. A transcriptionally and functionally distinct pd-1+ cd8+ t cell pool with predictive potential in non-small-cell lung cancer treated with pd-1 blockade. Nat Med. 2018 Jun 11;24(7):994–1004.

192. Palomero J, Panisello C, Lozano-Rabella M, Tirtakasuma R, Díaz-Gómez J, Grases

D, et al. Biomarkers of tumor-reactive CD4+ and CD8+ TILs associate with improved prognosis in endometrial cancer. J Immunother Cancer. 2022 Dec 1;10(12).

193. Ye Q, Song DG, Poussin M, Yamamoto T, Best A, Li C, et al. CD137 accurately identifies and enriches for naturally occurring tumor-reactive T cells in tumor. Clinical Cancer Research. 2014 Jan 1;20(1):44–55.

194. Seliktar-Ofir S, Merhavi-Shoham E, Itzhaki O, Yunger S, Markel G, Schachter J, et al. Selection of shared and neoantigen-reactive T cells for adoptive cell therapy based on CD137 separation. Front Immunol. 2017 Oct 10;8(OCT).

195. Duhen R, Fesneau O, Samson KA, Frye AK, Beymer M, Rajamanickam V, et al. PD-1 and ICOS coexpression identifies tumor-reactive CD4+ T cells in human solid tumors. Journal of Clinical Investigation. 2022 Jun 15;132(12).

196. Kortekaas KE, Santegoets SJ, Sturm G, Ehsan I, van Egmond SL, Finotello F, et al. CD39 identifies the CD4þ tumor-specific T-cell population in human cancer. Cancer Immunol Res. 2020 Oct 1;8(10):1311–21.

197. Kamphorst, Pillai RN, Yang S, Nasti TH, Akondy RS, Wieland A, et al. Proliferation of PD-1+ CD8 T cells in peripheral blood after PD-1–targeted therapy in lung cancer patients. PNAS [Internet]. 2017;114(19):4993–8. Available from: http://www.pnas.org/lookup/doi/10.1073/pnas.1705327114

198. Lone SN, Nisar S, Masoodi T, Singh M, Rizwan A, Hashem S, et al. Liquid biopsy: a step closer to transform diagnosis, prognosis and future of cancer treatments. Mol Cancer [Internet]. 2022;21(1):79. Available from: https://doi.org/10.1186/s12943-022-01543-7

199. Lu T, Li J. Clinical applications of urinary cell-free DNA in cancer: current insights and promising future [Internet]. Vol. 7, Am J Cancer Res. 2017. Available from: www.ajcr.us/ISSN:2156-6976/ajcr0066371

200. Ding S, Song X, Geng X, Liu L, Ma H, Wang X, et al. Saliva-derived cfDNA is applicable for EGFR mutation detection but not for quantitation analysis in non-small cell lung cancer. Thorac Cancer. 2019 Oct 1;10(10):1973–83.

201. Wang Y, Springer S, Mulvey CL, Silliman N, Schaefer J, Sausen M, et al. Detection of somatic mutations and HPV in the saliva and plasma of patients with head and neck squamous cell carcinomas [Internet]. 2015. Available from: https://www.science.org

202. Lee JS, Hur JY, Kim IA, Kim HJ, Choi CM, Lee JC, et al. Liquid biopsy using the supernatant of a pleural effusion for EGFR genotyping in pulmonary adenocarcinoma patients: A comparison between cell-free DNA and extracellular vesicle-derived DNA. BMC Cancer. 2018 Dec 10;18(1).

203. Song T, Mao F, Shi L, Xu X, Wu Z, Zhou J, et al. Urinary measurement of circulating tumor DNA for treatment monitoring and prognosis of metastatic colorectal cancer patients. 2019;57(2):268–75. Available from: https://doi.org/10.1515/cclm-2017-0675

204. Miller AM, Shah RH, Pentsova EI, Pourmaleki M, Briggs S, Distefano N, et al. Tracking tumour evolution in glioma through liquid biopsies of cerebrospinal fluid. Nature [Internet]. 2019;565(7741):654–8. Available from: https://doi.org/10.1038/s41586-019-0882-3

205. Baburaj G, Damerla RR, Udupa KS, Parida P, Munisamy M, Kolesar J, et al. Liquid biopsy approaches for pleural effusion in lung cancer patients. Mol Biol Rep [Internet]. 2020;47(10):8179–87. Available from: https://doi.org/10.1007/s11033-020-05869-7

206. Corcoran RB, Chabner BA. Application of Cell-free DNA Analysis to Cancer Treatment. New England Journal of Medicine. 2018 Nov;379(18):1754–65.

207. Lui YYN, Chik KW, Chiu RWK, Ho CY, Lam CWK, Dennis Lo YM. Predominant Hematopoietic Origin of Cell-free DNA in Plasma and Serum after Sex-mismatched Bone Marrow Transplantation [Internet]. 2002. Available from: https://academic.oup.com/clinchem/article/48/3/421/5641630

208. Sun K. Clonal hematopoiesis: background player in plasma cell-free DNA variants. Ann Transl Med. 2019 Dec;7(S8):S384–S384.

209. Leon SA, Shapiro DM, Yaros MJ. Free DNA in the Serum of Cancer Patients and the Effect of Therapy. Cancer Res. 1977;

210. Lo YMD, Corbetta N, Chamberlain PF, Rai V, Sargent IL, Redman CWG, et al. Presence of fetal DNA in maternal plasma and serum. The Lancet [Internet]. 1997 Aug 16;350(9076):485–7. Available from: https://doi.org/10.1016/S0140-6736(97)02174-0

211. Anker P, Mulcahy H, Qi Chen X, Stroun M. Detection of Circulating Tumour DNA in the Blood (Plasma/Serum) of Cancer Patients. Cancer and Metastasis Reviews [Internet]. 1999;18(1):65–73. Available from: https://doi.org/10.1023/A:1006260319913

212. Jahr S, Hentze H, Englisch S, Hardt D, Fackelmayer FO, Hesch RD, et al. DNA Fragments in the Blood Plasma of Cancer Patients: Quantitations and Evidence for Their Origin from Apoptotic and Necrotic Cells 1 [Internet]. Vol. 61, CANCER RESEARCH. 2001. Available from: http://aacrjournals.org/cancerres/article-pdf/61/4/1659/3252577/ch040101659p.pdf

213. Gormally E, Caboux E, Vineis P, Hainaut P. Circulating free DNA in plasma or serum as biomarker of carcinogenesis: Practical aspects and biological significance. Mutation Research/Reviews in Mutation Research [Internet]. 2007;635(2):105–17. Available from: https://www.sciencedirect.com/science/article/pii/S1383574206000986

214. Bronkhorst AJ, Ungerer V, Holdenrieder S. The emerging role of cell-free DNA as a molecular marker for cancer management. Biomol Detect Quantif [Internet]. 2019;17(February):100087. Available from: https://doi.org/10.1016/j.bdq.2019.100087

215. Diehl F, Schmidt K, Choti MA, Romans K, Goodman S, Li M, et al. Circulating mutant DNA to assess tumor dynamics. Nat Med [Internet]. 2008;14(9):985–90. Available from: https://doi.org/10.1038/nm.1789

216. Cheng F, Su L, Qian C. Circulating tumor DNA: a promising biomarker in the liquid biopsy of cancer. Oncotarget [Internet]. 2016;7(30). Available from: www.impactjournals.com/oncotarget

217. Gao Q, Zeng Q, Wang Z, Li C, Xu Y, Cui P, et al. Circulating cell-free DNA for cancer early detection. The Innovation. 2022 Jul;3(4):100259.

218. Wyatt AW, Annala M, Aggarwal R, Beja K, Feng F, Youngren J, et al. Concordance of Circulating Tumor DNA and Matched Metastatic Tissue Biopsy in Prostate Cancer. J Natl Cancer Inst. 2017 Dec 1;109(12).

219. Jahangiri L, Hurst T. Assessing the concordance of genomic alterations between circulating-free DNA and tumour tissue in cancer patients. Vol. 11, Cancers. MDPI AG; 2019.

220. Takeshita T, Yamamoto Y, Yamamoto-Ibusuki M, Tomiguchi M, Sueta A, Murakami K, et al. Comparison of ESR1 Mutations in Tumor Tissue and Matched Plasma Samples from Metastatic Breast Cancer Patients. Transl Oncol. 2017 Oct 1;10(5):766–71.

221. Grasselli J, Elez E, Caratù G, Matito J, Santos C, Macarulla T, et al. Concordance

of blood- and tumor-based detection of RAS mutations to guide anti-EGFR therapy in metastatic colorectal cancer. Annals of Oncology. 2017 Jun 1;28(6):1294–301.

222. Adalsteinsson VA, Ha G, Freeman SS, Choudhury AD, Stover DG, Parsons HA, et al. Scalable whole-exome sequencing of cell-free DNA reveals high concordance with metastatic tumors. Nat Commun. 2017 Dec 1;8(1).

223. Lanman RB, Mortimer SA, Zill OA, Sebisanovic D, Lopez R, Blau S, et al. Analytical and clinical validation of a digital sequencing panel for quantitative, highly accurate evaluation of cell-free circulating tumor DNA. PLoS One. 2015 Oct 16;10(10).

224. Schwarzenbach H, Stoehlmacher J, Pantel K, Goekkurt E. Detection and Monitoring of Cell-Free DNA in Blood of Patients with Colorectal Cancer. Ann N Y Acad Sci [Internet]. 2008 Aug 1;1137(1):190–6. Available from: https://doi.org/10.1196/annals.1448.025

225. Ignatiadis M, Dawson SJ. Circulating tumor cells and circulating tumor DNA for precision medicine: Dream or reality? Annals of Oncology [Internet]. 2014;25(12):2304–13. Available from: https://doi.org/10.1093/annonc/mdu480

226. Elazezy M, Joosse SA. Techniques of using circulating tumor DNA as a liquid biopsy component in cancer management. Vol. 16, Computational and Structural Biotechnology Journal. Elsevier B.V.; 2018. p. 370–8.

227. Liu S, Wang J. Current and Future Perspectives of Cell-Free DNA in Liquid Biopsy. Curr Issues Mol Biol. 2022 Jun 1;44(6):2695–709.

228. Bettegowda C, Sausen M, Leary RJ, Kinde I, Wang Y, Agrawal N, et al. Detection of Circulating Tumor DNA in Early-and Late-Stage Human Malignancies [Internet]. 2014. Available from: https://www.science.org

229. Namløs HM, Boye K, Mishkin SJ, Barøy T, Lorenz S, Bjerkehagen B, et al. Noninvasive detection of ctDNA reveals intratumor heterogeneity and is associated with tumor burden in gastrointestinal stromal tumor. Mol Cancer Ther. 2018 Nov 1;17(11):2473–80.

230. Lee TH, Montalvo L, Chrebtow V, Busch MP. Quantitation of genomic DNA in plasma and serum samples: higher concentrations of genomic DNA found in serum than in plasma. Transfusion (Paris) [Internet]. 2001;276. Available from: www.transfusion.org

231. Uchida J, Kato K, Kukita Y, Kumagai T, Nishino K, Daga H, et al. Diagnostic

accuracy of noninvasive genotyping of EGFR in lung cancer patients by deep sequencing of plasma cell-free DNA. Clin Chem. 2015 Sep 1;61(9):1191–6.

232. Sobczuk P, Kozak K, Kopeć S, Rogala P, Świtaj T, Koseła-Paterczyk H, et al. The Use of ctDNA for BRAF Mutation Testing in Routine Clinical Practice in Patients with Advanced Melanoma. Cancers (Basel). 2022 Feb 1;14(3).

233. Moynahan ME, Chen D, He W, Sung P, Samoila A, You D, et al. Correlation between PIK3CA mutations in cell-free DNA and everolimus efficacy in HR+, HER2-advanced breast cancer: Results from BOLERO-2. Br J Cancer. 2017 Mar 14;116(6):726–30.

234. Taly V, Pekin D, Benhaim L, Kotsopoulos SK, Corre D Le, Li X, et al. Multiplex picodroplet digital PCR to detect KRAS mutations in circulating DNA from the plasma of colorectal cancer patients. Clin Chem. 2013 Dec;59(12):1722–31.

235. Couraud S, Vaca-Paniagua F, Villar S, Oliver J, Schuster T, Blanché H, et al. Noninvasive diagnosis of actionable mutations by deep sequencing of circulating free DNA in lung cancer from never-smokers: a proof-of-concept study from BioCAST/IFCT-1002. Clin Cancer Res. 2014 Sep 1;20(17):4613–24.

236. Sakai H, Tsurutani J, Iwasa T, Komoike Y, Sakai K, Nishio K, et al. HER2 genomic amplification in circulating tumor DNA and estrogen receptor positivity predict primary resistance to trastuzumab emtansine (T-DM1) in patients with HER2-positive metastatic breast cancer. Breast Cancer. 2018 Sep 1;25(5):605–13.

237. Higgins MJ, Jelovac D, Barnathan E, Blair B, Slater S, Powers P, et al. Detection of tumor PIK3CA status in metastatic breast cancer using peripheral blood. Clinical Cancer Research. 2012 Jun 15;18(12):3462–9.

238. Li S, Hu R, Small C, Kang T yu, Liu C chi, Zhou XJ, et al. cfSNV : a software tool for the sensitive detection of somatic mutations from cell-free DNA. Nat Protoc. 2021;1–21.

239. Li S, Noor ZS, Zeng W, Stackpole ML, Ni X, Zhou Y, et al. Sensitive detection of tumor mutations from blood and its application to immunotherapy prognosis. Nat Commun [Internet]. 2021;12(1). Available from: http://dx.doi.org/10.1038/s41467-021-24457-2

240. Chan KCA, Woo JKS, King A, Zee BCY, Lam WKJ, Chan SL, et al. Analysis of Plasma Epstein–Barr Virus DNA to Screen for Nasopharyngeal Cancer. New England Journal of

Medicine. 2017 Aug 10;377(6):513–22.

241. Fernandez-Cuesta L, Perdomo S, Avogbe PH, Leblay N, Delhomme TM, Gaborieau V, et al. Identification of Circulating Tumor DNA for the Early Detection of Small-cell Lung Cancer. EBioMedicine. 2016 Aug 1;10:117–23.

242. Amant F, Verheecke M, Wlodarska I, Dehaspe L, Brady P, Brison N, et al. Presymptomatic identification of cancers in pregnant women during noninvasive prenatal testing. JAMA Oncol. 2015 Sep 1;1(6):814–9.

243. Corcoran RB, Chabner BA. Application of Cell-free DNA Analysis to Cancer Treatment. New England Journal of Medicine. 2018;379(18):1754–65.

244. Zill OA, Greene C, Sebisanovic D, Siew LM, Leng J, Vu M, et al. Cell-Free DNA Next-Generation Sequencing in Pancreatobiliary Carcinomas. Cancer Discov. 2015 Oct 1;5(10):1040–8.

245. Lowes LE, Bratman S V., Dittamore R, Done S, Kelley SO, Mai S, et al. Circulating tumor cells (CTC) and cell-free DNA (cfDNA)workshop 2016: Scientific opportunities and logistics for cancer clinical trial incorporation. Int J Mol Sci. 2016 Sep 8;17(9).

246. Brown P. The Cobas® EGFR Mutation Test v2 assay. Future Oncology [Internet]. 2016 Feb 1;12(4):451–2. Available from: https://doi.org/10.2217/fon.15.311

247. Dawson SJ, Tsui DWY, Murtaza M, Biggs H, Rueda OM, Chin SF, et al. Analysis of Circulating Tumor DNA to Monitor Metastatic Breast Cancer. New England Journal of Medicine. 2013 Mar 28;368(13):1199–209.

248. Lipson EJ, Velculescu VE, Pritchard TS, Sausen M, Pardoll DM, Topalian SL, et al. Circulating tumor DNA analysis as a real-time method for monitoring tumor burden in melanoma patients undergoing treatment with immune checkpoint blockade. J Immunother Cancer. 2014 Dec 16;2(1).

249. Faria G, Silva E, Da Fonseca C, Quirico-Santos T. Circulating cell-free DNA as a prognostic and molecular marker for patients with brain tumors under perillyl alcohol-based therapy. Int J Mol Sci. 2018 Jun 1;19(6).

250. Reinert T, Schøler L V., Thomsen R, Tobiasen H, Vang S, Nordentoft I, et al. Analysis of circulating tumour DNA to monitor disease burden following colorectal cancer surgery. Gut. 2016 Apr 1;65(4):625–34.

251. Kamat AA, Kim TJ, Landen CN, Lu C, Han LY, Lin YG, et al. Metronomic chemotherapy enhances the efficacy of antivascular therapy in ovarian cancer. Cancer Res. 2007 Jan 1;67(1):281–8.

252. Cabanero M, Tsao MS. Circulating tumour DNA in EGFR-mutant non-small-cell lung cancer. Vol. 25, Current Oncology. Multimed Inc.; 2018. p. S38–44.

253. Ashida A, Sakaizawa K, Uhara H, Okuyama R. Circulating Tumour DNA for Monitoring Treatment Response to Anti-PD-1 Immunotherapy in Melanoma Patients. Acta Derm Venereol [Internet]. 2017 Aug 7;97(10):1212–8. Available from: https://medicaljournalssweden.se/actadv/article/view/5005

254. Birkenkamp-Demtröder K, Nordentoft I, Christensen E, Høyer S, Reinert T, Vang S, et al. Genomic Alterations in Liquid Biopsies from Patients with Bladder Cancer. Eur Urol. 2016 Jul 1;70(1):75–82.

255. Spindler KLG, Pallisgaard N, Vogelius I, Jakobsen A. Quantitative cell-free DNA, KRAS, and BRAF mutations in plasma from patients with metastatic colorectal cancer during treatment with cetuximab and irinotecan. Clinical Cancer Research. 2012 Feb 15;18(4):1177–85.

256. Goyal L, Saha SK, Liu LY, Siravegna G, Leshchiner I, Ahronian LG, et al. Polyclonal secondary FGFR2 mutations drive acquired resistance to FGFR inhibition in patients with FGFR2 fusion-positive cholangiocarcinoma. Cancer Discov. 2017 Mar 1;7(3):252–63.

257. Russo M, Misale S, Wei G, Siravegna G, Crisafulli G, Lazzari L, et al. Acquired resistance to the TRK inhibitor entrectinib in colorectal cancer. Cancer Discov. 2016 Jan 1;6(1):36–44.

258. Parikh AR, Leshchiner I, Elagina L, Goyal L, Levovitz C, Siravegna G, et al. Liquid versus tissue biopsy for detecting acquired resistance and tumor heterogeneity in gastrointestinal cancers. Nat Med [Internet]. 2019;25(9):1415–21. Available from: https://doi.org/10.1038/s41591-019-0561-9

259. Chandarlapaty S, Chen D, He W, Sung P, Samoila A, You D, et al. Prevalence of ESR1 Mutations in Cell-Free DNA and Outcomes in Metastatic Breast Cancer: A Secondary Analysis of the BOLERO-2 Clinical Trial. JAMA Oncol. 2016 Oct 1;2(10):1310–5.

260. Chabon JJ, Simmons AD, Lovejoy AF, Esfahani MS, Newman AM, Haringsma HJ,

et al. Circulating tumour DNA profiling reveals heterogeneity of EGFR inhibitor resistance mechanisms in lung cancer patients. Nat Commun [Internet]. 2016;7(1):11815. Available from: https://doi.org/10.1038/ncomms11815

261. Diehl F, Schmidt K, Choti MA, Romans K, Goodman S, Li M, et al. Circulating mutant DNA to assess tumor dynamics. Nat Med. 2008;14(9):985–90.

262. Garcia-Murillas I, Schiavon G, Weigelt B, Ng C, Hrebien S, Cutts RJ, et al. Mutation tracking in circulating tumor DNA predicts relapse in early breast cancer [Internet]. 2015. Available from: https://www.science.org

263. Chaudhuri AA, Chabon JJ, Lovejoy AF, Newman AM, Stehr H, Azad TD, et al. Early detection of molecular residual disease in localized lung cancer by circulating tumor DNA profiling. Cancer Discov. 2017 Dec 1;7(12):1394–403.

264. Sausen M, Phallen J, Adleff V, Jones S, Leary RJ, Barrett MT, et al. Clinical implications of genomic alterations in the tumour and circulation of pancreatic cancer patients. Nat Commun. 2015;6:1–6.

265. Martin SD, Wick DA, Nielsen JS, Little N, Holt RA, Nelson BH. A library-based screening method identifies neoantigen-reactive T cells in peripheral blood prior to relapse of ovarian cancer. Oncoimmunology. 2018 Jan 2;7(1).

266. Bai Y, Ni M, Cooper B, Wei Y, Fury W. Inference of high resolution HLA types using genome-wide RNA or DNA sequencing reads. BMC Genomics. 2014 May 1;15(1).

267. Reynisson B, Alvarez B, Paul S, Peters B, Nielsen M. NetMHCpan-4.1 and NetMHCIIpan-4.0: Improved predictions of MHC antigen presentation by concurrent motif deconvolution and integration of MS MHC eluted ligand data. Nucleic Acids Res. 2021;48(W1):W449–54.

268. Cohen CJ, Zhao Y, Zheng Z, Rosenberg SA, Morgan RA. Enhanced antitumor activity of murine-human hybrid T-cell receptor (TCR) in human lymphocytes is associated with improved pairing and TCR/CD3 stability. Cancer Res. 2006 Sep 1;66(17):8878–86.

269. Haga-Friedman A, Horovitz-Fried M, Cohen CJ. Incorporation of Transmembrane Hydrophobic Mutations in the TCR Enhance Its Surface Expression and T Cell Functional Avidity. The Journal of Immunology. 2012 Jun 1;188(11):5538–46.

270. Cohen CJ, Li YF, El-Gamil M, Robbins PF, Rosenberg SA, Morgan RA. Enhanced

antitumor activity of T cells engineered to express T-cell receptors with a second disulfide bond. Cancer Res. 2007 Apr 15;67(8):3898–903.

271. Bohers E, Viailly PJ, Jardin F. Cfdna sequencing: Technological approaches and bioinformatic issues. Vol. 14, Pharmaceuticals. MDPI; 2021.

272. Newman AM, Lovejoy AF, Klass DM, Kurtz DM, Chabon JJ, Scherer F, et al. Integrated digital error suppression for improved detection of circulating tumor DNA. Nat Biotechnol. 2016 May 1;34(5):547–55.

273. Gros A, Parkhurst MR, Tran E, Pasetto A, Robbins PF, Ilyas S, et al. Prospective identification of neoantigen-specific lymphocytes in the peripheral blood of melanoma patients. Nat Med. 2016;22(4):433–8.

274. Vollbrecht T, Brackmann H, Henrich N, Roeling J, Seybold U, Bogner JR, et al. Impact of changes in antigen level on CD38/PD-1 co-expression on HIV-specific CD8 T cells in chronic, untreated HIV-1 infection. J Med Virol. 2010;82(3):358–70.

275. Eiva MA, Omran DK, Chacon JA, Powell DJ. Systematic analysis of CD39, CD103, CD137, and PD-1 as biomarkers for naturally occurring tumor antigen-specific TILs. Eur J Immunol. 2022 Jan 1;52(1):96–108.

276. Vandekerkhove G, Todenhöfer T, Annala M, Struss WJ, Wong A, Beja K, et al. Circulating tumor DNA reveals clinically actionable somatic genome of metastatic bladder cancer. Clinical Cancer Research. 2017 Nov 1;23(21):6487–97.

277. Lozano-Rabella M, Garcia-Garijo A, Palomero J, Yuste-Estevanez A, Erhard F, Farriol-Duran R, et al. Exploring the Immunogenicity of Noncanonical HLA-I Tumor Ligands Identified through Proteogenomics. Clinical Cancer Research [Internet]. 2023 Feb 24;OF1–16. Available from: https://aacrjournals.org/clincancerres/article/doi/10.1158/1078-0432.CCR-22-3298/718374/Exploring-the-Immunogenicity-of-Noncanonical-HLA-I

278. Garcia-Garijo A, Fajardo CA, Gros A. Determinants for neoantigen identification. Vol. 10, Frontiers in Immunology. Frontiers Media S.A.; 2019.

279. Paley MA, Kroy DC, Odorizzi PM, Johnnidis JB, Dolfi D V., Barnett BE, et al. Progenitor and Terminal Subsets of CD8+ T Cells Cooperate to Contain Chronic Viral Infection. Science (1979). 2012 Nov 30;338(6111):1220–5.

280. Sharpe AH, Pauken KE. The diverse functions of the PD1 inhibitory pathway. Vol.

18, Nature Reviews Immunology. Nature Publishing Group; 2018. p. 153–67.

281. Duraiswamy J, Ibegbu CC, Masopust D, Miller JD, Araki K, Doho GH, et al. Phenotype, Function, and Gene Expression Profiles of Programmed Death-1 hi CD8 T Cells in Healthy Human Adults . The Journal of Immunology. 2011 Apr 1;186(7):4200–12.

282. Yossef R, Tran E, Deniger DC, Gros A, Pasetto A, Parkhurst MR, et al. Enhanced detection of neoantigen-reactive T cells targeting unique and shared oncogenes for personalized cancer immunotherapy. JCI Insight. 2018 Oct 4;3(19).

283. Takahashi C, Mittler RS, Vella AT. Cutting edge: 4-1BB is a bona fide CD8 T cell survival signal. J Immunol. 1999 May 1;162(9):5037–40.

284. Vinay DS, Kwon BS. Role of 4-1BB in immune responses. Semin Immunol [Internet]. 1998;10(6):481–9. Available from: https://www.sciencedirect.com/science/article/pii/S1044532398901579

285. Zhang J, Huang D, Saw PE, Song E. Turning cold tumors hot: from molecular mechanisms to clinical applications. Vol. 43, Trends in Immunology. Elsevier Ltd; 2022. p. 523–45.

286. Andersen RS, Thrue CA, Junker N, Lyngaa R, Donia M, Ellebæk E, et al. Dissection of T-cell antigen specificity in human melanoma. Cancer Res. 2012 Apr 1;72(7):1642–50.

287. Poschke IC, Hassel JC, Rodriguez-Ehrenfried A, Lindner KAM, Heras-Murillo I, Appel LM, et al. The Outcome of Ex Vivo TIL Expansion Is Highly Influenced by Spatial Heterogeneity of the Tumor T-Cell Repertoire and Differences in Intrinsic in Vitro Growth Capacity between T-Cell Clones. Clinical Cancer Research. 2020 Aug 15;26(16):4289–301.

288. Zheng C, Fass JN, Shih YP, Gunderson AJ, Sanjuan Silva N, Huang H, et al. Transcriptomic profiles of neoantigen-reactive T cells in human gastrointestinal cancers. Cancer Cell. 2022 Apr 11;40(4):410-423.e7.

289. Yost KE, Satpathy AT, Wells DK, Qi Y, Wang C, Kageyama R, et al. Clonal replacement of tumor-specific T cells following PD-1 blockade. Nat Med [Internet]. 2019;25(8):1251–9. Available from: https://doi.org/10.1038/s41591-019-0522-3

290. Tailor TD, Rao X, Campa MJ, Wang J, Gregory SG, Patz EF. Whole exome sequencing of cell-free DNA for early lung cancer: A pilot study to differentiate benign from malignant CT-detected pulmonary lesions. Front Oncol. 2019;9(APR).

291. Vandekerkhove G, Todenhöfer T, Annala M, Struss WJ, Wong A, Beja K, et al. Circulating tumor DNA reveals clinically actionable somatic genome of metastatic bladder cancer. Clinical Cancer Research. 2017 Nov 1;23(21):6487–97.

292. Jahangiri L, Hurst T. Assessing the concordance of genomic alterations between circulating-free DNA and tumour tissue in cancer patients. Vol. 11, Cancers. MDPI AG; 2019.

293. Bos MK, Angus L, Nasserinejad K, Jager A, Jansen MPHM, Martens JWM, et al. Whole exome sequencing of cell-free DNA – A systematic review and Bayesian individual patient data meta-analysis. Vol. 83, Cancer Treatment Reviews. W.B. Saunders Ltd; 2020.

294. Vandekerkhove G, Todenhöfer T, Annala M, Struss WJ, Wong A, Beja K, et al. Circulating tumor DNA reveals clinically actionable somatic genome of metastatic bladder cancer. Clinical Cancer Research. 2017 Nov 1;23(21):6487–97.

295. Gerlinger M, Rowan AJ, Horswell S, Larkin J, Endesfelder D, Gronroos E, et al. Intratumor Heterogeneity and Branched Evolution Revealed by Multiregion Sequencing. New England Journal of Medicine. 2012 Mar 8;366(10):883–92.

296. Moreno F, Gayarre J, López-Tarruella S, del Monte-Millán M, Picornell AC, Álvarez E, et al. Concordance of Genomic Variants in Matched Primary Breast Cancer, Metastatic Tumor, and Circulating Tumor DNA: The MIRROR Study. JCO Precis Oncol [Internet]. 2019 May 10;(3):1–16. Available from: https://doi.org/10.1200/PO.18.00263

297. Chan KCA, Jiang P, Zheng YWL, Liao GJW, Sun H, Wong J, et al. Cancer genome scanning in plasma: Detection of tumor-associated copy number aberrations, single-nucleotide variants, and tumoral heterogeneity by massively parallel sequencing. Clin Chem. 2013 Jan;59(1):211–24.

298. Koeppel F, Blanchard S, Jovelet C, Genin B, Marcaillou C, Martin E, et al. Whole exome sequencing for determination of tumor mutation load in liquid biopsy from advanced cancer patients. PLoS One. 2017 Nov 1;12(11).

299. Huang A, Zhao X, Yang XR, Li FQ, Zhou XL, Wu K, et al. Circumventing intratumoral heterogeneity to identify potential therapeutic targets in hepatocellular carcinoma. J Hepatol [Internet]. 2017 Aug 1;67(2):293–301. Available from: https://doi.org/10.1016/j.jhep.2017.03.005

300. Merker JD, Oxnard GR, Compton C, Diehn M, Hurley P, Lazar AJ, et al. JOURNAL OF CLINICAL ONCOLOGY Circulating Tumor DNA Analysis in Patients With Cancer: American Society of Clinical Oncology and College of American Pathologists Joint Review. J Clin Oncol [Internet]. 2018;36:1631–41. Available from: https://doi.org/10.1200/JCO.2017.

301. Vignali PDA, DePeaux K, Watson MLJ, Ye C, Ford BR, Lontos K, et al. Hypoxia drives CD39-dependent suppressor function in exhausted T cells to limit antitumor immunity. Nat Immunol. 2022 Feb 1;

302. Sade-Feldman M, Yizhak K, Bjorgaard SL, Ray JP, de Boer CG, Jenkins RW, et al. Defining T Cell States Associated with Response to Checkpoint Immunotherapy in Melanoma. Cell. 2018 Nov 1;175(4):998-1013.e20.

303. Kurtulus S, Madi A, Escobar G, Klapholz M, Nyman J, Christian E, et al. Checkpoint Blockade Immunotherapy Induces Dynamic Changes in PD-1 – CD8 + Tumor-Infiltrating T Cells. Immunity. 2019 Jan 15;50(1):181-194.e6.

304. Krishna S, Lowery FJ, Copeland AR, Bahadiroglu E, Mukherjee R, Jia L, et al. Stem-like CD8 T cells mediate response of adoptive cell immunotherapy against human cancer [Internet]. 2020. Available from: https://www.science.org

305. van der Leun AM, Thommen DS, Schumacher TN. CD8+ T cell states in human cancer: insights from single-cell analysis. Nat Rev Cancer [Internet]. 2020;20(4):218–32. Available from: https://doi.org/10.1038/s41568-019-0235-4

306. Puig-Saus C, Sennino B, Peng S, Wang CL, Pan Z, Yuen B, et al. Neoantigen-targeted CD8+ T cell responses with PD-1 blockade therapy. Nature [Internet]. 2023 Mar 8; Available from: http://www.ncbi.nlm.nih.gov/pubmed/36890230

307. Prokhnevska N, Cardenas MA, Valanparambil RM, Sobierajska E, Barwick BG, Jansen C, et al. CD8+ T-cell activation in cancer comprises an initial activation phase in lymph nodes followed by effector differentiation within the tumor. Immunity [Internet]. 2023 Jan 10;56(1):107-124.e5. Available from: https://doi.org/10.1016/j.immuni.2022.12.002

308. Klicznik MM, Morawski PA, Höllbacher B, Varkhande SR, Motley SJ, Kuri-Cervantes L, et al. Human CD4 + CD103 + cutaneous resident memory T cells are found in the circulation of healthy individuals [Internet]. Vol. 4, Sci. Immunol. 2019. Available from: http://immunology.sciencemag.org/

309. Torcellan T, Hampton HR, Bailey J, Tomura M, Brink R, Chtanova T. In vivo photolabeling of tumor-infiltrating cells reveals highly regulated egress of T-cell subsets from tumors. Proc Natl Acad Sci U S A. 2017 May 30;114(22):5677–82.

310. Kanda Y, Okazaki T, Katakai T. Motility dynamics of T cells in tumor-draining lymph nodes: A rational indicator of antitumor response and immune checkpoint blockade. Vol. 13, Cancers. MDPI; 2021.

311. Zacharakis N, Chinnasamy H, Black M, Xu H, Lu YC, Zheng Z, et al. Immune recognition of somatic mutations leading to complete durable regression in metastatic breast cancer. Nat Med. 2018 Jun 1;24(6):724–30.

312. Lu YC, Yao X, Crystal JS, Li YF, El-Gamil M, Gross C, et al. Efficient identification of mutated cancer antigens recognized by T cells associated with durable tumor regressions. Clinical Cancer Research. 2014 Jul 1;20(13):3401–10.

313. Robbins PF, Lu YC, El-Gamil M, Li YF, Gross C, Gartner J, et al. Mining exomic sequencing data to identify mutated antigens recognized by adoptively transferred tumor-reactive T cells. Nat Med. 2013 Jun;19(6):747–52.

Appendix

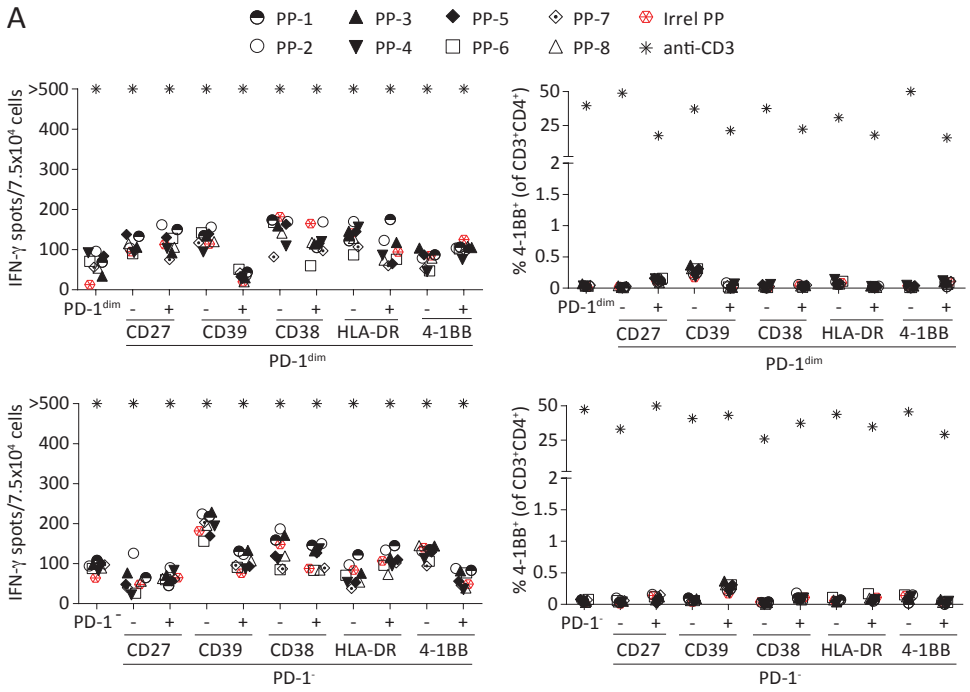

Appendix Figure 1. Screening against neoantigens of CD4⁺ PD-1^{dim} and PD-1⁻ T-cell populations sorted from peripheral blood of patient GOI-01. Autologous B cells pulsed with PPs encoding for neoantigens were co-cultured with the 33 CD4⁺ T-cell populations sorted from peripheral blood of patient GOI-01. After 20h, T-cell responses were evaluated by measuring the number of IFN-γ spots using IFN-γ ELISPOT (left) and the upregulation of 4-1BB by flow cytometry analysis (right). Data is representative of two independent experiments

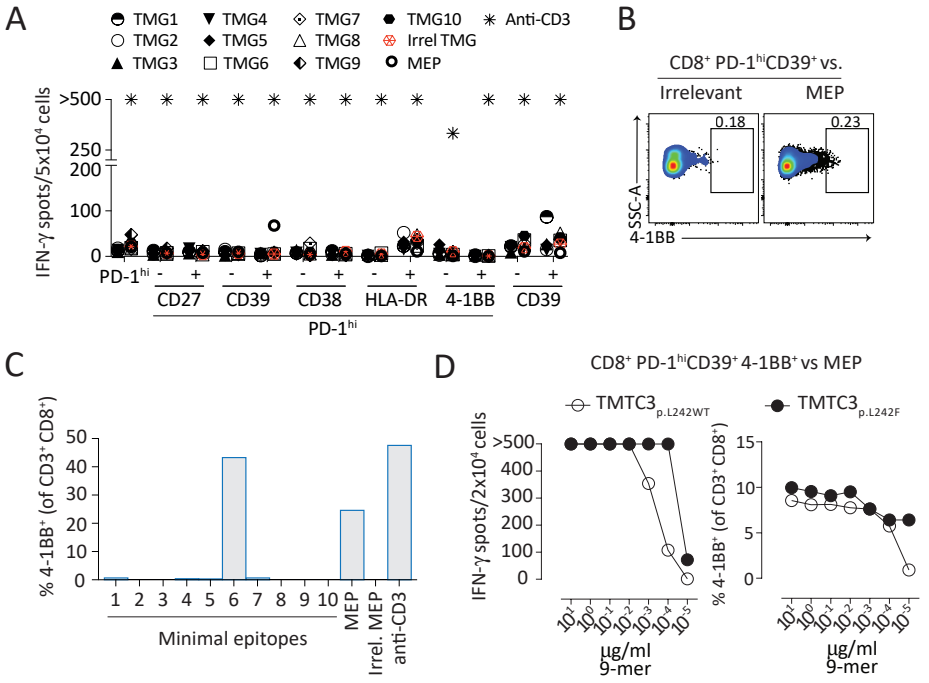

Appendix Figure 2. Neoantigen-specific T cells are detected in the CD8⁺ PD-1^{hi} CD39⁺ T-cell population sorted from peripheral blood in patient GOI-03. (**A**) Autologous B cells electroporated with TMGs encoding for neoantigens or pulsed with MEP were co-cultured with CD8⁺ T-cell populations sorted from peripheral blood based on the expression of PD-1 or CD39 alone or different levels of PD-1 in combination with CD27, CD38, CD39, HLA-DR and 4-1BB in patient GOI-03. After 20h, T-cell responses were evaluated by measuring the number of IFN-γ spots using IFN-γ ELISPOT. Only the results of the populations sorted based on PD-1^{hi} or CD39 alone or PD-1^{hi} in combination with CD27, CD38, CD39, HLA-DR and 4-1BB are shown. (**B**) Neoantigen-specific T cells were enriched from CD8⁺ PD-1^{hi} CD39⁺ T-cell population by FACS based on 4-1BB expression after 20h co-culture with B cells pulsed with MEP and *ex vivo* expanded for 14 days. Plots show gates used for sorting. Autologous B cells pulsed with an irrelevant MEP were used as negative control of T-cell activation. (**C**) To determine the specific mutation recognized, minimal epitopes contained in the MEP were independently pulsed onto autologous B cells at 1 μg/mL during 2h. B cells were then washed and co-cultured with the MEP-reactive CD8⁺ PD-1^{hi} CD39⁺ T cells enriched in (B). After 20h, the reactivity was measured by the upregulation of 4-1BB by flow cytometry as indicated in the y axis. (**D**) B cells were pulsed with serial dilutions of the wild-type (TMTC3$_{p.L242wt}$) or mutant (TMTC3$_{p.L242F}$) minimal epitopes and co-cultured with the neoantigen-reactive CD8⁺ PD-1^{hi} CD39⁺ T-cell population enriched by FACS in (B). T-cell reactivity was evaluated by measuring IFN-γ secretion by IFN-γ ELISPOT (left) and the upregulation of 4-1BB expression (right) after 20h of co-culture. ">500" denotes greater than 500 spots. Experiments were performed without technical duplicates. Data from A and C-D is representative from two independent experiments.

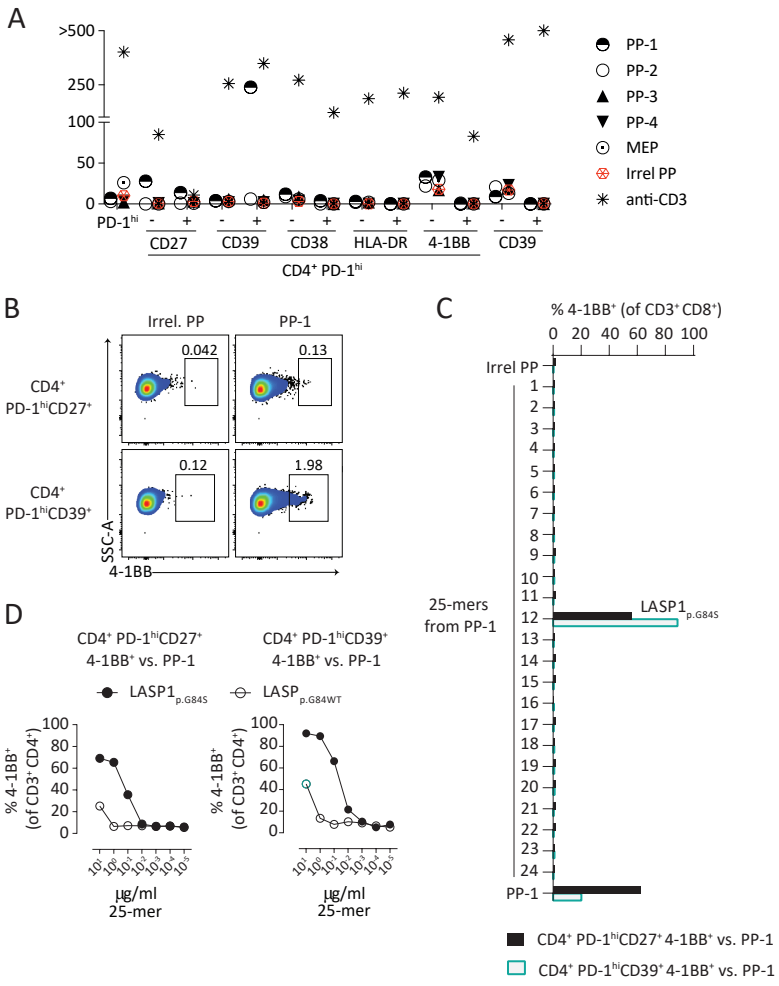

Appendix Figure 3. Identification of circulating CD4⁺ T cells recognizing the mutated antigen LASP1$_{p.G84S}$ in patient GOI-04. (**A**) Autologous B cells pulsed with PPs and a MEP encoding for neoantigens were co-cultured with CD4⁺ T-cell populations sorted from peripheral blood based on the expression of PD-1 or CD39 alone or different levels of PD-1 in combination with CD27, CD38, CD39, HLA-DR and 4-1BB in patient GOI-04. After 20h, T-cell responses were evaluated by measuring the number of IFN-γ spots using IFN-γ ELISPOT. Only the results of the populations sorted based on PD-1^{hi} or CD39 alone or PD-1^{hi} in combination with CD27, CD38, CD39, HLA-DR and 4-1BB are shown. (**B**) Neoantigen-specific T cells were enriched from CD4⁺ PD-1^{hi}CD27⁺ and PD-1^{hi} CD39⁺ T-cell populations by FACS based on 4-1BB expression after 20h co-culture with B cells pulsed with PP-1 and *ex vivo* expanded for 14 days. Plots show gates used for sorting. Autologous B cells pulsed with an irrelevant PP were used as negative control of T-cell activation. (**C**) To determine the specific mutation recognized, 25-mer peptides contained in the PP-1 were independently pulsed onto autologous B cells at 5 µg/mL overnight. B cells were subsequently washed and co-cultured with the PP-1-reactive CD4⁺ T cells enriched in (B) from the PD-1^{hi}CD27⁺ and PD-1^{hi}CD39⁺ T-cell populations. After 20h, the reactivity was measured by the upregulation of 4-1BB by flow cytometry as indicated in the axis. (**D**) B cells were pulsed with serial dilutions of the wild-type (LASP1$_{p.G84wt}$) or mutant (LASP1$_{p.G84S}$) 25-mers peptides and co-cultured with the neoantigen-reactive CD4⁺ T cells enriched in (B) from the PD-1^{hi}CD27⁺ (left) and PD-1^{hi} CD39⁺ (right) subpopulations. T-cell reactivity was evaluated by measuring the upregulation of 4-1BB expression after 20h of co-culture. Data from A and C-D is representative from two independent experiments.

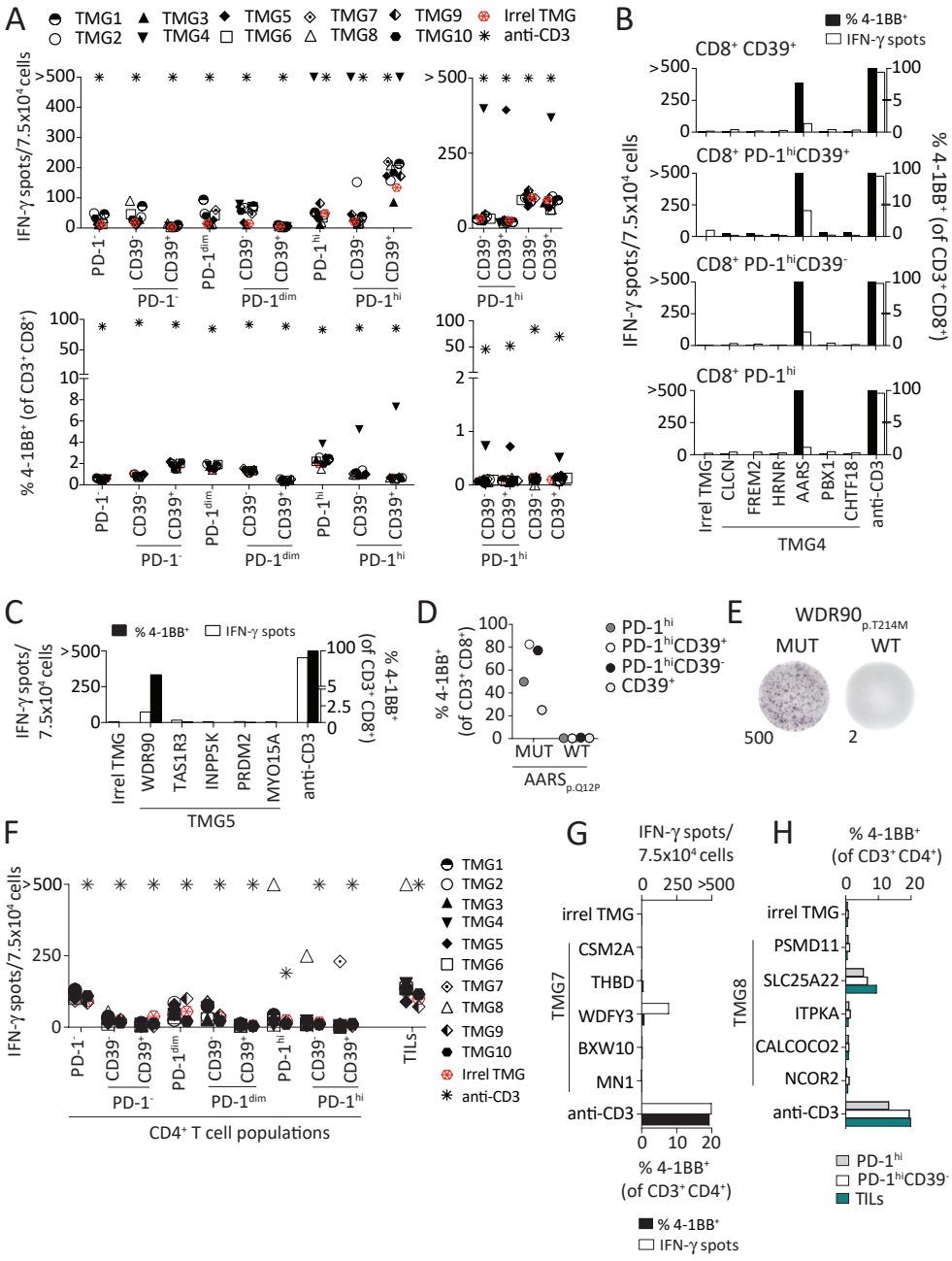

Appendix Figure 4. Identification of CD8⁺ and CD4⁺ neoantigen-specific PBLs and TILs in CRC patient GOI-05. **(A)** Reactivity of CD8⁺ T-cell populations sorted from peripheral blood when co-cultured with autologous B cells electroporated with TMGs encoding for NSMs identified by WES of TuBx DNA and cfDNA. T-cell recognition was evaluated by IFN-γ ELISPOT (top) and upregulation of the activation marker 4-1BB by flow cytometry analysis. **(B-C)** IFN-γ secretion measured by IFN-γ ELISPOT and flow cytometric analysis of 4-1BB expression on CD8⁺ (B) TMG4-reactive and (C) TMG5-reactive T-cell subsets following overnight co-culture with autologous B cells electroporated with

individual minigenes from TMG4 and TMG5. (**D-E**) Reactivity of (D) $AARS_{p.Q12P}$-specific and (E) $WDR90_{p.T214M}$-specific T-cell populations upon co-culture with autologous B cells electroporated with mutated (MUT) and wild-type (WT) $AARS_{p.Q12P}$ and $WDR90_{p.T214M}$ minigenes, evaluated by (D) 4-1BB expression by flow cytometry analysis or (E) IFN-γ secretion by IFN-γ ELISPOT. (**F**) Reactivity of circulating $CD4^+$ T-cell populations when co-cultured with autologous B cells electroporated with TMGs encoding for NSMs identified by WES of TuBx DNA and cfDNA, assessed by the secretion of IFN-γ by IFN-γ ELISPOT. (**G-H**) IFN-γ secretion measured by IFN-γ ELISPOT and/or flow cytometric analysis of 4-1BB expression on $CD4^+$ (G) TMG7-reactive and (H) TMG8-reactive T-cell subsets following an overnight co-culture with autologous B cells electroporated with individual minigenes from TMG7 and TMG8, respectively. “>500” denotes greater than 500 spots. Experiments were performed without technical duplicates. All data is representative from two independent experiments.

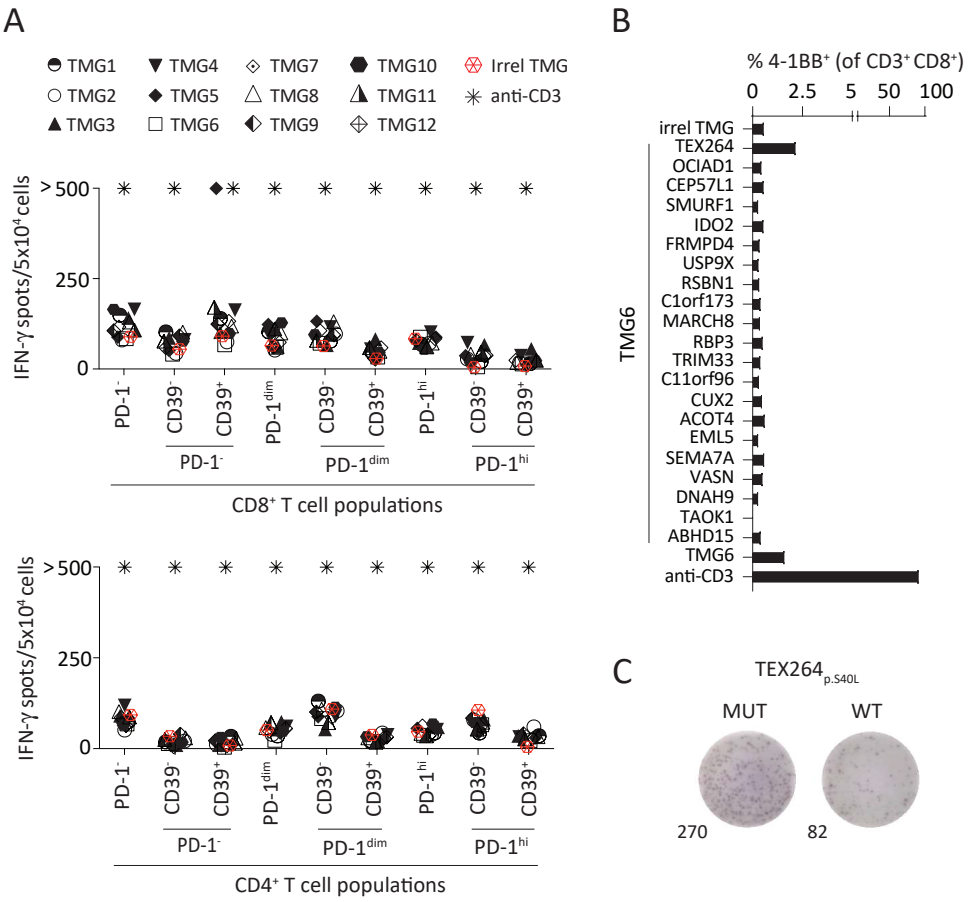

Appendix Figure 5. CD8⁺ PD-1⁻CD39⁺ PBL subset displayed neoantigen recognition in the CRC patient GOI-06. (**A**) Reactivity of CD8⁺ (top) and CD4⁺ (bottom) T-cell populations sorted from peripheral blood upon 20h of co-culture with autologous B cells electroporated with TMGs encoding for NSMs identified by WES of TuBx DNA. T-cell recognition was evaluated by measuring IFN-γ secretion by IFN-γ ELISPOT. (**B**) Reactivity of CD8⁺ PD-1⁻CD39⁺ T cells after a 20h co-culture with autologous B cells electroporated with individual minigenes from TMG5. Reactivity was measured by the upregulation of 4-1BB expression by flow cytometry. (**C**) Reactivity of CD8⁺ PD-1⁻CD39⁺ T lymphocytes upon co-culture with autologous B cells electroporated with mutated (MUT) and wild-type (WT) $TEX264_{p.S40L}$ minigenes, evaluated by IFN-γ ELISPOT. “>500” denotes greater than 500 spots. Experiments were performed without technical duplicates. All data is representative from two independent experiments.

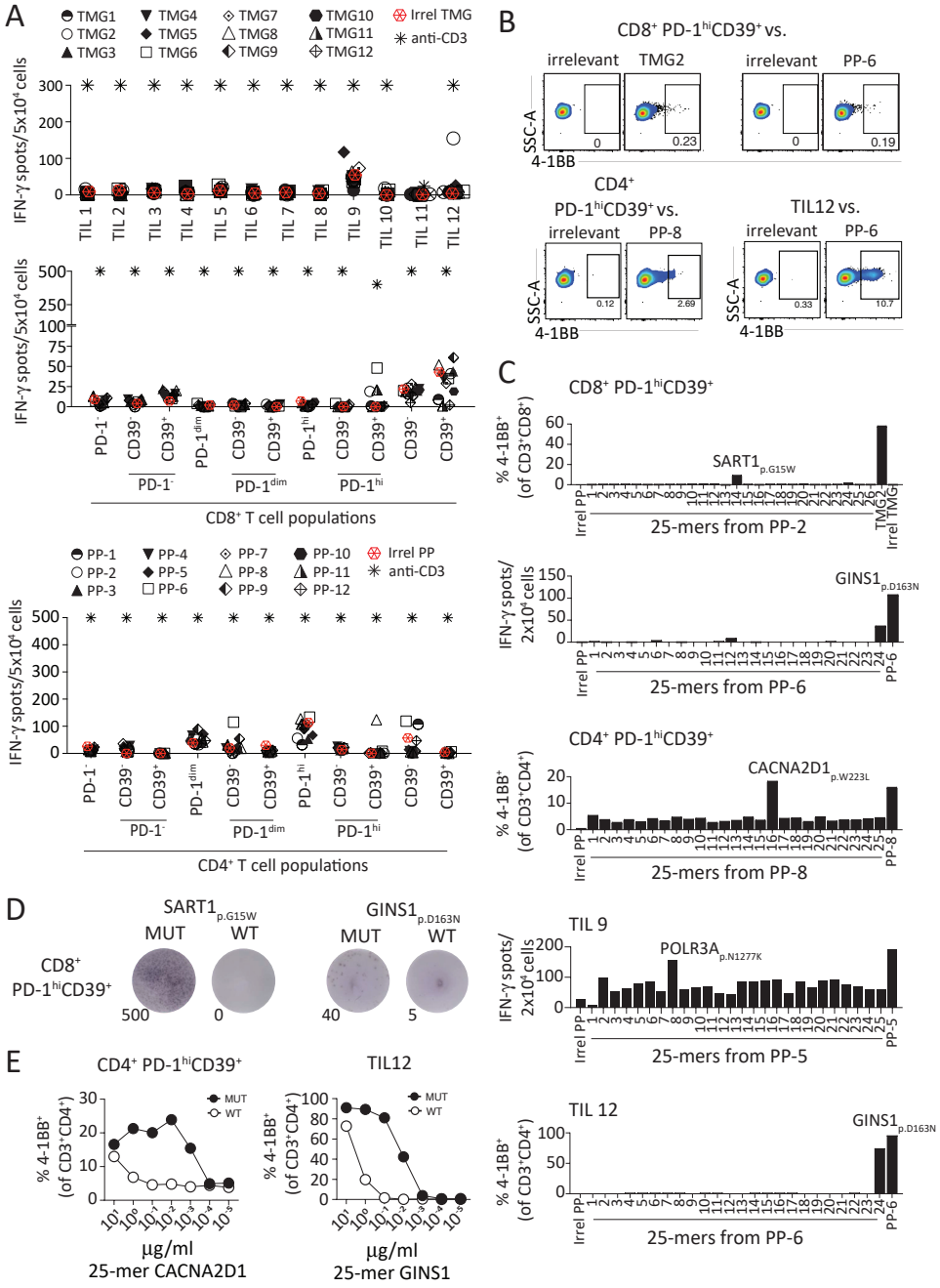

Appendix Figure 6. CD8⁺ and CD4⁺ PD-1^{hi}CD39⁺ PBLs and unselected TILs identified neoantigen reactivities in patient GOI-08. (**A**) Reactivity of TILs (top), CD8⁺ (middle) and CD4⁺ (bottom) PBLs upon 20h co-culture with autologous B cells electroporated with TMGs or pulsed with PPs encoding for somatic mutations identified by WES of TuBx DNA and/or cfDNA. IFN-γ secretion measured by IFN-γ ELISPOT is plotted. (**B**) CD8⁺ and CD4⁺ PD-1^{hi}CD39⁺ PBLs and TILs were co-cultured with autologous B cells either electroporated or pulsed with the respective TMGs and PPs that showed certain reactivity in (A) and CD8⁺ and CD4⁺ T cells that upregulated 4-1BB after 20h of co-culture were

FACS purified and expanded. Representative plots show the percentage of 4-1BB$^+$ live CD3$^+$CD8$^+$ or CD3$^+$CD4$^+$ lymphocytes. (**C**) Reactivity of TMG- or PP-reactive CD8$^+$ and CD4$^+$ PBLs and TILs unselected or isolated in (B) against autologous B cells pulsed with individual 25-mers from the respective TMG/PP. IFN-γ secretion by IFN-γ ELISPOT or the upregulation of 4-1BB expression by flow cytometry are plotted. (**D-E**) Reactivity of TMG- or PP-reactive CD8$^+$ and CD4$^+$ PBLs and TILs isolated in (B) upon co-culture with autologous B cells pulsed with mutated (MUT) and wild-type (WT) versions of the respective recognized peptides, evaluated by (D) IFN-γ ELISPOT or by (E) the upregulation of 4-1BB expression by flow cytometry. ">500" denotes greater than 500 spots. Experiments were performed without technical duplicates. Data from A, C-E is representative from two independent experiments.

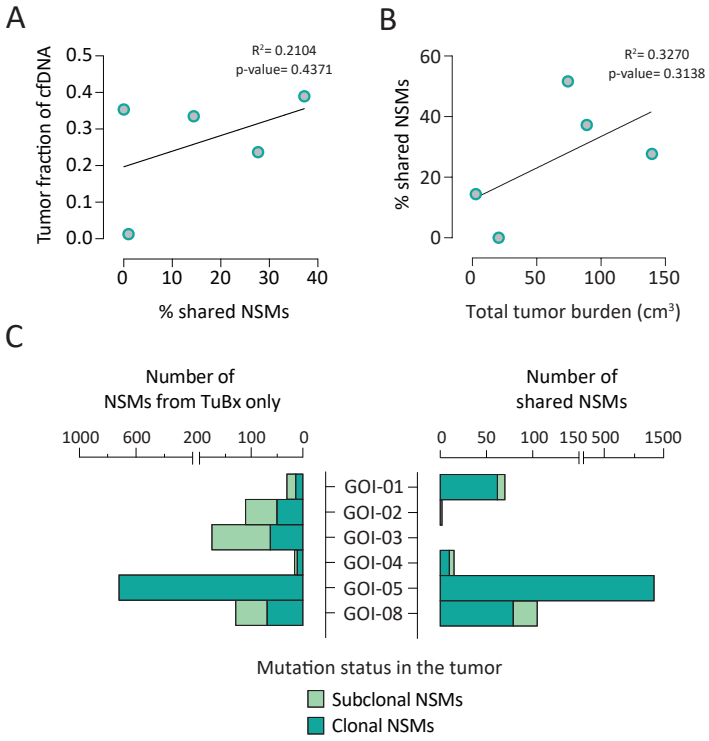

Appendix Figure 7. Correlative analysis of cfDNA and evaluation of the clonality of shared NSMs and NSMs only identified in TuBx DNA. (**A**) Correlation between tumor fraction of cfDNA and frequency of shared somatic NSMs between cfDNA and TuBx DNA. (**B**) Correlation between total tumor burden measured in cm^3 and the frequency of shared NSMs between cfDNA and TuBx DNA. (**C**) Number of clonal and subclonal NSMs identified in both TuBx DNA and cfDNA or only identified in TuBx DNA.

Appendix Table 1. RNA levels of expression of cancer germline antigens selected for immunological screening in patient GOI-07

Cancer germline antigen	Gene transcript expression in TuBx	Gene transcript expression in autologous TCL	Cancer germline antigen pool for screening
MAGE A3	30.266	-	1
MAGE A4	98.303	99.003	8
MAGE A6	39.747	-	1
MAGE A10	33.589	-	8
MAGE C1	33.589	-	2
MAGE C2	30.266	-	4
ACRBP	55.604	41.244	3
BRDT	-	37.514	7
DKKL1	59.538	62.458	5
DPPA2	36.055	32.293	5
ODF3	32.506	-	4
POTEE	32.506	48.568	6
PRAME	96.442	91.04	3
PRSS54	39.149	55.317	7
SPAG9	98.178	98.875	2
TEX14	49.375	47.153	6

Appendix Table 2. Co-expression of markers within PD-1$^-$, PD-1^{dim} and PD-1^{hi} T-cell populations in cancer patients and healthy individuals

		Number of markers co-expressed in CD4$^+$ T-cell subsets		Number of markers co-expressed in CD8$^+$ T-cell subsets	
ID	**PD-1 population**	**3**	**4**	**3**	**4**
Patients	PD-1^{hi}	14.44	2.41	16.64	10.9
	PD-1^{dim}	2.86	0.38	2.85	0.73
	PD-1$^-$	0.64	0.11	0.75	0.11
Healthy donors	PD-1^{hi}	2.15	0.05	4.99	1.07
	PD-1^{dim}	0.55	0.03	0.66	0.04
	PD-1$^-$	0.18	0.01	0.25	0.02